warwick.ac.uk/lib-publications

THE BRITISH LIBRARY
BRITISH THESIS SERVICE

Aspects of Continuity in Steel and Composite Frames

A Aziz Saim
Dip. in Civil Eng. (UTM. Malaysia)
B. Eng(Hons)(UTM, Malaysia)
M Sc. (Civil Engineering)(Sheffield, UK)

Department of Engineering

University of Warwick
United Kingdom

Thesis submitted to the University of Warwick for the degree of

Doctor of Philosophy

January 1998

BLANK IN ORIGINAL

Contents

Chapter 2

TEST ON BEAM-T0-BEAM END PLATE COMPOSITE

Chapter 4

Chapter 7

FURTHER DEVELOPMENT TO DIRECT DESIGN TO HORIZONTAL

Chapter 8

Summary

This thesis concerns the continuity in steel and composite frame and specifically the region of the connections. It reports on five main areas as follows:

1. Seven beam-to-beam connection tests were conducted to study the structural performance of composite end plate connections. Various parameters such as the types of connections, amount of reinforcement, beams sizes, and the degree of shear connection were investigated. The investigation confirmed a similar overall response of moment-rotation (M-ϕ) curves to beam-to-column tests and justified the restriction by current design codes of having partial shear connection in hogging moment region. A prediction method to estimate the initial stiffness of composite connection has also been proposed.

2. The effects of concrete encasement on structural response of end plate joints of slimfloor beams were investigated. Five specimens of beam-to-column connection of slimfloor were tested. Parameters such as end plate thickness and bolt sizes are included in the study. The results have shown that proper reinforcement and design are needed if the connections are to be considered as a composite joint.

3. Tests were carried out to improve the bond capacity of encased slimfloor. A total of six push-out tests each with different type of "shear enhancer" were performed. The load at initial slip is not greatly depend on the types of enhancer and there were indications that the resistance of the enhancer only became effective after slip, due to bond failure, had occurred.

4. As far as stability of composite beams in the negative moment region is concerned, local buckling has been identified as one of the problems. The action of reinforcement may reduce many hot-rolled section to be in Class 3. Studies were conducted on published data to explore the possibility of upgrading Class 3 to Class 1. The studies indicated that beams of Class 3 web showed the characteristics of beams with higher class if the connection was full strength. Many of the Class 3 beams used in composite beams can only be upgraded to Class 2 and not to Class 1.

5. A method applicable to the design of unbraced multi-storey frames to specified limits on horizontal sway deflection is proposed. Only simple calculation are required by the method and its application is illustrated by worked examples.

Acknowledgements

Declaration

I declare that the work presented in this thesis was carried out by the author and has not taken from any other research except where specific reference has been made. None of this work has been submitted for a higher degree at any other establishment.

Notations

M	Moment
ϕ	Relative angular rotation
M_{Rd}	Moment resistance
S_j	Rotational stiffness
ϕ_{Cd}	Rotation capacity
$M_{j,Rd}$	Moment resistance of a connection
$F_{t,Rd}$	Effective design tension resistance of bolt row
h_r	Distance from bolt-row to the centre of compression
$B_{t,Rd}$	Design tension resistance of a bolt
l_{eff}	Effective length of T-stub
$S_{j,ini}$	Initial rotational stiffness
k_i	Stiffness coefficient of component i
z	Lever arm
μ	Stiffness ratio
$M_{pl,Rd}$	Beam plastic moment resistance
D	Steel beam depth
D_b	Distance of row of bolts below the top of the beam
D_r	Distance of the reinforcement above the top of the beam
R_r	Tensile resistance of the reinforcement
f_{ys}	Yield stress of reinforcement

A_s	Total reinforcement area within the slab's effective breadth
R_b	Effective tensile resistance of the bolt row in accordance to Annex J of EC3[1-17]
R_w	Compressive resistance of web in compression
t_f	Flange thickness
R_f	Tensile resistance of flanges
y_c	Neutral axis depth above the bottom flange
f_{yw}	Yield stress of beam web
t_w	Thickness of the beam web
F_i	Force in the spring i,
k_i	Stiffness coefficient of the component i
E	Modulus of elasticity of steel
Δ_i	Deformation of the spring i.
K_{sc}	Translational stiffness of the shear connection
K_s	Translational stiffness of the reinforced slab in tension
k_{sc}	Stiffness of one connector
N	Number of shear studs provided
N_f	Number of shear studs required for full shear connection
A_r	Area of reinforcement
$f_{y,s}$	Yield strength of reinforcement
P_{Rd}	Design shear resistance of each shear stud determined from
d	Diameter of the shank of the stud

f_u	Ultimate tensile strength of stud but not greater than 500 N/mm^2
f_{ck}	Characteristic strength of concrete
E_{cm}	Secant modulus of concrete
h	Overall height of the stud
K_b	Total stiffness of a substitute frame
K_c	Total stiffness of substitute column
k_b, k_b	Distribution coefficient
σ_{sr1}	Reinforcement stress in the crack, when the first crack has formed,
σ_{sm}	Reinforcement stress in the crack, when the stabilised crack pattern has formed,
f_{yk}	Characteristic yield strength of reinforcement,
f_{tk}	Ultimate tensile strength of reinforcement,
ε_{smu}	Ultimate average strain of the embedded reinforcement,
ε_{su}	Ultimate strain of the unembedded reinforcement

PAGE
NUMBERING
AS BOUND

P.o - P.1-3.

- Unloading stiffness is almost the same as the initial stiffness.
- The curves fall between the ideals of "rigid" (vertical axis) and "pinned" (horizontal axis).

One way of obtaining moment-rotation curves is by the experimentation in the laboratory. This method is accurate but expensive. Experimental measurements of M-ϕ behaviour of steel beam-to-column connections have been reviewed by several researchers [1-11, 1-12, 1-13], which confirmed that particular moment-rotation characteristics are produced by different types of connections. However the data are of little direct usefulness to designers[1-14].

Other techniques of obtaining M-ϕ curve are described in Ref.[1-15] by Nethercot and Zandonini, classified into four main categories:

- Curve fitting
- Simplified analytical models
- Mechanical models
- Finite element analysis.

Jaspart and Maquoi[1-16] compared the similarities and differences of these categories, highlighting the advantages as well as disadvantages to assist others researchers who intend to develop mathematical predictions of joint behaviour.

Although an M-ϕ curve such as in Fig. 1-1 provides a means of discussing connection behaviour, it is too complicated for use as a basis for the consideration of joint flexibility in design. A simplified representation of M-ϕ curve (Fig. 1-3) for steel

connection is used by revised Annex J of EC3 [1-4] which defines three important properties in joint behaviour :

- moment resistance, M_{Rd}
- rotational stiffness, S_j
- rotation capacity, ϕ_{Cd}.

Methods for determining the moment resistance and rotational stiffness are given in revised Annex J of EC3 [1-17] described in the following sub-section.

1.1.2   Prediction method of connection response: Annex J of Eurocode3

A description of a connection response has to take into consideration all possible source of deformability within the joint area. In general, deformations may occur by shear deformations acting within the column web panel and bending deformations due to tensile or compression forces.

"Semi-continuous" is a term adopted by EC3[1-4] for frames which contain semi-rigid and/or partial-strength joints. By providing a method to predict the rotational stiffness and moment resistance for some types of joints, EC3[1-4] encourages the use of semi-continuous approach in design. However EC3[1-4] only provides a very limited advice to determine the rotation capacity of the steel frame joints.

1.1.2.1   Moment resistance of connection

The basic concept in determining the moment resistance $M_{j,Rd}$ is to identify each critical zone of the joint and to consider each potential limiting condition. The critical zones in which deformations may occur are identified as: the tension zone, the compression zone

and the shear zone (Fig. 1-4). The expression provided by EC3[1-4] to predict the moment resistance of a connection $M_{j,Rd}$ with a bolted end-plate is:

$$M_{j,Rd} = \sum_r h_r F_{t,Rd} \qquad (1.1)$$

where:

$F_{t,Rd}$ is the effective design tension resistance of bolt row r

h_r is the distance from bolt-row r to the centre of compression

r is the bolt row number.

The design tension resistance is based on a T-stub to model the column flange or the beam's end plate (Fig. 1-5 and Fig. 1-6). It is taken as the smallest value for three possible modes, determined as follows:

Mode 1: Complete yielding of the flange:

$$F_{t,Rd} = \frac{4\,M_{pl}}{m} \qquad (1.2)$$

Mode 2: Bolt failure with yielding of the flange:

$$F_{t,Rd} = \frac{2\,M_{pl} + n\sum B_{t,Rd}}{m+n} \qquad (1.3)$$

Mode 3: Bolt failure:

$$F_{t,Rd} = \Sigma B_{t,Rd} \qquad (1.4)$$

in which:

M_{pl} = $0.25\,l_{eff}\,t^2 f_y$

$B_{t,Rd}$ is   the design tension resistance of a bolt

l_{eff} is   the effective length of the T-stub

n = e_{min} but $\leq$ $1.25m$

e_{min} and m are as indicated in Fig. 1-5

In practice, usually more than one bolt row in tension are used in order to increase the stiffness and resistance of the end plate connection. In such cases it is generally necessary to consider both the maximum resistance of an individual bolt-row and the contribution of each bolt-row to the maximum resistance of two or more adjacent bolts rows within a bolt-group. For simplification however, the contribution of any bolt row may be neglected if the contribution of all other bolt rows closer to the centre of compression (normally located at the mid-thickness of the compression flange of the beam) are also neglected[1-17]. In any case the tensile forces of the bolt rows must not exceed compression resistance of the column web and also the resistance of compressive region of the beam.

1.1.2.2   *Rotational stiffness of steel connection*

The initial rotational stiffness $S_{j,ini}$ for the elastic range in EC3[1-4] is taken at a level of 2/3 of the design moment resistance $M_{j\,Rd}$. Beyond this range, the stiffness decreases until a plastic moment resistance $M_{j,Rd}$ is attained. When the moment in the joint reaches this value a constant plateau is assumed. The original Annex J attempted to calculate the secant stiffness at $M_{j,Rd}$ to be used in global analysis, and the initial stiffness $S_{j,ini}$ is then taken as a fraction of that rotational stiffness S_j. However in the revised rules[1-17] the rotational stiffness S_j is taken as a proportion of $S_{j,ini}$. Now for global analysis the rotational stiffness of a joint is simplified as $S_{j,ini}/2$[1-17].

The rotational stiffness of a joint S_j may be determined by the so-called "component method". By this, the flexibility of each relevant basic joint component is taken into

account. The method to determine the rotational stiffness in the revised Annex J[1-17] is summarised in Eqn. (1.5), given by

$$S_j = \frac{E\,z^2}{\mu \sum_i \frac{1}{k_i}}$$ (1.5)

where:

k_i is the stiffness coefficient representing each basic joint component

z   is the lever arm

μ is the stiffness ratio $S_{j,ini} / S_j$

$S_{j,ini}$ is the value of S_j when the moment $M_{j,Sd}$ is zero.

The stiffness ratio μ should be determined from:

$$\mu = \left[\frac{1.5\,M_{j,Sd}}{M_{j,Rd}} \right]^{\psi} \qquad \text{but } \mu \geq 1$$ (1.6)

in which the coefficient ψ ranging from 2.7 to 3.1 is obtained from the code. The value is based on an assessement of tests result by the code drafters. μ accounts for the reduction in stiffness beyond the expected elastic range.

1.1.3 Classification of steel connections

Connections in frames may be classified on the basis of their strength or rigidity which in turn identified the types of global analysis to be adopted in design. In EC3[1-4] connections are classified in relation to their rotational stiffness and moment resistance which in turn is related to framing systems which are simple, continuous or semi-continuous.

1.1.3.1   Classification by strength

In terms of strength, the connection is defined as either 'full strength', 'partial strength', or 'nominally pinned' depending upon its ultimate moment resistance $M_{j,Rd}$ relative to the beam plastic moment resistance $M_{pl,Rd}$. A connection is a full strength connection when the design moment resistance is equal to or greater than that of the connected beam ($M_{j\,Rd} \geq M_{pl\,Rd}$). On the other hand, a partial strength connection is one having a design moment resistance smaller than that of the connected beam. However to achieve full strength often requires a more expensive stiffened arrangement. EC3 allows the use of partial strength joints in frames analysed by plastic methods; as plastic hinges are expected to form in the joints, rotation capacity will now be required in the joints. The boundaries specified by the Revised Annex J of EC3[1-17] for strength classification of joint are illustrated in Fig. 1-7

The design plastic moment resistance $M_{pl,Rd}$ of a steel beam is taken as the product of the plastic modulus S_{xx} of the steel section multiplied to the design strength f_y of the steel.

1.1.3.2   Classification by stiffness

The connection is classified by stiffness as rigid, semi-rigid, or nominally pinned depending upon the M-ϕ behaviour. For this the initial rotational stiffness, $S_{j,ini}$ is determined and compared to boundaries, those of the Revised Annex J of EC3[1-17] being shown in Fig. 1-8(a) and 1-8(b). Separate boundaries are given for braced and unbraced frames. A rigid joint is one having high values of stiffness while a very flexible joint can be assumed as pinned. A connection having a stiffness in between the

two extremes may be classified as semi-rigid. By using semi-rigid connections, a designer may achieve worthwhile benefits in structural performance compared to simple design whilst avoiding a more expensive fabrication of rigid joints[1-18].

1.2   Composite construction

In the UK composite construction is commonly applied to floor systems. It uses composite action of a steel beam section with a concrete floor slab and possibly concrete encasement to increase the resistance and stiffness of the frame. Today most composite framed buildings utilise profiled steel decking in the slab and through-deck welding of shear connectors in the construction. One difference between steel and composite frames is the beam stiffness. The stiffness of the steel beam is usually constant along the span but that of the composite beam varies according to the nature of the moment (hogging or sagging moment).

The main structural benefits in using steel-concrete construction are[1-19] :

- Savings in steel weight are typically 30-50% over non-composite beams.
- The greater stiffness of composite beams mean that they can be shallower for the same span, leading to lower storey heights and savings in cladding cost or, alternatively, permitting more room for services.
- Construction periods are reduced compared to reinforced concrete construction.

However along with the benefits, serviceability problem such as deflection and vibration need to be addressed to. At present composite structural frames are usually limited to braced structures and simple construction due to the ease of design calculations in these cases.

EC4 [1-5] defines a composite frame as a 'framed structure for a building or similar construction works, in which some or all of the beams and columns are composite members and most of the remaining members are structural steel members'. Hence the treatment of composite frames in EC4[1-5] is closely related to steel frames in EC3[1-4]. In the UK today there is no code of practice regarding the composite frames or connections[1-8].

1.3   Composite joints

In composite construction, the concrete slab, with anti-cracking welded mesh around the column support, may be able to provide some continuity and additional strength and stiffness to the beam-to-column joint. However in braced frames, hogging moments always occurs at the joints. Normally the concrete cracks (due to low tensile strength) and the welded mesh fractures (due to its brittle nature) before the ultimate design load is reached, thus destroying any significant element of continuity[1-18]. However the introduction of reinforcing bars to provide tensile resistance into the concrete across the support can be cheap solution to this problem[1-20]. EC4[1-5] defines such a connection as a composite connection because it is 'a connection between a composite member and any other member in which reinforcement is intended to contribute to the resistance of the connection'. Composite action will also influence the connection's rotational stiffness by significantly increasing it over much of the range, altering the eventual mode of failure, and may well reduce its rotation capacity[1-21]. Hence all the key connection properties namely strength, stiffness and ductility will be affected (Fig. 1-9).

In composite structures, partial-strength composite connections may be used as a possible alternative to pinned or full-strength joints providing a substantial degree of continuity and reduces the importance of local buckling. By reasonable selection of the reinforcement, local flange buckling can be controlled. This is because reinforcement largely controls the balancing of compression in the steel section. Clearly such an approach leads to more economic solution than the use of rigid steelwork connections while achieving much of the benefits of continuity (greater load-bearing resistance, greater stiffness). The composite slab is also normally continuous over beam-to-beam connections; thus it is desirable to extend the idea of semi-rigid and/or partial strength joints to these connections. All composite beams in a floor could then be designed as semi-continuous rather than as simply supported.

In recent years, a substantial volume of testing and research designed to investigate the strength and rotational stiffness of composite beam-to-column connections in building has been undertaken. According to design codes for composite structures in the UK[1-7] and more widely in Europe[1-5] semi-continuous composite connections are allowed. However no application rules are given for the calculation of the properties of such connections. Research is still continuing (including this study) to provide acceptable design rules to assist the practising engineer to adopt this concept.

A comprehensive summary of the work until 1987 by several researchers on composite beam-to-column connection was carried out by Zandonini [1-22]. The main conclusion drawn from the summary were:

- Semi-rigid composite connections can be designed to possess high stiffness and ultimate strength. Moment capacities of the order of the negative plastic

moment of the composite beam may be achieved while maintaining simple detailing in the steelwork.

- The rotation capacity is significant and sufficient for a plastic beam mechanism to be activated, when proper detailing of the nodal zone is employed. Moreover, appropriate selection of the amount and grade of steel reinforcement in the slab allows local buckling of the steel members to be easily controlled, which is usually the critical factor affecting ductility.

- The single major factor governing the behaviour of the joint is the slab action. Models for these joints need to include not only connection parameters (number and distribution of connecting elements, prying action, and slip of bolts, for example), but also need to account for the way that composite action is developed in the beam (shear connection flexibility and strength, and distribution of shear studs)

In North America, Leon[1-23] outlined the distinction between three types of construction, namely pinned construction, semi-rigid construction and rigid construction, similar to the Eurocode classifications. He showed that by designing frames with semi-rigid connections using the composite floor system, economic advantage can be gained. The behaviour of semi-rigid composite connections subjected to gravity loading was investigated by Leon and Ammerman[1-24]. A useful design approach for the determination of beam deflections incorporating semi-rigid connection behaviour was provided. The study also confirmed that by using semi-rigid construction substantial weight savings and economic benefits can be achieved.

A substantial number of composite beam-to-column connection tests have been conducted in Europe, for example by Anderson and Najafi[1-25], Brown[1-26], Xiao et al[1-27] and Bernuzzi et al[1-28]. These confirmed the general observation that the reinforcing bars in the concrete substantially influence the strength and stiffness of the composite connection. The higher the amount of reinforcement provided, the lower was the contribution of the steel connection to the moment resistance of the composite connection itself. Basically, the moment-rotation response obtained by these researchers by way of testing is similar; linear at low load, followed by a reduction of stiffness. Further loading increased the rotation without significantly increasing the moment transmitted by the connection.

The findings of the researchers mentioned above contradicted to the conclusion drawn by Zandonini[1-22]. Instead of local buckling of steel member it is now recognised that the fracture of reinforcement in the concrete slab is the most critical factor affecting ductility in composite joint.

Compared to the considerable research effort on the composite beam-to-column connections, the attention given to composite beam-to-beam has been slight. In most existing codes of practice this subject is not covered in detail. One experimental study concerning beam-to-beam composite connections was conducted by Rex and Easterling[1-2] and involved four semi-rigid composite connections. The behaviour exhibited by these connections indicated that simple steel beam-to-beam connections can be turned into very stiff connections, with a moment resistance of the connection near to the plastic moment resistance of the steel beam. Bode and Kronenberger[1-29] tested a so-called "boltless" connection for interconnected floor beams with the main

beam underneath. Continuity and moment resistance in the negative bending region was provided by the reinforcing bars in the slab. It was shown that the type of joint tested provided a higher rotation capacity than necessary, and failure occured at a rotation of about 45 mrad.

1.3.1 Moment resistance of composite connections

The moment resistance of composite connections may be evaluated by plastic analysis based on a "stress block" approach, provided[1-30]:

- there is an effective compression transfer to and through the column (for beam-to-beam connections, compression transfer at the bottom flange)
- the amount of reinforcement is above a certain minimum, so that cracking of the concrete develops in a controlled manner
- there are sufficient shear connectors to develop the tensile forces in the reinforcement
- the reinforcement is effectively anchored on both sides of the connection
- the bolts provide sufficient resistance to vertical shear

1.3.1.1 Prediction method for moment resistance of connections: SCI model

An interim guide by SCI[1-30] provides a calculation method for the composite flush end plate connection (see Fig. 1-10). The model considered only the upper pair of bolts as effective in tension. Mode 1 failure (Fig. 1-6) is preferable to ensure that connection ductility is compatible with the extension of the reinforcement at the required rotation of the connection. The model also considered the effective portion of web depth that can resist compression before onset of local buckling (the maximum to be $19t_w\varepsilon$; t_w is

the web thickness and $\varepsilon = \sqrt{(p_y/275)}$ for steel of design strength, p_y). The moment of resistance of the composite connection could be determined by the expression:

$$M_{j.Rd} = R_r (D + D_r - 0.5\, t_f) + R_b (D - D_b - 0.5t_f) - R_w (0.5\, y_c) \qquad (1.7)$$

where :

$M_{j.Rd}$ = moment resistance of connection

D = steel beam depth

D_b = distance of row of bolts below the top of the beam

D_r = distance of the reinforcement above the top of the beam

R_r = tensile resistance of the reinforcement $= f_{ys}\, A_s$

f_{ys} = yield stress of reinforcement

A_s = total reinforcement area within the slab's effective breadth

R_b = effective tensile resistance of the bolt row in accordance to Annex J of EC3[1-17]

R_w = compressive resistance of web in compression $= y_c\, t_w\, f_{yw}$

t_f = flange thickness

R_f = tensile resistance of flanges

y_c = neutral axis depth above the bottom flange $= \dfrac{(R_r + R_b - R_f)}{t_w\, f_{yw}}$

f_{yw} = yield stress of beam web

t_w = thickness of the beam web

If:

$$R_f \quad > \quad R_b + R_r \qquad (1.8)$$

the plastic neutral axis lies in the beam bottom flange, thus the last term in Eqn.(1.7) can be omitted from the calculation.

For a bare steel connection, the first and the last terms in Eqn.(1.7) would be ignored in the calculation.

It is proposed in the guide that when $y_c > 0.5D$, the tensile resistance of the bolts should be neglected due to their low strain relative to the reinforcement.

Tables 1-1 and 1-2 present the comparison between the results of end plate connections test by several research group and the prediction method of the SCI[1-30]. From Tables 1-1 and 1-2 it can be seen that, except for a few cases, the approach proposed by the guide[1-30] is generally conservative.

1.3.1.2 Evaluation of connection moment of resistance : EC4 model

The model used is based on the "component" approach in which all the basic component of the joint subjected to tension, compression or shear are taken into consideration. The deformation and resistance characteristics of each individual component are evaluated. The components are then assemble to evaluate the characteristics of the whole joint. This approach has enabled much of the material presented in EC3 for steel joints to be applicable to composite joints to be designed to EC4. The distribution of internal forces is obtained by assuming the compression force is transferred at the centroid of the beam flange. For a composite connection without steelwork components effective in tension, the sole tension force is at the level of the layer of the reinforcing bar (Fig. 1-11).

The design resistance of the joint $M_{j,Rd}$ is associated with the design resistance F_{Rd} of the weakest joint component and is given in Eqn.(1.9) as follows:

$$M_{j,Rd} = F_{Rd} \cdot z \qquad\qquad (1.9)$$

where z is the level arm of the internal forces.

For joints in which the tensile components are critical, it is assumed that in the presence of rows of bolt in the connection, the reinforcing bars attain and sustain their design resistance while the top row of bolt reaches its resistance as predicted by EC3. In effect, it is assumed that the deformation capacity in tension possessed by the ductile rebars allows redistribution of internal forces to take place and additional bending resistance results from the steelwork connection. As in the SCI model, the redistribution between bolt rows can take place if the failure mode anticipated by Annex J of EC3[1-17] is ductile (Mode 1 failure). However if the resistance of compression zone and shear zone do not governed, the connection moment resistance of composite joint may be simplified as

$$M_{j,Rd} = M_{steel\,joint} + (\text{Design resistance of rebars x lever arm} \qquad (1.10)$$

The essential differences between EC4 and the SCI guide[1-30] are that the former:

   i)   is more general and resistance may therefore be limited by shear in the column web panel or compression in unstiffened column web,

   ii)   treats unbalanced loading therefore resistance may be limited by compression of concrete against column face,

   iii)   treats multiple bolt rows.

Xiao et al [1-31] carried out a series of tests on composite connections. In one of the series, flush end plates with multiple row of bolts in tension were used (specimens SCJ3, SCJ4, SCJ5 and SCJ6). The amount of reinforcement was varied. This type of joint gave comparatively high moment resistance with the rotation capacity ranging from 23 mrad to 46.9 mrad. Fracture of reinforcing bars dis not take place in all specimens. This confirmed the assumption that redistribution of internal forces takes place and hence additional resistance is contributed by the steelwork connection. In two specimens (SCJ4 and SCJ 6) in which the web and plate are stiffened respectively, shear stud failure was noted.

1.3.2 Initial stiffness of composite connections

For the steelwork components in a composite connection, the method in the revised Annex J of EC3[1-17] is applicable. The initial stiffness $S_{j,ini}$ is derived from the elastic stiffness of the joint components each represented by a spring. The relationship between force and deformation of this spring is given by:

$$F_i = k_i E \Delta_i \qquad (1.11)$$

where F_i is the force in the spring i,

k_i is the stiffness coefficient of the component i

E is the modulus of elasticity of steel

Δ_i is the deformation of the spring i.

An example of spring model for a beam-to-column composite joint, where the tensile force in the joint is resisted by a single layer of reinforcement bars, is given in Fig. 1-12. Subscripts 1, 10 and 11 represent, respectively, the components column web in shear, longitudinal reinforcement bars in tension and unstiffened column web in compression.

The force in each spring is equal to F, and z is the distance between the centre of tension and the centre of compression. The moment M_j acting in the spring model is equal to Fz. The rotation ϕ_j in the joint is equal to $(\Delta_1 + \Delta_{11} + \Delta_{10})/z$. The initial stiffness $S_{j,ini}$ is then calculated by the following expression:

$$S_{j,ini} = \frac{M_j}{\phi_j} = \frac{Fz}{\dfrac{\Delta_1}{z} + \dfrac{\Delta_{11}}{z} + \dfrac{\Delta_{10}}{z}} = \frac{Fz^2}{\dfrac{F}{E}\left(\dfrac{1}{k_1} + \dfrac{1}{k_{11}} + \dfrac{1}{k_{10}}\right)} = \frac{Ez^2}{\sum \dfrac{1}{k_i}} \qquad (1.12)$$

The spring model can also be adapted for both cases of multi-layers of reinforcement and multi bolt-rows in tension belonging to steelwork connection (Fig. 1-13). The layers of reinforcement are assumed to behave like bolt-rows in tension, but with different deformation characteristics. The deformations of the column flange in bending, the column web in tension, the end-plate in bending and the bolts in tension (given by k_4, k_5, k_6 and k_9 respectively) are added to form an effective spring for bolt row r, with a stiffness coefficient $k_{eff,r}$ (Fig. 1-13b). An equivalent effective spring with a stiffness coefficient of k_{eq}, acting at lever arm z, is then used to replace the spring for each bolt row (Fig. 1-13c). In order to calculate the initial stiffness $S_{j,ini}$, the term k_{eq} is used in Eqn. (1.12) instead of k_{10}. The coefficient $k_{eff,r}$, k_{eq} and the lever arm z can be determined from the formulae given in Annex J of EC3[1-17].

1.3.3   Classification of composite connection

As in bare steel connections, a similar approach as mentioned in Section 1.1.3 can be used to classify the composite connection according to strength or stiffness.

1.3.3.1 Classification of connection by strength

For classification by strength, the moment resistance of composite connection $M_{j,Rd}$ is compared to the plastic moment resistance of composite beam $M_{pl.Rd}$. The "stress

block" approach may be used to calculate the $M_{pl,Rd}$ of the composite beam. Fig. 1-14 shows a cross-section of a composite beam in hogging region, the relevant situation for classifying a composite joint in a braced frame. A composite connection is only considered as full strength if $M_{j,Rd}$ is equal or greater than $M_{pl,Rd}$. Otherwise it is considered as a partial strength connection.

1.3.3.2 Classification of connection by stiffness

The initial stiffness of the composite connection, $S_{j,ini}$, is compared to the boundaries for rigid and pinned connections expressed in terms of the beam stiffness (Fig. 1-8(a) and Fig. 1-8(b)). However the classification as rigid, semi-rigid or pinned depends on the value of either the cracked or uncracked flexural rigidity I_b of the connected beam. Normally cracked values is used in hogging moment regions because of the tendency of concrete to crack. Thus the cracked approach may be thought to be more appropriate. However, the cracks do not usually extend over the full length of the beam. Moreover, if the cracked stiffness is used it is more likely that the connection will be classified as rigid. This is because smaller value of the second moment of area is used. Compared to the alternative of a cracked stiffness, the uncracked value would therefore provide a more stringent design criterion[1-9].

1.4   Rotation capacity

As mentioned before, the key elements of moment-rotation characteristics are stiffness, moment resistance and rotation capacity. However, prediction methods are provided only for the stiffness and moment connection by EC3[1-4] and the revised Annex J of EC3[1-17]. The rotation capacity of a connection depends on the deformation response

of individual joint component and also the lever arm between these components. The deformation capacity is influenced by the length and ductility of the reinforcing bars and also the tension stiffening effect of concrete between cracks. A method to predict rotation capacity of each connection was described by Anderson and Kornenberger in a COST-C1 Publication [1-18]. It was based on the CEB-FIP model[1-32] of simplified stress-strain relationship of embedded reinforcing steel (Fig. 1-15), which is used to determine the elongation Δ_u between the centre-line of the column and the first shear connector on the beam. In Fig. 1.15, the following definitions apply :

σ_{sr1} is the reinforcement stress in the crack, when the first crack has formed,

σ_{sm} is the reinforcement stress in the crack, when the stabilised crack pattern has formed,

f_{yk} is the characteristic yield strength of reinforcement,

f_{tk} is the ultimate tensile strength of reinforcement,

ε_{smu} is the ultimate average strain of the embedded reinforcement,

ε_{su} is the ultimate strain of the unembedded reinforcement.

Fig. 1-15 enables Δ_u to be calculated when the rebars reach their ultimate strain, taken as the strain at maximum strength. Good agreement between the method and the test results for beam-to-column connection has been demonstrated[1-33].

The prediction method for rotation capacity extracted from Ref.[1-18] is summarised below. It makes use of the deformation of the shear connectors[1-34, 1-35] as well as the rebars.

Let K_{sc} be the translational stiffness of the shear connection defined by (refer to Fig.1-16) :

$$s = F_t / K_{sc} \tag{1.13}$$

where F_t is the design tension force slab and s is the slip at the steel-concrete interface close to the joint. The design moment at the composite joint, M is given by:

$$M = S_{j.ini}\phi + F_t h_s \qquad (1.14)$$

where $S_{j,ini}$ is the initial stiffness of the steelwork connection and h_s is the lever arm for the tension force. In addition the elongation Δ_s of the slab reinforcement is given by:

$$\Delta_s = F_t / K_s \qquad (1.15)$$

where K_s is the translational stiffness of the reinforced slab in tension, while the rotation ϕ of the composite joint is given by:

$$\phi = (\Delta_s + s) / h_s \qquad (1.16)$$

Combining the relationships for s, Δ_s and ϕ, the relationship for the moment becomes:

$$M = S_{j.ini} \phi + K_s h_s^2 \; \frac{1}{1 + K_s / K_{sc}} \cdot \phi \qquad (1.17)$$

Hence it can be seen that the effective stiffness of the slab is reduced by the factor:

$$\frac{1}{1 + K_s / K_{sc}} \qquad (1.18)$$

The stiffness K_{sc} for the shear connection is determined by elastic interaction theory and is given by:

$$K_{sc} = \frac{N k_{sc}}{\beta - \dfrac{\beta - 1}{1 + \alpha} \cdot \dfrac{h_s}{d_s}} \qquad (1.19)$$

where d_s is the distance between the line of action of the tension resistance of the slab to the centroid of the beam's steel section, and:

$$\alpha = \frac{E_a I_a}{d_s^2 E_s A_L} \qquad (1.20)$$

$$\beta = \sqrt{\frac{(1 + \alpha)N k_{sc} / d_s^2}{E_a I_a}} \qquad (1.21)$$

l is the length of the beam in hogging bending adjacent to the joint. k_{sc} is the stiffness of one connector - for a 19 mm diameter headed stud it may be taken as 100 kN/mm.

Knowing the stiffness of one connector (k_{sc}), the end slip, $s^{(A)}$, can then be determined. The force $F_s^{(A)}$ is then obtained from this slip and the stiffness of the shear connection K_{sc}.

At ultimate strain of rebars

$$F_s^{(B)} = A_s f_{us} \qquad (1.22)$$

The end slip may be assumed that

$$s^{(B)} = 2 s^{(A)} (Fs^{(B)} / F_s^{(A)}) \qquad (1.23)$$

Assuming that the centre of rotation is at the centre of the compression flange, the rotation capacity of the tension region is given by:

$$\phi_c = \frac{\Delta_u + s^{(B)}}{h_s} \qquad (1.24)$$

1.5   Composite Beam

It can be seen that classification of joint behaviour is related to that of the beam, and joint performance is influenced by beam components, such as the shear connection. The term composite beam is applied to steel beam for which continuity with a concrete or composite slab is preserved along their horizontal interface by the use of shear connectors. The most popular type of shear connector is the headed stud, welded through the deck as rapid process. The commonest size in building is the stud 19 mm in diameter and 100 mm long before welding. Studs with diameter exceeding 19 mm become significantly more expensive and difficult to weld[1-8]

Composite action increases load bearing resistance and stiffness, thus enabling a significant savings in steel weight and in construction depth[1-36]. The ultimate strength of a composite section may be dependent upon the interaction capacity of the shear connectors joining the slab to the beam.

Slip at the interface between the slab and the steel section is usually inevitable. This leads to the situation of ultimate strength as the possible limitation of which the force which can be developed in the rebars because of the limited shear connection. If the shear connection limits the flexural strength in this way, the beam is said to have "partial shear connection" [1-37]

1.5.1 Degree of shear connection

In order to determine the influence (if any) of the shear connectors, it is necessary to know their resistance. The main source of data on resistance of shear connectors are from various types of 'push-out' tests. They provides the relationship between shear force transmitted, P, and the slip at the interface, s. The load-slip relationship is influenced by many variables, including[1-8]:

- number of connectors in the test specimen,
- mean longitudinal stress in the concrete slab surrounding the connectors,
- size, arrangement, and strength of slab reinforcement in the vicinity of the connectors,
- thickness of concrete surrounding the connectors,
- bond at the steel-concrete interface,
- strength of the concrete slab.

BS5950:Part 3.1[1-7] differentiates between the design resistance of shear connectors, depending upon the region they are placed; 60% of characteristic strength in a negative moment region and 80% of characteristic strength given in Table 1-3. In EC4[1-5] no distinction is made between these two cases. Table 1-3 is applicable only when the stud material has particular properties (a minimum ultimate tensile strength of 450 N/mm^2 and an elongation of at least 15%).

In EC4[1-5] a different arrangement of push-out test is described,, incoporating greater amount of reinforcement and size of slab. The results obtained are less influenced by the splitting of the slab. As a result the EC4 methods gives better predictions for the behaviour of connectors in composite beam[1-38].

Although partial shear connection is an attractive method of design, because the number of shear connector provided can be related to applied moment rather than to moment resistance of the beam[1-8], it is allowed in most design codes only for the positive moment region.

Partial shear connection is not permitted in negative moment regions because of the concerns about the deformation capacity of the shear connectors in the zone of cracked concrete. The degree of shear connection is calculated by comparing the number of shear connectors provided to the number required based on tensile resistance of reinforcement. Following EC4[1-5]:

$$\frac{N}{N_f} = \frac{N\,P_{Rd}}{A_r f_{y,s}} \tag{1.25}$$

where,

N/N_f is the degree of shear connection

N is the number of shear studs provided

N_f is the number of shear studs required for full shear connection

A_r is the area of reinforcement

$f_{y,s}$ is the yield strength of reinforcement

P_{Rd} is the design shear resistance of each shear stud determined from

$$P_{Rd} = \frac{0.8 f_u \left(\frac{\pi d^2}{4}\right)}{\gamma_v} \tag{1.26}$$

or

$$P_{Rd} = \frac{0.29 \alpha d^2 \sqrt{(f_{ck} E_{cm}}}{\gamma_v} \tag{1.27}$$

whichever is smaller,

where

d is the diameter of the shank of the stud

f_u is ultimate tensile strength of stud but not greater than 500 N/mm^2

f_{ck} is the characteristic strength of concrete

E_{cm} is the secant modulus of concrete

$\alpha = $ $0.2[(h/d) + 1]$ for $3 \leq h/d \leq 4$;

$\alpha = $ 1 for $h/d > 4$,   and

h is the overall height of the stud

Partial shear connection arises if $N \, / \, N_f$ is less than unity.

Tests on composite connections with partial shear connection were carried out by Najafi [1-39] and have showed that both the stiffness and moment capacity were lower when compared to the full shear connection design. In one of the specimen with partial shear interaction failure by crushing of concrete around the shear connectors was observed. Law[1-40] investigated the effect between uniformly distributed and non-distributed shear connectors to the composite connection. His research showed that the different interaction between steel beam and slab moderately affects early response of the connection but significantly affected the connection response in the non-linear phase.

1.5 Slim floor construction

In the last ten years an innovative and economical method of constructing floors using beams, known as 'top' hat(also commonly referred to as 'hat beam')[1-41], has been developed in the Scandinavian countries. In these countries this form of construction

has dramatically increased the market share for steel framed multi-storey buildings. By adopting the same basic concept of 'top' hats various other systems are proposed and developed to suite local construction practice[1-42, 43, 44].

The 1990's saw the development of this approach into what is known as 'slim floor' construction, offering further benefits in addition to composite construction. Slim-floor construction is now making an impact into the market for multi-storey buildings[1-41, 1-45]. "Slim floor" is characterised by the supporting floor beam being contained within the depth of the floor deck. Various form of slim floor system are illustrated in Fig. 1-17, with Fig. 1-17(f) showing system that had been adopted in the UK [1-46] by November 1991. Several useful publications related to UK slim floor practice are available[1-41, 1-46]. A very recent development in the slim floor construction is the use of an Asymmetrical Beam (ASB)[1-47].

The slim floor composite system enables relatively long spans to be achieved with low construction depth. Other advantages include inherent fire protection and greater stiffness.

Research has been conducted on this form of construction to justify the proposed method of design within the UK. To date the work has been carried out with reference to simply supported beams. However, due to the overall slenderness of the system, this approach may not lead to the most economical solution since serviceability deflections can control the design. Substantial further improvement of the structural behaviour may be possible by understanding the joint action and by use of the inherent semi-continuity in the frame construction[1-48,1-49]. In a slim floor system the beam and joint may be encased by concrete and this will enhance the stiffness of the joint.

1.7 Concrete encasement of steel section

It has been recognised that the encasement of a steel beam in concrete would enhance the structural performance. An early code of practice[1-50] permitted the beam to be designed as a composite member if sufficient reinforcement was included to prevent spalling of concrete and a certain minimum dimension of encasement was also provided. Although such encasement may result in an economical design, this requires bonding and transfer of stress between the two dissimilar materials[1-51] of steel and concrete. In EC4[1-5], it is not allowed to take into account any reinforced concrete between the flanges of the steel beams with concrete-encased webs for the load bearing resistance and for deflection calculation. Kindmann et al[1-52] test have, however, indicated that the reinforcing bars and the concrete between the flanges influenced the calculation of the ultimate bending moment, the ultimate shear force and deflection.

Lawson et al [1-47] recognised the effects of composite action of the in-situ concrete with the steel section in developing the new asymmetric beam section for Slim-flor construction. The effects are to :

- increase the bending resistance of the steel section
- increase the stiffness, which reduces deflection of the beam
- provide inherent fire resistance and composite action in fire.
- increase shear resistance of the section, especially at opening.

Lawson et al[1-47] also acknowledged that the composite action of encased steel sections depends on the shape and size of the steel section, and on the use of any shear connection devices or embossment.

At any stage of loading, the horizontal shear that develops between a concrete slab, or encasement, and the steel beam needs to be resisted if the composite section is to act monolithically. Although the bond force and the frictional force that developed between the concrete slab and steel beam can be significant, they may be relied upon to provide the required interaction. The state of knowledge developed in traditional systems (concrete slab connected to the top flange of I-shaped steel beam) may not be adopted to the slim floor system directly. The fact that the beam is encased in concrete may influence both the interactions and the flexural behaviour[1-51].

It is clear from the research previously referenced that there is currently considerable interest in utilising bond and friction in the composite design of encased sections and to improve the bond capacity of encased beams by introducing one of of several types of 'shear enhancer'.

1.7.1 Related previous research on the bond strength

Many early tests referred to by Hawkins[1-53] have shown that the bond between the concrete and the steel section controls the behaviour of the encased beam. Hawkins[1-53] also reported that three limiting stress methods had been proposed by various previous researchers to determine the load at bond failure :

1.   The horizontal shear stress on the section of minimum width passing around the top steel is taken as about one tenth of concrete strength in compression.

2.   The horizontal shear stress per unit length of steel section divided by the perimeter of the steel beam is taken as about 170 psi (1.17 N/mm^2)

3.   The value of rate of change in axial force divided by the perimeter of steel section as 100 psi (0.7 N/mm^2).

In EC4[1-5] no application rules are given for the contribution of concrete encasement of a steel section to resistance in bending or vertical shear. However depending on types of encasement, EC4[1-5] state the average bond strength, due to bond and friction, should be taken as between 0-0.6 N/mm^2 in the design of composite columns.

Roik and Bergmann[1-54] also recognised that an exact determination of the bond stress due to applied loading is hardly possible. However they suggested a method to estimate this strength on the basis of elastic theory assuming uncracked concrete.

Roeder[1-51] reported studies by Bryston and Mathey on the typical push-out tests as shown in Fig 1-18. In the these studies, W14 steel sections were used with an embedded length of 607 mm and with tie reinforcement around the concrete core. Bond was permitted at the flanges only by applying foamed material to the web. The determination of an average bond stress was by averaging the applied load over the contact area. The average maximum bond stress was found to be in the range of 2.1 to 3.4 N/mm^2.

In the tests carried out by Roeder[1-51], W6 and W8 steel sections were used. The length of embedment varied between 590 mm to 890 mm. Concrete strength varied between 17.2 N/mm^2 and 48.2 N/mm^2. Except in one case, all the specimens failed by "full slip" i.e. the position of the steel section relative to the concrete encasement changes. No significant concrete cracking was observed even for the specimens with no tie reinforcement around the steel section. The average maximum bond stress recorded was between 0.6 N/mm^2 and 1.6 N/mm^2. However if the average was based on the flange perimeter only, a bond strength of 1.0 N/mm^2 to 2.5 N/mm^2 resulted. Roeder also evaluated the effect on the bond stress distribution in a specimen which has already slipped. He found that prior slip affects the bond stress distribution. It reduced the ultimate load capacity by 28 to 45%.

Twenty two specimens of W6, W8 and W10 sections were used by Hawkins[1-53] in his push-out experiments. The length of embedment varied between 0.1 m to 0.51 m. Both lightweight and normal weight concrete were used in the studies. Bond stresses in the range of 0.7 to 1.1 N/mm^2 were recorded. If the hypothesis that flanges contributed the majority of bond capacity was applied to Hawkins's experiments[1-53], the bond stress increased to between 1.3 N/mm^2 and 2.1 N/mm^2. Hawkins concluded that longer embedment resulted in smaller average bond stress and increase in concrete reinforcement had little effect on the maximum bond stress. However significant improvement of bond capacity after slip was noted.

The previously-referenced research related to encasement of asymmetric beam sections [1-47]. One objective of the testing was to determine the appropriate shear bond strengths and the effective perimeter around the section for this action. Both dynamic

and static load were applied in the test. The results from the dynamic testing indicated that the shear bond resistance was not adversely affected by this cyclic action. Shear bond strength in the range between 0.85 to 1.28 N/mm^2 was recorded.

1.8   Local Buckling and Section Classification

One effect of concrete encasement is to reduce the likehood that local buckling will affect the resistance of a beam[1-5]. Fig 1-19 shows two modes of flange and web local buckling failure. It normally occurs when component plates of the section distort out-of plane, but with the straight-line junctions at the intersections remaining straight.

Most steel structural members are in effect assemblies of thin plate elements, and so are prone under stress (possibly below the yield point of the material) to instability by buckling locally within each element. Local buckling is encouraged when there are localised distortions in compression flanges and/or the web, with the half-wave length of the buckle being of the order of the depth or width of the section [1-35, 1-55]. Local buckling is different from distortional buckling[1-56] and lateral buckling[1-57]. In distortional buckling the local and overall buckles interact while in lateral buckling no distortion of cross-section occurred and the mode is an overall one. With hot-rolled sections usually no immediate failure takes place when local buckling arises as there is a useful amount of deformation capacity available before the bending resistance of the section falls below the plastic moment[1-58]. Research on local buckling of steel beams has resulted in the establishment of flange proportions that guarantee that local flange buckling does not occur prior to the onset of strain hardening [1-59, 1-60].

As far as stability of composite beams in the hogging moment region is concern, local buckling (as in steel beams) has been identified as one of the problems. Due to the presence of reinforcing bars the level of the neutral axis always shifts toward the concrete slab. Hence, for any given rotation, the compressive strains in the steelwork are proportionately higher. When a composite beam is designed as continuous, local buckling of steel elements in compression often occurs in the negative (hogging) moment region (adjacent to the supports). Unlike the sagging region shear connectors and concrete may not provide direct restraint to the steelwork against this mode of buckling. The beam hogging moment of resistance may be reduced due to premature local buckling and the attainment of a plastic collapse mechanism in the beam may be prevented by the reduction of rotation capacity[1-25, 1-27].

The adverse effect that local buckling has on rotation capacity of steel beam is well known[1-61]. Sufficient rotation capacity is needed for the formation of collapse mechanism in the hogging regions if the beams are to be designed plastically. The development of a complete mechanism presumes a certain deformation capacity in the plastic hinges that are first to form. For full redistribution of bending moments in the structure the first hinges must be able to rotate without losing the moment resistance of the hogging region[1-57]. Rotation capacity can be defined as the ability to deform and to rotate at a critical cross-section while sustaining the expected moment resistance of the region. Among the parameters that govern rotation capacity are[1-57] the flange slenderness, the web stiffness and the steepness of the moment gradient.

Tests to determine the effect of local buckling on rotation capacity of composite beams under negative bending have been carried out[1-61, 1-62, 1-63]. Kemp and Dekker[1-

62] concluded that there is no clear justification for a difference in the local buckling provisions for steel and composite beams. The effectiveness of a continuous composite beam is largely dependent on avoiding premature local and lateral buckling of the bottom compression flange of the steel section so that the fully plastic moment can be developed and maintained as a ductile plastic hinge develops[1-64]. From theoretical and experimental studies on local buckling of composite beams in the hogging moment region Hamada and Longworth [1-65] had concluded that:

- The ultimate moment resistance of composite beams in negative bending is affected by local flange buckling unless a cover plate is used to stiffen the compression flange.

- An increase in the flange width:thickness ratio would decrease the bending resistance significantly.

- Local flange buckling is slightly affected by the amount of reinforcement and span length.

Local buckling may be eliminated from further consideration in design by restricting the ratio of width-to-thickness of the steel section's element. In the UK , BS 5400:Part 3 [1-66] was the first to define explicitly a cross-section as either compact or non-compact by fulfilling certain slenderness provisions. Compact sections are defined as those which can develop the full plastic moment before local buckling occurs and are able to sustain it after.

Design codes[1-3, 1-4, 1-5] commonly use a set of classifications based on limiting proportions of cross-sections. The cross-sections of steel sections are placed into four classes namely, plastic, compact, semi-compact and slender respectively. Table 1-4

shows the classification of the section based on maximum width-to-thickness ratios. The classifications are done separately for the flange and the web but in reality they interact. Codes also identify conditions for global analysis of the structure (see Table 1-5) either involving elastic analysis, or elastic analysis with specified limits of moment redistribution, or plastic analysis[1-60]. Present ideas regarding the behaviour of continuous composite beams are based on test results by Climenhaga and Johnson [1-61]. Slenderness limits were defined for the flange and web to ensure the availability of ductility to allow plastic global analysis. Hope-Gill[1-67] performed computer simulation to determine limits of allowable moment redistribution as a function of section slenderness. These limits formed the basis of the EC4 requirements.

EC4 [1-5] defined the four classes as follows :

Class 1 - The plastic sections are those which can form a plastic hinge with sufficient rotation capacity allowing for plastic analysis to be applied.

Class 2 - The compact sections are those which can develop their plastic moment resistance but with limited rotation capacity.

Class 3 - The semi-compact sections are those in which the calculated stress in the extreme compression fibre of the steel member can reach its yield strength, but local buckling is liable to prevent development of the plastic moment resistance.

Class 4 - The slender sections are those in which it is necessary to make explicit allowances for the effects of local buckling when determining their moment resistance or compression resistance.

Fig 1-20 demonstrates the effect of local buckling on each of class of section.

An approach known as "hole-in-web" method[1-5] can be used effectively to upgrade from Class 3 web to Class 2, but not allowed to upgrade to Class 1. The method discounts the portion of the web that do not participate in bending (Fig. 1-21).

1.9   Framing type

The inherent stiffness of composite elements has a beneficial effect on frame deflection, but application to unbraced frames is not well-established. For unbraced bare steel frames, control of sway deflection at working load may well govern design of the frame.

1.9.1   Unbraced frame

In unbraced frames, the lateral stiffness is provided by the flexural rigidities of the beams and columns, connected by moment-resisting joints. Thus some degree of continuity is essential for the overall stability of the frame. The detailing of the connection may be expensive to ensure the frame stability. However unbraced frames offer more flexibility in architectural planning than braced construction[1-68].

Although design based on plastic analysis promises greater economy than use of elastic methods, this economy often cannot be realised in unbraced frames. This is because control of sway deflection at service load governs the design of many such structures[1-69]. The basic effect of sway under the lateral load[1-70] is to reduce the moment at a windward connection from the value initially reached under gravity load, while the connection on the leeward side is more heavily loaded.

In designing unbraced frames, both the ultimate strength and the recommended limits under service load for horizontal deflection or sway need to be satisfied. Fig 1-22[1-71] indicated the limit recommended by EC3[1-4]. It is important that member sections are selected in some optimum manner, to compensate to some extent for the very stiff construction needed to resist sway.

One of the popular methods for the design of low-rise unbraced frames is the 'wind moment method'[1-72]. For the purpose of analysis and design the members are assumed to be pinned-ended under gravity load and thus have only designed to transfer 'eccentricity' moment to column. Under horizontal load the connections are considered as rigid. The resulting joints are in reality relatively flexible in construction[1-73, 1-74].

Fig. 1-23 illustrates the effect of connection flexibility on the behaviour of unbraced multi-storey frames studied by Gerstle[1-72]. Figures 1.23(b) - (e) show column moment and deflected shape of the frames, for four different beam-to-column connection stiffness. Increase in connection stiffness changes the response of the frame from flexural cantilever behaviour to the shear type response. He noted two effects of the rotational connection flexibility on unbraced frames :

- The joint rotation contributes to the overall frame deformations, in particular the frame sway under lateral load.
- The joint rotation will affect the distribution of internal forces and moments in beam and columns.

Anderson and Islam[1-75] developed optimal design formulae to limit sway by means of subframes of beams and columns (see Fig. 1-24). Three assumptions were made. Firstly, vertical loads are assumed to have negligible effect on horizontal deflections.

Secondly, a point of contraflexure is taken to exist under horizontal loading at the mid-height of the column (except in the bottom storey) and at the middle length of each beam. The third assumption was to divide the total horizontal shear between the bays in proportion to their relative width.

Very promising results were obtained when tested against "exact" analysis, even for frames which did not have equal bay widths or storey heights. However, the assumed points of contraflexure, together with a given sway index, would not themselves produce expressions for direct design. The extra device which made this possible was that of minimising the summation of (second moment of area x length) for the members in any storey - a form of approximate minimum weight design.

To tackle the same problem, Wood and Roberts[1-76] invented a graphical method (Fig. 1-25) of predicting side sway in the design of multi-storey building. A substitute frame concept (Fig. 1-26) was used as the basis for that method. To use the analysis, each storey of the actual frame must be replaced by an equivalent structure having the form of Fig. 1-26. The actual frame was transformed into a substitute beam-column structure, as shown in Fig. 1-27.

From Fig. 1-26 the moment M_{bt} in the top beam at the beam-column junction is given by slope-deflection as:

$$M_{bt} = \frac{4EI_{bt}}{L_t}\theta_t \qquad (1.28)$$

From Fig. 1-27 for the typical beam AB in the actual frame with end rotations $\theta_A = \theta_B$, slope-deflection gives

$$\text{end moment} \quad = \quad \frac{2EI_b}{L}(2\theta_A + \theta_B) = \frac{6EI_b}{L}\theta \qquad (1.29)$$

The basis of substitute frame is that[1-77] :

(i)   for horizontal loading on the real frame, the rotation of all joints at any one level are approximately equal, and

(ii)   each beam restrains a column at both ends.

Therefore from Eqn.(1.28) and Eqn.(1.29), the beam's inertia in the substitute frame should be based upon $(6/4) I_b = 1.5 I_b$. It follows from (ii), that the total stiffness of K_b of a substitute frame is

$$K_b \quad = \quad \Sigma(2 \times 1.5 I_b/L) \quad = \quad \Sigma(3I_b/L) \qquad (1.30)$$

For the substitute column, the stiffnesses are summed:

$$K_c \quad = \quad \Sigma(I_c/h) \qquad (1.31)$$

By analysing the frame using the stiffness distribution method suggested by Wood[1-77], Wood and Roberts[1-76] were able to develop the chart shown in Fig. 1-25, in which

$$k_t = \frac{K_c + K_u}{K_c + K_u + K_{bb}} ; \qquad k_b = \frac{K_c + K_l}{K_c + K_l + K_{bb}} \qquad (1.32)$$

where k_t and k_b are distribution coefficient, suffices u and l refer to upper and lower adjacent column stiffness, and K_{bt} and K_{bb} are the top and bottom beam stiffness of that storey, in all cases for the substitute frame. The method has the advantage that through use of substitute frames it deal more easily with frames with some irregularity.

1.10 Scope and Purpose

The main objective of this present work is to study a number of aspects of continuity in steel and composite buildings, and in particular the connections. The review of previous research shows that further work is justified in order to realise in practice the benefits of continuity and composite action in frames.

(1)   *Tests on beam-to-beam composite connections*

In normal practice the composite floor will typically span 3 m while columns will be spaced on grid of at least 6 m. Thus the floor will be supported by secondary beams which then transfer the load to primary beams. It is necessary to develop moment in beam-to-beam connections to benefit from continuity throughout the frame. For the above purposes, a series of beam-to-beam connection tests was conducted by the present author. These tests and their assessment form a substantial part of this thesis.

(2)   *Tests on encased end plate joints for slimflor beams*

Established methods for slim-floor apply to simply supported beams. Further economic benefits can be achieved if the beam can be designed as semi-continuous. Tests were carried out on three encased and two bare steel end plate connections to determine whether the encasement provided in the slim-floor construction affected the connection's response in a beneficial way.

(3)   *Push-out tests*

There is currently considerable interest in recognising and improving the bond capacity of encased beams, including introduction of 'shear enhancers'. A total of six push-out test were performed and the suitability of such innovations is assessed and appraised.

(4)   *Local buckling*

Continuity has the disadvantage that composite beams become prone to local buckling in the negative moment region. The adverse effect that local buckling has on rotation capacity of steel beam is well-known. Ideally the proportion of composite sections should be chosen so that they are Class 1 or Class 2, but the action of the reinforcement in lifting the neutral axis causes many hot-rolled section to be in Class 3. These can be upgraded to an effective web in Class 2. The author has conducted studies on published data to explore the possibility of up grading section in Class 3 to Class 1.

(5)   *Direct design to horizontal sway limitation*

A method applicable to the design of unbraced multi-storey frames to specified limits on horizontal sway deflection is presented. This method of design results from a combination from the works of Wood and Roberts [1-76] and Anderson and Islam[1-75]. Both rigid and semi-rigid joints may be included in the method. The current method is applicable to bare steelwork only.

References

1-1   Leon, R.T., and Zandonini, R., "Composite Connections", Constructional Steel Design. An International Guide, Ed. Dowling, P.J., Harding, J.E., Bjorhovde, R., Elsevier Applied Science Publishers, London, 1992, pp 501-522.

1-2   Rex, C.O., and Easterling, W.S., "Partially Restrained Composite Beam-To-Girder Connections", Engineering Journal, 4th Quarter 1995. AISC pp 145-158.

1-3   BS 5950. Part 1 1990. "Structural use of steelwork in building: Code of practice for design in simple and continuous construction". British Standard Institution. London.

1-4   EUROCODE 3, "Design of Steel Structure, Part1.1 General Rules and rules for buildings"., Brussels, 1992

1-5   EUROCODE 4, "Design of Composite Steel-Concrete Structures", Brussels, 1992.

1-6   American Institute of Steel Construction, "Load and Resistance Factor Design Specification for Structural Steel Buildings", AISC, Chicago, 1993.

1-7   BS 5950 : Part 3: Section 3.1: 1990, "Design of simple and continuous composite beams". British Standard Institution, London.

1-8   Johnson, R.P., Composite Structures of Steel and Concrete, Volume 1 Beams, Slabs, Columns, and Frames for Buildings. 2nd Edition. Blackwell Scientific Publications, Oxford, UK, 1994.

1-9   Anderson, D., and Brown, N., "Design of composite connection according to ENV 1994-1, Annex J", IABSE 15th Congress Report, Copenhagen 1996. pp 975-983.

1-10   Anderson, D.A., Colson, and A., Jaspart J., "Connections and Frame Design for Economy". New Steel Construction, October 1993, pp 30-33.

1-11   Nethercot D.A., "Steel to column connection- a review of test data." CIRIA, London, 1985.

1-12   Goverdhan A.V., "A collection of experimental moment-rotation curves and evaluation of prediction equation for semi-rigid connection". MSc. Thesis, Vanderbilt University, Nashville, 1984.

1-13   Kishi N., and Chen W.F., "The collection of tests on steel beam-to-column connections." Report CE-STR-86-26, School of Civil Engineering. Purdue University. 1986.

1-14   Morris, G., Huang J., and Scerbo M., "Accounting for connection behaviour in steel frame design", Canadian Journal of Civil Engineering. Vol. 22. 1995. pp 955-969.

1-15   Nethercot, D.A., and Zandonini, R., "Methods of prediction of joint behaviour: Beam-to-column connections. Structural Connections", Stability and strength (ed. Narayanan R.), Elsevier Applied Science, London, 1989, pp 23-62.

1-16   Jaspart, J.P., and Maquoi, R., "Survey of existing types of joint modelling", COST PROJECT C1, Semi-rigid behaviour. October 1992.

1-17   Revised annex J : Joints in building frames. Eurocode 3: Part 1.1. ENV 1993-1-1/pr A2.

1-18   Composite Steel-Concrete Joints in Braced frames for Buildings. (ed. D. Anderson,), European Commission European Cooperation in the Field of Scientific and Technical Research, Brussels,COST-C1,1997.

1-19   Narayanan R., "Design Developments in Long Span Flooring System in the UK", Proceeding of the International Conferences on Steel and Aluminium Structures. Singapore. 1991, pp 11-22.

1-20   Mathys, J.H., "Multi-storey Steel Buildings A new Generation", The Structural Engineer, 65A, No.2 February, 1987. pp 47-51.

1-21   Nethercot, D.A., "Design of Composite Connections", The Structural Engineer, 75, No 13/4 July 1995. pp 218-219.

1-22   Zandonini, R., "Semi-rigid composite joints". Structural connections: Stability and Strength, ed. R. Narayanan. Elsevier Applied Science Publishers, 1989, pp. 63-120.

1-23   Leon, R.T., "Semi-rigid composite construction", Journal of Constructional Steel Research. Vol 15 1990, pp. 99-120.

1-24   Leon R.T., and Ammerman, D.J., "Semi-rigid composite connections for gravity loads", Engineering Journal, AISC, 27(1), pp. 1-11.

1-25   Najafi, A. and Anderson, D., "Composite connection with structural steel end plate", Report to Steel Construction Institute, No.2 to No.4, Department of Engineering, University of Warwick,UK.

1-26   Brown, N. "Aspects of sway frame design and ductility of composite end plate connections", PhD Thesis, University of Warwick, UK, 1995.

1-27   Xio, Y., Nethercot, D.A., and Choo, B.S., "Moment resistance of composite connections in steel and concrete", Constructional Steel Design: World Development., (ed. Dowling, P.J., et.al.), Elsevier Applied Science Dec 1992. pp 331-343.

1-28   Bernuzzi, C., Salvatore, N., and Zandonini, R. "Semi-rigid composite joints: Experimental studies", Connections in Steel Structures II: Behaviour, strength and design conference, Pittsburgh Pennsylvania, USA.

1-29   Bode, H., and Kronenberger, H.-J.: " Behaviour of composite joints and their influence on semi-continuous beams", Proceeding of the Engineering Foundation Conference. Composite Construction III, Irsee, 1996.

1-30   Lawson, R. M., and Gibbons, C., "Moment connections in composite construction: Interim guidance for end-plate connections", The Steel Construction Institute, Publication 143. Ascot, UK.

1-31   Xiao, Y., Nethercot, D. A., Choo, B. S., "Moment resistance of composite connections in steel and concrete", Constructional Steel Design: World Development. (ed. P.J. Dowling et al.) Dec 1992. Elsevier Applied Science

1-32   CEB-FIB mode Code 1990. Comite' Euro-International du Beton, Lausanne, 1990.

1-33   Bode H., Kronenberger H-J, and Michaeli W., "Composite Joints-Further Experimental Results". IABSE Conference: Composite Construction - Conventional and Innovative, Innsbruck, Sept 1997. pp433-438.

1-34   Aribet J.M., "Influence of slip on the shear connection on composite joint behaviour", Third International Workshop on Connections in Steel Structures. Trento, Italy. May 1995.

1-35   Aribet J.M., "Proposed clause J.4.5 in Annex J for EN 1994-1.1", Paper AR 11, Laboratoire de Structure et Mecanique Applique. INSA. Rennes, France. Dec. 1995.

1-36   Lawson R.M., Taylor J.C., Smith D.G.E. "Commentary on BS 5950: Part1:Section 3.1." The Steel Construction Institute . 1993.

1-37   Price A.M., Anderson D. , "Composite Beams", Constructional Steel Design, An International Guide. (ed. Dowling et al). 1992. pp421-442.

1-38   Johnson, R.P., Anderson, D., "Designers' handbook to Eurocode 4: Part 1.1, Design of steel and composite structures". Thomas Telford, London 1993.

1-39   Najafi, A.A., "End plate connections and their influence on steel and composite structures", PhD thesis. University of Warwick. 1992

1-40   Law, CLC, "Planar no-sway frames with semi-rigid beam-to-column joints" Phd Thesis, University of Warwick 1983.

1-41   Mullett D.L., Slim floor design and construction. The Steel Construction Institute. Publication 110, 1992.

1-42   Inha, T., "New composite beams and slab in Finland", Constructional Steel Design: World Development, Elsevier Applied Science. 1992, pp297-306

1-43   Lawson R.M., Owens G.W., Mullet D.L., "Slim floor construction in UK", Constructional Steel Design : World Development. Elsevier Applied Science. 1992. pp317-330.

1-44   Leino T., "Results from two series of tests on typical Finnish steel beam to composite column connections". COST PROJECT C1, Proc. 2nd State of the Art Workshop, Parague, October 1994. pp 165-174.

1-45   Mullet, D.L., and Lawson, R.M., "SlimFloor Construction Using Deep Decking", Publication P127. The Steel Construction Institute. 1993

1-46   Design in Steel 2 Slim Floor Construction. British Steel - Sections, Plates & Commercial Steels.

1-47   Lawson, M., Mullet, D., Rackham, J., "Slimdek: Development and Testing", New Steel Construction, June/July 1997. pp 19-22.

1-48   Bernuzzi C., and Zandonini R., "Design of semi-continuous non-sway composite frames with slim floor beams", 5th International Colloquium on Stability of Metal Structures. Chicago 1996.

1-49   Bernuzzi C., Gadotti F., and Zandonini R., "Joint action in slim floor systems", 4th Pacific Structural Steel Conference. Singapore. October 1995.

1-50   BS117. British Standard Institution.

1-51   Roeder C.W., "Bond stress of embedded steel shapes in concrete", Proc. of the US/Japan Joint Seminar on Composite and Mixed Construction, Washington. July 1984. ASCE. pp227-240.

1-52   Kindmann R., Bergmann R., and Cajot L-G, Schleigh "Effect of reinforced concrete between the flanges of the steel profile of partially encased composite beams. J, Construct. Steel Research (27). 1993 pp 107-122.

1-53.   Hawkins N.M., "Strength of Concrete-Encased Steel Beams", Civil Engineering Transaction. Inst. of Eng. Australia 1973. CE15 pp 39-45.

1-54   Roik K., and Bergmann R., "Composite column", Constructional Steel Design : An International Guide. Elseveir Applied Science. 1992. pp 443-470.

1-55   Oehler D.J., and Bradford M.A., "Composite steel and concrete structure member, Fundamental behaviour",. Pergamon, Elsevier Science Ltd. 1995.

1-56   Bradford M.A., and Trahair N.S., "Distortional buckling of I-beam", J. Struct. Div. ASCE Vol. 107, No ST2, 1981, pp 355-370.

1-57   Trahair N.S., and Bradford M.A., "The behaviour and design of steel structures", Chapman and Hall, London. 1988.

1-58   Kuhlmann U., "Definition of flange slenderness limits on the basis of rotation capacity values", J. Construct. Steel Research. 14 1989. pp21-40.

1-59   Haaijer G., and Thurlimann B., "Inelastic buckling in steel" Transactions, ASCE Vol. 125, No 3023, 1960. pp 308-344.

1-60   Lay M.G., "Flange local buckling in wide-flange shapes", J. of Struct. Div. ASCE Vol. 91 No ST6, Proc. Paper 4554, Dec 1965 pp 95-116.

1-61   Climenhaga J.J., and Johnson R.P., "Local buckling in continuous composite beams", The Structural Engineer. No 9 Vol. 50 Sept. 1972. pp 367-374.

1-62   Kemp A.R., and Dekker N.W., "Available rotation capacity in steel and composite beams.", The Structural Engineer. Vol. 69, No 5, March 1991. pp 88-97

1-63   Bradford M.A., and Gao Z., "Distortional buckling solutions for continuous composite beams.", Journal of Structural Engineering. ASCE. Vol 118. No 1. January 1992.

1-64   Kemp A.R., Trechero P., and Dekker N., "Ductility effect of end details in composite beams.", Composite Construction in Steel and Concrete II, Proceedings of an Engineering Foundation Conference, ASCE, Potosi, June 1992, pp 413-428.

1-65   Hamada S., and Longworth J., "Buckling of composite beams in negative bending.", J. of Struct. Div. ASCE. No ST11 1974 pp 10917-2221.

1-66   BS 5400. "Steel, concrete and composite bridges." British Standard Institution, 1979.

1-67   Hope-Gill M.C., "Redistribution in composite beam." , The Structural Engineer. Vol57B No1. March 1979, pp 7-10.

1-68   Chen W.F., and Lui E.M., "Beam-to-column moment-resisting connections.", Steel Framed Structures : Stability and Strength. (ed. Narayanan R.) Elsevier Applied Science Publishers, London, 1985

1-69   Anderson D., and Lok T.S., "Design studies on unbraced, multi-storey frames.", The Structural Engineer, Vol. 61B, No2, June 1983, pp 29-34.

1-70   Cunningham R., and Taylor C., "Practical design allowing for semi-rigid connections.", Connections in Steel Structures II: Behaviour, Strength, and Design. Proc. AISC April 1991. pp 380-390.

1-71   Essentials of Eurocode 3, "Design Manual for Steel Structures in Building.", ECCS No65, 1991.

1-72   Gerstle K.H., "Flexibly connected steel frames.", Steel Framed Structures : Stability and Strength. (ed. Narayanan R.) Elsevier Applied Science Publishers, 1985. pp 205-239.

1-73   Joints in Simple Construction Volume 1: Design Methods., The Steel Construction Institute, Ascot 1990.

1-74   Joint in Simple Construction Volume 2: Practical Application., The Steel Construction Institute, Ascot 1992.

1-75   Anderson, D., and Islam, M.A., "Design of multi-storey frames to sway deflection limitations.", The Structural Engineer, 57B(1), pp 11-17.

1-76   Wood, R.H., and Robert, E.H., "A graphical method of predicting side-sway in the design of multi-storey buildings.", Proc. ICE, Pt 2, 59, 1975. pp353

1-77   Wood R.H., "Effective lengths of columns in multi-storey buildings.", Structural Engineer, 52(7),pp235-244, (8),pp295-302, (9),pp341-346.

Table 1-7[1-30] : **Summary of tests on composite connections carried out at the University of Warwick.**

Connection Type	Bar Rein- forcement %	Test Moment kNm	Rotation at Failure mRad	Connection Moment Resistance kNm		Composite Beam Negative Resistance kNm	Test Theory (With Bolts)	Failure Mode
				With Bolts	No Bolts			
Flush end plate 305 UB	Steel only	105	56	64	·	173	1.64	Yielding of column flange
	0.55	179	27	150	86	221	1.19	Fracture of rebars + mesh
	1.1	262	36	219	202	248	1.20	Fracture of rebars + mesh
	1.65	302	56	264	303	271	1.14	Local buckling of beam flange
Extended end plate 305 UB	1.1	291	40	248	202	248	1.17	Local buckling of beam flange
Flush end plate 457 UB	1.1 (8T12)	416	14	328	276	451	1.27	Fracture of rebars + mesh
	1.0 (4T16)	390	47	295	211	450	1.32	Fracture of rebars + mesh

Notes:
1. The reinforcement consisted of bars and A142 mesh. The mesh reinforcement is neglected in the calculation of the moment resistance of the connection and the beam.
2. The connection moment resistance includes the tensile action of the bolts. The corresponding value without the tensile action of the bolts is also given.
3. The beam moment resistance is that in negative bending including the bar reinforcement.
4. The first six tests were carried out using a 305 × 165 UB 40 in S275 steel. The last two tests were carried out using a 457 × 152 UB 52.

Table 1-2[1-30] :   *Tests on flush end plate composite connection*

Reference	Test Ref	Beam	Reinforcement (Bar and Mesh) %	Connection Moment Resistance		Test Moment kNm	Test Theory With Bolts	Test Theory Without Bolts
				With Bolts	Without Bolts			
Xiao, Nethercot & Choo[13]	SCJ3	305x165UB40	0.2	102	29	86	0.84	2.97
	SCJ4	305x165UB40	1.0	226	195	201	0.89	1.03
	SCJ5	305x165UB40	1.0	226	195	241	1.06	1.24
	SCJ6	305x165UB40	1.2	202	156	158	0.78	1.01
	SCJ7	305x165UB40	1.0	226	195	205	0.90	1.05
	SCJ15	305x165UB40	1.0	202	156	186	0.92	1.19
Li, Nethercot & Choo[20,21]	CJS-1	254x102UB25	0.90	159	120	181	1.14	1.51
	CJS-2	254x102UB25	0.90	159	120	173	1.09	1.44
	CJS-3	254x102UB25	0.90	159	120	149	0.94	1.24
	CJS-4	254x102UB25	0.90	159	120	160	1.01	1.33
	CJS-5	254x102UB25	0.90	159	120	195	1.23	1.63
	CJS-6	254x102UB25	0.90	159	120	174	1.10	1.45
Puhak, Smotlak & Zandonini[17]	SJB10	IPE300	0.71	148	132	209	1.43	1.58
	SJB14	IPE300	1.21	250	187	261	1.05	1.40
Law & Johnson[16]	JX1	457x191UB67	0.72	313	257	354	1.13	1.38
	JX2	457x191UB67	0.72	313	257	370	1.18	1.44
	JY1	457x191UB67	0.72	313	257	384	1.23	1.49
	JC1	457x191UB67	0.72	313	257	449	1.43	1.75
	JC2	457x191UB67	0.45	410	319	530	1.29	1.66
Anbert & Lachal[17]	A2	IPE360	0.53	215	119	296	1.38	2.49
	A3	HEA200	0.53	108	74	152	1.41	2.05
	A4	IPE360	0.53	215	119	297	1.38	2.49
	C1	IPE360	0.74	249	166	344	1.38	2.07
	C2	IPE360	0.74	249	166	326	1.31	1.96
	C3	IPE360	0.74	249	166	288	1.16	1.74

Notes: 1.   Reinforcement includes mesh reinforcement in these tests.
2.   The connection moment resistance excludes the tensile action of the bolts. The corresponding value without the tensile action of the bolts is also given.

Table 1-3:   Characteristic resistance (kN) of headed stud shear connectors from BS 5950:Part 3

DIMENSION OF STUD SHEAR CONNECTORS (mm)			CHARACTERISTIC STRENGTH OF CONCRETE (N/mm^2)			
DIAMETER	NOMINAL HEIGHT	AS-WELDED HEIGHT	25	30	35	40
25	100	95	146	154	161	168
22	100	95	119	126	132	139
19	100	95	95	100	104	109
19	75	70	82	87	91	96
16	75	70	70	74	78	82
13	65	60	44	47	49	52

Table 1-4 : Comparison of maximum width to thickness ratios of section

Element	Code	Classification of Section[*]			
		Class 1 Plastic	Class 2 Compact	Class 3 Semi-compact	Class 4 Slender
Outstands[**] of flanges (rolled sections)	EC3 and EC4	10ε	11ε	15ε	unlimited
	BS 5950: Pts1 & 3	8.5ε	9.5ε	15ε	unlimited
(welded section)	EC3 and EC4	9ε	10ε	14ε	unlimited
	BS5950: Pts 1 & 3	7.5ε	8.5ε	13ε	
Webs[***] (bending)	EC3 and EC4	72ε	83ε	124ε	unlimited
	BS5950: Part 1	79ε	98ε	120ε	
	Part 3	64ε	76ε	114ε	
(compression)	EC3 and EC4	33ε	38ε	42ε	unlimited
	BS5950: Part 1	39ε	39ε	39ε	
	Part 3	32ε	38ε	38ε	

Notes:
* $\varepsilon = (275/p_y)^{0.5}$ for BS5950 and $\varepsilon = (235/p_y)^{0.5}$ for Eurocodes
**   Different outstand limit defined for rolled and welded sections
***   Web in bending correspond to neutral axis in mid-depth. Webs in compression correspond to neutral axis in flange.

Table 1-5 :   Classifications of composite beams and condition for global analysis

Section	Moment resistance and mode of failure	Analysis of load effect	Resistance based on
Class 1 Plastic	Failure after resistance maintained over plateau of displacement	Plastic, or elastic with moment redistribution	Plastic resistance moment
Class 2 Compact	Failure after reaching plastic resistance, but no plateau of displacements	Elastic, limited redistribution	Plastic resistance moment
Class 3 Semi-compact	Failure before plastic resistance is reached	Elastic, no redistribution	Stress limit of yield
Class 4 Slender	//	//	Effective section at yield
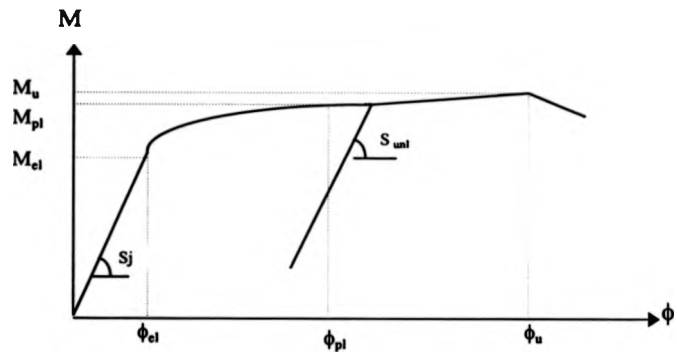
Fig. 1-1 :   Idealised moment-rotation characteristic
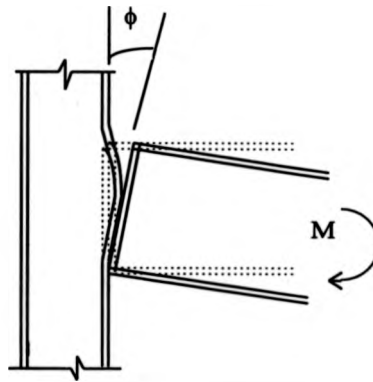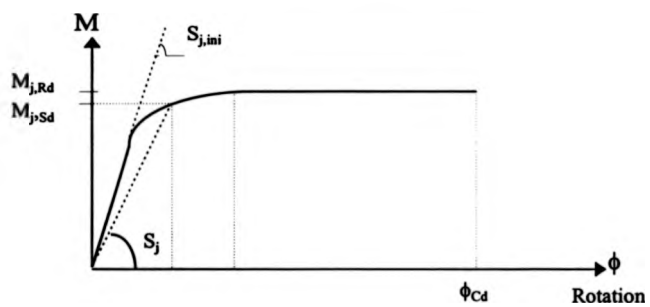

Fig. 1-2 :   Rotation of a connection

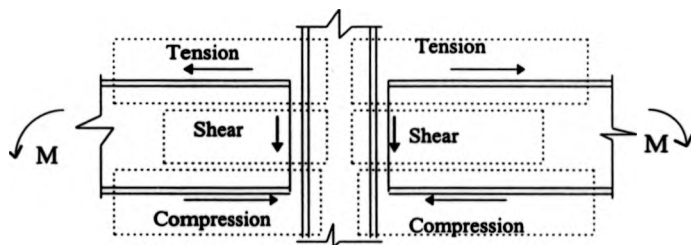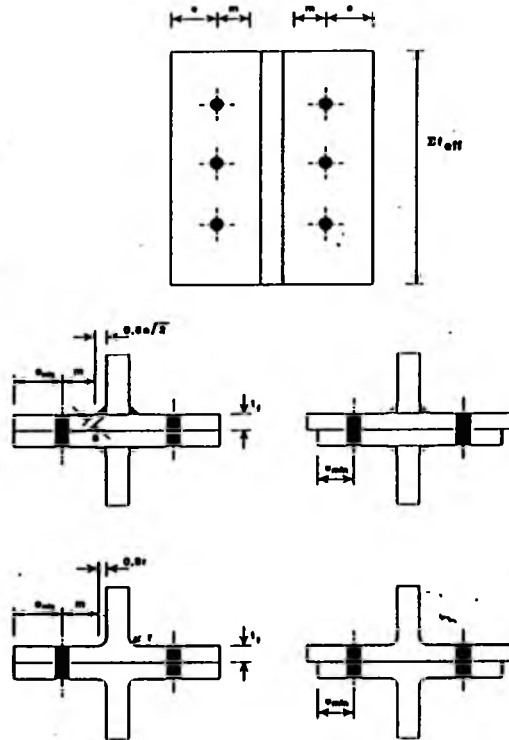*Fig. 1-3 :   Simplified M-φ curves*

Fig. 1-4 : Critical zone in a typical joint

Fig. 1-5 : Dimension of equivalent T-stub flange

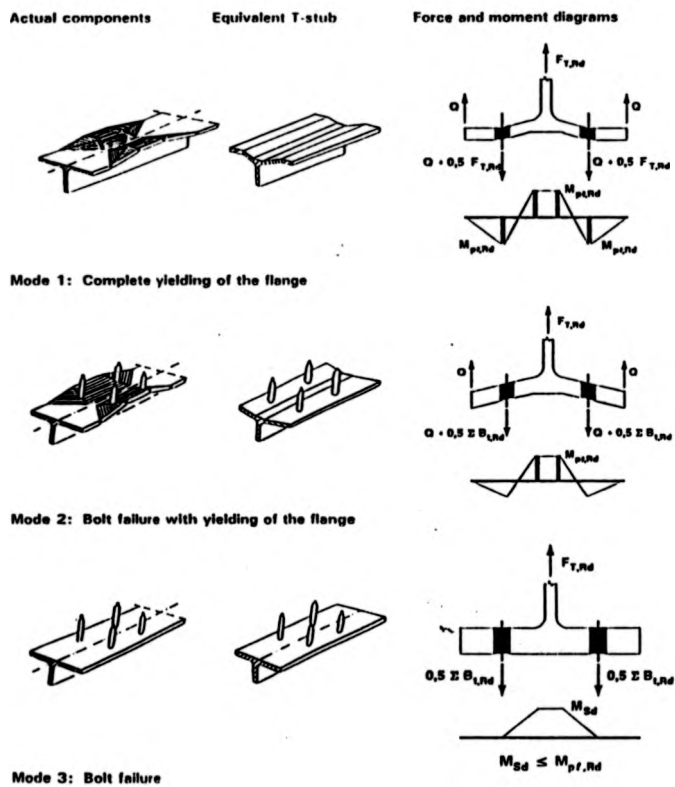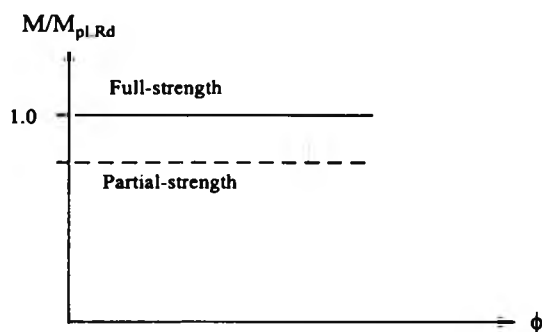*Fig. 1-6 : Failure modes of actual components and equivalent T-stub flanges*

$M/M_{pl.Rd}$

Full-strength

1.0

Partial-strength

ϕ

Fig. 1-7 :   Classification by moment resistance

M

1. Rigid if $S_{j,ini} \geq 8EI_b/L_b$
2. Semi-rigid
3. Nominally pinned if
   $S_{j,ini} \leq 0.5EI_b/L_b$

1

2

3

ϕ

M

1. Rigid if $S_{j,ini} \geq 25EI_b/L_b$
2. Semi-rigid
3. Nominally-pinned if
   $S_{j,ini} \leq 0.5EI_b/L_b$

1

2

3

ϕ

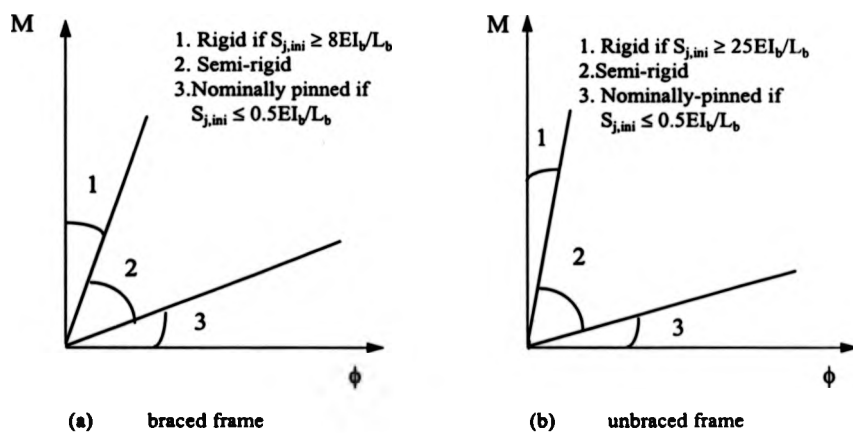(a)   braced frame

(b)   unbraced frame

Fig. 1-8 :   Boundaries for stiffness classification of a joint for
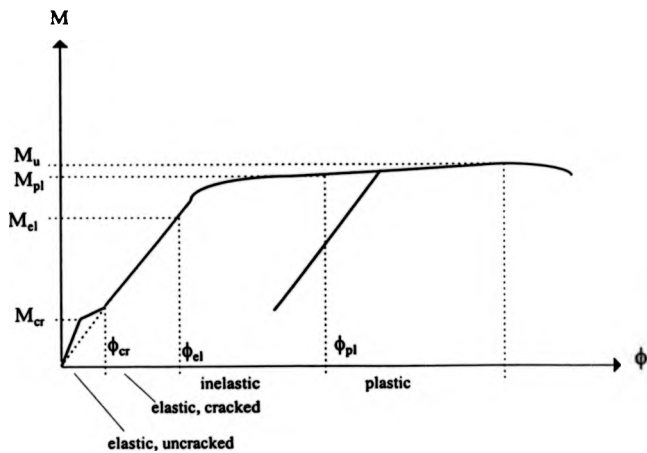*braced and unbraced frame*

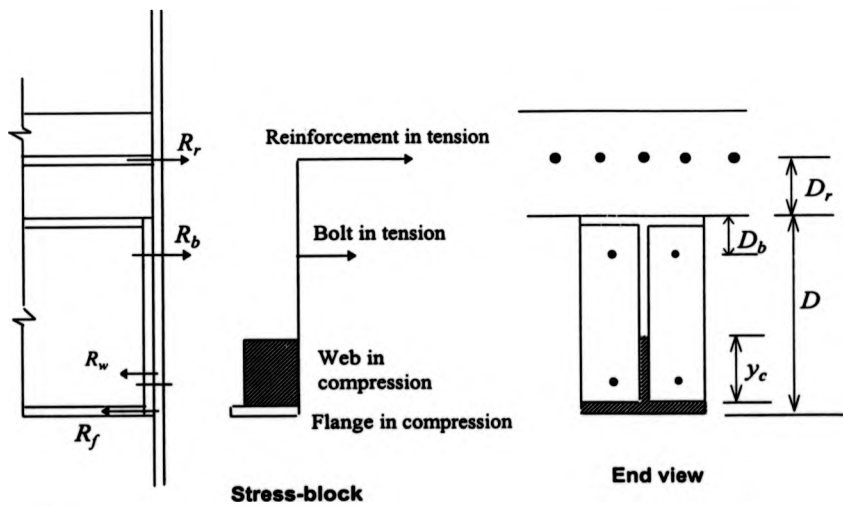*Fig. 1-9 : Typical moment-rotation curve for composite connection*

Fig. 1-10 : Stress block analysis of moment resistance of a composite connection
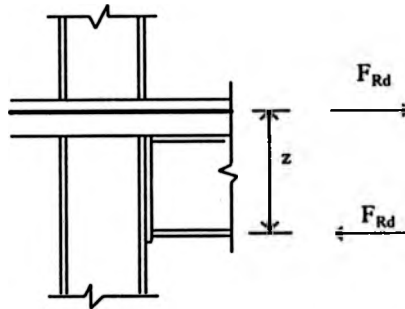
Fig. 1-11 : *EC4 model in calculating moment resistance of composite connection*
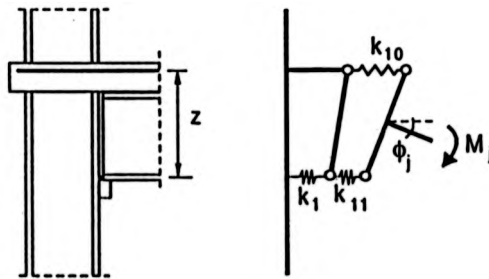

Fig. 1-12 : *Spring model - simple case*
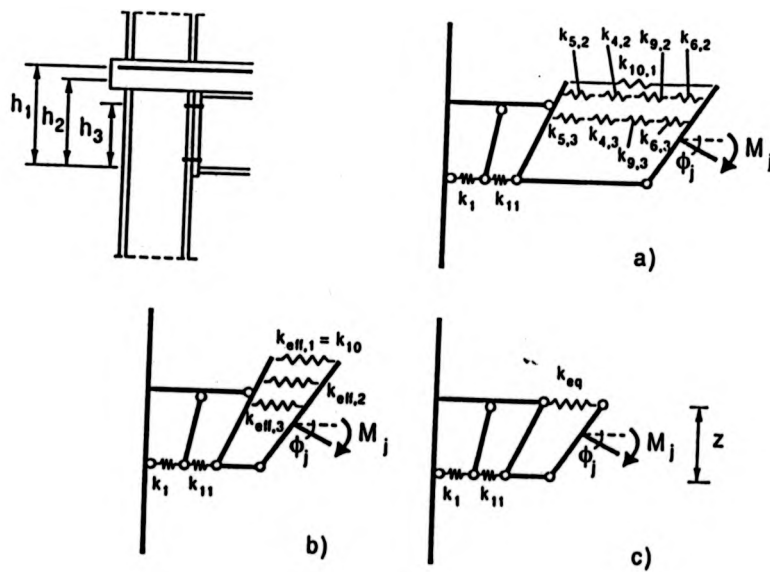
Fig. 1-13 :   *Spring model for a beam-to-column end plated joint*
with two bolts rows in tension
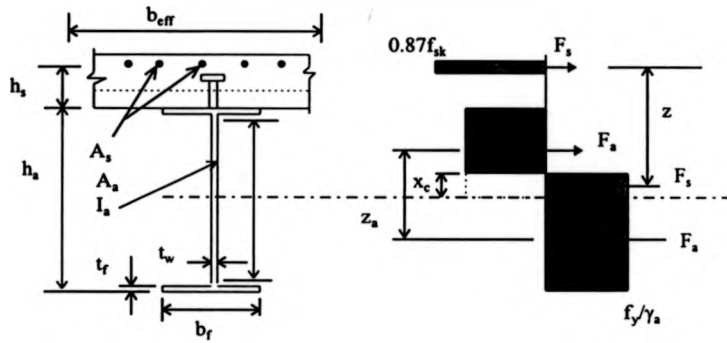
Fig. 1-14 :   *Stress block analysis of hogging moment resistance of composite beam*
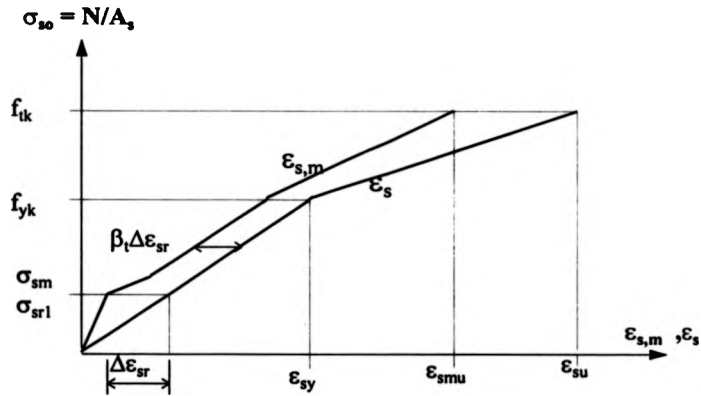
Fig. 1-15 :   *Simplified stress-strain relationship of embedded reinforcing steel*
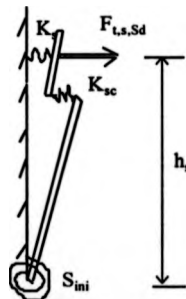
Fig. 1-16 :   *The model of shear connection deformation*
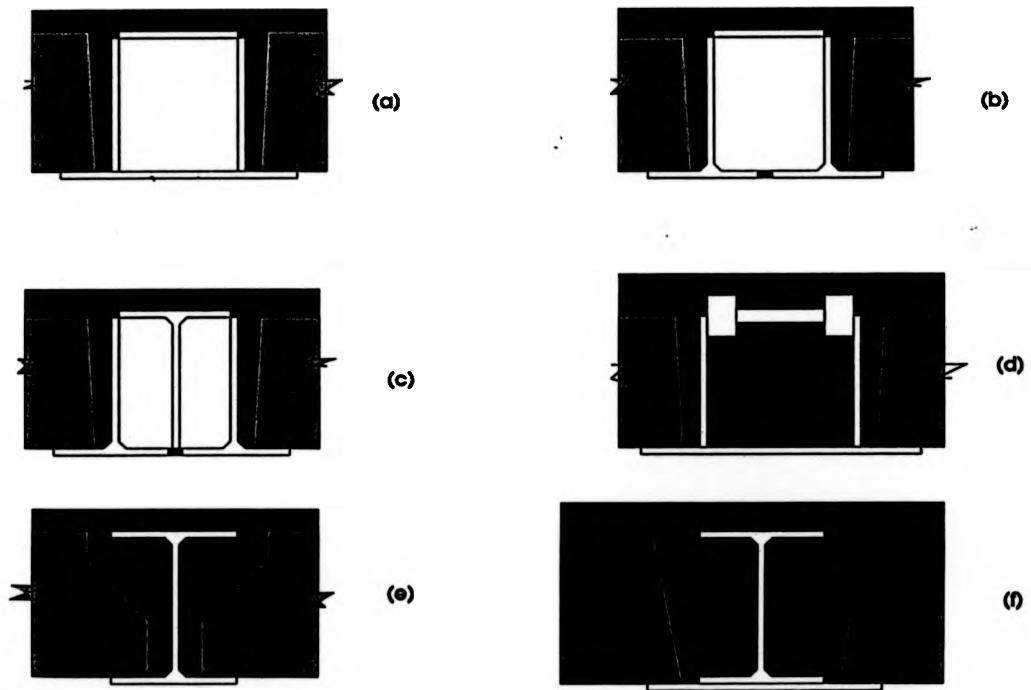
Fig. 1-17 :   Various type of slim floor beam
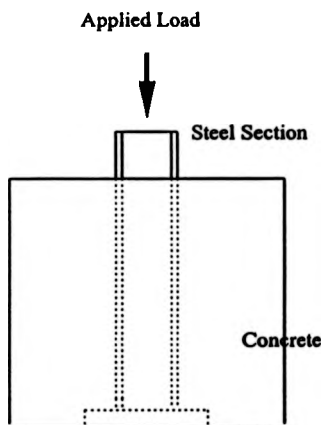
Fig. 1-18 :   Typical push-out test
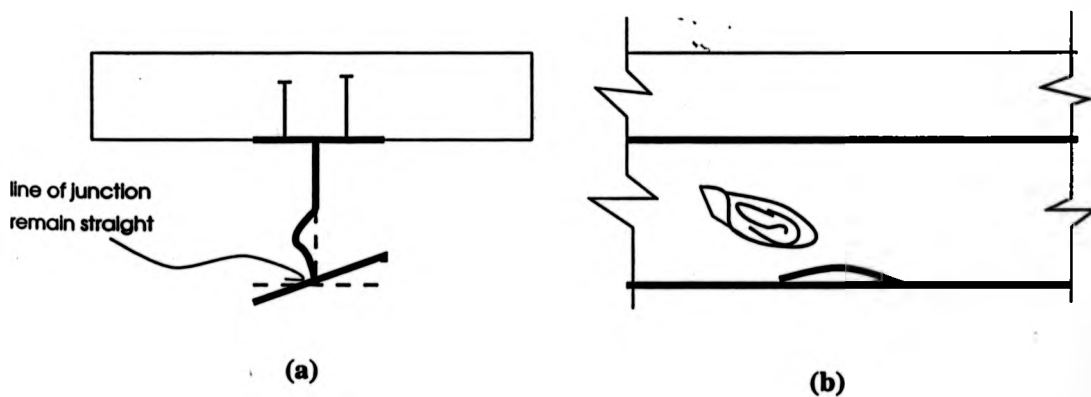
Fig. 1-19 :   Local buckling of web and bottom flange
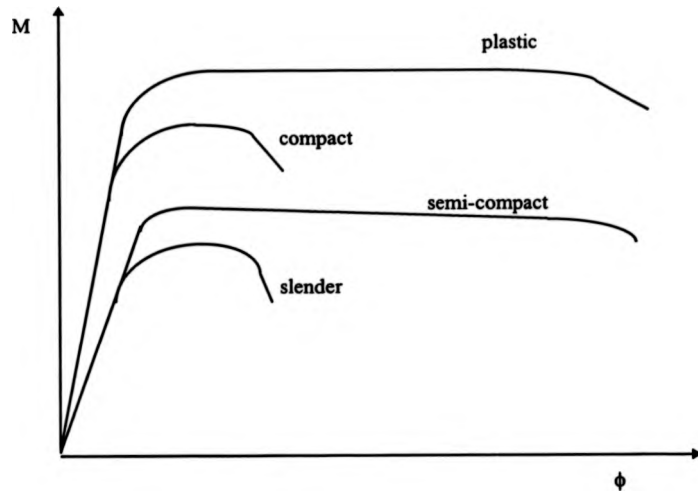
Fig. 1-20 : *Classification of section limited to local buckling*
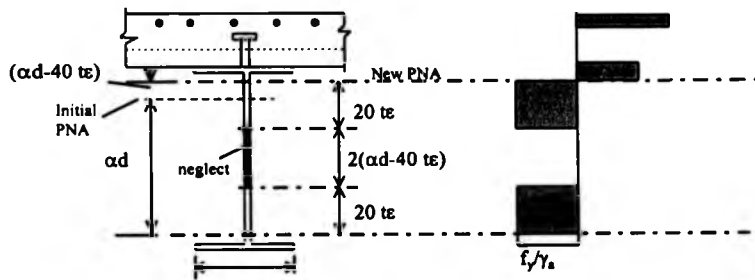
Fig. 1-21 : *Use of effective web in Class 2 for a section in hogging bending with a web in Class 3*

$$\delta_1 \le h_1/300$$
$$\delta_2 \le h_2/300$$
$$\delta_0 \le h_0/500$$

(a) Multistorey

Portal frames without gantry cranes $\delta < h/150$

Other buildings $\delta < h/300$

(b) Single storey
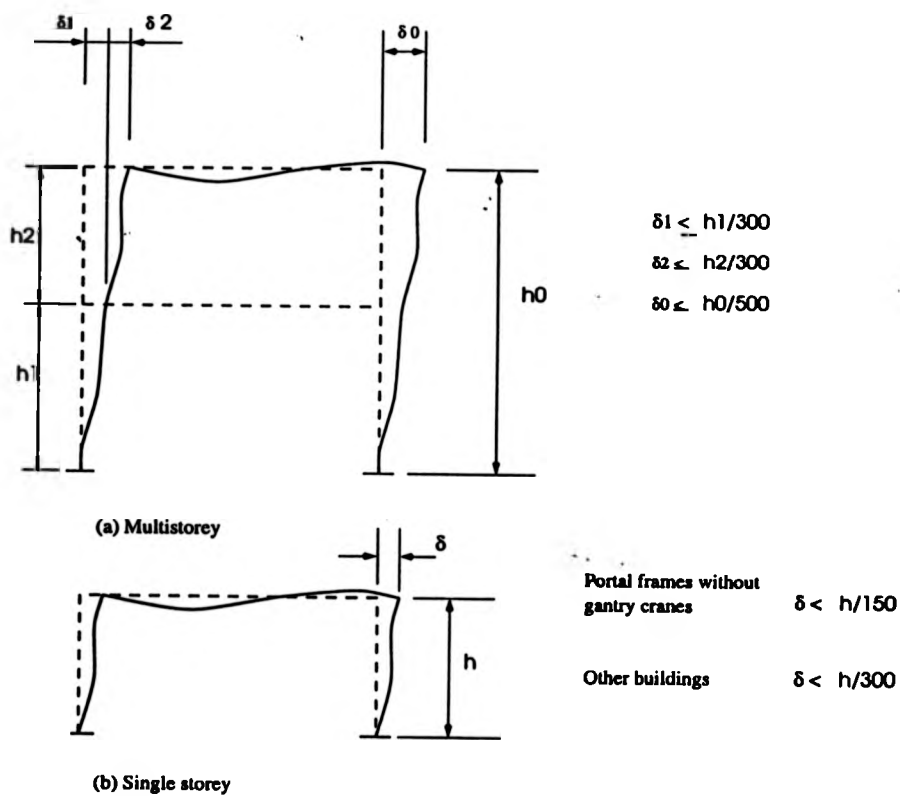
Fig. 1-22 :   Recommended limits for horizontal deflections
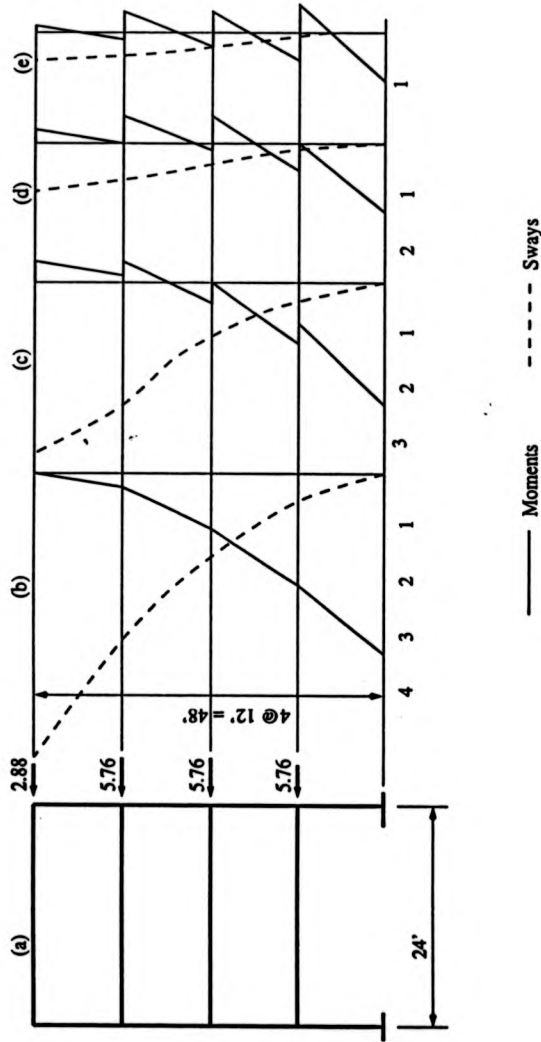
Fig. 1-23 : Effect of connection flexibility on frame sway and column moments

——— Moments   - - - - - Sways
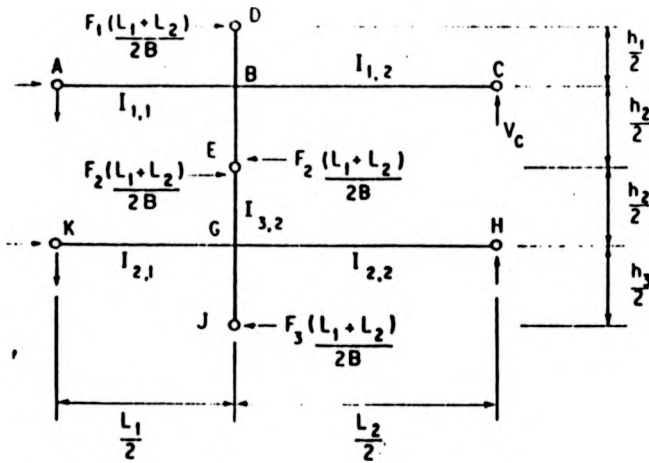
Fig. 1-24 :   *Anderson and Islam's subframes
for intermeadiate storeys*
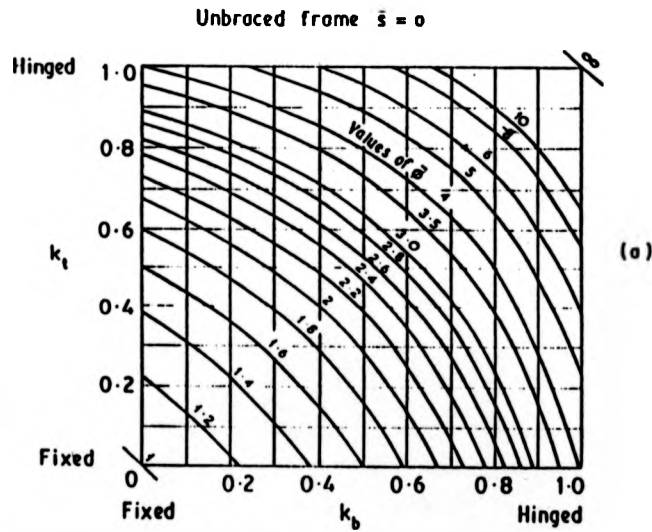
Fig. 1-25 :   *Values of $\overline{\Phi} = (\Delta/H) / (FH/12EK_c)$ for Grinter frame.*
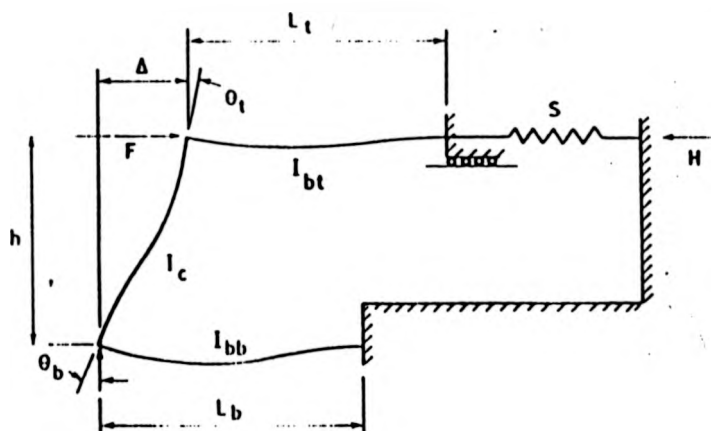
Fig. 1-26 :   Single-storey substitute frame
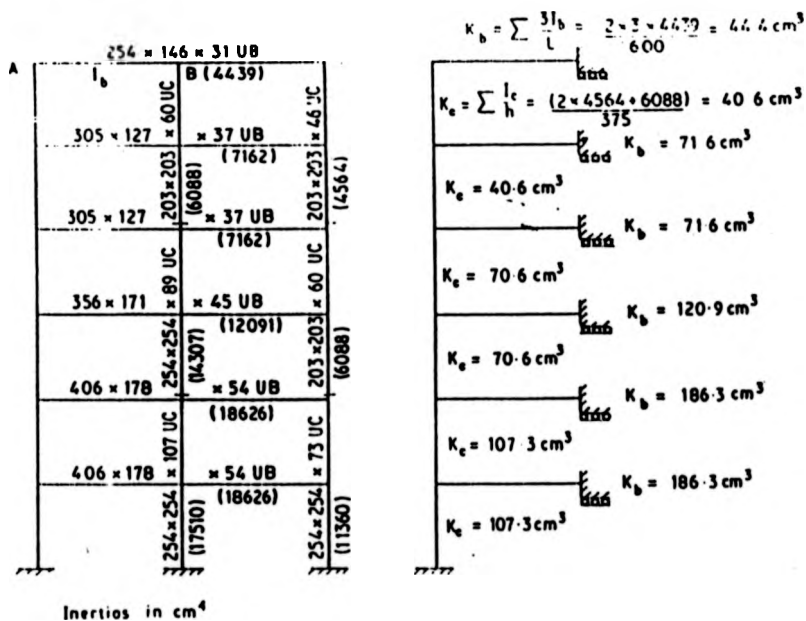
Fig. 1-27 :   Multi-storey substitute frame.

Chapter 2

TESTS ON BEAM-TO-BEAM END PLATE COMPOSITE CONNECTIONS

2.1   Introduction

A typical floor plan of steelwork framing supporting a composite floor is shown in Fig. 2-1. Several forms of composite joints may arises as such a typical floor plan ; namely beam-to-column joints (major and minor axes) and beam-to-beam joints. Much of the experimental research[2-1, 2-2, 2-3] carried out so far on composite connections has been concerned with beam-to-column connections. A significant benefit in braced frames credited to such connections is the reduction in depth of floor beam resulting from the hogging moments developed in the connections.

The tests described below were planned and performed to study the behaviour of composite beam-to-beam joints. As explained in Chapter 1, compared to composite connections between beams and columns, studies on beam-to-beam composite connections are very few in number. However, beam-to-beam joints need to be used in order to realise the benefit of continuity consistently throughout the building frame. It is necessary to develop moment resistance, stiffness and ductility in such joints, in a similar manner to beam-to-column joints. This arises because the composite floor will

typically span 3 metres, but columns will be spaced on a grid of at least 6 metres. At least half of the beams supporting the floor will not be connected directly to the columns, but will be supported by primary beams by means of beam-to-beam connections. Thus research is necessary on end plate beam-to-beam connections, in order to investigate their performance in building frames. Presumably though, much of the research findings in composite beam-to-column connections will be applicable to composite beam-to-beam connections.

2.2   Test configuration

The general configuration of the author's specimen is shown in Fig. 2-2. In each test cantilevers representing the hogging moment region of semi-continuous secondary beams were connected to each other via the web of a short length of primary beam. The primary beam in turn was bolted at each end to short steel columns reacted against the laboratory's strong floor as shown in Fig. 2-3. Loading was applied in a balanced way as far as possible. This arrangement was intended to represent an internal connection. In comparison to external connections, there is a continuity of the slab across the primary beam (see Fig. 2-1) to mobilise the strength of the reinforcement.

In practice, unbalanced loading at internal connections will arise under pattern loading conditions (see Fig. 2-4a), to be resisted the twisting of primary beam (Fig. 2-4b). However, due to the normally low torsional rigidity GJ, only a little rotational restraint is provided by the primary beam and thus it is reasonable to assume balanced moments. Likewise, it is believed that the unbalanced loading will not prevented significant moment resistance being developed due to continuity effects in the slab and the beams.

2.3   Design of test specimens

2.3.1   General specimen description

Two series of experiments were conducted. A first series (BTB1-BTB3) involved the use of a shallow section (356x171UB45) in grade S275 steel as secondary beams. This section was deliberately chosen as the flanges are only Class 2 (compact) the effect of local buckling is more likely to be noticeable in the study. The second series (BTB4-BTB7) adopted the deeper section 457x152UB, of the same grade. The tests on joints with deeper beams (over 400 mm) by Najafi [2-1] and Brown[2-3] had shown a marked enhancement on the moment of resistance when compared to the smaller beams. However rotation capacities of those beams were very much less. Therefore one of the aim for the second series was to study the potential problem of poor ductility in end plate connections with deeper beams.

The steelworks details are illustrated in Fig. 2-5 and Fig. 2-6 respectively. The selection and design of the steelwork connection in the test specimens were based on the recommendation of SCI/BCSA Connections Group[2-4, 5]. A summary of the series of experiments and the parameters investigated are presented in Table 2-1.

2.3.2   Bare steel test

BTB1 and BTB4 were bare steel specimens and the first test performed in each series. These tests were intended to act as a control to the remainder of the tests on composite specimens. This allowed a comparison to be made to the improved connection performance due to composite action.

2.3.3   Choice of structural steel section

It is suggested in reference [2-6] that for internal spans of continuous composite construction, the appropriate span-to-depth (L/D) ranges between 25 to 30 before serviceability criteria influence the design. The choices of the steel sections and the required length for the cantilever regions were based on this recommendation. The points of load application were 1.41 m (for BTB1-BTB3) and at 1.61 m (for BTB4-BTB7) from the face of primary beam's web. These lengths represented points of contraflexure of semi-continuous composite secondary beams of 9 m and 12 m span respectively.

2.3.4 Concrete slab

For all the composite specimens, the construction conformed to general practice. The steel decking used was the PMF CF46 of 0.9 mm thickness, manufactured by Precision Metal Forming Ltd (UK). The overall concrete slab depth was 120 mm. In practice the minimum depth of composite slab is controlled by 'insulation' in fire, usually between 100 to 150 mm[2-7]. Normal density concrete of grade 30 was used throughout the test.

The effective breadth of the slab is not a precise figure, as it depends on the form of loading and position along the beam. It is usually found that bending capacity of a composite beam is relatively insensitive to the precise value of effective breadth of slab used[2-7]. The width of 1100 mm was adopted for all the composite specimens. This was based on the recommendations of EC4[2-8] and BS5950: Part 3.1[2-9] for effective breadth of the concrete flange in hogging bending for a span of 9 m.

2.3.5 Shear connectors

To resist the longitudinal shear and the uplift forces caused by the tendency for the slab to separate from the beam, headed studs of 19 mm diameter and a height of 100 mm (before welding) were used as shear connectors. They are the most popular type to be use in composite construction. The studs were welded through the troughs of the metal decking profile using a special hand tool in the laboratory. With the exception of BTB7 the number of studs welded on each secondary beam were intended to provide full shear connection for the reinforcement used in the slab. It was based on the calculated design shear stud strength of 73.13 kN recommended in *Clause 6.3.2* of EC4[2-8]. The strength of the reinforcing bar was assumed 500 N/mm^2. Fig. 2-7 shown the shear stud positions provided in the tests.

2.3.6 Reinforcement

High yield T16 bars were used as longitudinal reinforcement. An A142 mesh supplemented the rebars to provide transverse reinforcement and also to reduce shrinkage cracking. The rebars were aligned and tied to the mesh which in turn was held by plastic spacers of 30 mm height. This effectively reduced the cover from the upper surface of the slab to 28 mm. Additional reinforcement of 2R8 was placed diagonally at each beam's free end as a precautionary measure against premature failure due to punching shear at load point.

The rebars were varied between 4 to 6 in number to provide 1% to 1.5% of the effective area of the concrete. As the metal decking was placed transversely on the beams, the effective area of the concrete considered was that above the ribs of the decking. The number of rebars provided were expected to give good ductility [2-3]. All the rebars were continuous across the primary beam and were evenly spaced. The maximum clear

distance between bars met the requirements of BS8110[2-10] for 30% redistribution of moment. The reinforcement details are shown in Fig. 2-8.

2.3.7 Choice of connection geometry

End plate joints are widely used in steel construction in the UK. Besides being neat and robust in handling, they are quite versatile in that they can tolerate moderate offsets in erection and they can be used with skewed beam. Relatively thin (10 mm) end plates were used for the connections in the tests, and so the joints would be regarded as nominally-pinned when of bare steel[2-4, 2-5].

A standard weld size of 8 mm weld were applied to attach the end plates to the secondary beam. Fillet welds of this size are generally recognised as being reliable and will normally need little testing beyond the usual visual inspection[2-5].

Ordinary bolts of M20 Gr.8.8 were used as they are commonly available as an industrial standard. It has been shown that they are suitable for 90% of the connections in a typical multi-storey frame[2-5]. The bolts are placed at cross centres 90 mm (Figs.2.5 and 2.6), again to provide some flexibility in the joints. In BTB3 bolts were not provided for the top row of bolt holes. It was intended at first to provide additional reinforcement for BTB3 to reduce the specimen to one with partial shear connection. However, the holes for the top bolts in the steelwork connection were misaligned by the fabricator by 5 mm. The decision was made to carry out the test by omitting the top bolts, thus making the connection similar to the "boltless" composite connections investigated in Germany[2-11].

2.4 Preparation of specimen

The delivery and the fabrication of steelwork was arranged by The Steel Construction Institute which was the principal sponsor of the tests. To prepare a specimen, each secondary beam was placed on two specially-made steel supports with the end plates lining each other at a suitable distance apart. The primary beam was lowered by the crane into position and was bolted together with the secondary beams. A torque wrench was applied to tighten up the bolts to 190 Nm to maintain consistency between specimens.

For the composite tests, the bolted specimen was lowered down into a casting rig and restrained by adjustable supports to both primary and secondary beams. This effectively created the conditions for propped construction. The required size of metal deckings was cut, positioned and aligned transversely on the secondary beam. The shear connectors were welded through the deck to the flange of the beam. Edge trim 120 mm deep (conforming to the overall depth of the slab) was riveted to the decking to complete the formwork for concreting. The reinforcement (including the mesh) were then fixed in the manner already described in Section 2.3.6.

The concreting was done in the laboratory. Prior to actual casting of the concrete, trial mixes were made out. Ordinary Portland Cement, uncrushed coarse and fine aggregate were used throughout. The mix was designed as normal density concrete with a characteristic strength of 30 N/mm^2 based on the 28-day cube strength, a maximum 20 mm aggregate and a slump of between 30-60 mm.

2.5   Test rig

The test rig essentially comprised two "goal posts" at each end of the test specimen. It was made up from lengths of pre-drilled steel sections already available in the laboratory, and was designed by the author to be capable of resisting a maximum unfactored midspan load of 500 kN (Plate 2-1(a)). A factor safety of 1.4 was applied in the design of the members. The bolts were assumed capable of resisting single shear of 70 kN. The test frames were braced and bolted down to the strong floor. A general arrangement of the rig is shown in Fig. 2-9(a) and 2-9(b).

The load was applied by two independent jacks mounted on the test rig at 1410 mm (for BTB1-BTB3) and at 1610 mm (for BTB4-BTB7) from the face of primary beam's web. The secondary beams were supported by primary beams which were bolted at each end to a short steel column. Although this simple arrangement will not simulate the actual behaviour of the primary beam, it would not affected significantly the measured moment- rotation behaviour of the connection as the rotations are measured relative to the primary beam. The load was transferred to the specimen through an arrangement of rollers and a knife edge (Fig. 2-10) which ensure the verticality of the load during testing. The jacks reacted against the laboratory strong floor through the test rig.

2.6   Supplementary Test on Materials

2.6.1   Concrete

Casting of 150x150x150 mm cubes for compression tests and 200x100 mm diameter cylinders for splitting tensile strength tests was carried out at the same time as the

specimen was cast. The cubes were tested at 7 days, at 28 days and on the test days. The cylinders were tested on the day of the connection test to determine the tensile splitting strength. The splitting tensile strength f_{ctm} was taken as

$$f_{ctm} = \frac{2F}{\pi d l} \quad (\text{N/mm}^2) \tag{2.1}$$

where $\qquad$ F = maximum applied force (N)

$\qquad\qquad$ d = cylinder diameter (mm)

$\qquad\qquad$ l = cylinder length (mm)

The procedure for making and testing the cubes and cylinders are given in BS 1881[2-13]. The specimen were placed in the test rig when the concrete strength had reached at least 30 N/mm². All the concrete test results are summarised in Table 2-2.

2.6.2 Structural steel and reinforcement

Standard coupons were made in the laboratory from the end plate, and from both the web and the flanges of the steel beam using an additional 300 mm length supplied by the fabricator from the same rolling. One sample 300 mm in length was cut for each length of rebar used in the tests. The standard tensile test was carried out in accordance to BS EN 10 002-1[2-14]. The results are tabulated in Table 2-3 and Table 2-4, respectively.

2.7   Instrumentation

The general instrumentation is shown in Fig 2-11. Five electronic inclinometers were used to measure the rotation of the connection directly. One inclinometer was fixed to the primary beam and another two at each end of the secondary beams. Both the absolute and relative rotations to the primary beam were recorded so as to provide full

information to enable the moment-rotation relationships to be obtained. A comparison study carried out by Najafi[2-1] confirmed that the electronic inclinometers are able to give accurate readings.

Two displacement transducers were used to measure deflections (one at each end) under the loading position. They were also used to control the balance of the specimen especially at the later stages of loading. Another two transducers positioned near to the connections were used to record any vertical slip between the secondary beam and the primary.

Choice of strain gauges depends upon the expected behaviour of the material under loading condition. The horizontal strains on the steel beam's flanges and web were measured by single PL-10 type strain gauges haveing a strain limit of 2%. PRS-10 type rosette $(0, 90, 45^0)$ strain gauges (also having limiting strains of 2%) were adopted on the steel beams' webs in order to obtained vertical, horizontal and diagonal strains. The surface of the steel sections were ground before the gauges were glued on them.

It was anticipated that each test would be carried out until the fracture of the rebar, so higher strains were expected for such components. The post-yield strain gauges YL-10 capable of measuring strain from 10 to 20% were applied on the reinforcing bars. The rebars need to be ground at the position where the gauges were to be glued. This effectively reduced the area of the reinforcing bars. These strain gauges were also to be embedded in the concrete and special protection was needed. The compressive strains of the web and flanges were measured on both the bare specimens. It was decided not to strain gauge the rebars in BTB5, BTB6 and BTB7 after the general strain behaviour had been established in the earlier tests (BTB2 and BTB3).

The measurement of the loads was by way of two 50-ton load cells.

2.8 Calibration of instruments

The calibration was carried out before the first test to ensure each item of instrumentation performed satisfactorily.

The calibration of load cells was carried out using a previously-calibrated compression machine with connection to a digital voltmeter. Load was applied to the load cell by the compression machine. Loads was applied up to the expected level to be used in the experiment and the corresponding voltages were plotted to obtain a general form of a straight line equation

$$y = mx + c \tag{2.2}$$

The value of constants from Eqn. 2.2 were supplied as data to the software available in the laboratory.

The electrical inclinometers were calibrated using a purpose-built rig available in the laboratory. The rig basically consists of a metal plate of 150x600 mm and a stopper fixed to a base. Three inclinometers can be fixed to the metal plate and calibrated simultaneously. Slip gauges were used to lift up one end of the plate thus creating an angle which was detected by a data logger. The process was repeated with slip gauges of different sizes to obtain more data. This data was plotted and a straight line equation as in Eqn. 2.2 was obtained. The value of constants in the equation were entered to the software to be use in the experiment.

The transducers were also calibrated by using purpose-built equipment in the laboratory. The rig included a base to which a micrometer was fixed at the other end. The

transducer, which was connected to a data logger, was secured into position. The barrel of the micrometer was adjusted to a position (datum). The response of the transducer was detected by the data logger. Slip gauges of several sizes were applied to provide the required displacements. The process was repeated several times to acquire the necessary data. The data was then plotted and a straight line equation was obtained to determine the necessary constants. The constants were supplied as data to the software to be use in the tests.

The instrumentation was wired to a data acquisition system which was connected to a computer to monitor each test. The reading passed from the data logger was processed by software available in the laboratory and monitored on the computer screen. Data was printed and also stored on hard disk.

2.9   Test Procedure

Before each test, visual inspections of the test rig and specimen were conducted. The overall performance of the apparatus was checked by loading each specimen to 15 kN in 5 kN increments and then unloaded to 5 kN. The beams were then loaded again in stages up to two-thirds of the predicted ultimate resistance of the connection (considered to be the elastic limit) calculated using Equation 2.3 (see Section 2.10) before being unloaded to 5 kN. At each load stage, instantaneous readings were recorded and the specimen was then left for 5 minutes before further readings were recorded. The specimens were then loaded further to determine the ultimate behaviour. Marking of concrete crack pattern was also carried out at each load level.

Graphs of moment-rotation curves (M-ϕ) were plotted during the tests as guides to the general behaviour of specimen. In the elastic range, the moment was taken as the

controlling test parameter. At higher load (in the plastic range) the M-ϕ curves showed marked increased in rotation without significant increase of moment. The amount of the moment increments in this range was based on deflection increments at each end of the secondary beam.

The tests were terminated when one of the following conditions arose:

1.   The rotation was over the limit of practical interest, which was judged to be 40 mrad. Joints achieving a rotation capacity of 40 mrad can assuredly be use in plastic design of frame[2-11].

2.   Fracture of the rebars, which limited the rotation capacity of a composite specimen.

3.   If further loading could be dangerous, for example because of potential bolt fracture.

2.10   The predicted resistance of connection

In the design of the test specimens, nominal dimensions and characteristic material properties were used because the actual properties could not be determined until the experiment was completed. However for the end plate, the material properties were taken from Najafi's tests[2-1] and the value of yield strength of reinforcement f_{yrf} was taken based on Brown's work[2-3] as 500 N/mm^2 The resistance moments M_{cr} of the structural steel connections were calculated in accordance of Annex J of EC3[2-12]. The predicted resistance contributed by the reinforcement, which formed composite connection, was added to that of the bare steel. Thus:

$$M_{cc} = M_{cs} + M_{crf} \qquad (2.3)$$

where,

M_{cc} is resistance moment of composite connection,

M_{cs} is resistance moment of bare steel connection,

M_{crf} is resistance moment due to reinforcement.

and,

$$M_{crf} = A_{rf} f_{yrf} l_{rf} \qquad (2.4)$$

where,

A_{rf} is the total area of reinforcement provided,

f_{yrf} is the yield stress of the reinforcement,

l_{rf} is the lever arm (taken as distance between centre of reinforcement to the centre of compression flange).

2.11 Test Observation

The results of the tests are summarised in Table 2-5. The calculated moment resistance M_{cc} was based on Eqn. 2.3. Maximum experimental moments of resistance of the connections M_{exp} (averaging both sides) are taken from the respective M-ϕ curves attained in the tests. These moments were calculated by multiplying the applied load by the lever arm of 1.41m for BTB1-BTB3 and 1.61m for BTB4-BTB7. All test results are presented against the connection moment. The rotations ϕ_u relate to the maximum experimental moment M_{exp} while ϕ_{ult} is the ultimate rotation at failure. Both rotations are the average value between the two sides. They were measured relative to the primary beam. The degree of shear connection and mode of failure of each specimen are also indicated in Table 2-5.

Moment-rotation curves (M-ϕ) for all the tests are given in Fig. 2-12 to Fig. 2-18. Plate 2-1 to Plate 2-7 show the specimens BTB1 to BTB7 respectively. The average strain responses are plotted in Fig. 2-19 to Fig. 2-21. The following sub-sections outline the main observed behaviour of the connections during the tests.

2.11.1   *Specimen BTB1*

The moment-rotation curves for BTB1 are presented in Fig. 2-12. Generally at low moment the response of the two connections were generally not similar. After the applied moment surpassed the predicted moment of 45 kNm the response of the two connections was similar. Substantial reduction in stiffness was recorded at higher moment, although there was a continued rise in resistance after the "knee" of the curve; this is typical of bare end plate connections[2-15].

It was observed during unloading that the curves showed the unexpected response (see Fig. 2-12a) of being non-linear. It is believed that the difficulty of controlling the load balance on the two cantilevers during unloading contributed to this behaviour. Evidence for this is obtained when the average value is plotted as in Fig. 2-12b, resulting in a more typical response for such connections.

The predicted moment resistance of connection BTB1 based on the assumed and nominal properties was 45 kNm (see Section 2.10) This was achieved at the rotation of 10 mrad. The mode of failure expected was mode 2 i.e. failure of bolts combined with end plate yielding. At this moment level, the top part of end plate had noticeably deformed transversely (Plate 2-1b), resulting in prying forces on the bolts. It was observed that at a moment level of about 60 kNm, the end plate between first row and

second row bolts showed sign of bending (Plate 2-1c). No measurement suggested that vertical slip had occurred.

The test was terminated after the moment reached 97 kNm for the fear of possible bolt fracture. The rotation had reached more than 40 mrad and the calculated tensile bolt force corresponding to the applied moment was about 175 kN per bolt.

The curves of moment against average compressive strain (Fig. 2-19) showed that for the whole duration of the test the lower flanges were under compressive strain. There was also an indication from the results in the figure that the bottom flanges strain started to exceed the yield strain at a moment of about 55 kNm. The web at the level of 1st row bolt was under tensile strain(Fig. 2-20) throughout the test.

The connection was inspected after the test. It was found that the top bolts had stripped and the end plates were still slightly bent between the 1st row and 2nd rows of bolts. No visible deformation had occurred in the steel beams. From Fig 2-12b it was found that the initial rotational stiffness $S_{j,ini}$ of the connection of BTB1 was 10.9 kNm/mrad This test confirmed that the bare steel joints do possess some significant degree of moment resistance and initial rotational stiffness.

2.11.2 *Specimen BTB2*

Specimen BTB2 consist of a composite connection as shown in Fig. 2-1. Four T16 rebars representing 1% of effective area of concrete slab (see Section 2.3.6) were provided to further contribute to the resistance of the connection. The average concrete cube strength on the test day was 50 N/mm^2 .

The first transverse crack occurred at the moment of 35 kNm for the left beam, about 110 mm from the centreline of the primary beam. Further increase in moment extended both the length and width of the initial crack. However only after the moment reached 70 kNm was formation of new transverse cracks on the right beam observed, at 120 mm from the centreline of primary beam. It was noticed that a transverse crack always initiated around the position of transverse mesh bar. Longitudinal cracks started to appear at the moment level of 240 kNm at several positions where the rebars were located. Plate 2-2a shows the crack pattern after the test was completed.

The moment-rotation behaviour of BTB2 is plotted in Fig. 2-13. It shows that above a moment of 200 kNm, a great reduction in stiffness occurred. The curve after the "knee" was not smooth compared to BTB1, due to the fracture of the bars of the mesh on both sides.

At a rotation of about 20 mrad (at 260kNm) the lower flange of the left beam started to show sign of local buckling (see Plate 2-2c). It was realised also that the left beam had twisted slightly at this moment level. After visible local buckling began, it was difficult to increase the moment level further. At a rotation of about 39 mrad a loud 'bang' was heard and the moment decreased considerably, indicating that one of the rebars had fractured (Plate 2-2b). The fracture occurred at the position where strain gauges were located. No significant slip was recorded at the beam-slab interface.

The top part of the end plate started to deform noticeably when the load was at 170 kN (240 kNm). The end plate was observed to bend between 1st row and 2nd row of bolt beginning at a moment of 250 kNm. Except for the local buckling of lower flanges of the beam, no other noticeable deformation occurred on the steel sections.

The recorded strain on the bottom surface of the lower flanges (Fig. 2-19) indicated that they had yielded before the ultimate moment. The direct strain reading on the web at the level of the first row bolt (Fig. 2-20) shows a compressive strain at a low load. This may imply that the neutral axis is higher than 1st row bolt level because the concrete slab was not cracked and thus of higher stiffness. However at about 50 kNm the reading changed to the tensile strain suggesting that the neutral axis moved down after cracking had occurred.

Upon completion of the test, the concrete in the area of beam-to-beam connection was broken out. It was found that a reinforcing bar and all the bars of the mesh parallel to one secondary beam had fractured. Neither the shear studs on the primary beam nor the first studs on the secondary beams showed signs of permanent deformation.

2.11.3   Specimen BTB3

When the specimen was placed in the test rig, it was found that it was not level along the secondary beams. It was discovered that the top and bottom flanges of the primary beam were not parallel to each other, with the top flange having a tranverse slope of 1:100 (Plate 2-3b) relative to the bottom flange. The average concrete cube strength on the test day was 44 N/mm^2.

The M-ϕ curve of the test is given in Fig. 2-14. The loading procedure applied to the specimen was the same as for BTB2. It was observed that the connection of the left beam recorded a negative value of rotation up to a moment level of 120 kNm, despite applying balanced load. This may due to the initial imperfection (distortion) of the primary beam.

2-19

The crack development was similar to that observed in BTB2 except that there was a distinct crack along the centreline of the primary beam (Plate 2-3a). The maximum moment achieved however was 240kNm at the rotation of about 6 mrad, afterwhich an almost horizontal plateau followed. The test was terminated at the rotation of about 40 mrad after considerable deformation of the end plates was observed.

As with specimen BTB2 only negligible slip occurred at the steel-slab interface and there was no evidence to suggest vertical slip between the end plates and the web of primary beam. The concrete was broken up after the test for inspection of embedded materials. All the bars of the mesh were fractured but no noticeable permanent deformation of the studs had taken place. There were signs of a slight local buckling (Plate 2-3c) to the beam flanges.

2.11.4 *Specimen BTB4*

The bare steel specimen BTB4 was the first of the second series, in which a stiffer connection and a deeper beam were used. Direct correlation was to be made to three other composite joints BTB5, BTB6, and BTB7 which had the same steel details.

The moment-rotation curves for BTB4 are presented in Figs. 2-15(a) and 2-15(b). The M-ϕ response was generally similar to that bare specimen BTB1 (i.e. extensive reduction in stiffness at higher loads). Compared to Fig 2-12 of BTB1, higher stiffness and resistance moment was obtained with BTB4.

Bending of the end plate was apparent between rows two and three at a moment level of 96 kNm and the top parts of the end plate had noticeably deformed transversely (Plate 2-4b). No noticeable deformation of the end plate occurred between bolt rows one and two.

After the rotation had reached more than 40 mrad the test was terminated. Inspection after the test showed that permanent deformation had occurred to the end plate; however no observable deformation remained in the steel beams, nor was there any indication of bolts stripping.

2.11.5   *Specimen BTB5*

Transverse cracking in the concrete started at about 100 mm on the right of the joint region at a moment level of 48 kNm. Increase in moment extended this initial crack. A subsequent new crack was observed to take place at a moment of 103 kNm at about 120 mm to the left of the connection. The cracks formation is shown in Plate 2-5a.

The moment-rotation curves are given in Fig. 2-16. The "knee" of M-φ curve was reached at the moment of about 310 kNm below which the response was substantially linear. The post-"knee" behaviour however showed a well-developed plateau. The first mesh bar fractured at a rotation of about 5 mrad, corresponding to a moment of 330 kNm. Slight deformation of the end plate was also observed at this stage. Several mesh bars fractured subsequently, which resulted in dips in the M-φ curves, when compared to those for bare steel connection BTB4.

Slight deformation of the end plates was observed at a rotation of 18 mrad. During unloading it was noticed that at a rotation of 23 mrad the steel pad of the uni-directional rocker of the right beam on which load was applied (refer to Fig. 2-10) had slid about 10 mm transversely. On further reloading, slight local buckling of the bottom flanges of beams was observed at 320 kNm. The rotation had achieved 25 mrad at this level.

Attempts to increase moment further only showed a marked increase in rotation under constant moment. At about 45 mrad a very loud sound (identical to BTB2) was heard and the load dropped very significantly, indicating a rebar had fractured. The moment was about 350 kNm and the test was terminated.

The specimen was inspected and the concrete was broken up around the joint region after the test. It was confirmed that the entire width of the mesh and a rebar had fractured (Plate 2-5b) However there was no indication of permanent deformation of the shear studs. Local buckling of the lower flanges of the secondary beam had occurred, and also the end plates were deformed between bolt rows two and three (Plate 2-5c).

2.11.6 Specimen BTB6

By omitting the nearest stud to the connection in each secondary beam, the degree of shear connection of specimen BTB6 effectively reduced ("partial shear" according to BS5950[2-9] but still "full shear" according to EC4[2-8]). It also increased the distance of the first shear connector from the centre of the connections to 424 mm instead of 199mm (Fig. 2-7).

The first transverse crack of the concrete slab was observed at the position of the first stud at a moment of 56 kNm. This crack widened and extended as the load increased further (Plate 2-6a). Longitudinal cracks started to form mainly at the rebar positions at 225 kNm.

The moment-rotation curves of BTB6 is given in Fig. 2-17. The behaviour of the M-ϕ curves is generally similar to that of BTB5, although the "knee" was more gentle. This may due to the increase of the length of reinforcing bar contributing greater flexibility to the connection.

At the moment of about 315 kNm a loud sound was heard and there appeared a wide crack at the position of first studs (Plate 2-6a); the load dropped considerably. It was thought that two bars of the mesh fractured at almost the same instance. End plates were beginning to bend between the bolt rows two and three when the moment was 206 kNm. At a rotation of 12 mrad, local buckling of beam flange was noticeable (Plate 2-6c). This corresponded to a moment of 340 kNm.

The test was terminated after a rotation of over 40 mrad had been achieved and was due to excessive deflection. After the test the concrete slab was broken up for inspection. As in other previous composite specimens, all the mesh bars parallel to the secondary beams had fractured but no significant permanent deformation of shear studs was observed.

2.11.7   Specimen BTB7

In BTB7 two additional rebars were added to increase the amount of reinforcement to 1.5% of the effective concrete area. This increase in turn caused the shear connection to be "partial".

The first transverse cracks on the concrete were observed on both sides of the primary beam at about 100 mm from the centre line at a moment of 56 kNm. The next new cracks (about 300 mm from centre line) and the extension of the previous cracks were observed at the moment of 88 kNm. The cracking coincided approximately the position of the transverse bars of the mesh. Compared to all previous specimens, further load increments did not widen the existing cracks extensively at the joint region.

The moment-rotation behaviour of BTB7 is plotted in Fig 2-18. The lower flange of the left beam showed sign of local buckling at 370 kNm with a corresponding rotation of 6

mrad. Permanent deformation of end plate between bolts of rows two and three was also observed (Plate 2-7b). At about 390 kNm it was realised that the top flange of left beam was hogging and a long longitudinal crack was occurring along the position of studs on the left beam (Plate 2-7a). Further attempts to raise the load were not successful and only registered a marked increased in rotation. At a rotation of about 25 mrad it was found that there was slip of 14 mm between steel and concrete interface at the end of the left beam.

The test was terminated when the rotation was about 30 mrad due to excessive "bowing" of the upper flange and the detachment of profile steel decking from the steel section of the left beam. A total slip of 20.4 mm was recorded on the left end beam (Plate 2-7d) although only negligible slip on the right beam. After the concrete had been broken at, it was observed that all the shear studs of the left beam had been deformed permanently (Plate 2-7c). However no deformation of shear studs of the right beam was visible.

2.12 Conclusions

(i)   Tests to determine the behaviour of beam-to-beam end plate connections were performed. The parameters varied in the tests are the type of connections, the amount of reinforcement, the depth of steel beam and the degree of shear connection provided.

(ii)   It was confirmed that the moment resistance of connections can significantly be enhanced by providing moderate reinforcement.

(iii)   It was found that there was a similar overall response of $M\text{-}\phi$ curves to beam-to-column tests[2-1, 2-3].

(iv)   The failure modes (mesh and rebar fracture, local buckling) were alo similar to beam-to-column joints.

(v)   Greater ductility was observed when the length of rebar to first stud was increased (BTB6).

(vi)   For full shear connections (BTB2, BTB3, BTB5 and BTB6) no permanent deformation of shear connector was noticed.

(vii)   On the other hand, partial shear connection (BTB7), greater loss of resistance at large slip had occurred followed by permanent deformation of shear connectors.

(viii)   The "boltless" connections did possess a comparable degree of moment resistance to that of normal connection. It may provided an economic alternative solution.

References

2-1   Najafi, A.A., "End plate connections and their influence on steel and composite structures", PhD Thesis, University of Warwick, 1992.

2-2   Li, T., "The analysis and ductility Requirements of semi-rigid composite frames", PhD Thesis, University of Nottingham, 1995.

2-3   Brown, N., "Aspects of sway frame design and ductility of composite end plate connection". PhD Thesis, University of Warwick, 1995.

2-4   "Joints in Simple Construction. Vol. 1: Design Methods", Steel Construction Institute, Ascot, and British Constructional Steelwork Association, London, 1993.

2-5   "Joint in Simple Construction. Vol. 2: Practical Applications", Steel Constructional Institute, Ascot, and British Constructional Steelwork Association, London. 1995.

2-6   Lawson, M., and Wickens, P., "Composite beams", Steel Designers' Manual Fifth Edition, ed. G.W. Owens and P.R. Knowles, Blackwell Scientific Publications, 1992, pp 592-619.

2-7   Lawson, R.M., "Design of composite slabs and beams with steel decking", Publication No 055, Steel Construction Institute, Ascot, 1993.

2-8.   Eurocode 4, "Design of Composite Steel and Concrete Structures, Part 1: General Rules and Rules for Building". 1991.

2-9   BS 5950: Part 3, "Code of practice for design in composite construction, Section 3.1: Design of simple and continuous beams., British Standard Institution. 1990.

2-10   BS8110, "Structural use of concrete. part 1. Code of Practice for design and construction". British Standard Institution. London, 1985.

2-11   "Composite steel-concrete joints in braced frames for buildings" (ed. D. Anderson), COST C1, Brussels, 1997.

2-12   Eurocode 3, "Design of Steel structures, Part 1.1 General Rules and Rules for Building", European Committee for Standard, 1992,

2-13   BS 1881, " Testing of concrete", British Standard Institution, London, 1983.

2-14   BS EN 10 002-1: "Tensile testing of metallic material, Part 1" British Standard Institution, London,1990.

2-15 Bose, B., Youngson, G.K., and Wang, Z.M., "An appraisal of the design rules in Eurocode 3 for bolted end plate joints by comparison with experimental results", Proc. Instn Civ.Engrs Structs & Bldgs, 116 May 1996. pp 221-234.

2-27

Table 2-1: Beam-to-beam composite connection tests

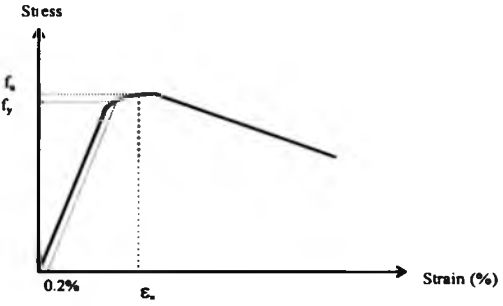| Test No	Secondary Beam	Primary Beam	End Plate	Rebar	Notes
BTB1	356x171UB45	457x152UB52	10 mm	-	Bare steel test
BTB2	-do-	-do-	-do-	1%	
BTB3	-do-	-do-	-do-	-do-	Omit top row bolts
BTB4	457x152UB52	533x210UB82	10 mm	-	Bare steel test
BTB5	-do-	-do-	-do-	1%	
BTB6	-do-	-do-	-do-	1%	Omit 1st stud on each beam
BTB7	-do-	-do-	-do-	1.5%	Increased area of reinforcement

Table 2-2: Results of Concrete Strength Tests

Specimen	7 days (Average) N/mm^2	Test day (Average) N/mm^2	28 days (Average) N/mm^2	Tensile Strength f_{ctm} (Average) kN
BTB2	41.8	50.0	54.3	134
BTB3	37.3	44.1	50.1	116.3
BTB5	40.8	45.9	52.1	106.3
BTB6	40.5	44.9	46.5	122.3
BTB7	42.3	50.0	54.5	111.4

Table 2-3 : Coupon Test Results of Steel Sections

(i) Sample fo coupon test

(ii) Position of test sample

BTB1-BTB3	Average Yield Stress f_y N/mm²	Average Ultimate Stress f_u N/mm²	Average Elongation at fracture %	Average Young Modulus E kN/mm²
Secondary Beam (flanges)	315	462	34	191
Secondary Beam (webs)	384	530	30	210
Main Beam (flange)	318	488	33	196
Main Beam (web)	383	525	31	215
End Plate	258	425	35	196
BTB4-BTB7	Average Yield Stress f_y N/mm²	Average Ultimate Stress f_u N/mm²	Average Elongation at fracture %	Average Young Modulus E kN/mm²
Secondary Beam (flanges)	291	475	32	196
Secondary Beam (web)	348	519	33	215
Main Beam (flanges)	310	496	36	210
Main Beam (web)	333	494	32	194
End Plate	258	425	35	196

Table 2-4 : Tensile test result for the reinforcement

	Average Yield Stress f_y	Average Ultimate Stress f_u	f_u/f_y	Average Elongation at fracture	Average Young Modulus E	Average Ultimate Strain ε_u
	N/mm^2	N/mm^2		%	kN/mm^2	%
BTB2	505	594	1.18	22	195	14.1
BTB3	510	601	1.18	22	192	12.9
BTB5	508	605	1.19	22	197	13.3
BTB6	509	604	1.19	22	196	12.0
BTB7	508	599	1.18	22	191	13.3
A142 mesh	616	642	1.04	12	208	N/A

Table 2-5 : Summary of the test results

| Test	Shear Connection	Reinforcement	M_{cc} kNm	M_{esp} kNm	ϕ_{esp} mrad	ϕ_{ult} mrad	Mode of failure
BTB1	-	-	45	68	43.4	43.4	Deformation of end plate and bolt stripped
BTB2	FULL	(4T16) 1%	221	253	32	41.5	Fractured of mesh plus rebars and local buckling of lower flanges.
BTB3	FULL	(4T16) 1%	195	235	9	40	Deformation of end plate and excessive bending
BTB4	-	-	78	123	27	42	Deformation of end plate
BTB5	FULL	(4T16) 1%	292	350	46	54	Fracture of mesh plus rebar and local buckling of lower flanges
BTB6	FULL	(4T16) 1%	292	335	37	53	Excessive cracking of concrete, local buckling of lower flanges and deformation of end plate
BTB7	PARTIAL	(6T16) 1.5%	398	398	8	15	Significant slip at interface, deformation of stud and local buckling.
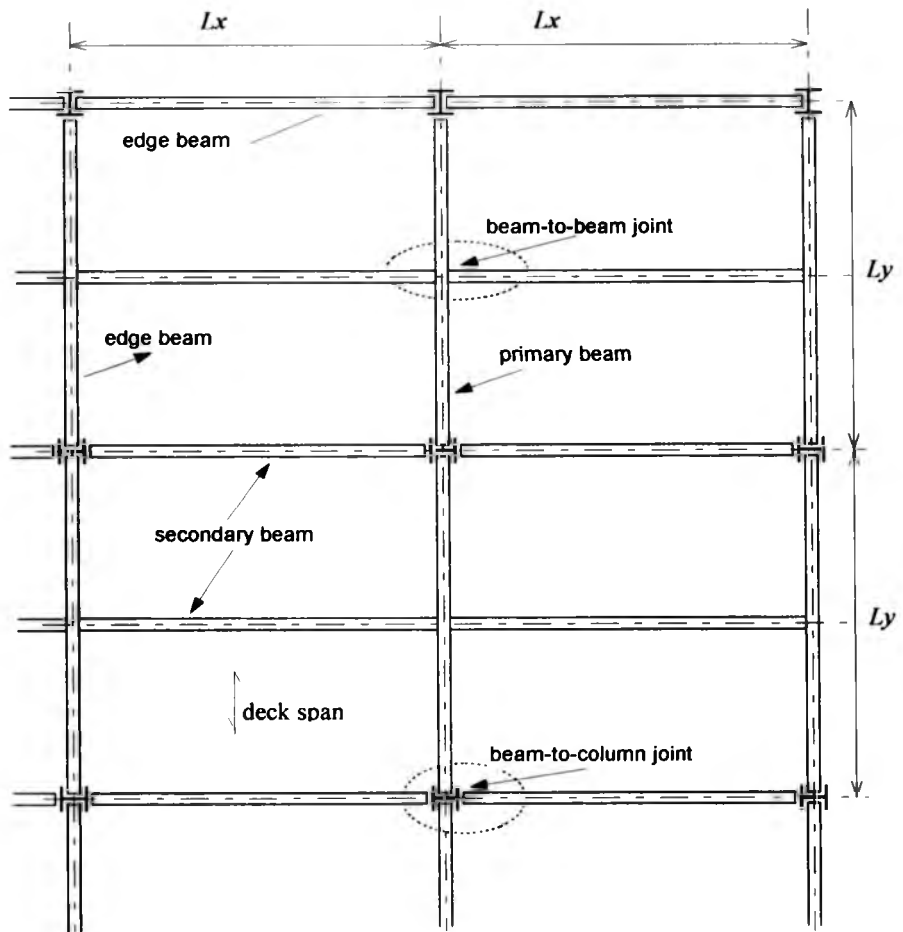
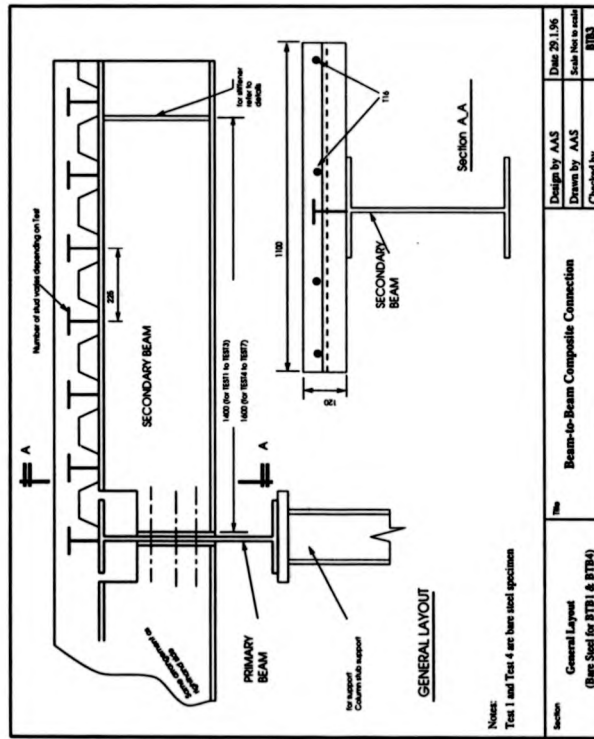*Fig. 2-1 : Typical floor plan of composite construction*

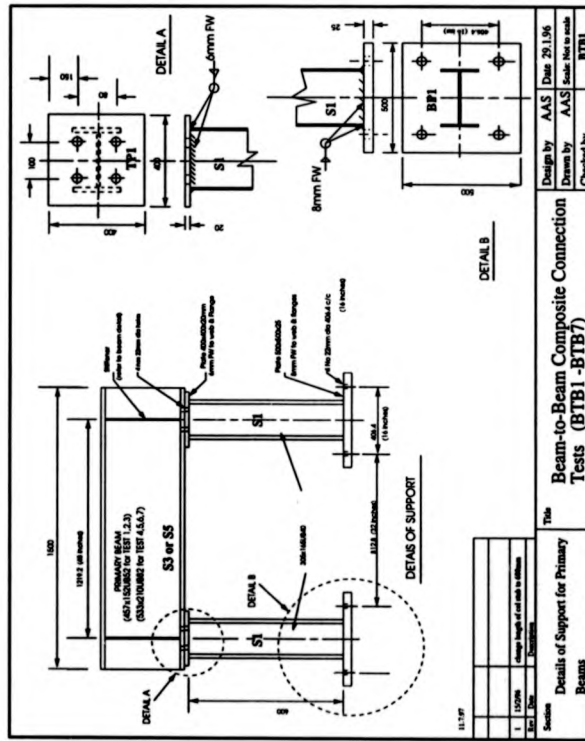*Fig. 2-2 : General arrangement of specimens*

Fig. 2-3 : Details of short steel column
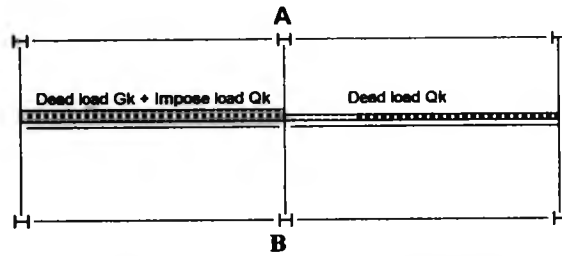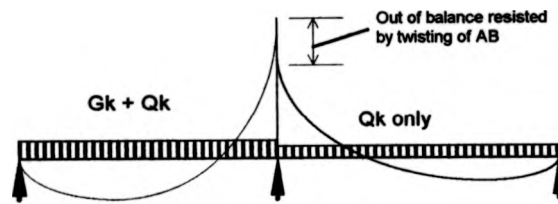
(a) The possibility of unbalanced load on beam configuration

(b) Unbalanced moment

Fig. 2-4 : Justification for assumed balanced moment

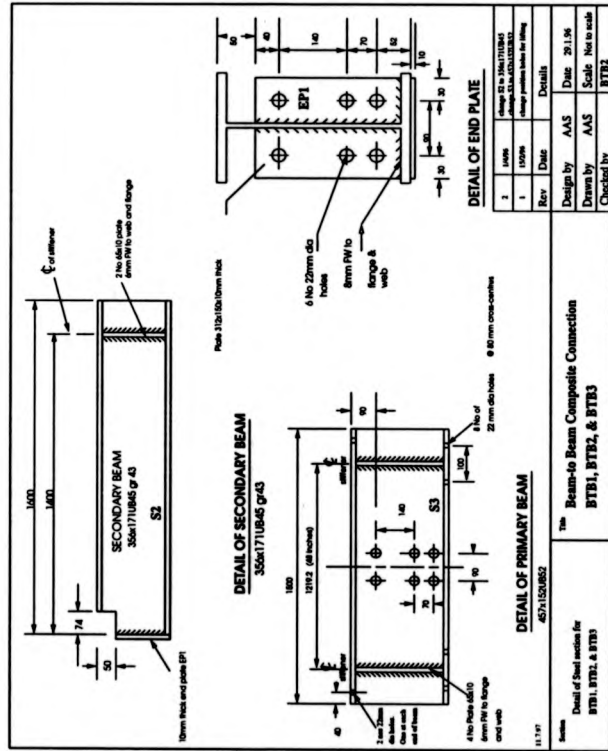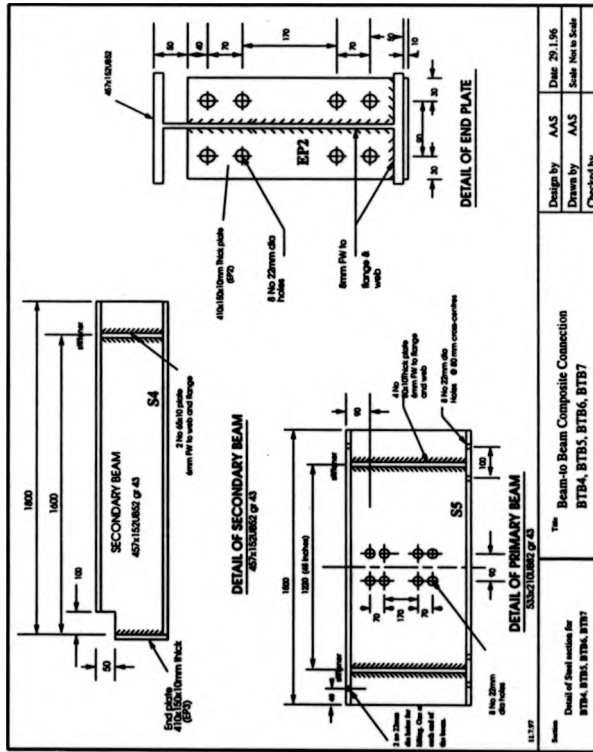Fig. 2-5 : Steel details for BTB1, BTB2 and BTB3

Fig. 2-6 : Steel details for BTB4 - BTB7
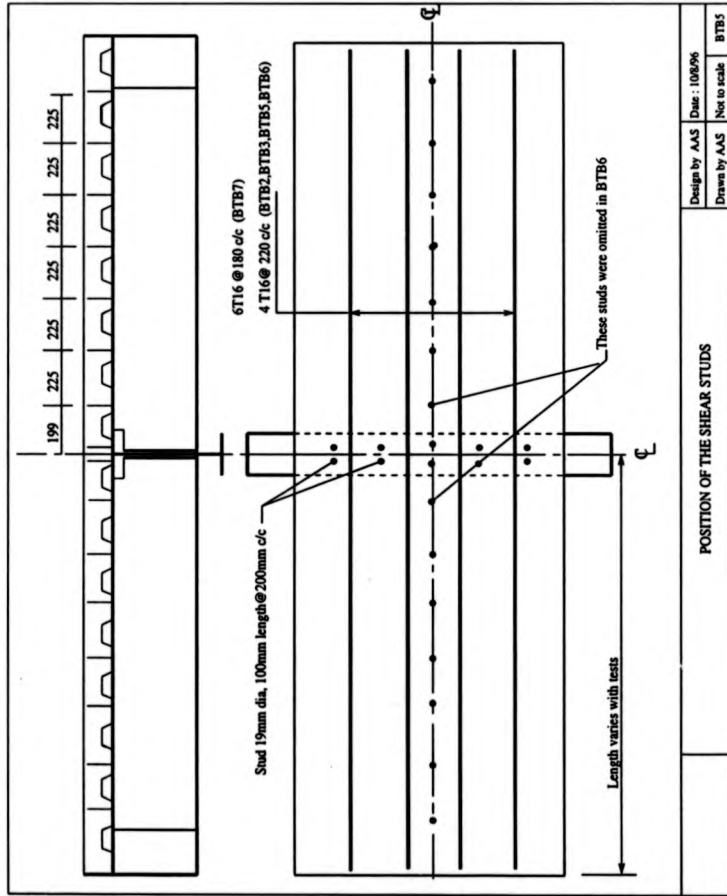
Fig. 2-7 : Position of shear studs
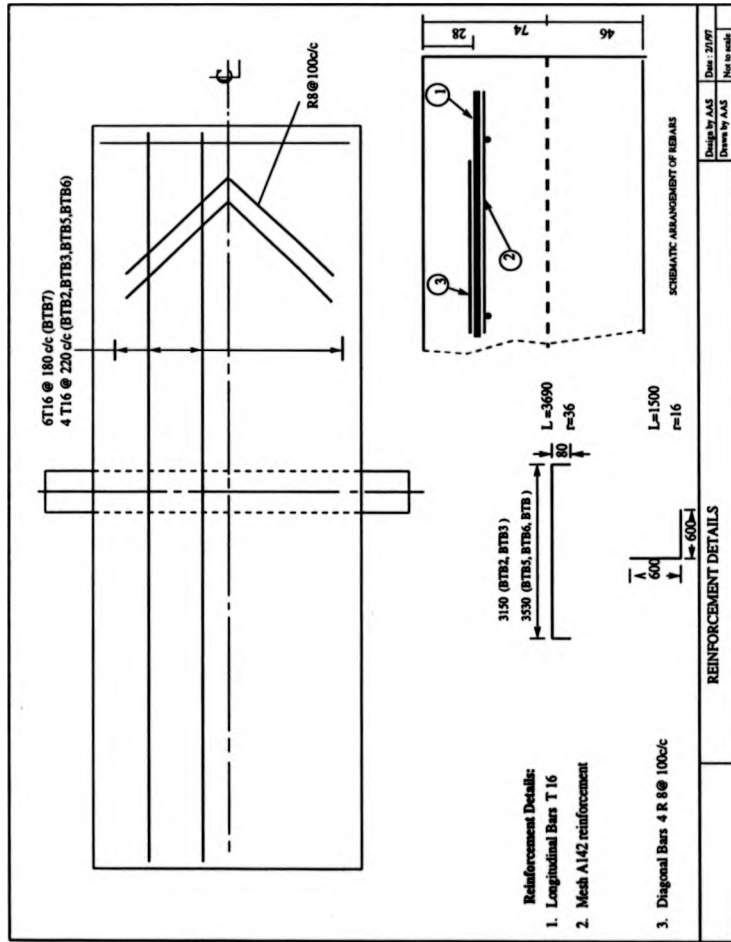
Fig. 2-8 : Reinforcement details

Fig. 2-9a : Front elevation of test rig
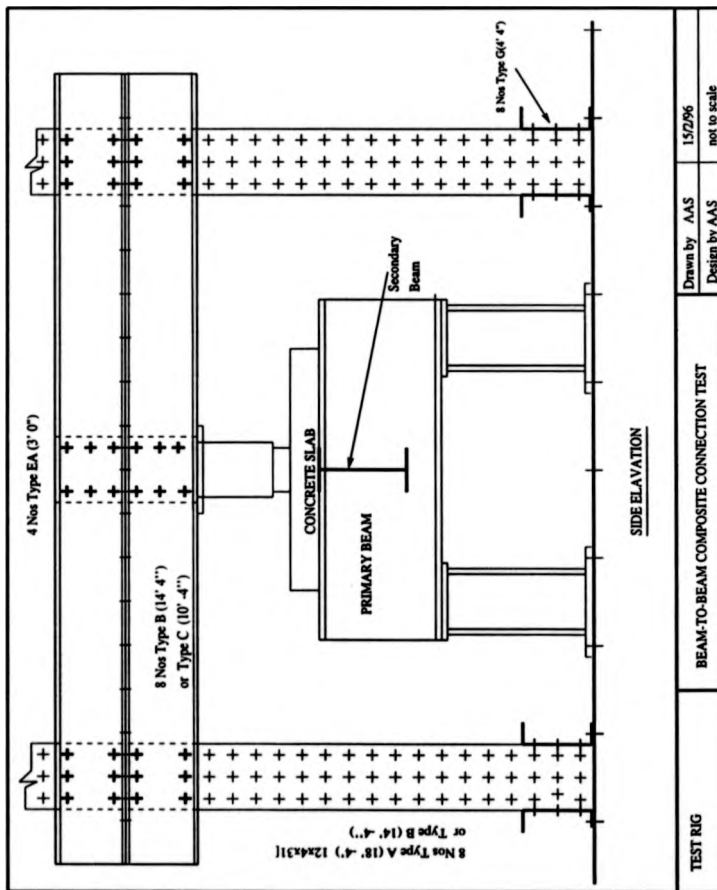
Fig. 2-9b : Side elevation of test rig
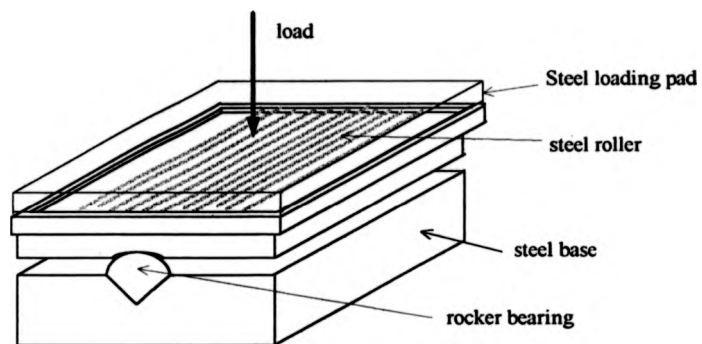
Fig. 2-10 : Uni-directional rocker for load application point
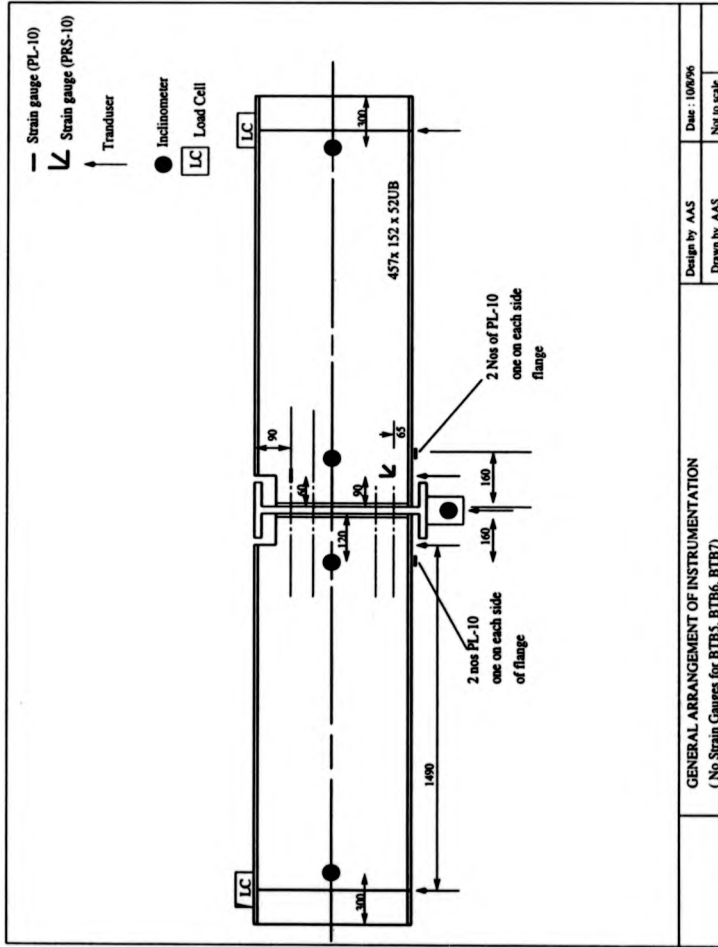
Fig. 2-11 : General arrangement of instrumentation on steel beam

BTB1
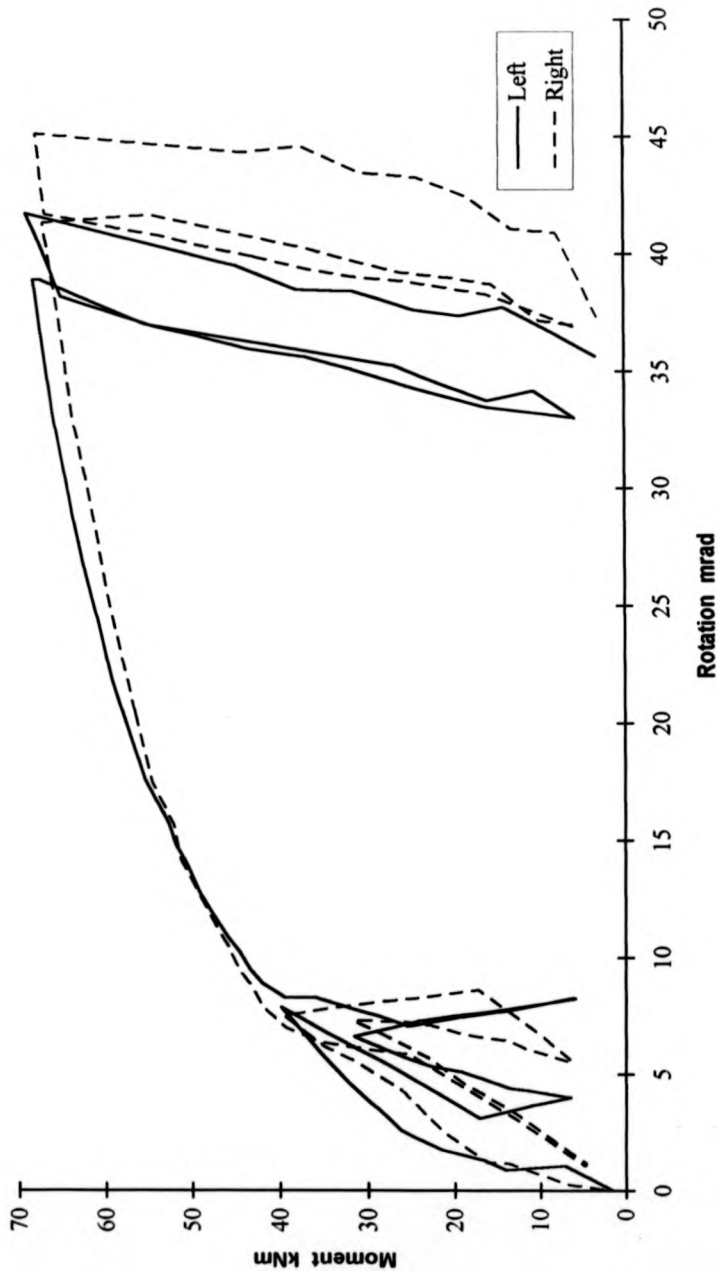
Fig. 2-12a : Moment vs Rotation (BTB1)

BTB1
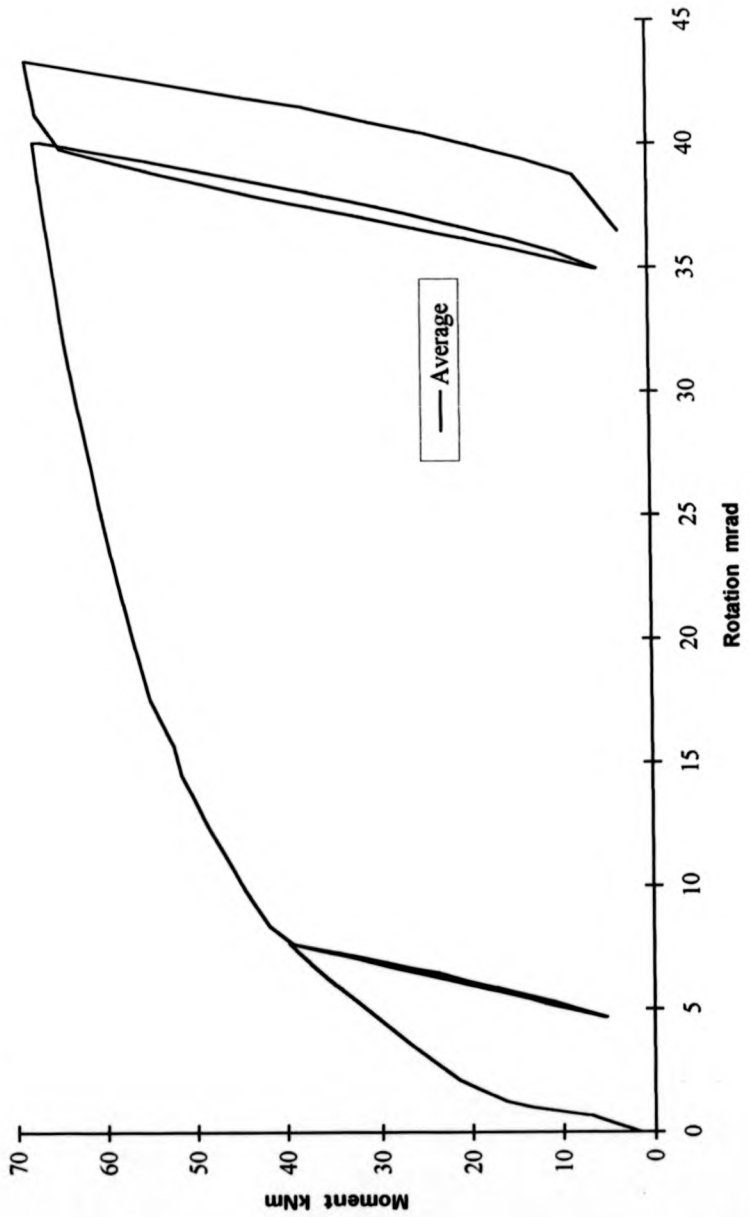
Fig. 2-12b : Average value of Moment vs Rotation for BTB1

BTB2
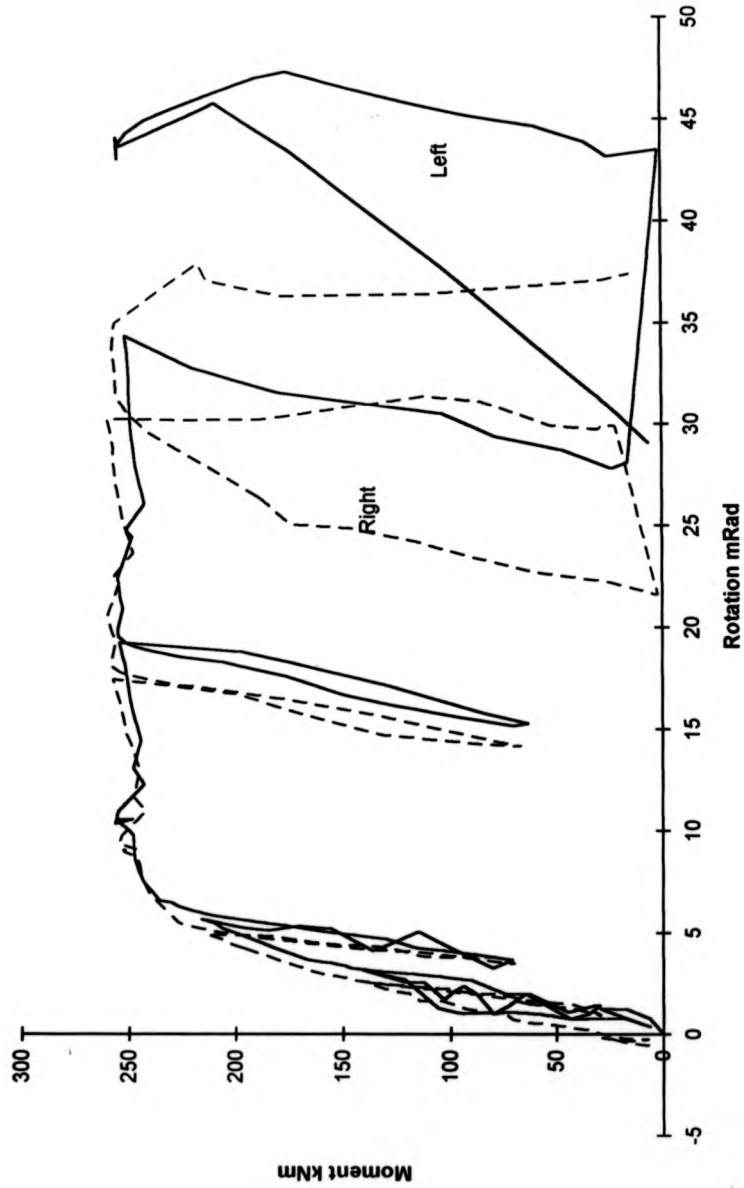
Fig. 2-13a : Moment vs Rotation (BTB2)
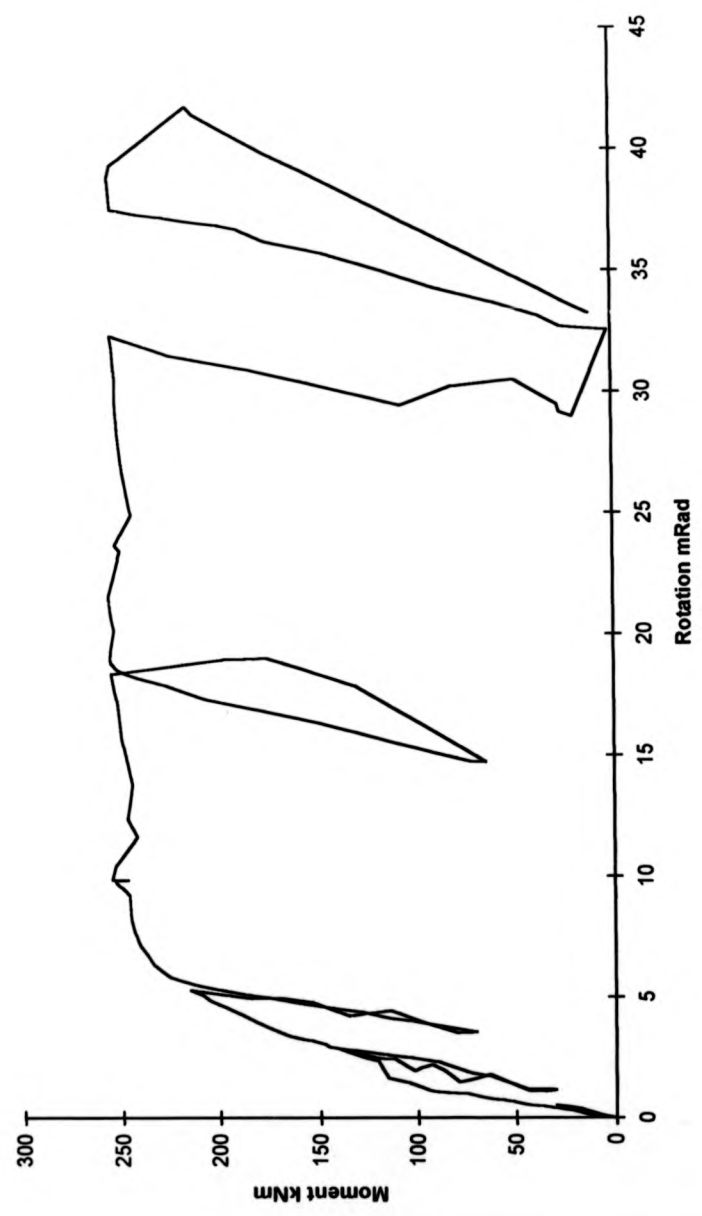
Fig. 2-13b: Average value of Moment vs Rotation for BTB2
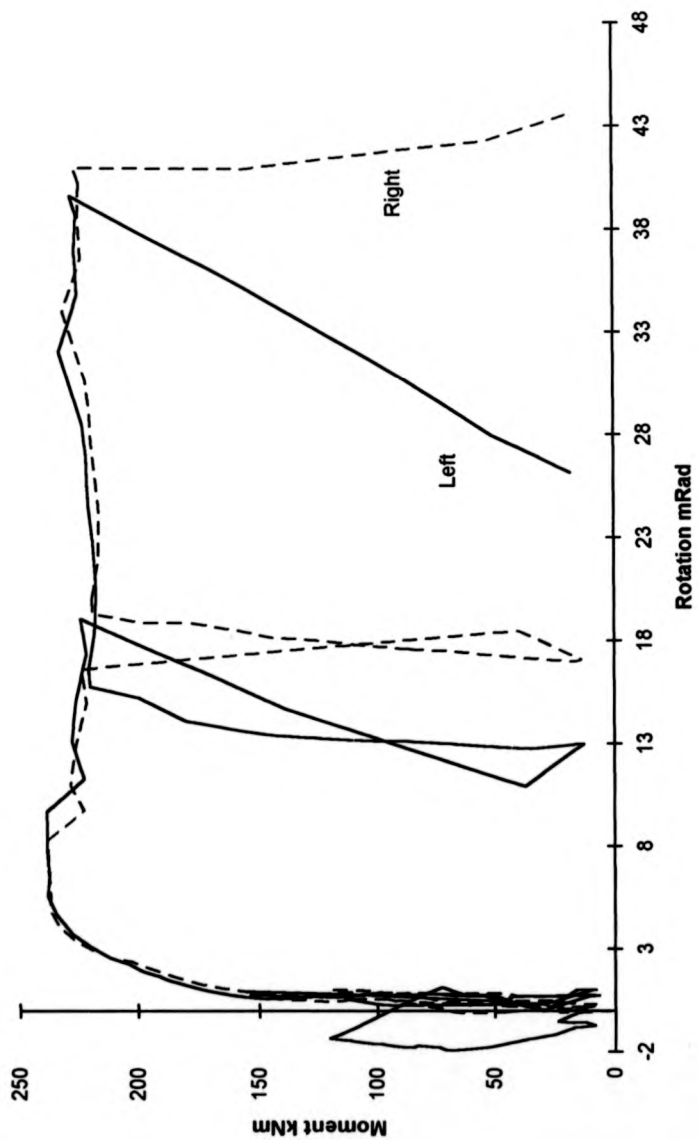
Fig. 2-14a : Moment versus Rotation (BTB3)

BTB3
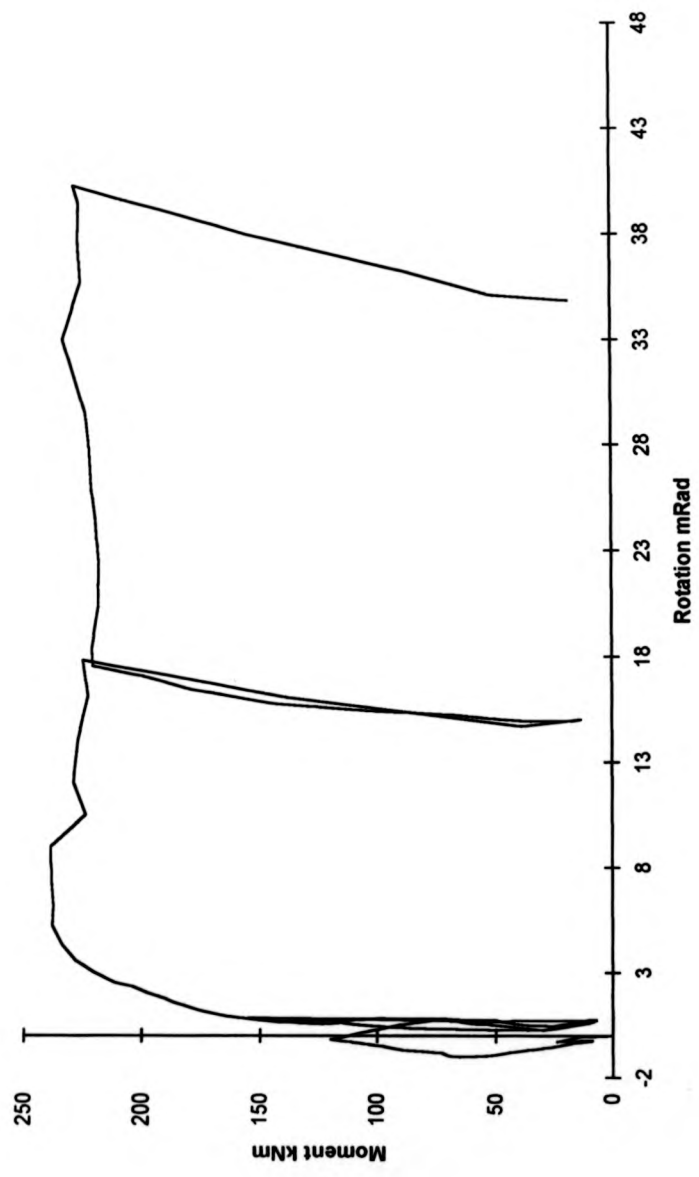
Fig. 2.14b : Average Value of Moment vs Rotation (BTB3)

BTB4
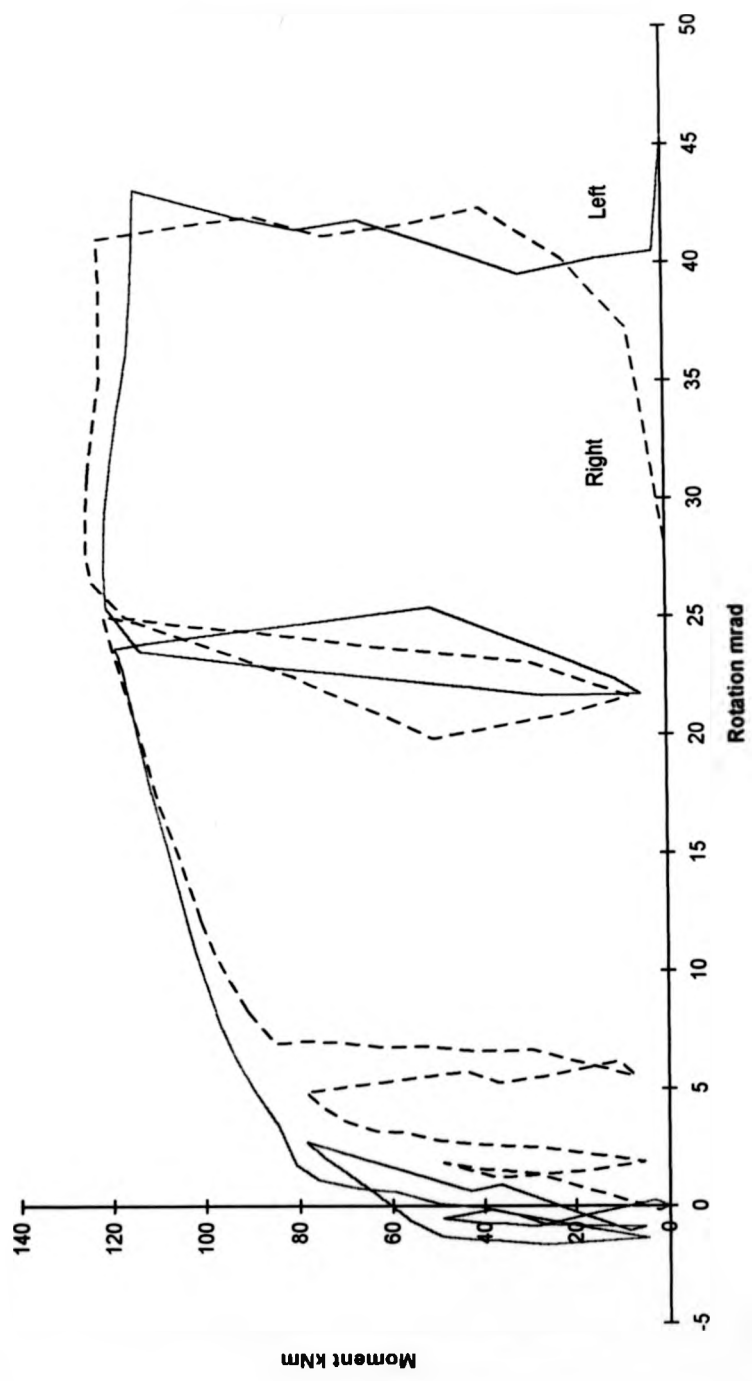
Fig. 2-15a : Moment vs Rotation (BTB4)

BTB4
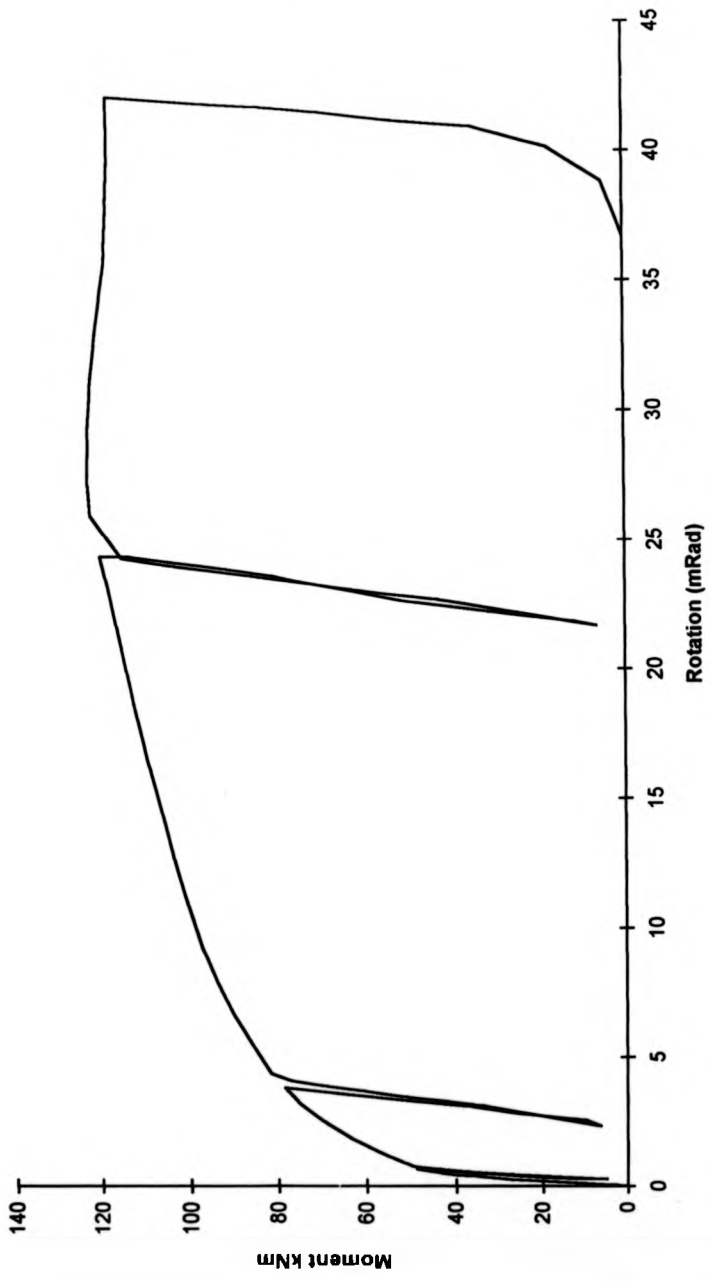
FIG. 2.15b : Average Value of Moment vs Rotation (BTB4)

BTB5
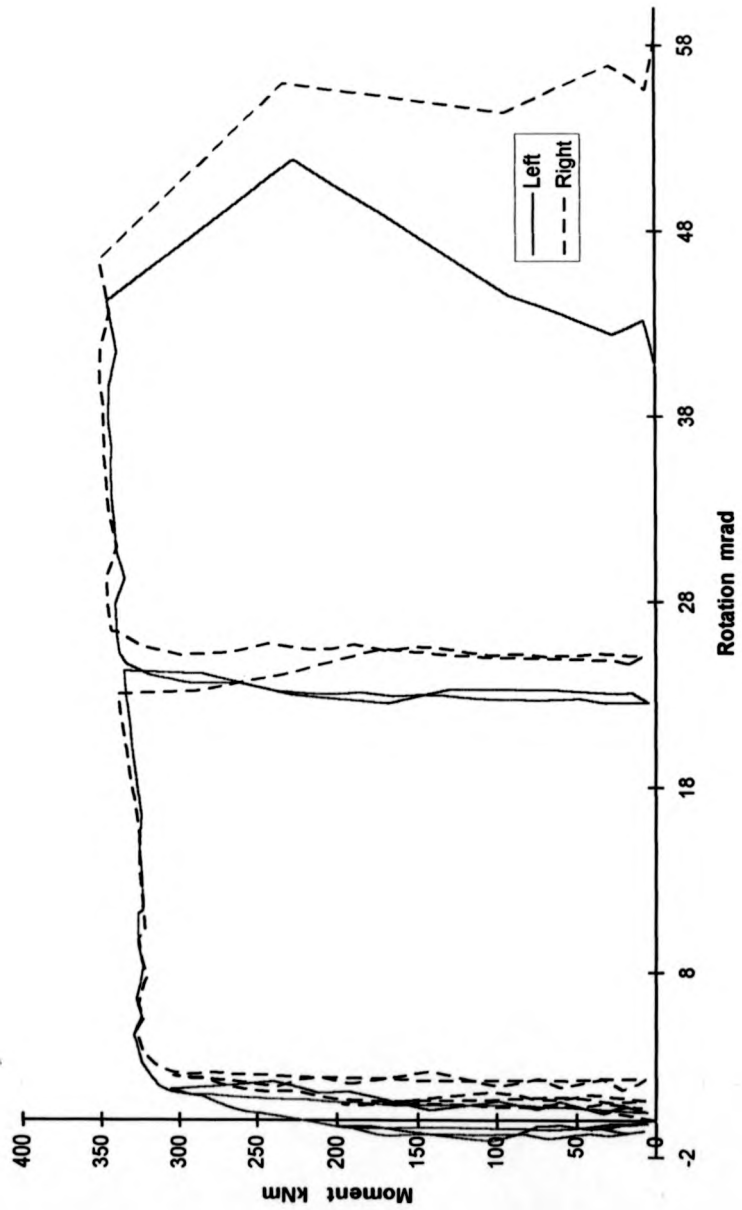
Fig. 2-16a : Moment vs Rotation (BTB5)
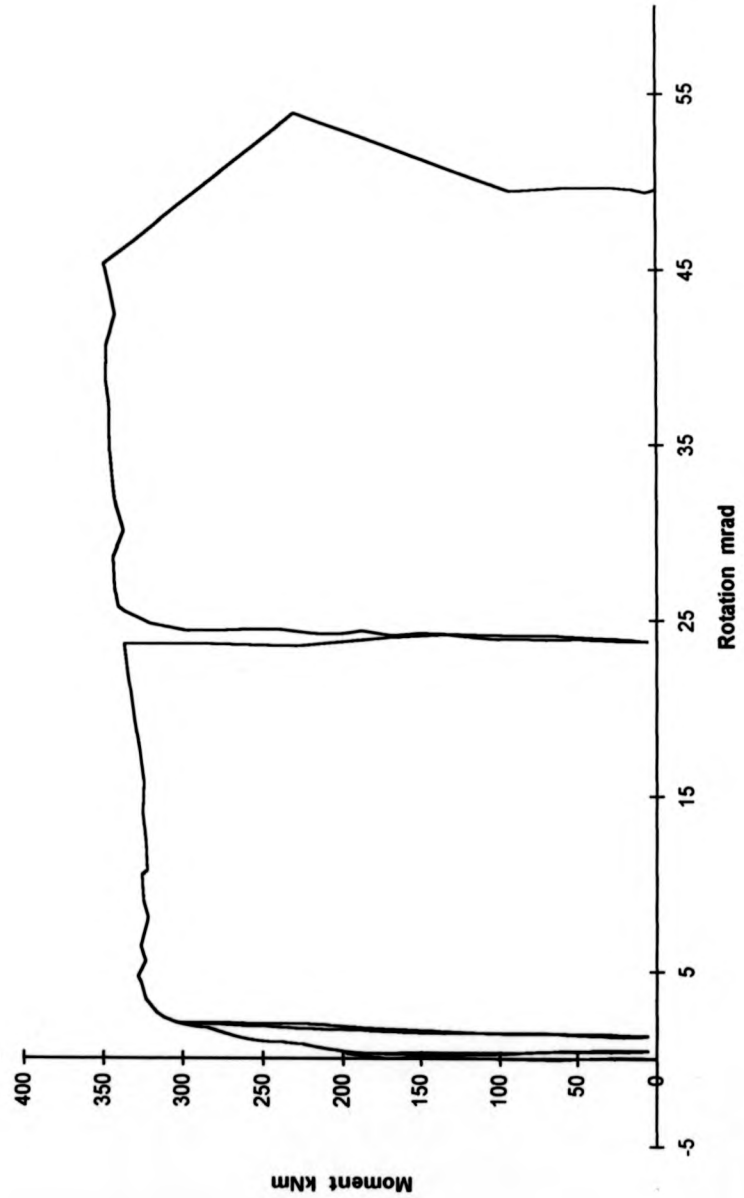
Fig. 2-16b : Average value of Moment vs Rotation (BTB5)

BTB6
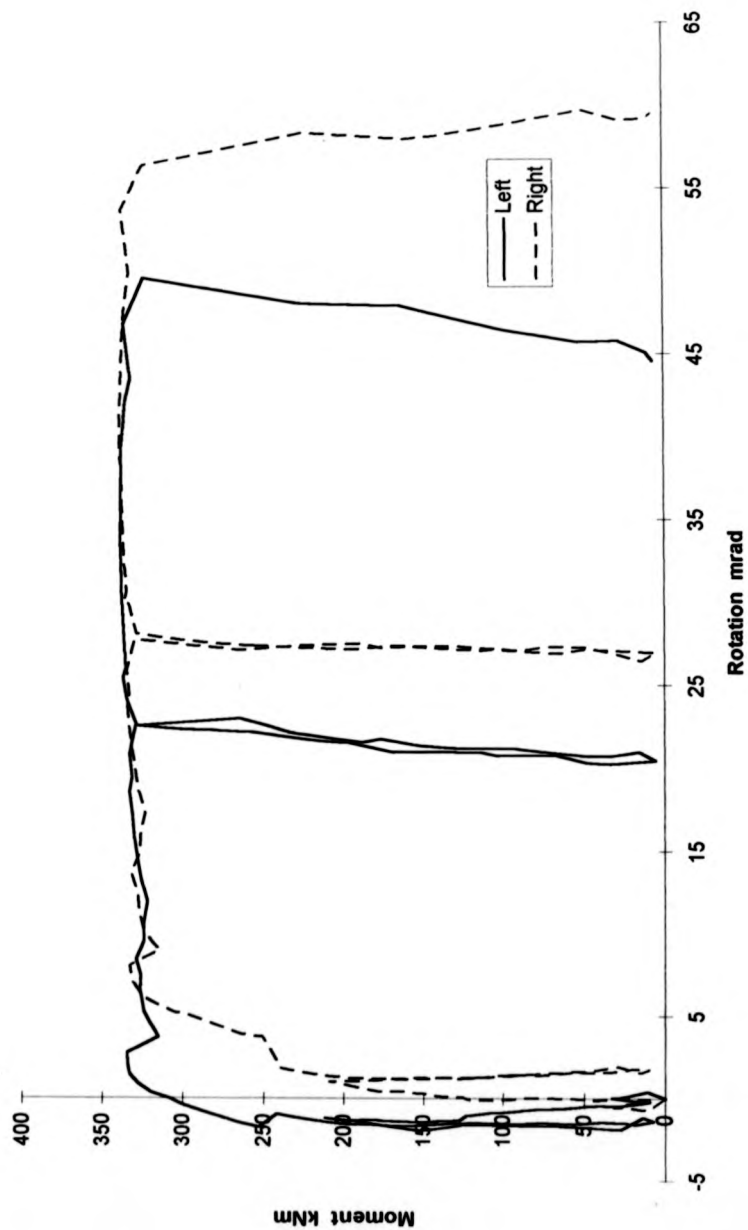
Fig. 17a : Moment vs Rotation (BTB6)
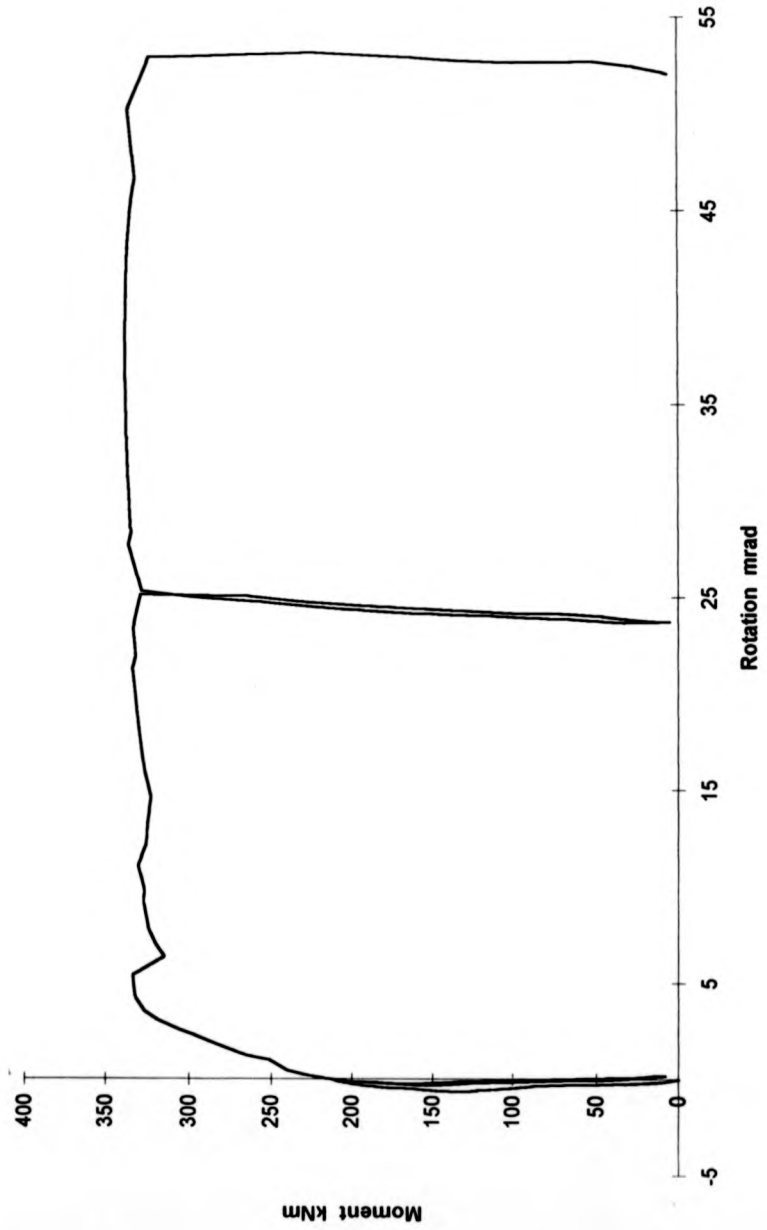
Fig. 2-17b : Average value of Moment vs Rotation for BTB6
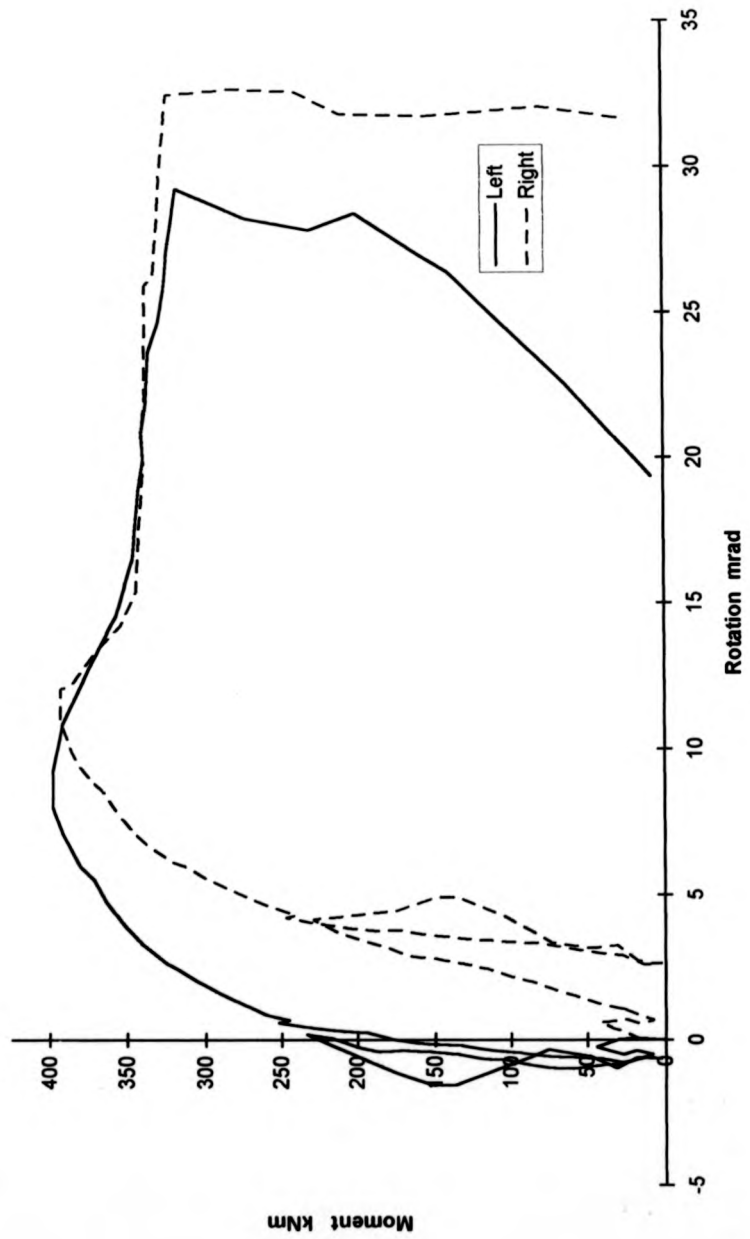
Fig. 2-18a : Moment vs Rotation (BTB7)
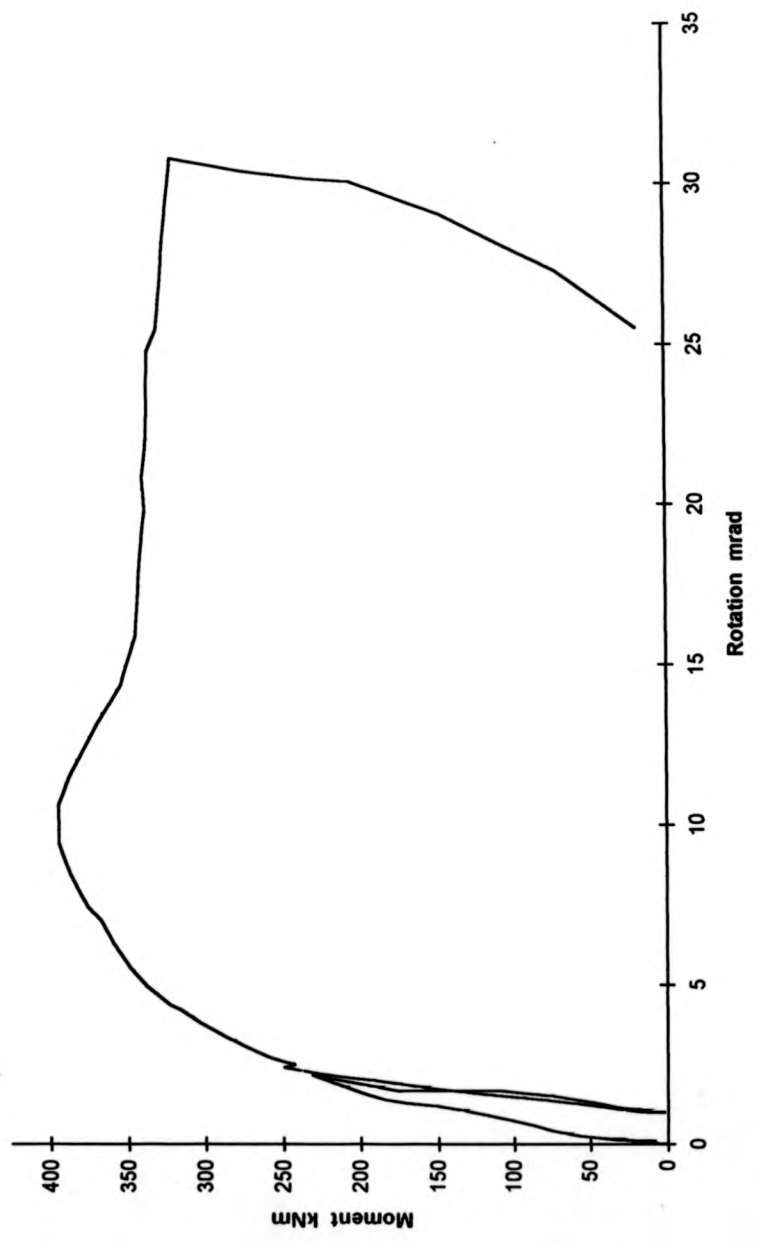
Fig. 2-18b : Average value of Moment vs Rotation for BTB7
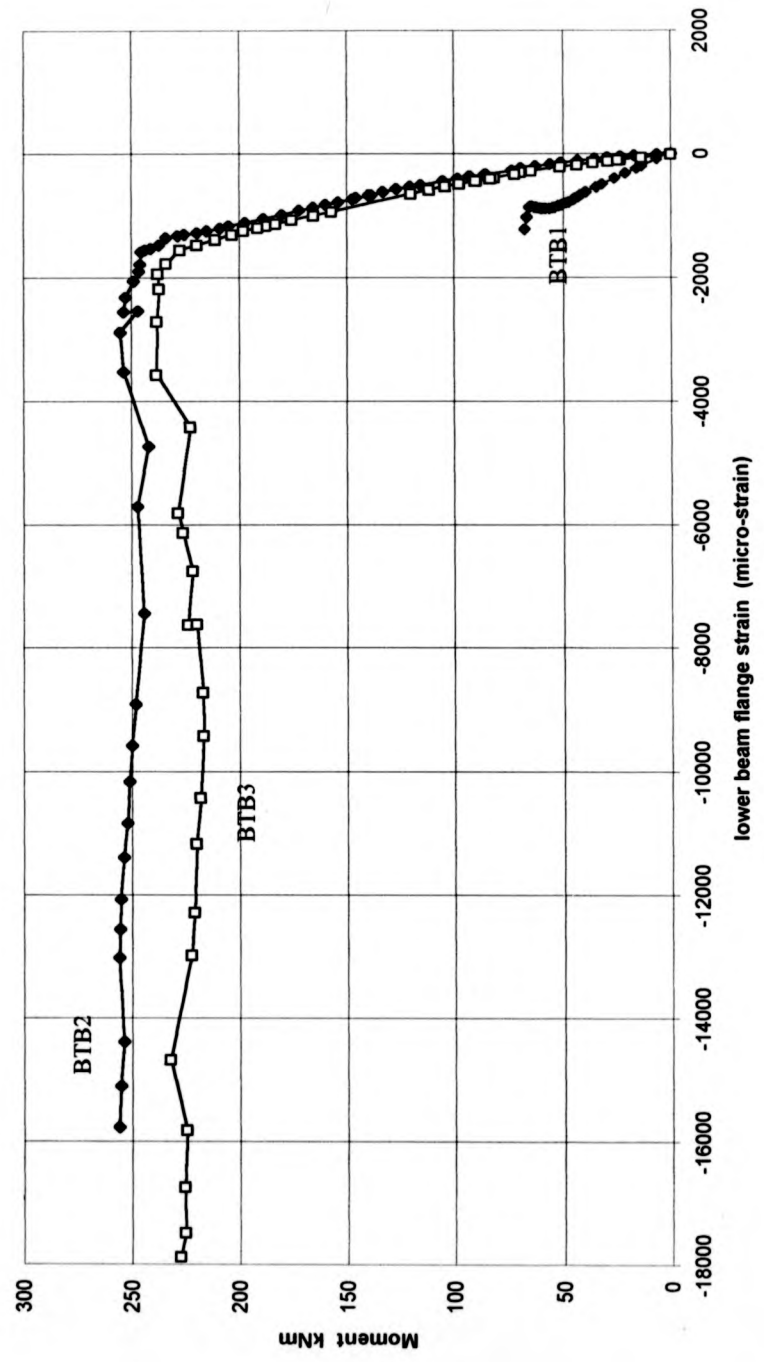
Fig. 2-19 : Comparison of lower flange beam strain
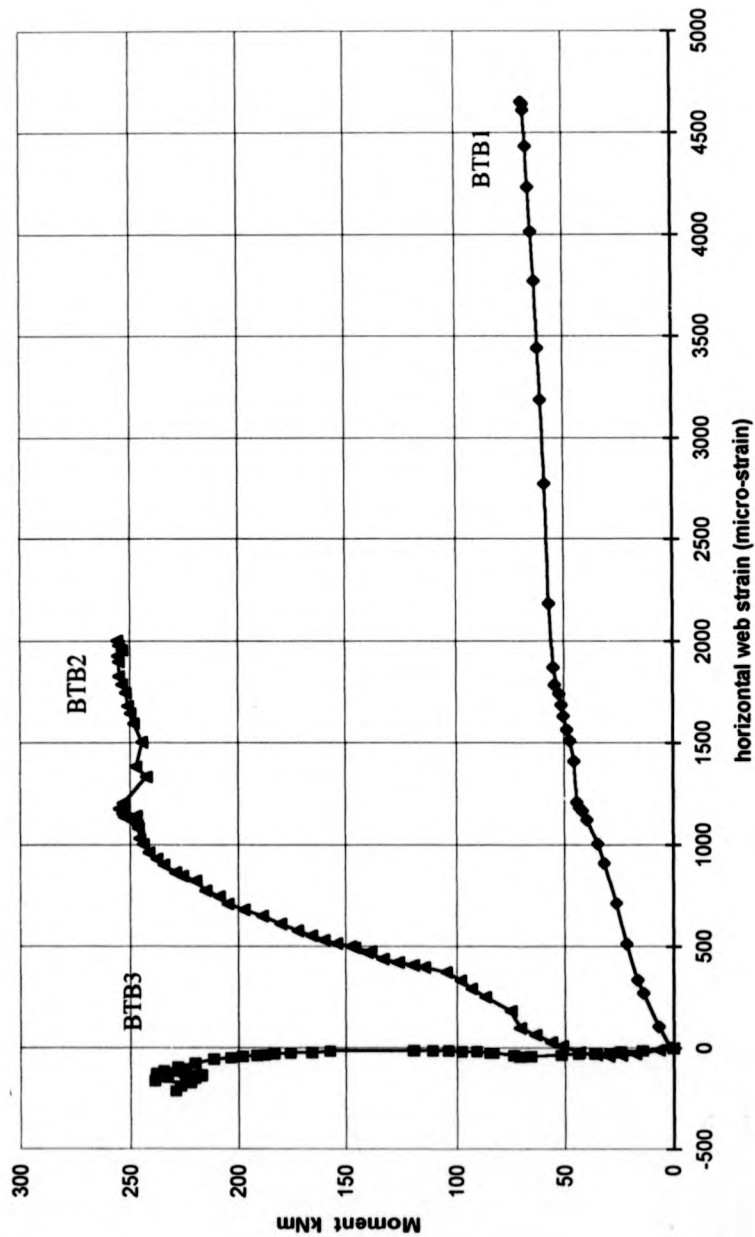
Fig. 2-20 : Comparison of beam web horizontal strain

Moment vs rebar strain(BTB2)
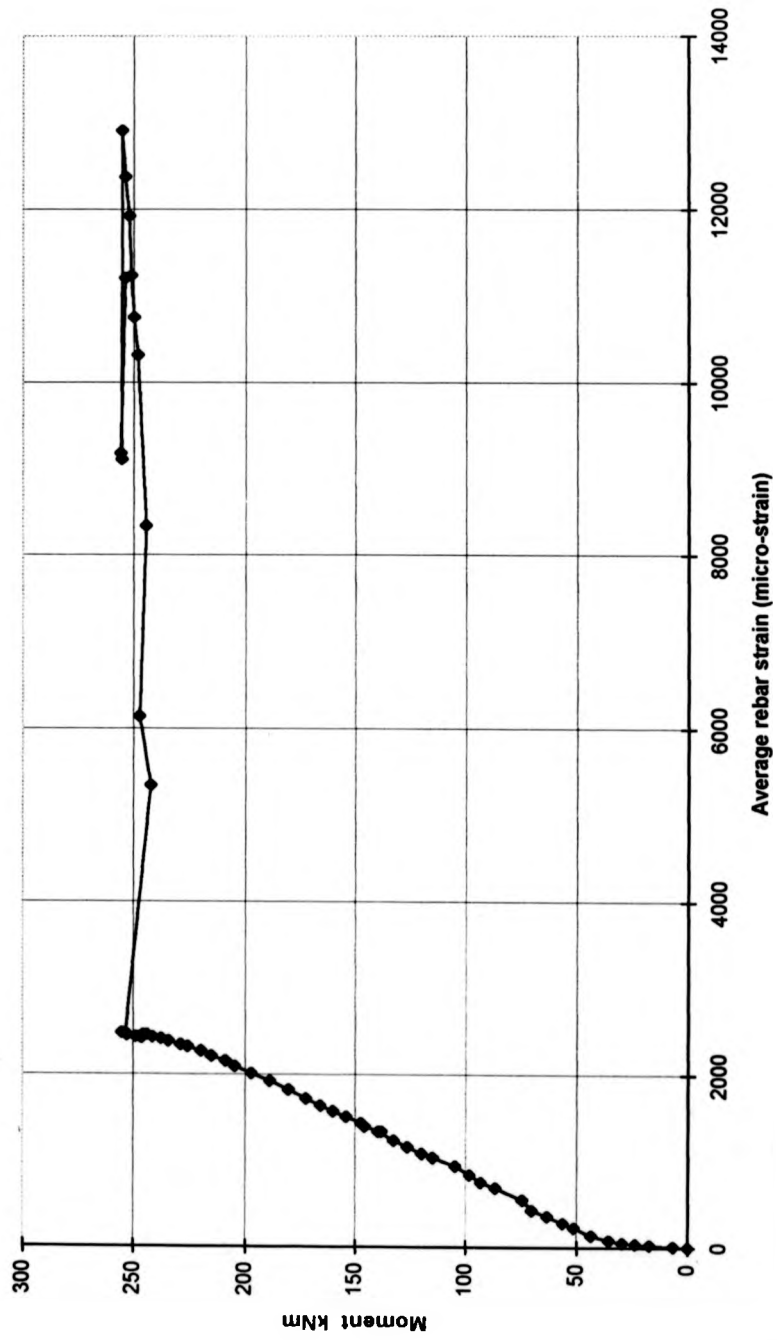
Fig. 2-21 : Average rebar strain of the most critical rebar for BTB2
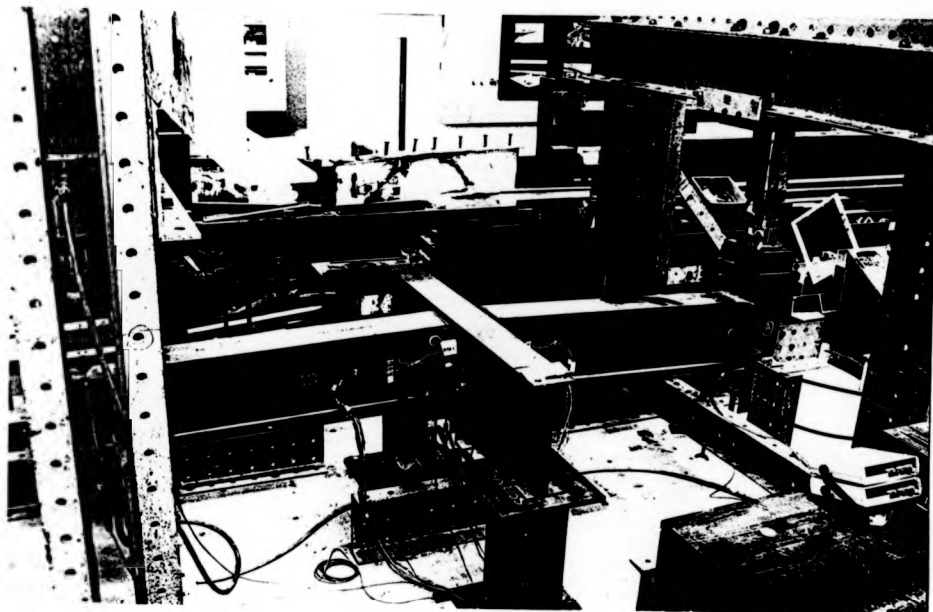
Plate 2-1(a) :General view of BTB1 after the test

Plate 2-1 (b) : Tranverse deformation of end plate

Plate 2-1(c) : Bending of end plate between 1st row and 2nd row bolt

__PLATE 2-1 : Specimen BTB1__
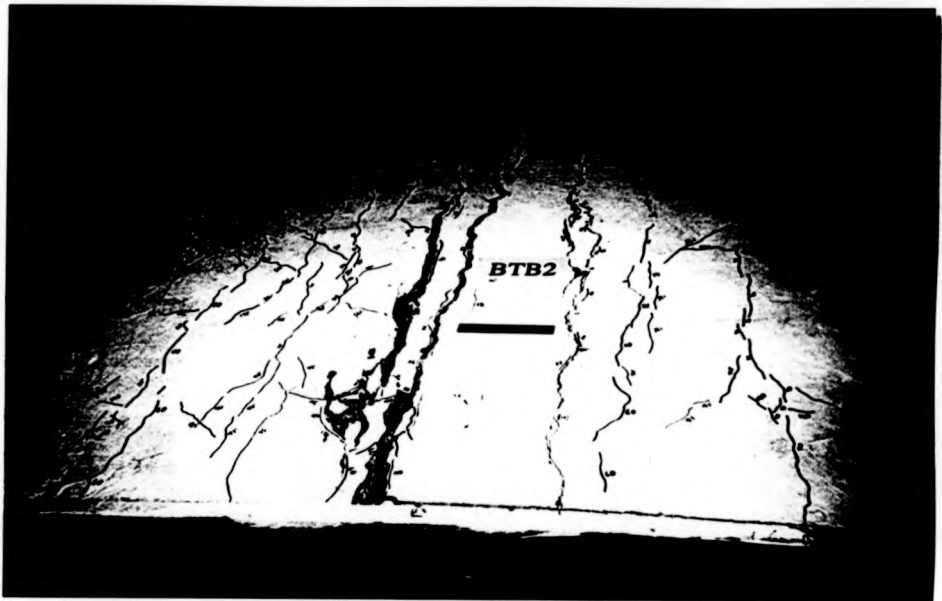
Plate 2-2(a) : Cracks pattern of BTB2
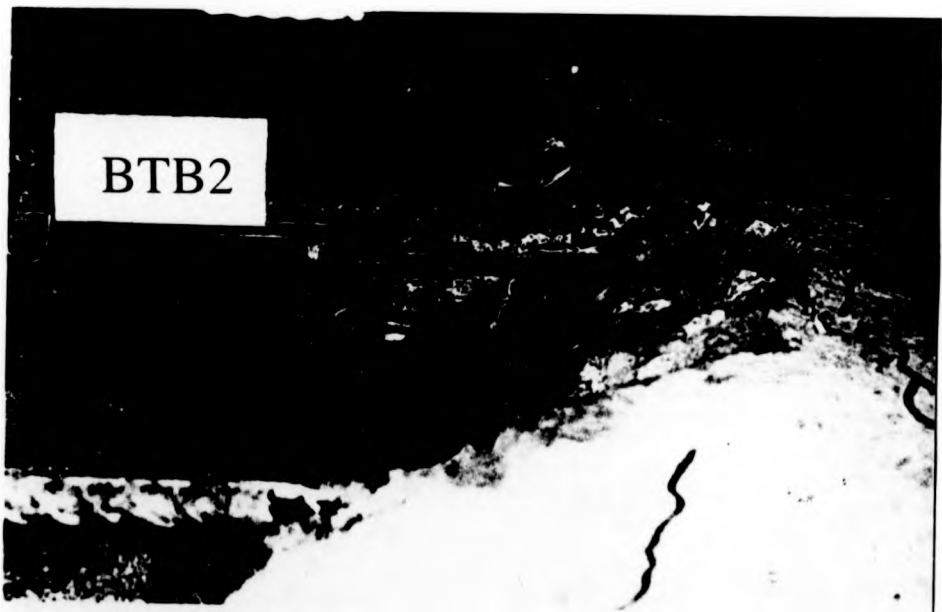
Plate 2-2(b) : Rebar and mesh fractured
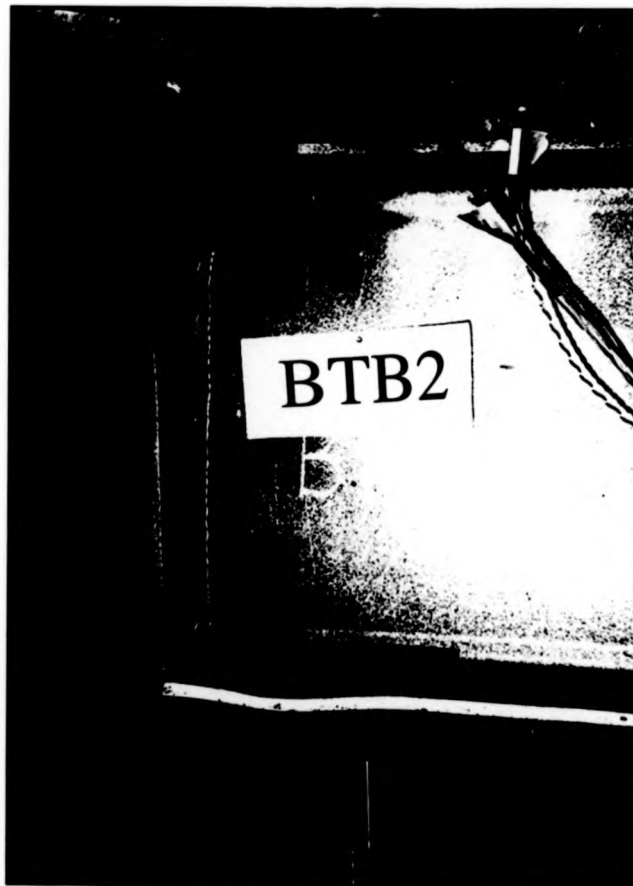
Plate 2-2(c) : Local buckling and end plate deformation (BTB2)

PLATE 2-2 : Specimen BTB2

Plate 2-3(a) : Cracks pattern of BTB3
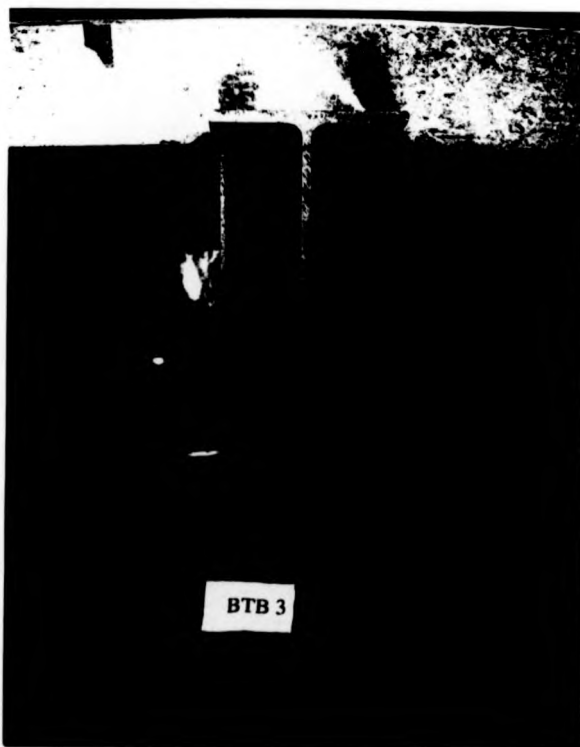
Plate 2-3(b) : Flanges of primary beam not parallel
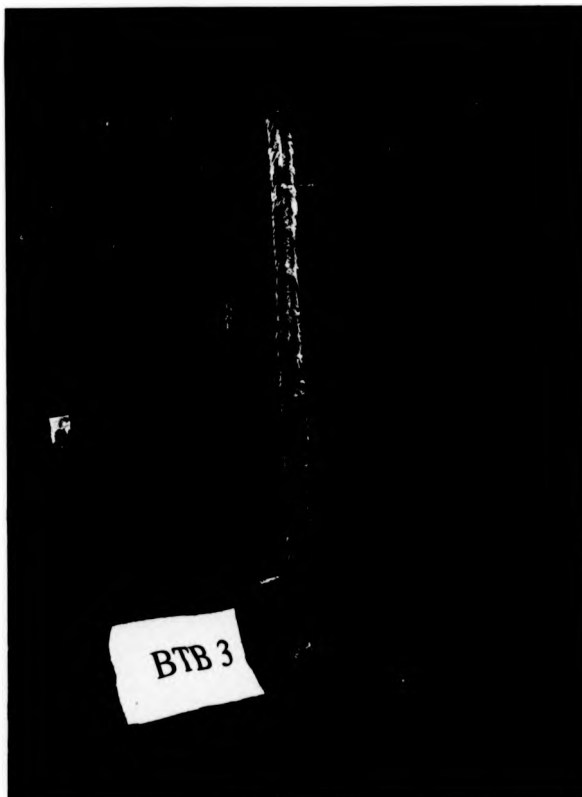
Plate 2-3(c) : Deformation of end plate and local buckling of lower flange

PLATE 2-3 : Specimen BTB3

Plate 2-4(a) : General view of BTB4 after the test

Plate 2-4(b) : Deformation of end plate

PLATE 2-4 : Specimen BTB4
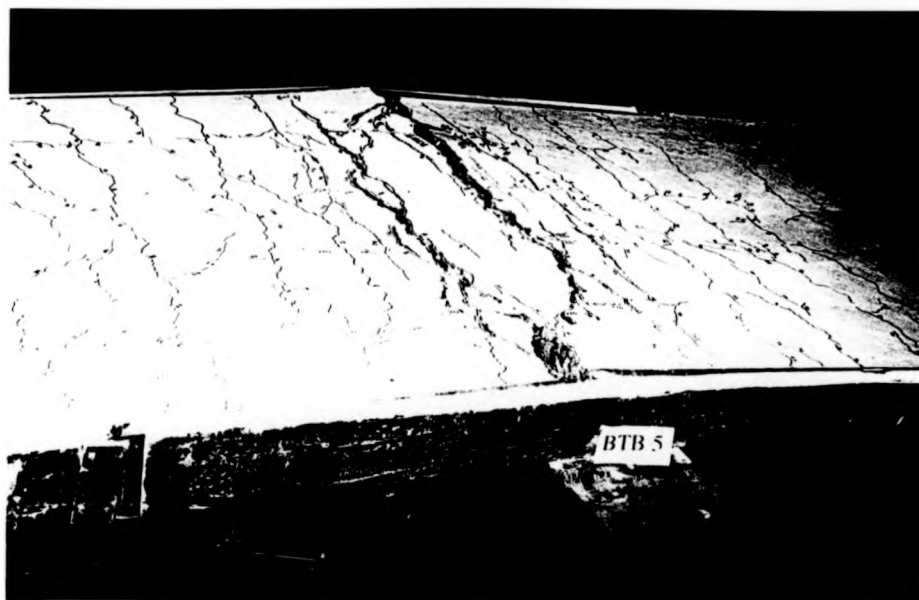
Plate 2-5(a) : Cracks pattern of BTB5

Plate 2-5(b) : Fractured rebar and mesh

Plate 2-5(c) : Deformation of end plate and local buckling of lower flange

PLATE 2-5 : Specimen BTB5
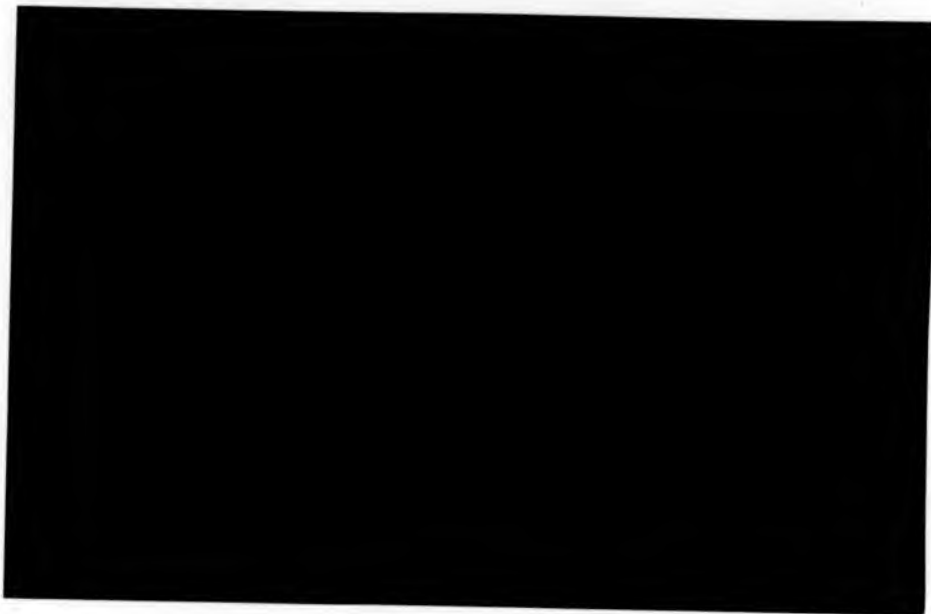
Plate 2-6(a) : Wide cracks at shear studs position (BTB6)

Plate 2-6(b) : No deformation occured to shear stud
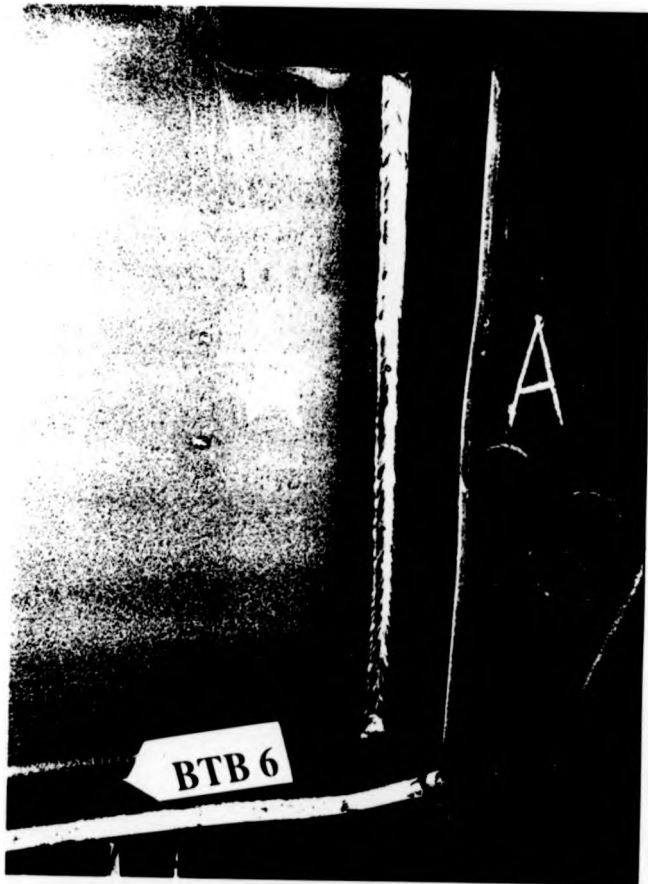
Plate 2-6(c) : Local buckling of lower flange and deformation of end plate

PLATE 2-6 : Specimen BTB6
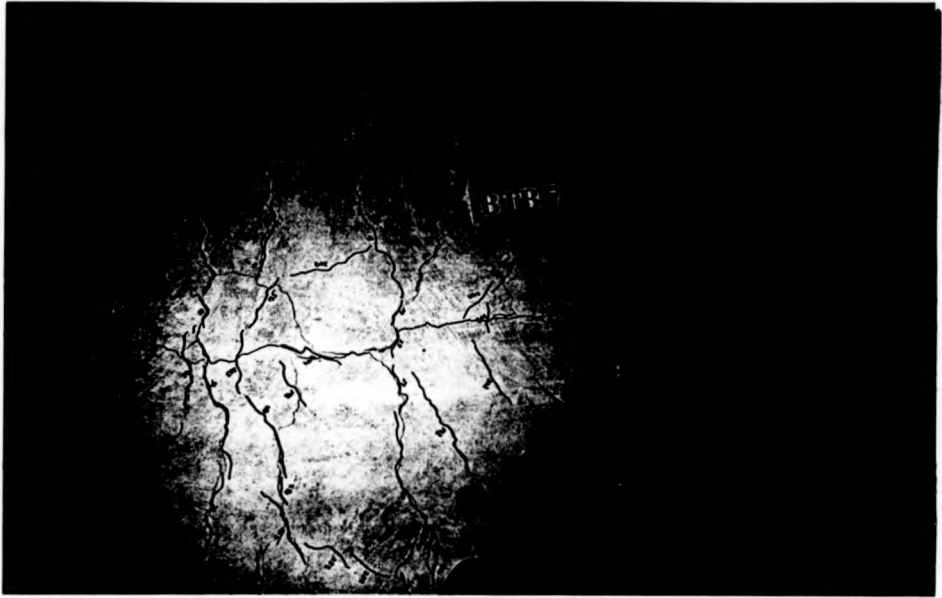
Plate 2-7(a) : Cracks pattern of left beam

Plate 2-7(b) : Local buckling of lower flange and the deformation of end plate
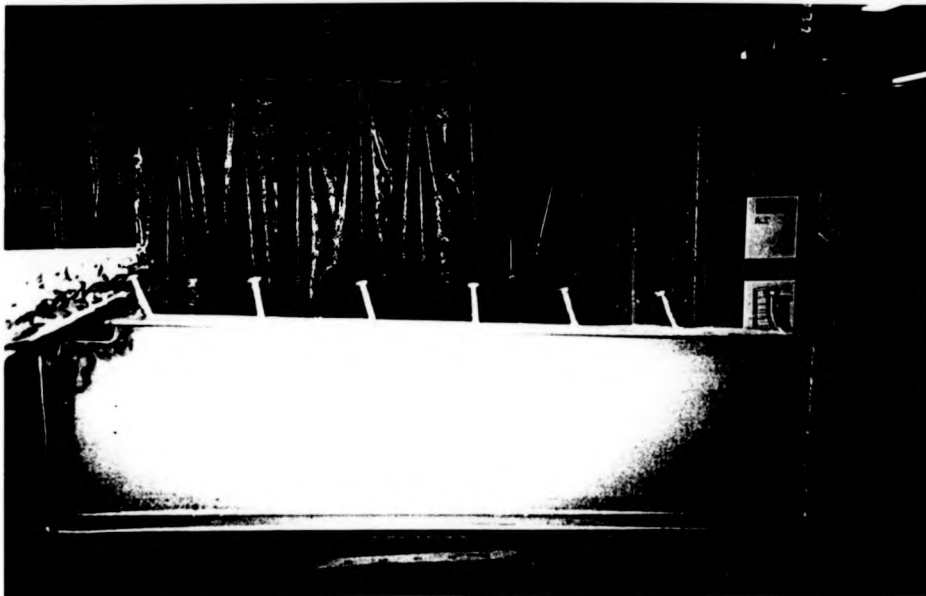
Plate 2-7(c) : Deformed shear stud connectors

Plate 2-7(d) : Slip at steel and concrete slab interface

PLATE 2-7 : Specimen BTB7

Chapter 3

ASSESSMENT AND ANALYSIS OF BEAM-TO-BEAM COMPOSITE CONNECTION TESTS

3.1   Introduction

The testing procedure and test observations have been described in Chapter 2. The experimental results are now compared with the predictions for the key elements of the moment-rotation characteristic namely the stiffness, moment resistance and rotation capacity of the joint.

The predicted resistance of both beam and connection are based on measured thicknesses and material properties as given in Table 3-1 and Table 3-2, although nominal values of plastic modulus S_{xx} and second moment area I_{xx} are taken for the proposed calculations. Additionally classifications both by strength and rotational stiffness have been made according to EC3[3-1] and EC4[3-2]. This requires calculation of beam properties, as explained in Chapter 1. The symbols in this diagram have already bee defined in Chapter 1. For the proposed classifications the experimental values of the initial stiffness $S_{j,ini}$ are taken from the gradient of the loading-unloading part of the

average M-ϕ curves obtained in the test. The moment rotation curves of all the tests have been given in Figs. 2-12 to Fig. 2-18.

A prediction method for estimating the initial stiffness $S_{j,ini}$ of connection based on the model[3-12] shown in Fig. 3-1 is given in this chapter. The predicted $S_{j,ini}$ is compared to the experimental result for the verification of the method and also to the results of several previous researchers[3-3, 3-4].

In the tests variation in some parameters were investigated. The effects in the tests of the various changes made are also presented and discussed in this chapter.

3.2   *Classification of section for local buckling*

The beams' plastic hogging moment resistance $M_{pl.Rd}$ were determined based on the formulae of Appendix B and Appendix C of BS 5950 Pt 3.1[3-5]. The calculation takes into consideration the "hole-in-the-web" approach which had been described in Chapter 1. The contribution of the mesh was not taken into account in this ultimate limit states calculation due to its low ductility (see Table 2-4). The classification of the steel and composite beams for local buckling was carried out by comparing the maximum width-to-thickness ratios for both the flanges and the webs of the section to the limit specified in *Table 4.1* and *Table 4.2* of EC4[3-2].

Table 3-3 gives the member classification for local buckling. It can be seen that the bare steel sections (BTB1 and BTB4) were classified as Class 2 (compact) and Class 1 (plastic). The effects of composite action to the beams however increases significantly the moment resistance of the beam but the same time reduces the class of the section to Class 3 (semi-compact). This is due to the shift in the position of plastic neutral axis which results in more depth of web being in compression. Thus the section was more

prone to local buckling. As can be seen from Table 2-5, local buckling is one of the modes of failure for connections BTB2, BTB5, BTB6 and BTB7.

3.3 Classification of bolted end plate beam-to-beam connections

The procedure to classify the connections (both composite and steel only) has already been described in Chapter 1. Classification limits have been proposed in terms of both strength and rotational stiffness for joints in braced frames. Prior to classifying the connections, the moment resistance of the connection needs to be established first.

For the bare steel connections, the tensile resistance of the steelwork components (the bolts, welds and the end plate) were determined using Annex J of EC3[3-6]. The moment resistances were then calculated, multiplying the tensile resistances by the respective the lever arm (from the mid-level of the bolts to the middle of lower (compression) flange).

For the composite connections on the other hand, the moment resistances of the connections were evaluated by two methods. The first method used the prediction model of the interim SCI guide[3-7] for flush end plate connections. The second one was to use the EC4[3-2] method. Both of the methods are outlined in Chapter 1.

Table 3-4 gives the comparison between the moment of resistance obtained from the tests and the predicted values. For the composite connection the corresponding values without the tensile action of top row bolts are also given. It can be seen that the predictions from both methods produce a significant underestimate of the true moment achieved in the test. However it can also be seen that the predicted moment resistance of the connections approximate to the "knee" of the experimental moment-rotation curves (Fig. 2-12 to Fig. 2-18). The "knee" refers to a position on the moment-rotation curves

where substantial loss of stiffness begins to show. It is understandable because the revised Annex J of EC3[3-6] itself, of which the prediction methods depend, attempts to predict the moment at this point on the moment-rotation curves. Although it is recognised that it will not represent the true moment resistance the predicted values would always produces a safe design. Factors which influence the ultimate resistance, particularly strain-hardening and membrane effects, are not considered by the prediction model.

The presence of reinforcement affected the moment resistance of the connection. From Table 3-4, it can be seen that by providing only 1% of reinforcing bar there was an increase of between 2.7 and 3.7 times that of the steel only connection. Other researchers' findings, tabulated in Table 1-1 and Table 1-2 (extracted from the SCI interim guide[3-7]) also confirm the substantial contribution of reinforcement to the moment resistance of such connections.

In comparing the predicted moment resistance of the composite connections by the SCI method and the Eurocodes, the results are usually comparable to each other for the same amount of reinforcement used. However there was a notable difference for the specimen with highest percentage reinforcement (BTB7). This is because the total tensile force now required part of the web to be in compression to maintain equilibrium. The SCI method[3-7] then bases the calculated resistance on a reduced lever arm.

3.3.1 Classification by strength

As mentioned in Chapter 1, classification by strength, in relation to the moment resistance of the connected member, divides connections into "full strength" and "partial strength". The classification is tabulated in Table 3-3. From this, all the connections tested are classified as "partial-strength". The steel-only connections of BTB1 and

BTB4 has the lowest strength ratios of 0.27 and 0.36 respectively. The remainder all had strength ratios of at least 70% of the connected beam's plastic hogging moment of resistance. It is noticeable how the addition of the reinforcement causes a substantial increase in the strength ratio, even though the resistance of the beam also increases. This indicates how effective composite joints are in providing substantial increase in moment resistance.

3.3.2 Classification by stiffness

The classification of steel connection by stiffness (relevant to BTB1 and BTB4) is based on the revised Annex J of EC3[3-6]. In this classification the initial stiffness of the connection $S_{j,ini}$ is compared to the boundaries for rigid and pinned connections expressed in term of beam stiffness as indicated in Fig. 1-8. From Fig. 1-8 it can be seen that if the initial stiffness is between those two boundaries, the connection is classified as semi-rigid . The beam spans L_b for BTB1-BTB3 and BTB4-BTB7 were taken as 9.0 m and 12.0 m respectively. As explained in Chapter 2, these spans correspond to reasonable L/D ratios for the specimens.

For the composite connections, the classification depends on whether the cracked or uncracked flexural rigidity EI_b of the connected beam is taken. The tendency of concrete in hogging regions is to crack and thus the cracked approach may be thought to be more appropriate. However the cracking does not usually extended over the full length of the beam, as a substantial proportion is in sagging bending. Moreover, if the cracked stiffness is used, there is more likelihood that the connection will be classified as rigid, because a smaller value of the beam's flexural rigidity will apply. Thus the uncracked value would provide a more severe criterion. A further argument is that the classification rules are based on a limited loss of restraint to the columns. As restrained

columns approach collapse, the end moment reverses, and thus the concrete in the joint will be compressed; this leads to the uncracked beam stiffness being more appropriate. For comparison, both values of cracked and uncracked flexural rigidity were taken in the classification process. A modular ratio of 15 was used in determining the elastic properties of the uncracked composite section. This value makes an allowance for a proportion of the loading to be long-term.

The experimental initial stiffnesses of the connections $S_{j,ini}$ are presented in Table 3-5. The experimental values were taken from the gradient of the loading-unloading part of the M-ϕ curves of each test.

The classification indicated in Table 3-5 was based on the experimental $S_{j,ini}$. All joints except BTB1 were rigid, irrespective of whether (for the composite joints) the cracked or uncracked beam stiffness was used. For BTB2 and BTB3, which have semi-rigid steelwork connections as BTB1, it is shown that the reinforcement provides sufficient additional rigidity to the connections for them to be classified as rigid.

3.4   Rotation capacity

The rotation capacity of a connection depends on the deformation response of individual joint components and also the lever arm between these components. The deformation capacity is influenced by the length and ductility of the reinforcing bar and also the tension stiffening effect of concrete between cracks. The predicted rotation capacity of each connection was calculated based on the method outlined by Anderson and Kornenberger in a COST publication [3-8]. Good agreement between the values obtained using method and the test results for beam-to-column connections has been demonstrated. However as the author's tests involved beam-to-beam connections, it was

thought appropriate to determine the deformation capacity of the joint on the basis of a length measured from the centre-line of the primary beam to the nearest shear connector on the secondary beam. The corresponding rotation capacity is obtained by taking account of the lever arm of the joint.

The predicted rotation capacities calculated from the formulation mentioned above are given in Table 3-5 and compared to the ultimate rotation obtained from the test results. For BTB7 the ultimate rotation was taken as 15 mrad (refer Fig. 2-18b) due to the shape of the M-φ curve.

Bode et al[3-9] emphasised that the prediction method provides correct results only if failure of the reinforcement or the shear connectors occurs. In two tests (BTB2 and BTB5) the mode of failure was the fracturing of the reinforcement. The results indicated that except for the test BTB7, the predicted rotation capacity underestimates the ultimate rotation obtained from the test. In the test, plastic deformation (i.e. local buckling) of the lower part of the beam's section was included in the determination of the rotation capacity. However, in the predicted method, these deformations were ignored. This may explain the underestimation of the value.

The predicted value for BTB2 is more similar to its test result than BTB5 although the fracture of the rebar was the mode of failure in both specimens. In BTB2 the difference is only 16% but in BTB5 (with deeper beam) the difference is more than 40%.

BTB7 was the partial shear connection and the failure was due to permanent deformation of shear studs. The prediction method did not give a comparable rotation capacity for connection BTB7. From Table 3-5 it can be seen that partial shear connection limits the rotation capacity (due to the deformation capacity of shear studs).

It can thus substantiate the recommendation of the current design practice not to permit partial shear connection in the hogging moment region.

3.5   Assessment of the tests results

In this section the effect on M-ϕ curves of varying the amount of reinforcement, the degree of shear connection, the arrangement of shear connectors and beam depth will be discussed.

3.5.1   General remarks on beam-to-beam tests

In the beam-to-beam tests the beams were connected to the web of the main beam by end plates. These were bolted together through the web of the main beam. They could only be partial-depth though, in order to clear the flange outstand of the main beam. Since the top part of the end plate was not welded to the top flange of the secondary beam it would not be as stiff as the flush and extended types which would normally be used in beam-to-column connections. This also tends to make the location of the bolt rows closer to the centre of compression; thus less contribution was expected from the bolts to the resistance of the composite joint. The interim SCI guidelines[3-7] suggests that the contribution of the bolts to the tensile resistance should be ignored for partial depth end plate connections. By omitting the tensile bolt contributions, no substantial effect is made to the predicted moment resistance of connection (refer to Table 3-4).

3.5.2   The reinforcement

Reinforcement in the concrete slab is the most important factor influencing the strength and stiffness of the composite connections. A suitable amount of reinforcement is essential to provide a degree of continuity in a semi-rigid design. Ductility of reinforcement is required in composite connections as it enables rotation of the

connection without reducing its moment resistance, and to allow redistribution to take place.

The ductility of reinforcing bars is expressed as the percentage elongation based on a standard gauge length. The minimum elongation at fracture of 12% is specified by BS 4449[3-10] for high tensile bars. In EC4[3-2], references are made to EC2[3-11] regarding the ductility requirement of the reinforcing steel. Two types are classified according to ductility characteristics : normal or high. These are based on elongation at maximum strain ε_u , and the ratio of ultimate stress and the yielding stress f_u / f_y. For high ductility reinforcing steel the minimum values specified for ε_u and f_u / f_y are 5% and 1.08 respectively.

The results obtained from tensile tests (see Table 2-4) indicate an elongation at fracture of 22% for all the reinforcing bars used in the experiments. The strain ε_u was at least 12%, and the average ratio for f_u / f_y was over 18% is shown in Table 2-4. This means that the reinforcing bars used in the experiment conformed to the ductility requirements of both UK and European practice.

3.5.3   Influence of reinforcement on joint behaviour

The presence of reinforcement alters the position of the plastic neutral axis and puts more of the web into compression. It is well known that this normally changes the class of the section to semi-compact (see Table 3-3). The moment-rotation curves of the tests, including those with a bare steel connection corresponding to the composite joints, are shown in Fig. 3-2 and Fig. 3-3. From the curves, it can be seen that there was no clear plateau for the bare steel connection even at high rotation. This may be due to the

"membrane" effects in the end plates and that the secondary beams compression flanges stiffens the connection at large rotation.

The moment-rotation curves (Fig. 3-2 and Fig. 3-3) also demonstrate clearly the influence of the reinforced concrete slab on the overall behaviour. The initial stiffness and moment resistance increase due to the presence of reinforcement within the slab. The rupture of reinforcement in BTB2 and BTB5 limits the rotation capacity of those joints.

The effects of varying the amount of reinforcement are illustrated in Fig. 3-3 by comparing BTB5 to BTB7. In BTB5 the amount of reinforcement was 1% while in BTB7 it was 1.5%. The moment resistance of the joint with the greater reinforcement was higher. Higher rotation capacity of test BTB7 was expected from the increase in the reinforcement which in turn cause greater compression forces and therefore possible plastic deformation of the bottom flange. However BTB7 demonstrated low ductility behaviour compared to BTB5. This is because the greater reinforcement reduced BTB7 to partial shear connection, resulting in reduction of interaction at the concrete-steel interface.

3.5.4   Effect of different type of steel connection

Comparing specimens (BTB2 and BTB3) with the same amount of reinforcement, the tests show the influence of the bolt in the upper row of the steelwork connection. In BTB3 the row of top bolts were absent. The M-ϕ curves in Fig. 3-2 demonstrate that the moment resistance of BTB2 is just slightly higher than that of BTB3. The stiffness and ductility of both BTB2 and BTB3 are comparable. This indicates that the type of steel connection is much less influential in contributing to moment resistance of composite joint than the reinforcement.

The influence of beam depth on the behaviour of the composite joint (BTB2 and BTB5) is shown in Fig. 3-4. The reinforcement ratio used was the same although in the steelwork connection there were two rows of top bolts provided in BTB5, compared to only one in BTB2. The increase in stiffness and resistance due to the higher beam depth is apparent. The beam depth also influences the rotation capacity of the joint. Fracture of reinforcement limits the rotation curves in both tests. Contrary to other findings [3-8], an increase of beam depth leads to a higher experimental rotation capacity.

The predicted rotation capacities using the method outlined by Anderson and Kronenberger[3-8] also showed a marked decrease for deeper beams (Table 3-7). The method considers only the slip and reinforcement deformation. Plastic deformations of the compression flange was ignored although it can contributed to the rotation by way of local buckling. Permanent deformation (local buckling) of lower flange was observed in both BTB2 and BTB5 which explained why there was a distinct different between the prediction values and the test values.

3.5.5 Effect of shear connection in the composite beam

Composite action within the joint is ensured by the shear connectors placed along the connected beams. These connectors should possess adequate strength and deformation characteristics as they have to transfer horizontal shear forces between the steel section and concrete slab. In the tests, headed studs of 19 mm diameter and 100 mm nominal height were utilised. It has been shown in many tests that the load-slip behaviour of these headed stud is generally non-linear. Several inter-related factors affect the degree of shear connection, such as:

(i) The strength of concrete. Studs may reach their maximum load when concrete surrounding them fails, but in stronger concrete, they shear off.

(ii) The number of shear stud connectors provided.

(iii) The shear resistance of the stud.

(iv) The area and strength of reinforcing bar.

The influence of the degree of shear connection was investigated. In BTB7 the degree of shear connection was reduced to 84% by increasing the amount of reinforcement. Comparison made to a full shear connection of 125% of BTB5 (see Fig. 3-3) indicates that the partial shear connection had very little effect on initial stiffness, but significant reduction in secant stiffness at peak moment. As the curve reached about the level of predicted M_{Rd} (370 kNm) the rotation is diminished to less than 15 mrad due to the load-slip characteristics of the partial-shear connection. The influence of the degree of shear connection on rotation capacity depends on the real failure mode, in this case shear connector failure.

The arrangement of shear connectors near the joint may also influence the joint behaviour. In test BTB6 the effect of omitting the first stud in the secondary beam was studied. Again by comparing to BTB5 (Fig. 3-3), there was no significant drop in moment resistance. A greater distance between the joint and the first shear connectors adjacent to the joint resulted in higher ductility and hence higher rotation capacity resulted. This would be expected from the model used to predict the rotation capacity. From the M-ϕ curves a slight decrease in stiffness was observed

3.6   Prediction method for initial stiffness

Stiffness predictions have previously assumed that concrete in tension has no stiffness. In hogging bending only the reinforcement and the shear connectors contribute to stiffness[3-8]. The length of reinforcement taken in the COST-C1 proposals[3-8] for beam-to-beam joints is from the centre of the column to the outside of the column flange, i.e. to the face of the connection. More logically though, the method to predict the rotation capacity should examine the rebars between the centre-line and the first shear connector to the beam, because it is only through the connectors that composite action is achieved.

In this section of the thesis, the author reports an investigation into the use of this approach for prediction of initial stiffness, taking account of tension stiffening. This would permit a unified treatment for both stiffness and rotation capacity. Furthermore, for beam-to-beam joints there is no column and therefore stiffness based on the rebar length to the first connector is clearly the relevant distance.

The tension-stiffening method is based on the model by CEB-FIB [3-12] of a simplified stress-strain relationship of embedded reinforcing steel as shown in Fig. 3-1. The attainment of yield point 3 on the Fig. 3-1 is considered for initial stiffness calculation. The influence of slip is accounted for in the model.

Effective modulus at yield

With reference to Fig. 3-1 and the definitions given in Chapter 1:

At level 1,

the average strain ε_{sr1} of embedded reinforcement can be calculated as follows[3-12]:

$$\varepsilon_{sr1} = \frac{f_{ctm}}{E_c} \tag{3.1}$$

where

f_{ctm} is the concrete tensile strength
E_c is modulus of concrete

The stress of the embeddment reinforcement is given as follows:

$$\sigma_{sr1} = \frac{f_{ctm}}{\rho_{s,eff}}\left(1 + \frac{E_s}{E_c}\cdot\rho_{s,eff}\right) \tag{3.2}$$

where E_s is the reinforcement modulus, and

$$\rho_{s,eff} = \frac{2.0\cdot A_s}{A_c}$$

A_s is the effective area of reinforcement
A_c is the effective area of concrete slab

At level 2,

the stress of reinforcement at this level is given by

$$\sigma_{srn} = 1.3\sigma_{sr1} \tag{3.3}$$

the strain of reinforcement is given by

$$\varepsilon = \frac{\sigma_{srn}}{E_s} - \beta_t\cdot\Delta\varepsilon \tag{3.4}$$

and $$\Delta\varepsilon = \varepsilon_{sr2} - \varepsilon_{sr1} = \frac{\sigma_{sr1}}{E_s} - \frac{f_{ctm}}{E_c} \tag{3.5}$$

where β_t is the curve parameter taken as 0.4 for short term loading and 0.2 for long term loading

At level 3,

the strain of the reinforcement is given by

$$\varepsilon_{s,m} = \frac{f_{y,r}}{E_s} - \beta_t\cdot\Delta\varepsilon \tag{3.6}$$

$f_{y,r}$ is the yield strength of reinforcement

Thus the effective modulus at this level, is given by :

$$E = \frac{f_{y,r}}{\varepsilon_{sm}} \tag{3.7}$$

Slip of the shear connection

Account may be taken of the influence of slip between the slab reinforcement in tension and the steel profile by the model of Aribert[3-13] shown in Fig. 3-5.

K_{sc} is the translational stiffness of the shear connection defined by [3-8]:

$$F_{t,s,Sd} = K_{sc} \cdot s \tag{3.8}$$

The stiffness K_{sc} for shear connection is established by elastic interaction theory[3-13,3-8] and is given by:

$$K_{sc} = \frac{N \, k_{sc}}{\left(\beta - \dfrac{\beta - 1}{1 + \alpha} \cdot \dfrac{h_s}{d_s} \right)} \tag{3.9}$$

where

N is the number of shear connector provided

h_s is the lever arm for tension force

d_s is the distance between the line of action of the tension resistance

of the slab to the centroid of the beam's steel section, and:

$$\alpha = \frac{E_a I_a}{d_s^2 \, E_s \, A_L} \tag{3.10}$$

$$\beta = \sqrt{\left[\frac{(1+\alpha) \cdot N \, k_{sc} \, l \, d_s^2}{E_a \, I_a} \right]} \tag{3.11}$$

l is the length of hogging bending adjacent to the joint

k_{sc} is the stiffness of one connectors

E_a is the modulus of elasticity of steel section

I_a is second moment of area of steel section

E_s is the modulus of elasticity of reinforcement

A_L is the area of reinforcement

Aribet[3-13] suggested k_{sc} to be taken as 0.7 P_{Rk} (refer Fig. 3-6).

Using the model in Fig. 3-5, the design moment of the composite joint is:

$$M = S_{j,ini} \cdot \phi + F_{t,s,Sd} \cdot h_s \tag{3.12}$$

while the elongation Δ_s of the slab reinforcement is given by:

$$F_{t,s,Sd} = K_s \cdot \Delta_s \tag{3.13}$$

and the rotation of composite joint is:

$$\phi = (\Delta_s + s) / h_s \tag{3.14}$$

Combining Eqns (3.8), (3.13) and (3.14), Eqn (3.12) becomes :

$$M = S_{j,ini} \cdot \phi + K_s h_s^2 \cdot \frac{1}{1 + \dfrac{K_s}{K_{sc}}} \cdot \phi \qquad (3.15)$$

Based on proposal[3-13] the reduction factor of $K_s h_s^2$ the effective stiffness of slab becomes:

$$\frac{1}{1 + \dfrac{K_s}{K_{sc}}} = \frac{1}{1 + \dfrac{E_s k_l}{K_{sc}}} \qquad (3.16)$$

k_l is based on length of the reinforcement considered,

for beam-to-column connection $\qquad k_l \quad = \quad \dfrac{A_s}{\dfrac{h_c}{2} + a}$,

a is the distance from face of column to stud
h_c is the column depth
A_s is the area of reinforcement

for beam-to-beam the distance k_l considered is from centre-line of primary beam to the first stud therefore the reduced stiffness due to slip is given by:

$$k_{reduced} \quad = \quad k_l \frac{1}{1 + E_s k_l / K_{sc}} \qquad (3.17)$$

If there is no direct steelwork connection i.e. only slab reinforcement, the initial stiffness is calculated by:

$$S_L = E \, k_{reduced} \; z^2 \qquad (3.18)$$

where

$$E \quad = \quad \frac{E_{effective}}{E_s}$$

z = lever arm taken from mid-level of the reinforcement to the middle of compression flange.

If the direct contribution of steelwork connection is taken into account the expression from revised Annex J[3-5] is taken as follows:,

Rotational stiffness is given as[3-5]:

$$S_j \quad = \quad \frac{E z^2}{1/k_l} \qquad (3.19)$$

where k_i is the stiffness factor for a component i.

the value S_j may be taken from the bare steel connection or by expression given by revised Annex J[3-5]

$$z \quad = \quad \frac{\sum_r k_{eff,r} \cdot h_r^2 + \sum_s k_{reduced,s} \cdot h_s^2}{\sum_r k_{eff,r} \cdot h_r + \sum_s k_{reduced,s} \cdot h_s^2} \qquad (3.20)$$

$$k_{eq} = \frac{\sum_r k_{eff,r} \cdot h_r + \sum_s k_{reduced,s} \cdot h_s}{z}$$ (3.21)

where :

h_r is the distance between bolt row r and the centre of compression

h_s is the distance between reinforcement and centre of compression.

The predicted initial stiffness is then taken as

$$S_L = E \, k_{eq} \, z^2$$ (3.21)

A worked example of initial stiffness prediction based on test BTB2 is given in Appendix A1.

3.6.1 Verification of the prediction method

The value of steelwork stiffness may also be determined using Ref. [3-5]. However in the prediction method the stiffness of the steelwork obtained from the steel-only connection in the test was combined with the predicted slab stiffness to obtain the predicted initial stiffness of composite joint. The results are then compared with the tests and tabulated in Table 3-6. It can be seen from Table 3-6 that, with the exception of BTB5, the method proposed can be used to predict initial stiffness of composite connection from the author's tests satisfactorily. No explaination has been found for BTB5, although both experimental and predicted stiffnesses are so high that the joint is effectively rigid.

The expressions outlined in Section 3.6 were also applied to predict the initial stiffness for the composite tests conducted by Brown[3-3] and Najafi[3-4]. The results are compared to the respective experimental specimens in Table 3-6. It can be seen that the predicted values are comparable to the test result.

3.7   *Conclusions*

(i)   The moment resistance of end plate composite beam-to-beam can be predicted satisfactorily by the method specified by the SCI[3-7] and Annex J of EC3 (taking the reinforcement as an extra row of bolt) although both of the models are based on the beam-to-column connection type. The prediction by both methods underestimated the moment resistance achieved in the tests.

(ii)   Comparison between the methods of SCI[3-7] and Annex J of EC3 (refer to Table 3-4) shows that for the moderately deep steel section in the tests the similarity is remarkable. However for the deeper steel section, the SCI method gives slightly lower results.

(iii)   It was confirmed from both tests and analysis that the reinforcement in the concrete slab has very important effects on the moment resistance of composite connections. Moderate amounts of reinforcement provided significantly increased the moment resistance and the rotation capacity of the connection. However higher reinforcement may change the mode of failure, and hence limit the rotation capacity achieveable. This can be seen from the test results of specimen BTB7.

(iv)   A higher amount of reinforcement reduced the degree of shear connection to partial shear (BTB7). Partial shear connection in hogging moment region reduced the interaction of concrete-steel interface and hence the rotation

3-19

capacity. The results of BTB7 justified the restriction imposed by current design codes of not having partial shear connection in hogging moment region.

(v)   The method outlined in Ref.[3-8] provides a satisfactory method to predict the rotation capacity of a composite joint.

(vii)   A prediction method to estimate the initial stiffness is presented and applied to the tests result. This method provides a comparable result in predicting the initial stiffness of composite connections.

References

3-1   DD ENV 1993-1-1: 1992, "Eurocode 3: Design of Steel Structures, Part 1.1:General rules and Rules for Buildings". British Standard Institution, London, 1992.

3-2   DD ENV 1994-1-1: 1992, "Eurocode 4: Design of Composite Steel and Concrete Structures, Part 1.1: General Rules and Rules for Buildings". British Standards Institution, London, 1994.

3-3   Brown N. D., "Aspects of sway frame design and ductility of composite end plate connections". PhD Thesis, University of Warwick, UK, 1995

3-4   Najafi, A. A., "End plate connections and their influence on steel and composite structures". PhD Thesis, University of Warwick, UK, 1992.

3-5   BS 5950, "Structural Use of Steelwork in Building; Part 3: Design in Composite Construction, Section 3.1: Code of Practice for Design of Simple and Continuous Composite Beams". British Standard Institution, London, 1990.

3-6   Eurocode 3: Part 1.1, "Revised annex J : Joints in building frames". ENV 1993-1-1.

3-7   Lawson, R. M., and Gibbons C., "Moment connections in composite construction: Interim guidance for end plate connections". SCI Publication 143, The Steel Construction Institute, 1995.

3-8   Composite steel-concrete joints in braced frames for buildings, (ed. D. Anderson),European Commission European Cooperation in the Field of Scientific and Technical Research, COST-C1, Brussels 1997.

3-9   Bode H., Kronenberger H., and Michaeli W., "Composite joints - Further Experimental Result". Innsbruck Sept. 1997.

3-10   BS 4449 : "Specification for carbon steel bars for reinforcement to concrete". British Standard Institution. 1985.

3-11   Eurocode 2:Part 1: "Design of Steel Structures: General Rules and Rules for Buildings. ENV 1992-1-1. 1992.

3-12   CEB-FIB Model Code 1990. Comite' Euro-International du Beton, Lausanne, 1990.

3-13   Aribet, J.M., "Proposed clause J.4.5 in Annex J for EN 1994-1.1.", Laboratoire de Structures et Mecanique Applique. INSA, Rennes, France. Dec. 1995.

Table 3-1 : Summary of dimension and properties of BTB1-BTB3

		BTB1	BTB2	BTB3
Primary beam 457x152UB52	t_{wb}	7.7	7.7	7.7
Secondary beam 356x171UB45	D mm	352	352	352
	B mm	171	171	171
	t_f mm	9	9	9
	t_w mm	6.7	6.7	6.6
	d_w mm	312.2	312.2	312.2
	S_x cm^3	773.7	773.7	773.7
	I_x cm^4	12091	12091	12091
	$f_{y,f}$ N/mm^2	315	315	315
	$E_{y,f}$ kN/mm^2	191	191	191
	$f_{y,w}$ N/mm^2	384	384	384
	$E_{y,w}$ kN/mm^2	210	210	210
	A cm^2	57	57	57
Composite slab	B_{eff}	-	1100	1100
	D_s		120	120
	D_r		84	84
	D_p		46	46
	D_s-D_p		74	74
	$d_s=(0.5D+D_r)$		260	260
	A_r		804	804
	$f_{y,s}$		505	510
	$f_{u,s}$		594	601
	ε_{su}		14.1	12.9
	E_s		195	192
	b_{eff}		1100	1100
	f_{cu}		50	44.1
	f_{ctm}		4.26	3.7
	E_c		35	33.33
End plate	t_p	10.3	10.3	10.3
	$f_{y,p}$	258	258	258
	$f_{u,p}$	425	425	425
Bolts	M20, gr. 8.8	1	1	

Table 3-2 : Summary of dimension and properties of BTB5-BTB7

		BTB4	BTB5	BTB6	BTB7
Primary beam 533x210UB82	tw	10.6	9.6	9.6	9.8
Secondary Beam 457x152UB52	D mm	449.8	449.8	449.8	449.8
	B mm	152.4	152.4	152.4	152.4
	t_f mm	10.4	10.5	10.5	10.4
	t_w mm	8.0	7.9	8.0	7.9
	d_w mm	407.7	407.7	407.7	407.7
	S_x cm^3	1094	1094	1094	1094
	I_x cm^4	21345	21345	21345	21345
	$f_{y,f}$ N/mm^2	291	291	291	291
	$E_{y,f}$ kN/mm^2	196	196	196	196
	$f_{y,w}$ N/mm^2	348	348	348	348
	$E_{y,w}$ kN/mm^2	215	215	215	215
	A cm^2	66.5	66.5	66.5	66.5
Composite slab	B_{eff}		1100	1100	1100
	D_s		120	120	120
	D_r		84	84	84
	D_p		46	46	46
	D_s-D_p		74	74	74
	d_s=(0.5D +D_r)		308.9	308.9	308.9
	A_r		804	804	1206
	$f_{y,s}$		508	509	508
	$f_{u,s}$		605	604	599
	ε_{su}		13.3	12.0	13.3
	E_s		197	196	191
	b_{eff}		1100	1100	1100
	f_{cu}		45.9	44.9	50.0
	f_{ctm}		3.38	3.89	3.54
	E_c		33.77	33.48	35
End plate	t_p	10.3	10.3	10.3	10.3
	$f_{y,p}$	258	258	258	258
	$f_{u,p}$	425	425	425	425
Bolts	M20, gr. 8.8	1	1	1	1

Table 3-3 : Summary of resistance moments

Test	Test Moment (M_{exp}) kNm	Moment of resistance of beam (hogging) $(M_{pl.Rd})$ kNm	$\dfrac{(M_{exp})}{(M_{pl.Rd})}$	Classification by strength	Member classification*
BTB1	68	255	0.27	partial-strength	F-class 2 W-class 1
BTB2	253	329	0.77	partial-strength	F-class 2 W-class 3
BTB3	235	327	0.72	partial-strength	F-class 2 W-class 3
BTB4	123	337	0.36	partial-strength	F-class 1 W-class 1
BTB5	350	434	0.81	partial-strength	F-class 1 W-class 3
BTB6	335	438	0.76	partial-strength	F-class 1 W-class 3
BTB7	398	444	0.90	partial-strength	F-class 1 W-class 3

Notes:
1. F - flange
2. W - web

Table 3-4 : Comparison of connection moment resistance

Test	Bar rein-force ment	Degree of shear connection	Moment resistance of connection $(M_{j,Rd})$* kNm		Moment resistance of connection $(M_{j,Rd})$** kNm		Test moment (M_{exp}) kNm	$\dfrac{(Mexp)}{(M_{j,Rd})}$***
			with tensile bolt	without tensile bolt	with tensile bolt	without tensile bolt		
BTB1	-	-	27		27	-	68	2.52
BTB2	1%	1.26	202	175.2	202	175	253	1.25
BTB3	1%	1.25	177	177	177	177	235	1.32
BTB4	-	-	54	-	54	-	123	2.28
BTB5	1%	1.25	269	215	270	216	350	1.30
BTB6	1%	1.07	269	215	270	216	335	1.24
BTB7	1.5%	0.84	367	313	378	324	398	1.05

Notes:

*	Based on SCI[3-7] method
**	Based on EC3 & EC4
***	Based on EC3 & EC4 with bolt

Table 3-5 :   Summary of connection stiffness

Test	Initial Stiffness (Test) kNm/mrad	Initial Stiffness (Predicted) kNm/mrad	Rotational stiffness S_j at M_{rd} kNm/mrad	$\dfrac{S_{j,ini}}{S_j \text{ at } M_{Rd}}$	Ultimate rotation (Test) ϕ_u mrad	Predicted rotation capacity mrad	Connection classification based on stiffness (uncracked)	Connection classification based on stiffness (cracked)
BTB 1	10.9	17.2	1.58	6.9	>43.4	-	semi-rigid	semi-rigid
BTB 2	82.5	65	38.7	2.1	41.5	35	rigid	rigid
BTB 3	62.5	53	45.2	1.4	>40	35.6	rigid	rigid
BTB 4	45.6	59.9	4.4	10.4	>42	-	rigid	rigid
BTB 5	341.8	171	9.05	37.7	54	31.2	rigid	rigid
BTB 6	184.3	149	60	3.1	>53	51.1	rigid	rigid
BTB 7	195	194	42.4	4.6	15	36	rigid	rigid

Notes:
1. Ultimate rotation is the average value of left and right beams

Table 3-6 :   Comparisons of predicted initial stiffness to tests results

| Ref of test	Brown's		Najafi's			Author's test				
	2	3	S4F	S8F	S12F	BTB2	BTB3	BTB5	BTB6	BTB7
Shear connectors	19 mm dia by 100mm welded stud					19 mm dia by 100mm welded stud				
End plate thickness	15	15	15	15	15	10				
Reinforcement (including mesh) mm^2	966	966	614	1067	1519	966	966	966	966	1368
k_{sc} (kN/mm)	100					100				
Number of stud N	7					6	6	7	6	7
$S_{j,ini}$ (from steelwork) kNm/mrad	33	33	10.4	10.4	10.4	10.9	10.9	45.6	45.6	45.6
Predicted initial stiffness S_j	118	116	48.1	60.7	60.3	65	53	171	149	194
$S_{j,ini}$ (Experimental)	110	100	42.8	62	77.7	82.5	62.5	341.7	184.3	195
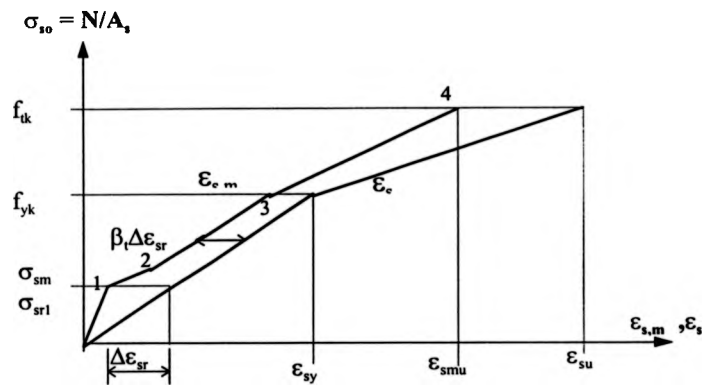
Fig. 3-1:   Simplified stress-strain relationship of embedded reinforcing steel
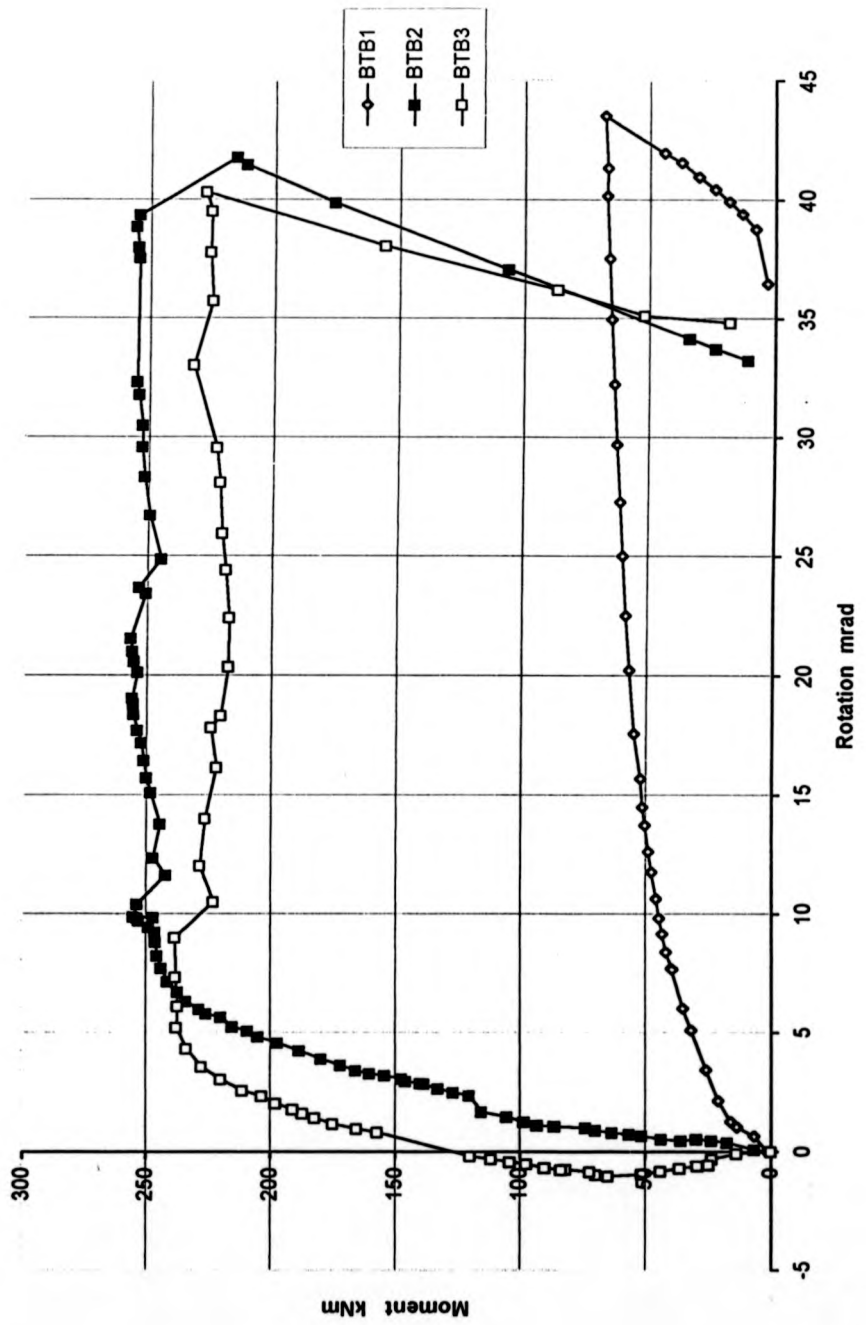
Fig. 3-2 : Comparison of M-φ curves
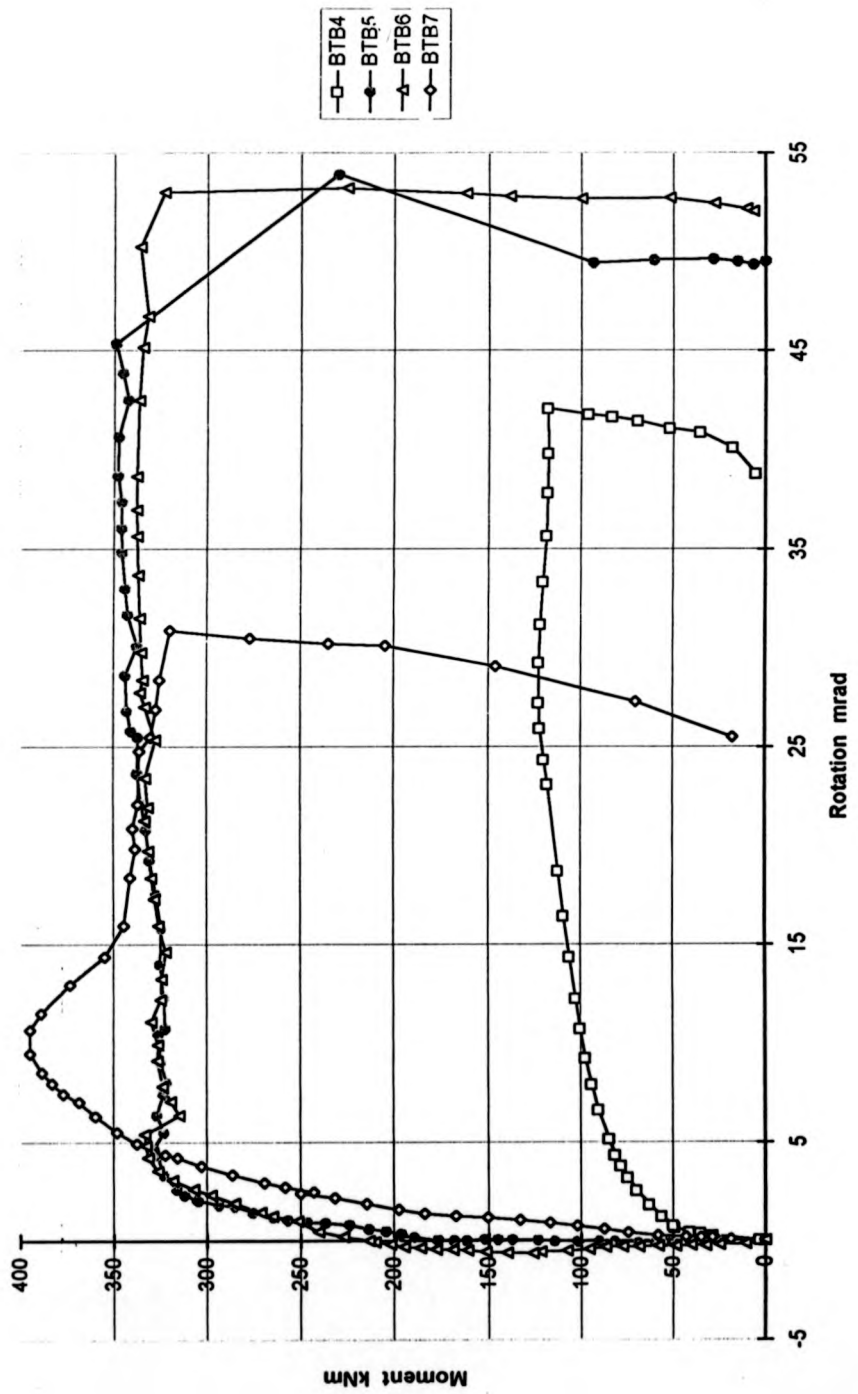
Fig. 3-3. : *Comparison of moment-rotation curves*
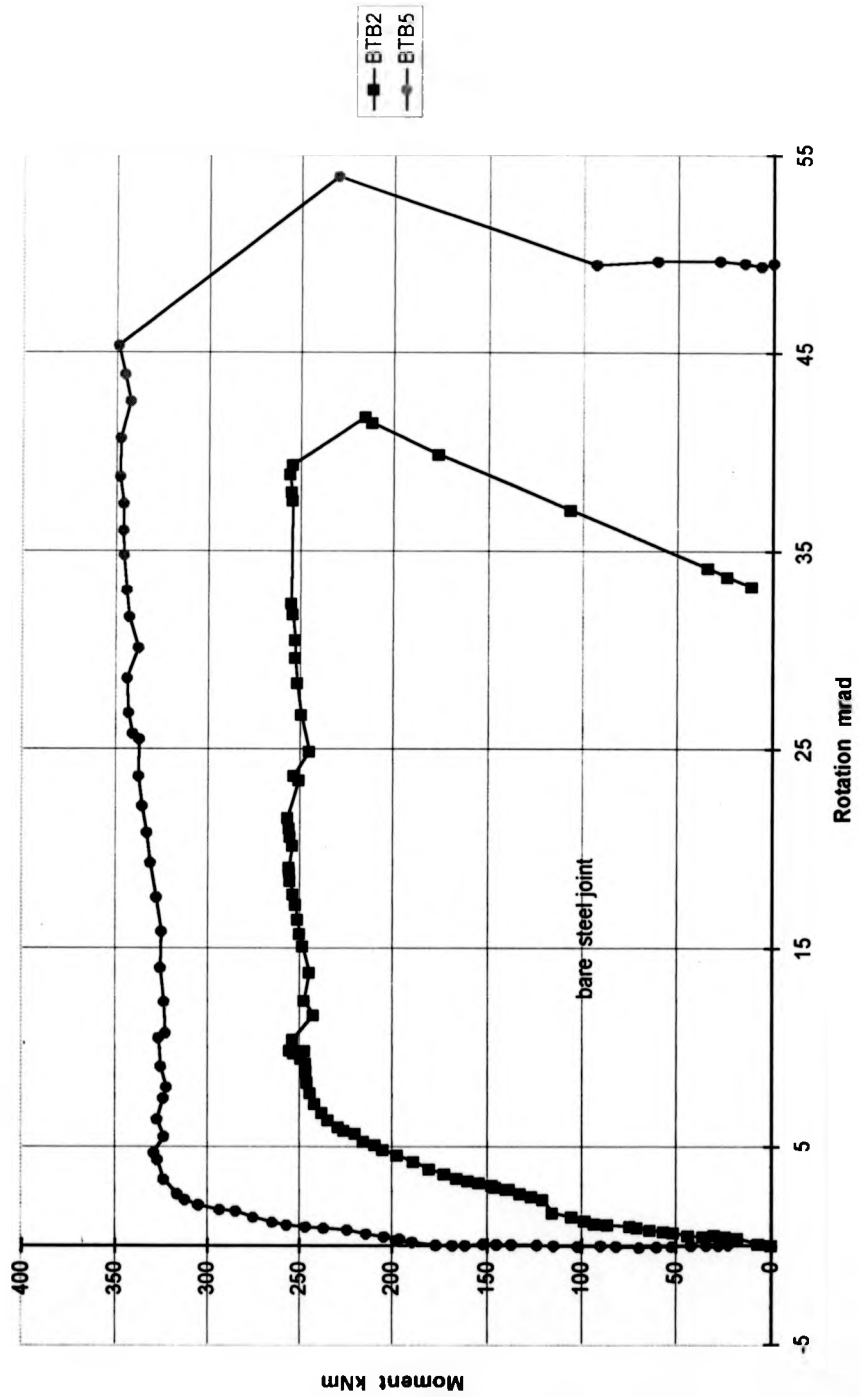
Fig. 3-4 : Influence of beam depth on joint behaviour
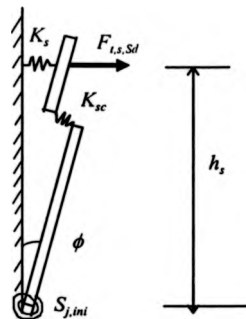
Fig. 3-5 :   *Spring model*
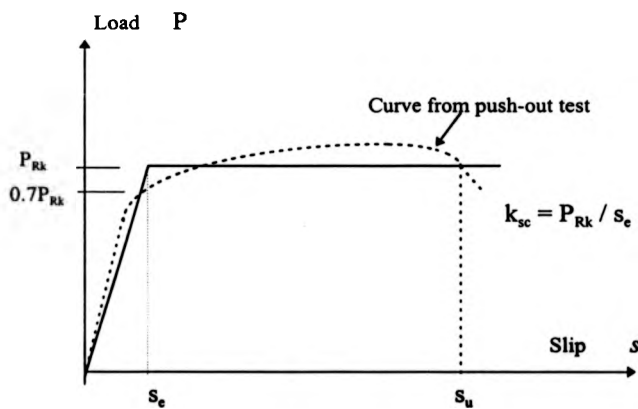
Fig. 3-6 : Values of k_{sc}

Chapter 4

TESTS ON ENCASED FLUSH END PLATE BEAM-TO-COLUMN JOINTS FOR SLIMFLOR BEAMS.

4.1 Introduction

This chapter concerned a series of five tests conducted at the University of Warwick on slimflor beams where flush end plates formed the beam-to-column connections. Development and studies of slim floor beams have been so far carried out with reference to simply supported beams. However, due to the overall slenderness of the system, often this approach may not lead to the most economical solution[4-1] as serviceability deflections usually control the design. It is now recognised that even nominally-pinned joints provide some moment resistance in practice which can provide a useful reduction in mid-span deflections. In the slim-floor system the beam and joint may be encased and this could further stiffen the joint. Thus the main aim of the tests were to investigate the effect of concrete encasement to the joints of continuous slimflor beams.

4-2 Test configuration

The general configuration of the tests is shown in Fig. 4-1 and Fig. 4-2. This was proposed by Steel Construction Institute as the test programme's sponsor. It consisted of two cantilever beams connected to each other through the flanges and web of a column.

This balanced cruciform arrangement was intended to simulate the action of moment and shear produced in a continuous beam. It also aimed to represent the connections to the internal columns of a braced frame.

4.3   Design of test specimen

Three encased slimflor beam specimens (SFB1, SFB2, SFB3) were tested. The beams were 254UC89 sections with 460 mm wide by 15 mm thick flange plates continuously welded with a 6 mm fillet weld to the underside. The pair of beams were connected to a stub length of 254UC89 section acting as the column. The grade of steel used was S355 (Grade 50). The choice was based on the fact that this grade provides optimum structural efficiency for slimflor beams[4-2].

For comparison of the joint performance two tests (TEST4 and TEST5) were carried out using the bare steel sections of 254UC89. The plate to the bottom flange was omitted because this would not significantly influence the joint performance.

The construction details for the encased and the bare specimens are illustrated in Fig. 4-1 and Fig. 4-2, respectively.

The behaviour of end plate connections depends on the thickness of the plate. The thickness of end plate and the bolt size were varied for each specimen. For SFB1 and SFB2, 15 mm thick end plates of grade S275 were used, but a more flexible 10 mm thick end plate of the same grade was used for SFB3. Connections with end plates are required for this slimflor type of construction because in practice they have to resist torsion caused by loading on one side of the floor during construction[4-3].

Four bolts which satisfy BS 5950[4-4] edge distance and other detailing requirements were used. Bolts of 24 mm diameter grade 8.8 were used in SFB2 while smaller bolts of 20 mm diameter were adopted for specimens SFB1 and SFB3. Mesh reinforcement (A142), which is used to control shrinkage cracks in current construction practice, was included with 20 mm concrete cover. TEST4 had the same 10 mm end plate and 20 mm diameter bolts as SFB3, and TEST5 had the same arrangement of steelwork connection as SFB2. Table 4-1 summarises the test parameters of all the specimens.

For SFB1, SFB2 and SFB3 the whole of the top flange and the web of the steel beams were encased by a lightweight concrete of design cube strength 30 N/mm². Lightweight concrete were chosen because it enables longer spanning of the unpropped slab and beam during construction, but makes little difference to the ultimate limit state behaviour. The concrete was designed to use a maximum aggregate size of 12 mm, and a slump of 75 mm. In practice the slump values were found to be in range of 65-90 mm and the concrete strengths on the day of testing were in the range of 30-50 N/mm².

4.4   Preparation of specimen

The fabrication and delivery of the steelwork components was arranged by The Steel Construction Institute. To form the specimens, the two beams were aligned on supports with a suitable gap for the column. The steel joint was then assembled into position with its bolts. The bolts were initially tightened using an ordinary spanner. A torque wrench was then applied to tighten the bolts to a torque of 190 Nm to maintain consistency between specimens.

Concreting for the composite specimens (SFB1, SFB2, SFB3) was carried out inside the laboratory. The formworks were constructed from plywood. Provision was made for

100x100x100 mm cubes for compression tests and 6 cylinders (200 mm x 100 mm diameter) for tension tests. Prior to actual concreting several trial mixes were conducted. Concrete mix design was based on Boral Lytag technical notes[4-5]. The cubes were tested at 7 days, 28 days and on the day of the connection tests. The specimens were lifted into the test rig when the concrete strength had reached a minimum of 30 N/mm². The results of the compressive strength tests of the concrete are tabulated in Table 4-2.

Standard steel coupons were made in the laboratory from both flanges and webs of the steel sections according to BS EN 10 002-1[4-6]. Similarly, coupons were also made from the end plates and the base plates. They were cut from the additional 300 mm length from the same rolling supplied by the fabricator. All the coupon test results are summarised in Table 4-3.

4.5   Test rig

The general arrangement of the test rig is shown in Plate 4-1. The loading frame was designed by the author and constructed using the same standard pre-drilled steel channels members as for the tests described in Chapter 3. The test rig was secured to the strong floor of the laboratory. The column of the specimen was supported on a steel base plate which allowed unrestrained rotation about the major-axis but prevented rotation about the minor-axis (Plate 4-2). The steel base plate was fixed on the centre of a large concrete slab (Plate 4-1) which provide suitable working space for observation of the specimen during the test. The loads were provided by two independent jacks at each end of cantilever beams through a roller-type bearing (see Fig. 2-10). This feature accommodated the small horizontal displacement of the top surface of the beam due to vertical bending deformation. The arrangement ensured that the load applied would stay vertical.

Two independent jacks were used to apply loads on each cantilever. The centre of each loaded area was 1383 mm from the face of the column section. The position of loading represented approximately the point of contraflexure in a full-span beam.

4.6   Instrumentation

In order to quantify the moment resistance, stiffness and rotation capacity, the instrumentation proposed in the test was to enable measurement of the moment-rotation response of the connection. Having assembled the test specimen, all the instruments were mounted on the specimen as shown in Fig. 4-3. They were designed to measure the following :

a)   **Rotations** : electronic inclinometers were used to measure directly the rotation of the column and the relative rotation of beams to the column. One inclinometer was fixed to the column while the remaining four were bolted to the beams in each test. Ideally, the inclinometer should be positioned at the centre line of the beams. For SFB1, SFB2 and SFB3 however, the inclinometer had to be screwed to a specially made plate welded to the bottom of the compound plate, to avoid being encased in concrete. A comparison study carried out by Najafi[4-7] confirmed that the electronic inclinometers are able to give accurate readings.

b)   **Deflection** : displacement transducers were used to measured the deflection of the specimen under the loading points and also to control the load balance of the specimen. The results of the deflections from the transducer could be use to check the electronic inclinometer reading.

c)   **Slip** : two transducers were placed at each end of the encased beam specimens to check whether any horizontal slip occurred between the section and the concrete casing. Two other transducers were used, each being fixed near the connection to checked the vertical slip.

d)   **Loads** : two 25-t load cells were used at the loading points of each specimen.

The calibration of the instruments was carried out in a manner described in Section 2.7. The instruments were wired to a data acquisition system which was connected to a computer to monitor each test. Data was printed and stored on disk. After the tests for SFB1 and SFB2 it was decided to put strain gauges on the column flange of specimen SFB3 so as to monitor the deformation of the column flange.

4.7   Test procedure

Each specimen was initially loaded to 15 kN in 5 kN increments and then unloaded to 5 kN, to check the overall performance of the apparatus. In general the beams were then loaded up in stages to two-thirds of the predicted ultimate resistance of the connections, deemed to be about the elastic limit, and then unloaded to 5 kN to monitor their unloading stiffness. The specimens were then loaded again to determine the ultimate behaviour.

The load stages was based on approximately constant increments of applied load in the elastic phase, as load was assumed as the controlling test parameter. After this point the spacing of load increments was determined by deflection. After each load stage instantaneous readings were recorded. The specimen was then left for 10 minutes when further readings were recorded. Marking of the concrete crack pattern was also carried

out at each load stage. Graphs of M-ϕ curves were plotted during the tests as a general guide to behaviour of the specimen during the test.

All tests were terminated when the rotation was above the limit of practical interest, or when the general moment-rotation behaviour had been well-defined.

4.8   Test observation

4.8.1   Behaviour of SFB1

The connections for specimen SFB1 were two nominally identical end plates of 15 mm thickness in Grade 43 steel with 4 bolts of 20 mm diameter grade 8.8 . The responses of the two connections were generally similar at low moments. At these levels both sides showed a linear moment-rotation (M-ϕ) behaviour but demonstrated non-linear behaviour at higher moment as illustrated in Fig. 4-4. The first wire mesh fractured at a rotation of about 15 mrad. It was indicated by a drop of moment in the M-ϕ curves before regaining its expected level after further load by jacking. During the test several loading-unloading steps were carried out so as to obtain a measure of the initial rotational stiffness $S_{j,ini}$ of the connection.

The moment resistance of the connection in the test was found to exceed by more than 50% the moment resistance (48.8 kNm) calculated based on Annex J of EC3[4-8]. The concrete was ignored in the calculation. The measured properties were used to calculate this moment of resistance. It was predicted by Annex J that the mode of failure would be mode 2 (yielding + bolt failure). At a moment level of about 80 kNm a loud 'bang' was heard and the load dropped suddenly. It was decided to stop the test at this stage. A rotation exceeding 45 mrad was achieved during the test.

Curves of moment against deflection for both left and right beam are shown in Fig. 4-5. The first formation of hairline cracks in the concrete for SFB1 was found in the vicinity of the connection parallel to column flange at a moment of 14kNm. These cracks later formed the main cracks of the beam. As moment increased to 24 kNm a new transverse crack formed further from the column. At moment level of 35 kNm another new crack developed further away still from the column flange. Plate 4-3 indicates the pattern of cracking.

A check was carried out to see if the beam twisted during the test ; no twisting occurred to the beams.

Upon completion of the test, concrete in the area of the connection was broken out to investigate the behaviour of the elements in that vicinity. There was evident deformation of the end plate but no significant deformation occurred in the column flanges. It was found that that all the mesh had fractured and one bolt was failing due to stripping which perhaps contributed to the loud `bang' sound. However there was no evidence of local buckling to the web or flanges of the steel beams.

4.8.2 Behaviour of SFB2

Compared to specimen SFB1 the connections for SFB2 were stiffer as a larger bolt diameter was used (24 mm diameter Grade 8.8). As expected the response showed an increase in moment resistance. However the M-ϕ curves (Fig. 4-6) were generally of similar shape to those of SFB1 (i.e. linear at lower moment and non-linear behaviour for the higher levels). The first mesh fractured occurred at a rotation of 10 mrad.

The moment resistance of the connection calculated on the basis of Annex J of EC3[4-8] based on measured material properties was 62.9 kNm. The concrete was ignored in the

calculation. However in the test the attained moment resistance of the connection was well over that value. The SFB2 connection demonstrated a capability of reaching a rotation of over 30 mrad. The test had to be discontinued owing to excessive deflection when the measured maximum bending moment was 110 kNm. Fig. 4-7 shows the deflection behaviour of the beam with moment. By calculation, the predicted mode of failure would be mode 1 (yielding of end plate/column flange).

At a moment of 14 kNm the first cracks in concrete were observed around the area of connections i.e. parallel to column flange. At 21 kNm new cracks formed at about 200 mm from the column flange. As in specimen SFB1, the transverse cracks formed further away from the column as load increased. Longitudinal cracks formed at about 400 mm from the column face at 55 kNm.

After the concrete around the connection was broken out, it was found that excessive deformation of column flanges and end plates were the main cause of the failure for the connection (see Plate 4-4). However, as with SFB1, there was no local buckling to the web or flanges of the beams.

4.8.3 Behaviour of SFB3

With a more flexible 10 mm thick end plates and 20 mm diameter bolts of Grade 8.8, the expected connection stiffness for the specimen SFB3 was much less compared to specimens SFB1 and SFB2. However, the response to increasing moment still showed a similar general pattern to that of SFB1 and SFB2 (see Fig. 4-8). The first mesh fractured was however at a lower rotation of about 10 mrad. Fig. 4-9 illustrates the response of the beam deflection to the moment increments of the specimen.

The calculated moment resistance of the connection based upon Annex J of EC 3[4-8] was 40.1 kNm. However the test showed the connection able to resist a much higher ultimate moment. As in previous tests the calculation was carried out using the measured material properties, ignoring the concrete. The predicted mode of failure was mode 1 (yielding of end plate/column flange).

During the test the left and right connections had slightly different responses at early stages of loading; the left connection demonstrated a higher rotation at the same applied moment. Both connections recorded a rotation well above 30 mrad before the test was terminated. At the moment of about 45 kNm there was a 'snapping' noise indicating mesh fracturing and this deteriorationcaused the moment to drop to 35 kNm. The test was terminated when the measured bending moment resistance had reached about 60 kNm, at a rotation of more than 45 mrad.

The cracking of concrete was concentrated almost entirely around the vicinity of connection and the first formation of a crack was found at a moment of 14 kNm. As in specimens SFB1 and SFB2 only negligible slip was recorded at the free end of the beam.

After the concrete casing was broken out, excessive deformation of end plates was identified as the main causes of failure for the connection (see Plate 4-5) confirming the predicted mode of failure.

4.8.4   Behaviour of TEST4

This specimen comprised bare steel sections having the same end plate connection as SFB3 but without the compound plate at the bottom flange. The M-ϕ curves as indicated in Fig. 4-10 showed a linear behaviour at the early stages of loading. The moment

against deflection (Fig. 4-11) also showed a linear behaviour at the early stages of loading. At a moment of 21 kNm a slight gap was observed between the column flange and the end plate. As moment increased this gap became wider. At 51 kNm noticeable bending was observed in the end plates. Although specimen TEST4 had the same connection arrangement as SFB3, the calculated moment of resistance was slightly lower at 36.6 kNm, due to different value of material properties (see Table 4-3).

It was decided to end the test when the applied moment was about 65 kNm at about 55 mrad to avoid the possibility of the bolts fracturing. Deformation of the end plates was the principal cause of failure. No local buckling of flanges and web was observed. Plate 4-6 indicated how the end plate had deformed.

4.8.5   Behaviour of TEST5

Compared to the previous specimen the connections in specimen TEST5 were stiffer as larger bolts and thicker end plates were used. From the M-ϕ curves (Fig. 4-12) it was observed that initially the rotation increased linearly as the applied moment increased. At the beginning of the test the right hand beam gave a negative rotation reading. It was thought that initial curvature of the end plate of the connection on the right hand beam contributed to this (see Plate 4-7). The moment-deflection curves (Fig. 4-13) also indicated that deflection increased linearly as the applied load increased.

The calculated moment resistance was 66.1 kNm. It was higher than the calculated moment of resistance for SFB2 (62.9 kNm) although both had the same end plate arrangement. Again this was due to the slight difference in the measured material properties. The predicted mode of failure was mode 2 (yielding + bolt failure). At the early stage of the test the nuts were tack welded to the end plate as a precautionary

measure against catastrophic bolt failure. It was decided to stop the test at about 96 kNm to avoid the danger of the bolt fracturing; the calculated bolt force was than approximately 250 kN. At this juncture the rotation had reached just 25 mrad.

4.9   Assessment of Test Results

The average values of M-φ curves for all the specimen are illustrated in Fig. 4-14a to Fig. 4-14e inclusive. Table 4-4 shows the summary of the mode of failure calculated based on the basis of Annex J of EC3[4-8]. The value of the tensile strength of the bolt was obtained by reference to the values determined through the experiment by Godley and Needham[4-9]. The comparisons indicated that the ultimate tensile strength of bolts were 28% above the nominal value.

The predicted and the experimental resistance moments (M_{Rd}) are given in Table 4-5, along with the failure modes. The predicted values are based on measured material properties. Annex J of Eurocode 3[4-8] were used to predict the resistance moments of the connections, ignoring the concrete. The proposals by Jaspart[4-10] formed the basis by which the prediction for the experimental values were derived. The experimental moment of resistance of each connection was defined as the moment at one third of the initial stiffness of the test. This stiffness may be obtained from the initial response of the specimen or more conveniently, from the unloading-reloading response at a later stage of the test.

The failure modes during the tests were identical to those predicted by Annex J. However the calculations show that Annex J of EC3[4-8] significantly underestimates the moment reached in all the tests. Two values of M_{Rd} from the tests for SFB1, SFB2, and SFB3 are given in Table 4-5. This is because there are two different values of "initial" rotational stiffness S_{ji}. One is the response before the mesh fractures. The

second is from the unloading-reloading response after the mesh had fractured. Except for SFB3 (left) all the experimental resistance moments were greater than the calculated values.

None of the specimens (except SFB1 left) showed a peak in the M-φ curve. No test exhibited a true plastic plateau. This behaviour is typical of steel end plate joints in which brittle modes of failure have been prevented. In SFB1 (left), both fracture of the mesh and bolt stripping had occurred.

As previously mentioned, initial rotational stiffness of a connection can be determined from the unloading parts of the M-φ curves in a test. These are recorded in Table 4-6. The two values result from the notable difference observed for all the encased specimens before and after the mesh fractured. It is found from Table 4-6 that after the mesh fractured, and the concrete had cracked significantly, the initial stiffness value is similar to that given by the corresponding bare steel test.

Table 4-6 also shows the values of rotational stiffness at various stages of loading. There were two calculated values for initial stiffness based on ENV 1993-1-1/pr A2[4-11]; one by considering the stiffened column web due the effect of encasement; the other by including the column flexibility.

Effects of encasement

The concrete encasement effects can be clearly seen from Fig. 4-15 and Fig. 4-16 for comparison between SFB3 and TEST4 and comparison between SFB2 and TEST5 respectively. At low rotation there is a much higher initial rotational stiffness for the encasement specimens. However, after the concrete had cracked and the first mesh fractured the stiffnesses were comparable to the corresponding bare steel value. From

the comparison in Table 4-6 there is evidence that encasement by concrete can enhance the initial stiffness of a slimflor connection by a factor of between 1.5 to 2.4 .

Effects of different end plate thickness

Difference in the end-plate thickness result in different M-ϕ behaviour of the connection. In Fig. 4-17, SFB1(with 15mm end plates) registered a higher initial rotational stiffness than SFB3(with 10mm end plates). At 30 mrad the measured bending resistance of SFB1 is about 60% higher than SFB3. However, the measured rotation indicated SFB3 was more ductile than SFB1.

Effects of different bolt sizes

From Fig. 4-18, the larger M24 bolts used in SFB2 had little effect on the initial rotational stiffness when compared to SFB1(with 20 mm dia. bolt). However at 30 mrad, the bending resistance of SFB2 was 12% higher than SFB1.

Comparison between inclinometer and transducer reading

In all the tests the measured rotations were compared to the deflection Δ divided by the length of 1513 mm, which was the distance on the undeformed specimen from the centreline of the column to the displacement transducer. Fig. 4-19a to Fig. 4-19e indicated a good correlation between the two readings, the contribution from the beam's flexibility being very small due to the stiffness of the section employed.

4.10 Classification of Connections

EC3[4-8] requires that the type of joint be classified against the particular limits depending upon the form of framing adopted i.e. braced or unbraced frame. In order to carry out this classification the non-dimensional quantities $\bar{m}$ and $\bar{\phi}$ are required. The moment-rotation curves of all tests are presented in non-dimensional form ($\bar{m}$ - $\bar{\phi}$) in

Fig.4-20 using the method from EC3 for classification of connections in braced frames. The beam span L was taken as 7.5 m and a cracked beam section and measured material properties were taken to determine the properties of the beam section. From Fig.4-20 the connections can be classified by strength, as "partial-strength ", and by stiffness, as "semi-rigid". Use of an uncracked beam section would result in the same classifications.

Classification of connections using the revised Annex J' ENV 1993-1-1/pr A2[4-11] was also carried out (see Fig. 1-8). Classification by stiffness confirmed that all the connections were semi-rigid. However classification by strength resulted in all the connections being nominally pinned because their design moment resistances $M_{j,Rd}$ were not greater than 0.25 times the moment resistance required for a full-strength joint.

4.11 Conclusions

(i)   It has been found from the experimental and analytical studies that Annex J conservatively estimates the moment resistance of the slimflor connections.

(ii)   It was confirmed that encasement by concrete significantly increases the initial stiffness of end plate slimflor connections.

(iii)   After the mesh fractured and significant concrete cracking had occurred, the initial stiffness decreased to that of bare steel connections.

(iv)   Classification of connections by stiffness confirmed that all the end plate connection tested were semi-rigid.

(v)   The procedure of Annex J can be used to predict accurately the mode of failure.

(vi)   The moment of resistance of joints with more flexible end plates are just 6% over the values predicted by Annex J. However with thicker end plates significant increases in resistance arise (40%) as compared to the predicted value.

(vii) In the tests, all the rebar the mesh fractured at a moment greater than two third the value of the design moment. This observation indicates that the mesh could be assumed to be effective in deflection calculation for SLS.

(viii) Proper reinforcement and design are needed if a slimflor's beam-to-column connection is to be considered as a composite joint.

References

4-1. Bernuzzi C, Gadotti F, and Zandonini R., "Joint action in slim floor system", 4th Pacific Structural Steel Conference, Singapore, 1995.

4-2. *"Design in Steel 2, Slim floor Construction"*. British Steel publication 1996.

4-3 "Bending resistance and rotational stiffness of connections in encased steel sections", Document RT 594, Draft 01. The Steel Construction Institute, September 1996.

4-4 BS5950:Part1, "Code of practice for design in simple and continuous construction: hot rolled sections". British Standard Institution, London, 1990.

4-5. "Guidelines on the properties, Designs and Specification of Lytag structural lightweight concrete", Technical Notes, Boral Lytag.

4-6 BS EN 10 002-1:"Tensile testing of metallic material, Part 1: method of test and ambient temperature", British Standard Institution, 1990.

4-7. Najafi A.A., "End plate connections and their influence on steel and composite structures", PhD Thesis, University of Warwick, 1992.

4-8 Eurocode No.3, "Design of steel structures, Part 1 General rules and Rules for building", Commission of the European Communities. ENV 1993-1.

4-9 Godley M.H.R. and Needham F.H., "Comparative tests on 8.8 and HSFG bolts in tension and shear". *The Structural Engineer* Vol. 60A, No3, March 1982. pp 94-99.

4-10. Jaspart J.P., "Design and ultimate resistance for joints"., COST C1 Working group Meeting on Steel and Composite, Graz. December 1995.

4-11 Eurocode 3 : Part 1.1. "Revised annex J : Joints in building frames". ENV 1993-1-1/pr A2.

Table 4-1 : Test parameters

Specimen	End plate thickness (mm)	Bolt sizes (mm dia.)	Type of beams	
SFB1	15	20	Encased	Bottom flange plate
SFB2	15	24	Encased	Bottom flange plate
SFB3	10	20	Encased	Bottom Flange plate
TEST4	10	20	Bare	–
TEST5	15	24	Bare	–

Table 4-2   :   Concrete Compressive Strength

TEST	7 days N/mm²	28 days N/mm²	Day of Testing
SFB1	31.4	49.2	49.2
SFB2	35.0	49.2	49.2
SFB3	38.3	50.5	43.1

Table 4-3 : Summary Based On Coupon Tests

Specimen	t ep mm	f_y ep N/mm²	t flange mm	f_y flange N/mm²	t web mm	f_y web N/mm²	t bottom flange plate* mm	f_y bottom flange plate. N/mm²
SFB1	15.2	229	16.6	335	10.5	341	14.6	443
SFB2	15.2	229	16.6	335	10.5	341	14.6	443
SFB3	10.1	331	16.6	335	10.5	341	14.6	443
TEST4	10.0	307	16.7	359	10.3	331	-	-
TEST5	13.2	361	16.7	359	10.3	331	-	-

Table 4.4: Failure Mode according to Annex J of EC3

Specimen	Bolt size	F_t eplate kN	Mode	F_t col kN	Mode	F_t bolt kN	mode	F_t bolt** kN
SFB1	M 20	254.3	2	299.7	2	352.8	3	451
SFB2	M 24	328	1	377.7	2	508.3	3	654
SFB3	M 20	209	1	299.7	2	352.8	3	451
TEST4	M 20	189.7	1	310	2	352.8	3	451
TEST5	M 24	344.4	2	310	2	508.3	3	654

Notes:

1. Mode 1 : Complete yielding of plate/column flange
2. Mode 2 : Bolt failure + yielding
3. Mode 3 : Bolt failure
4. * Bottom flange plate
5. ** Value from Table4 of Godley & Needham[4-9]

Table 4-5: Moment resistance of connection and failure mode

Test	Connection details	M_{Rd} * (calculated) kNm	M_{Rd} ** (Test) left kNm	M_{Rd} ** (Test) right kNm	M_{plRd} (Base on steel alone) kNm	Failure Mode (predicted) ***	Failure Mode (Test)
SFB1	20 mm bolt 15 mm end plate 15 mm bott plate	48.8	67.5 85	68 76	469.1	2	bolt stripping end plate deformation mesh fracture conc crack
SFB2	24 mm bolt 15 mm end plate 15 mm bott plate	62.9	85 98	89.5 81	469.1	1	column flange and end plate deformation mesh fracture conc crack
SFB3	20 mm bolt 10 mm end plate 15 mm bott plate	40.1	39 43	46 51	469.1	1	end plate deformation mesh fracture conc crack
TEST4	20 mm bolt 10 mm end plate	36.6	47.5	49.3	410	1	end plate deformation
TEST5	24 mm bolt 15 mm end plate	66.1	97	100	410	2	end plate deformation

Notes: *   based on measured value and Annex J
           **   based on Sj inl/3 (Jaspart)
           ***   1.   Yielding of end plate/column flange
                                 2.   Yielding + bolt
failure

                                 3.   Bolt failure

Table 4-6 : Values of Rotational Stiffness S_j

Specimen	Initial Stiffness Sj ini (Test) Left kNm/rad	(Test) Right kNm/rad	Initial Stiffness Sj ini (Calc) # kNm/rad	Initial Stiffness Sj ini (calc)## kNm/rad	Stiffness Sj at MRd. (calc) kNm/rad	Stiffness Sj (Sji/3)** Left kNm/rad	Right kNm/rad	Stiffness Sj at calc MRd*** left kNm/rad	right kNm/rad	Stiffness Sj at 2/3MRd. Left kNm/rad	Right kNm/rad	MRd **** (calc) kNm
SFB1	17540 7770	20930 8780	14060	11210	3750	5850 2590	6976 2928	10910	12510	13700	18550	48.8
SFB2	23410 10140	16130 9730	15050	11830	3960	7800 3380	5377 3244	11960	8340	16760	12220	62.9
SFB3	11950 6860	15350 10360	7580	6670	2230	3920 2290	5100 3455	3580	7430	8610	14050	40.1
TEST4	6010	6290	7580	6670	2230	2000	2096	3440	4070	5420	5730	36.5
TEST5	8210	9050	15050	11830	3960	2740	3016	6070	74040	8630	9110	66.1

Notes : # not considering column web flexibility due to encasement (ENV 1993-1-1/prA2)

considering column web flexibility (ENV 1993-1-1/prA2)

** based on Jaspart [7]

*** based on graph plotted in the test
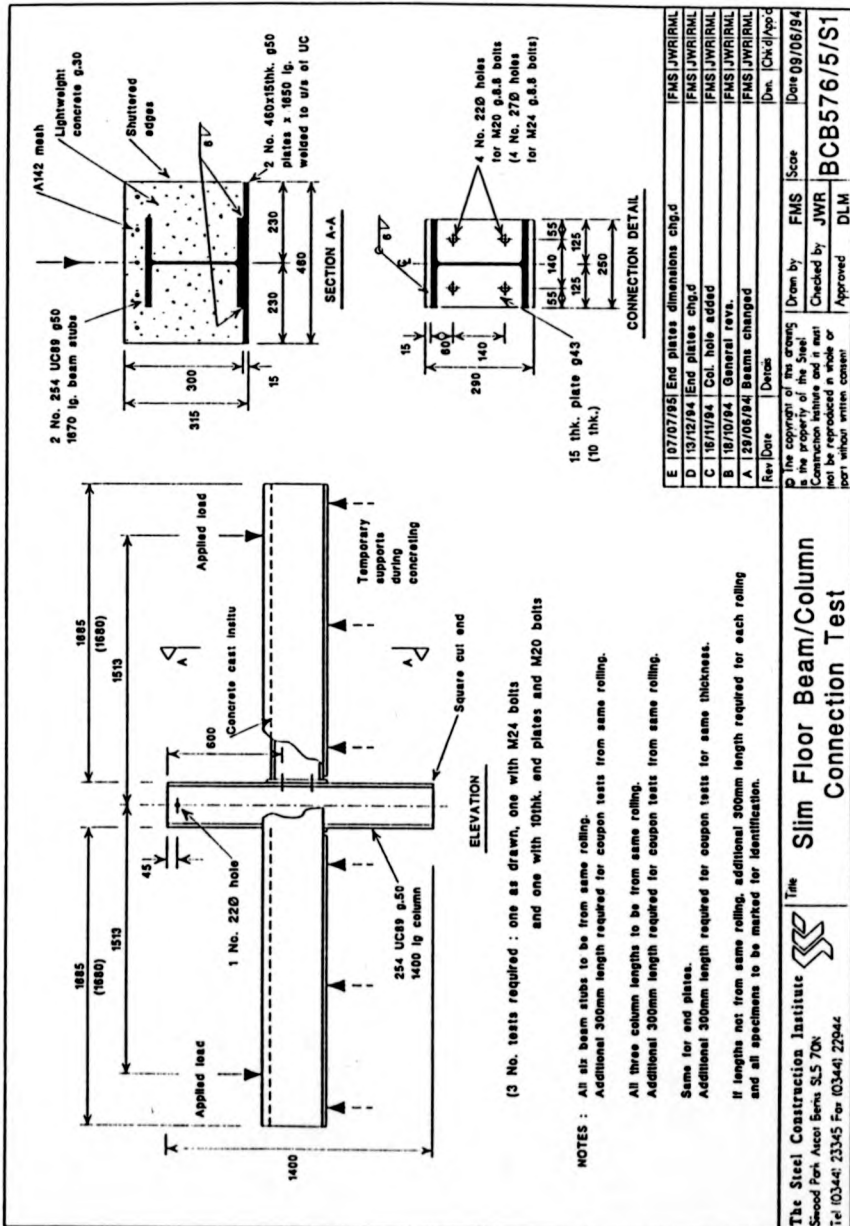
**** based on Annex J
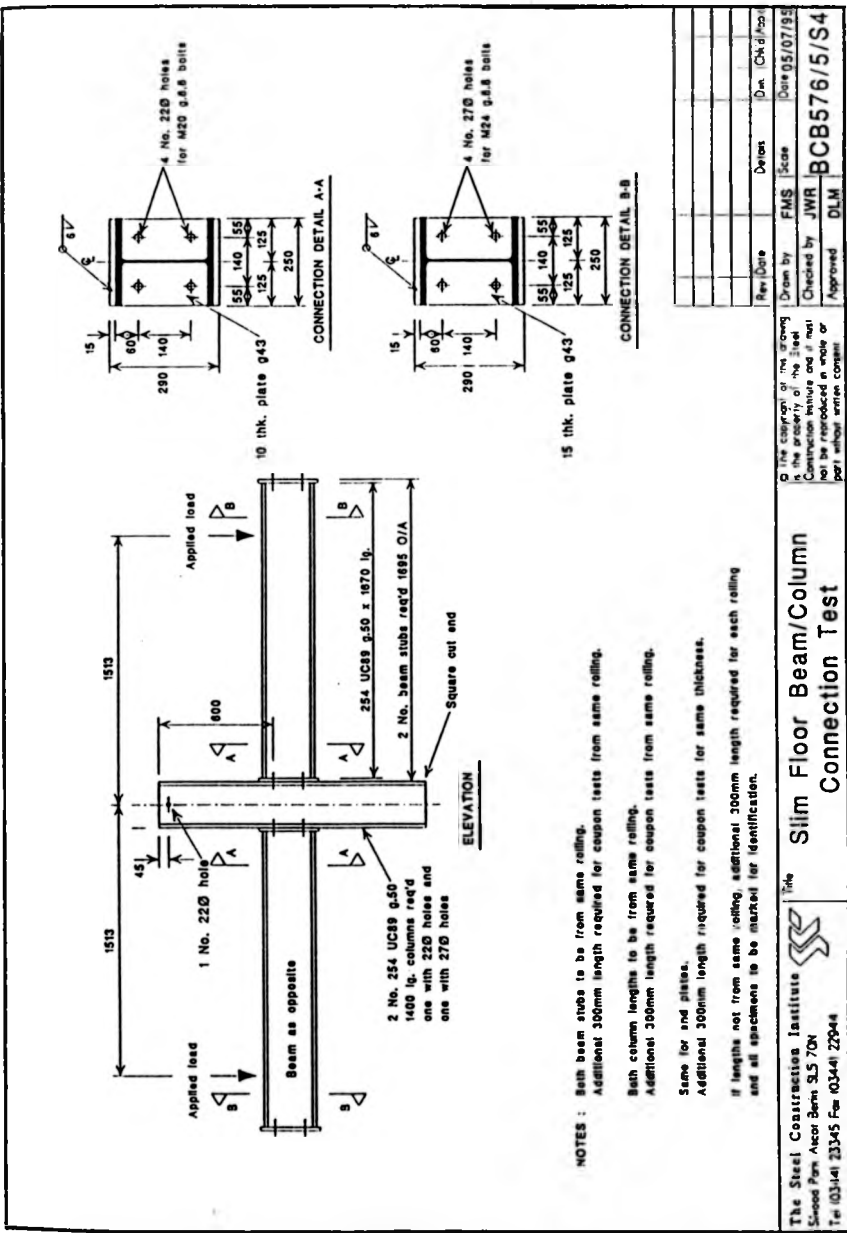
Fig. 4-1 : Details for SFB1, SFB2 and SFB3.

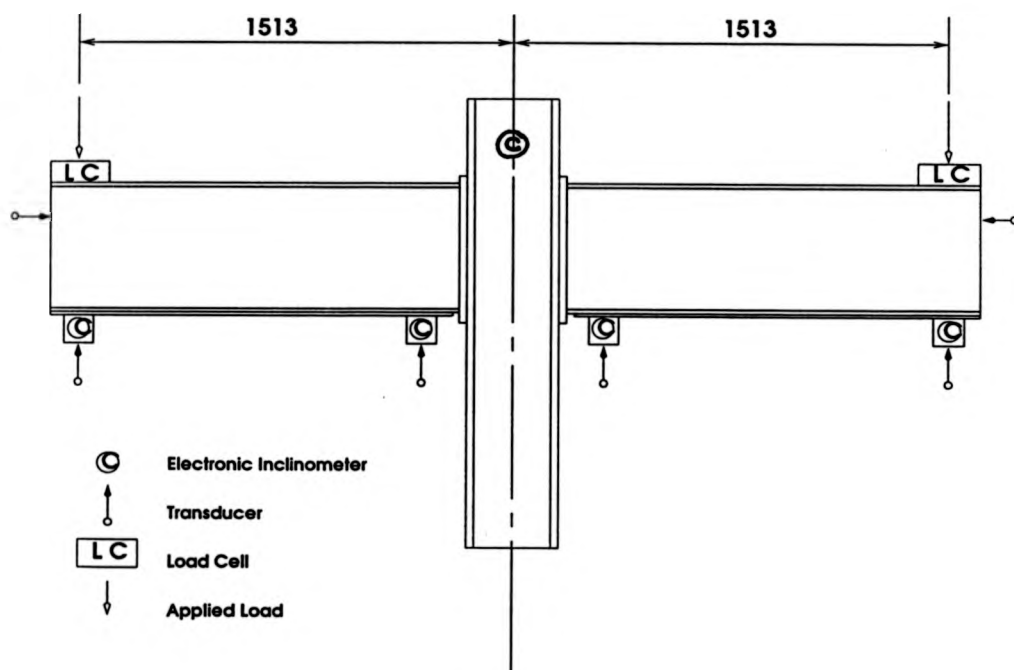*Fig. 4-2 :   Details for TEST4 and TEST5.*

Fig. 4-3 :   Instrumentation

Fig. 4-4 : Moment vs Rotation for SFB1

SFB1

Fig. 4-5 : Moment vs Deflection for SFB1

SFB2

End plate 15mm
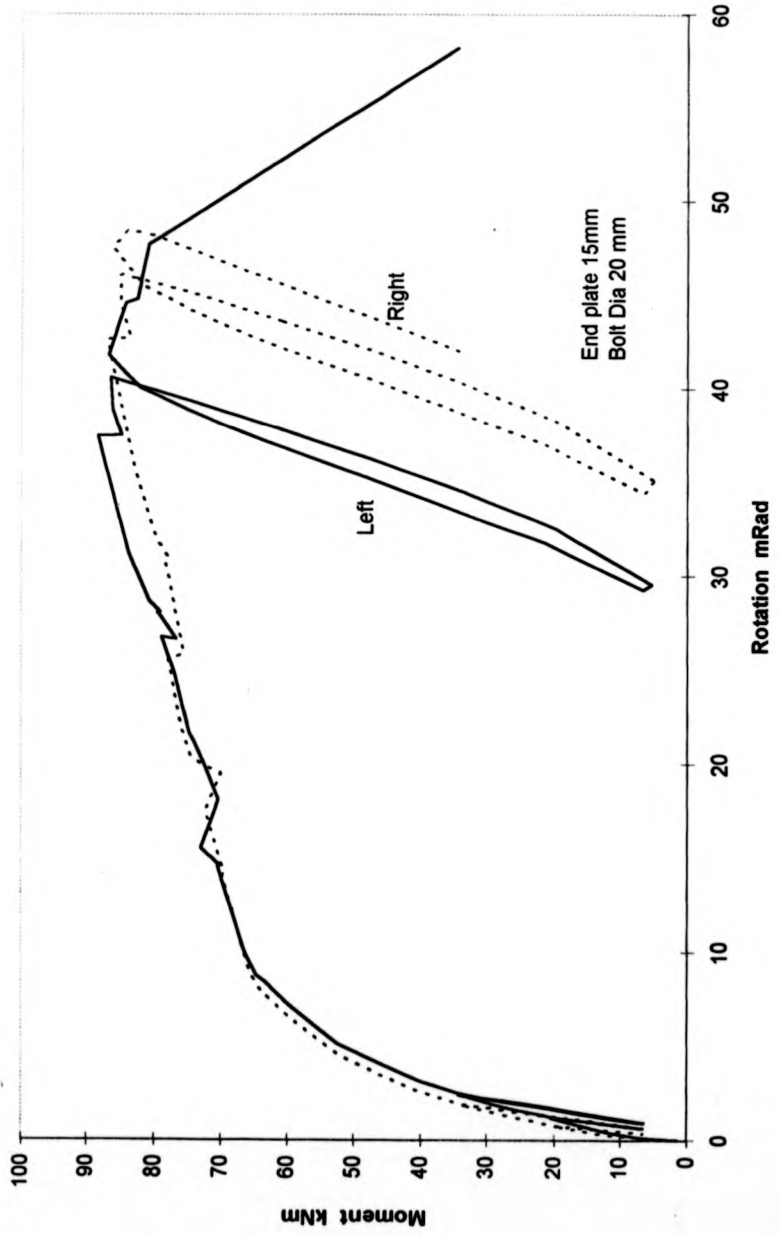Bolt dia. 24 mm

Moment   kNm

Rotation mRad

Right

Left

Fig. 4-6 : Moment vs Rotation for SFB2

SFB2

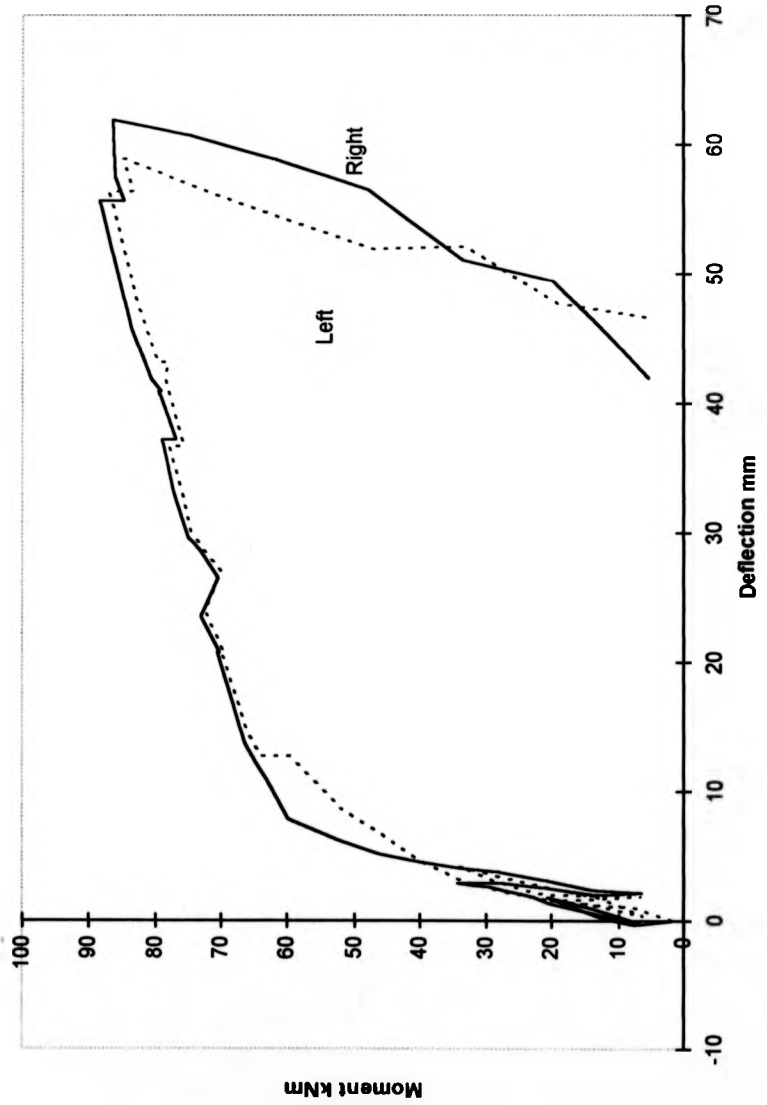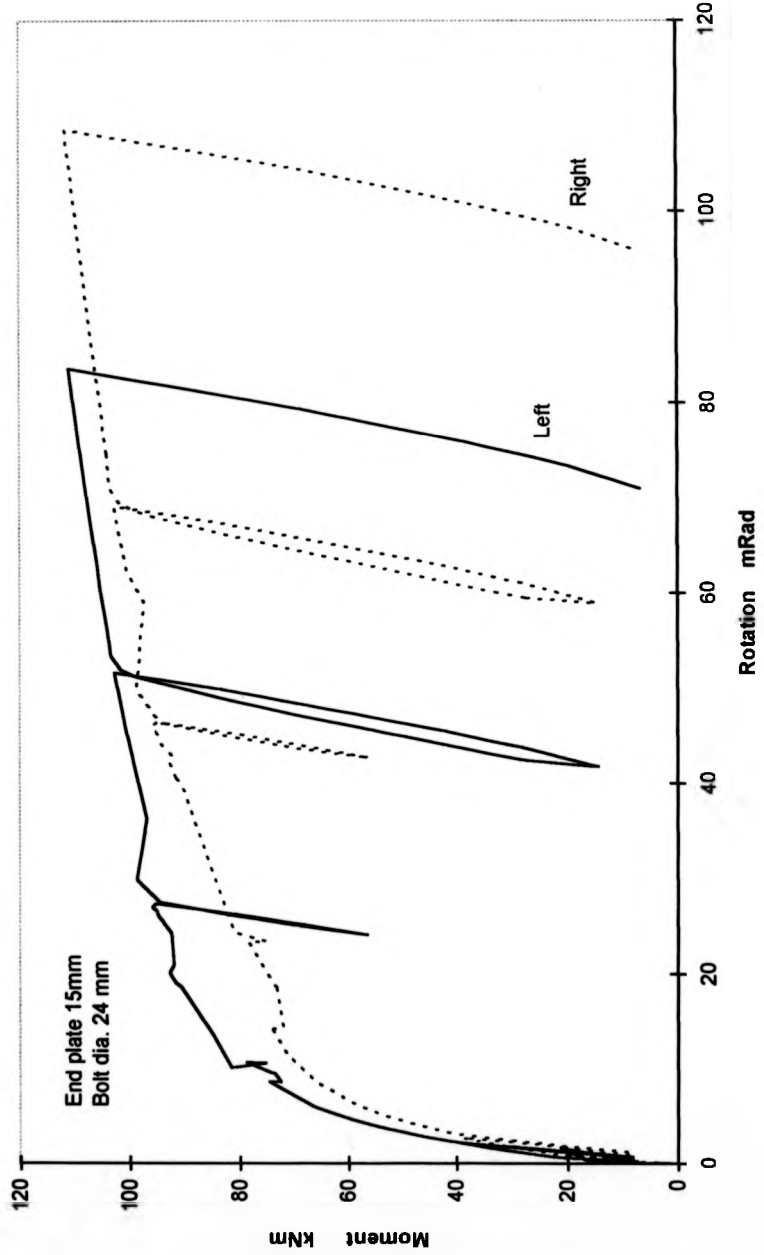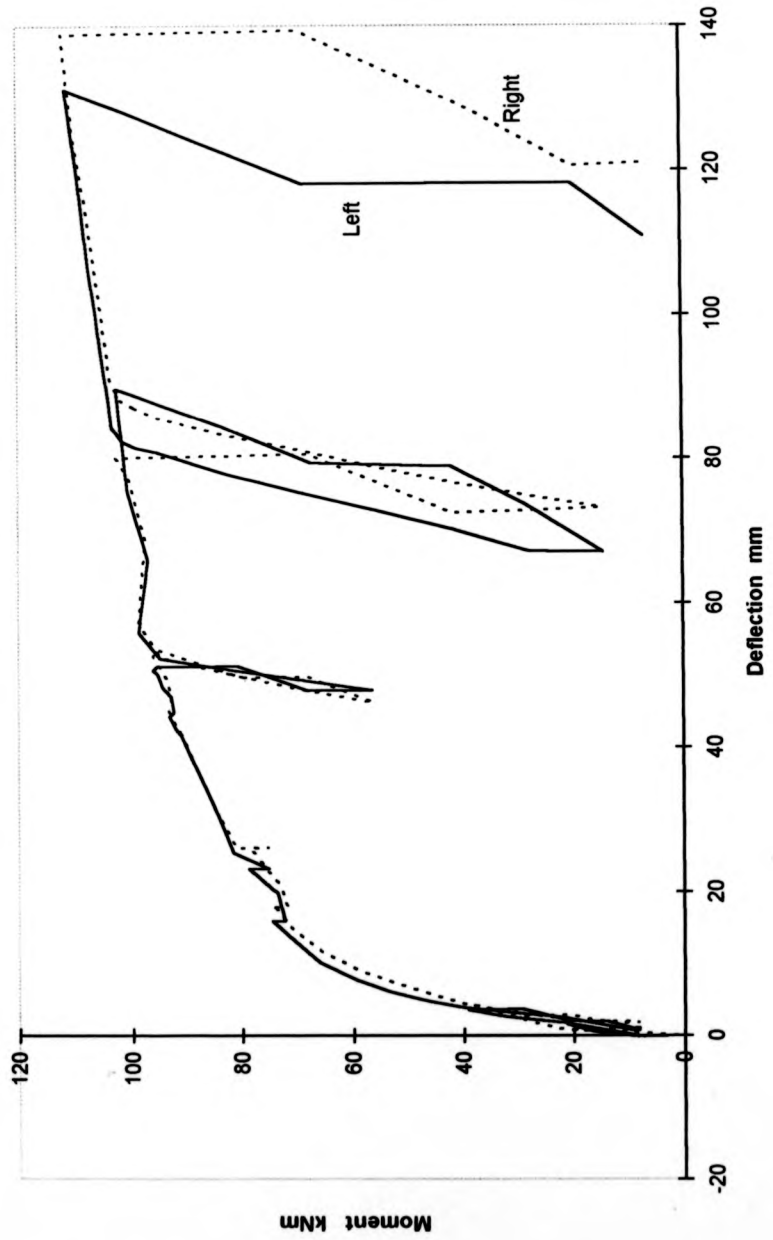*Fig. 4-7 : Moment vs Deflection for SFB2*
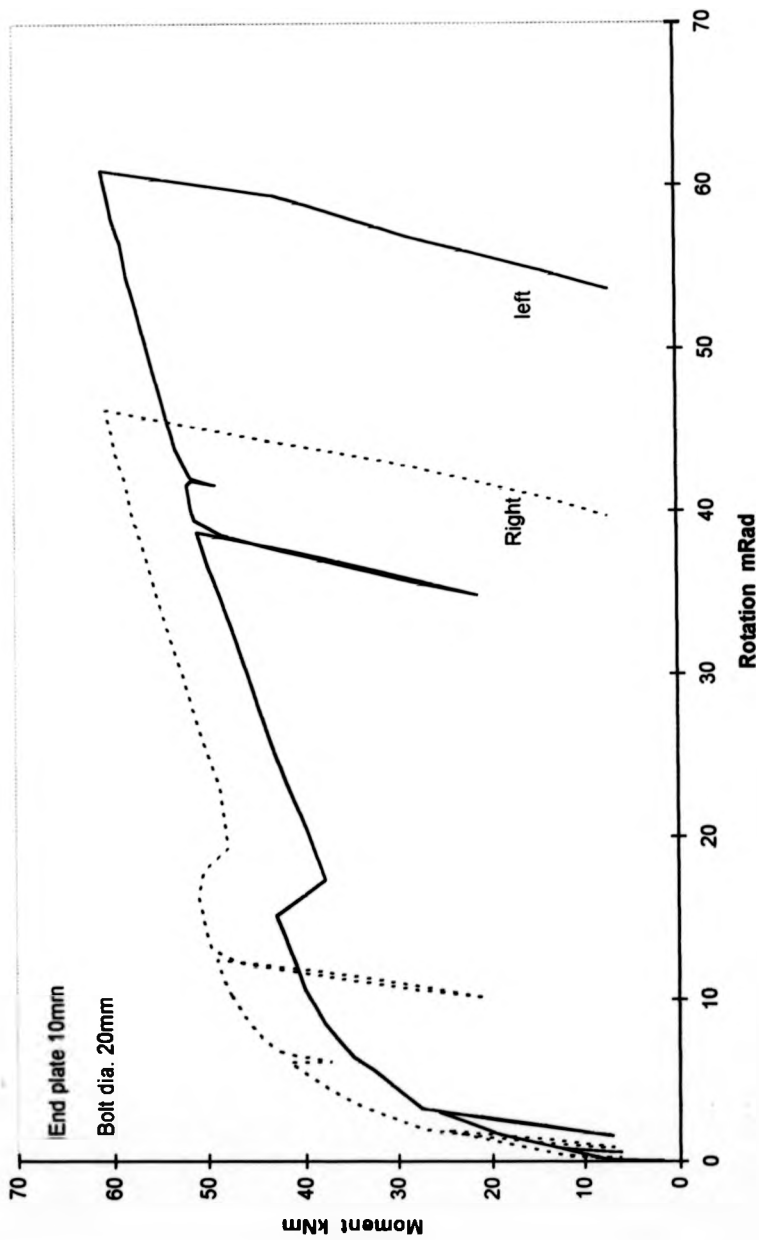
Fig. 4.8 : Moment vs Rotation for SFB3
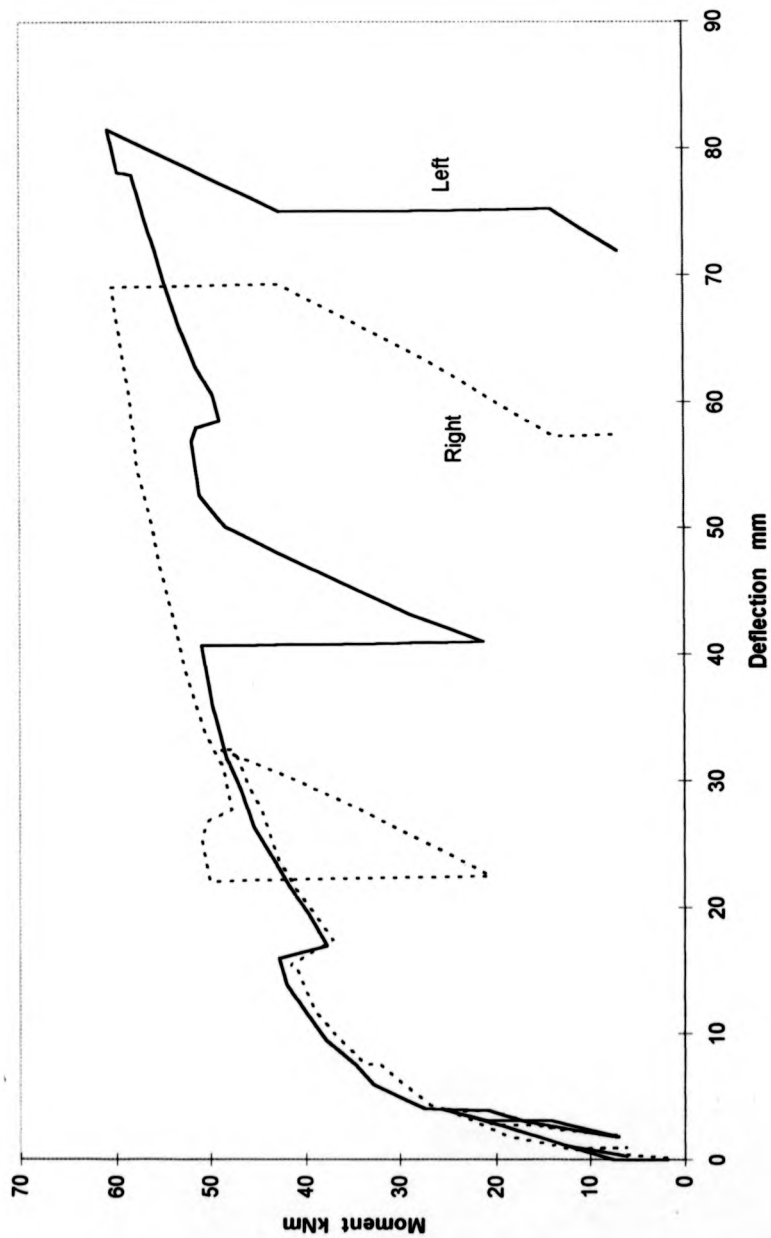
Fig. 4-9 : Moment vs Deflection for SFB3
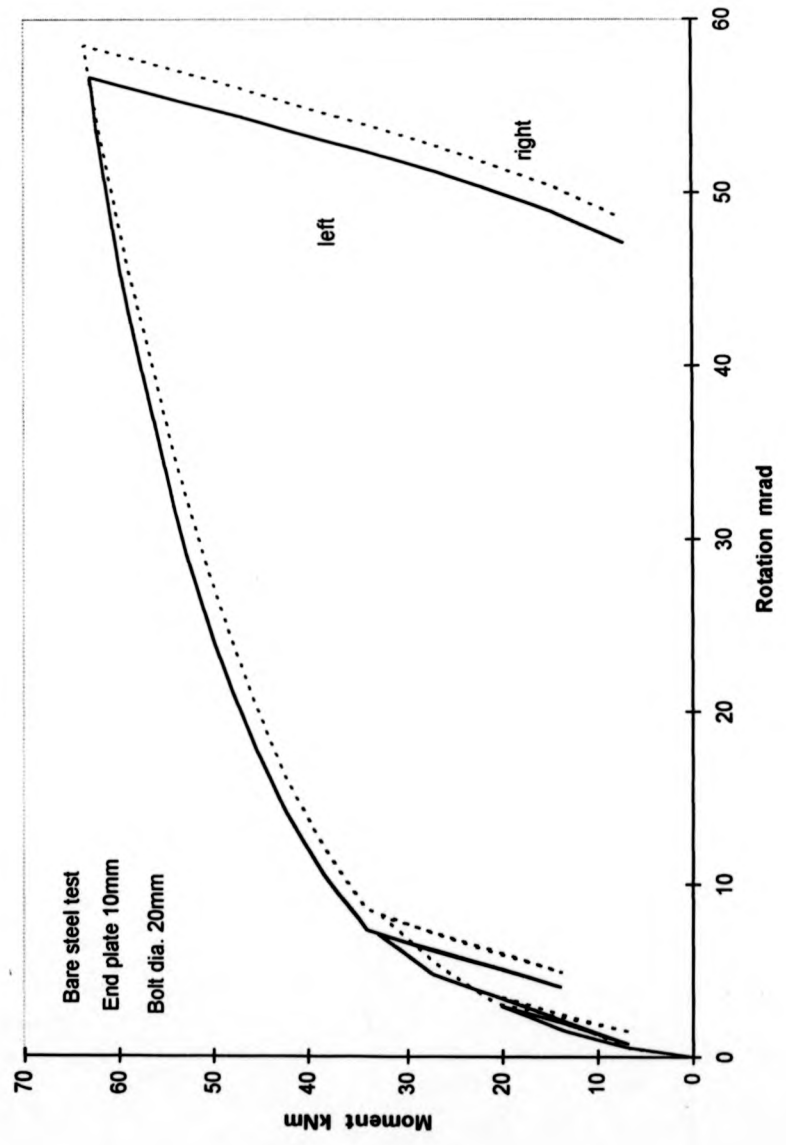
Fig. 4-10 : Moment vs Rotation for TEST4

TEST4
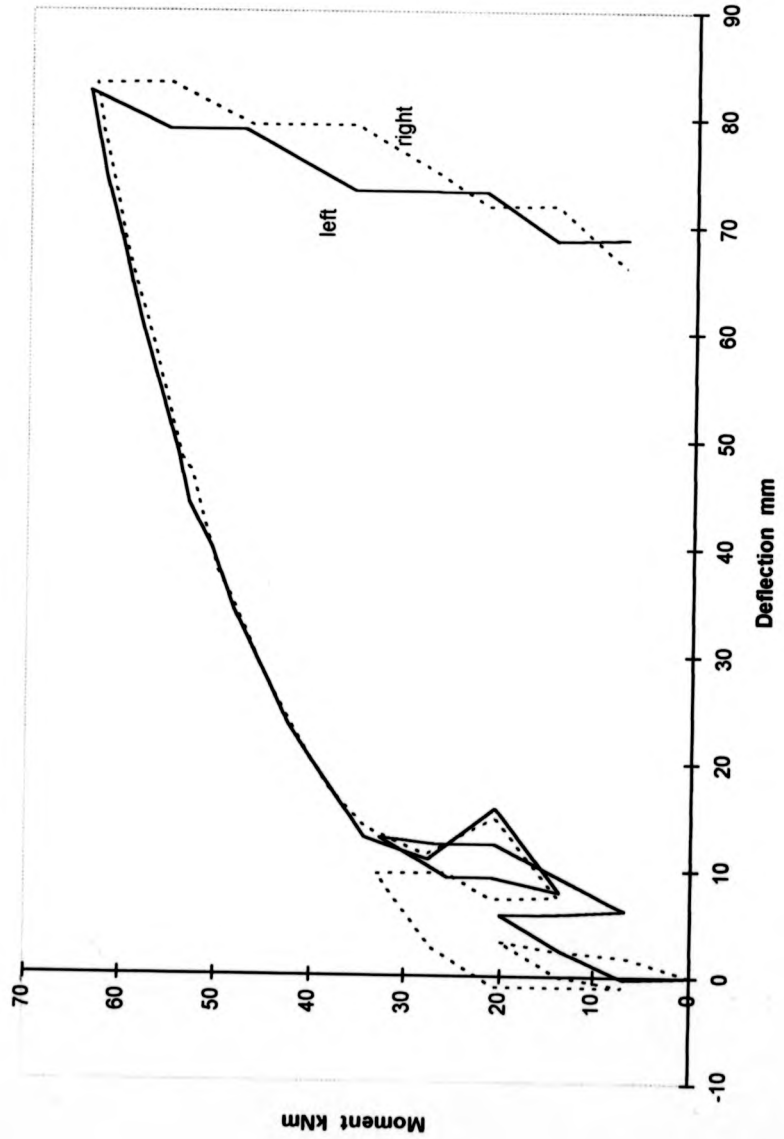
Fig. 4-11 : Moment vs Deflection for TEST4
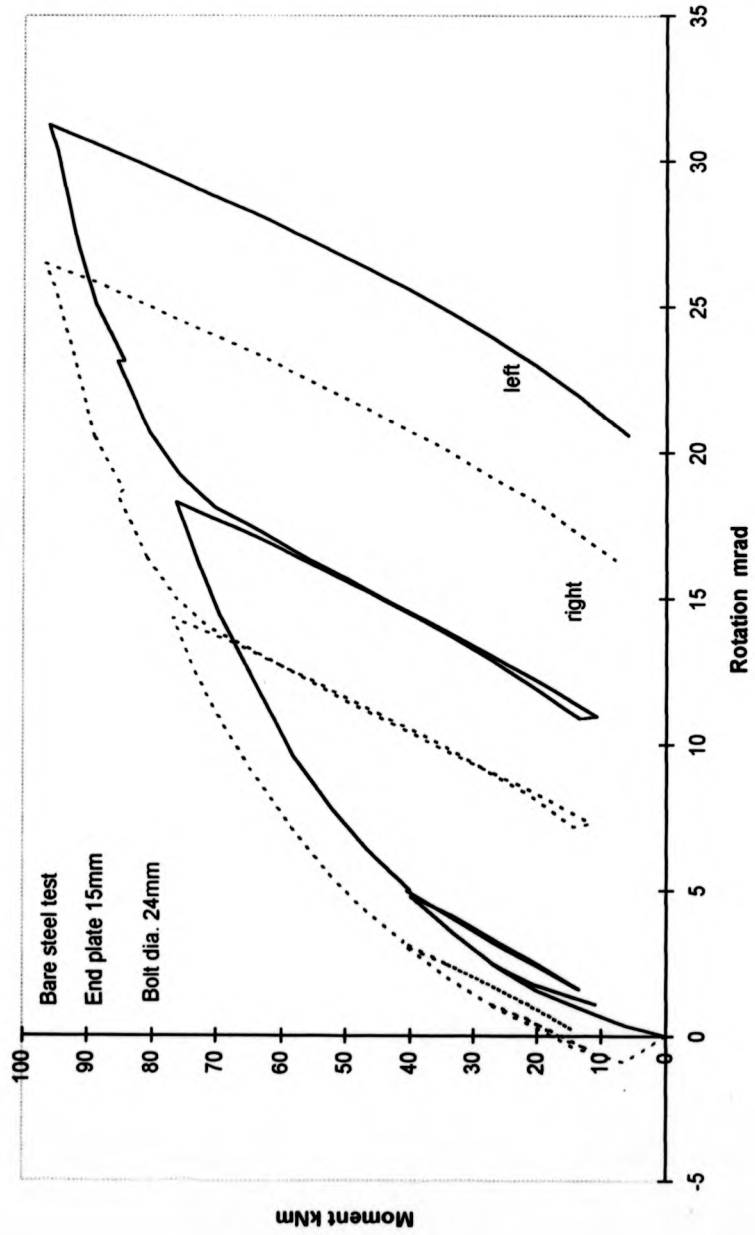
Fig. 4-12 : Moment vs Rotation for TEST5

TEST5
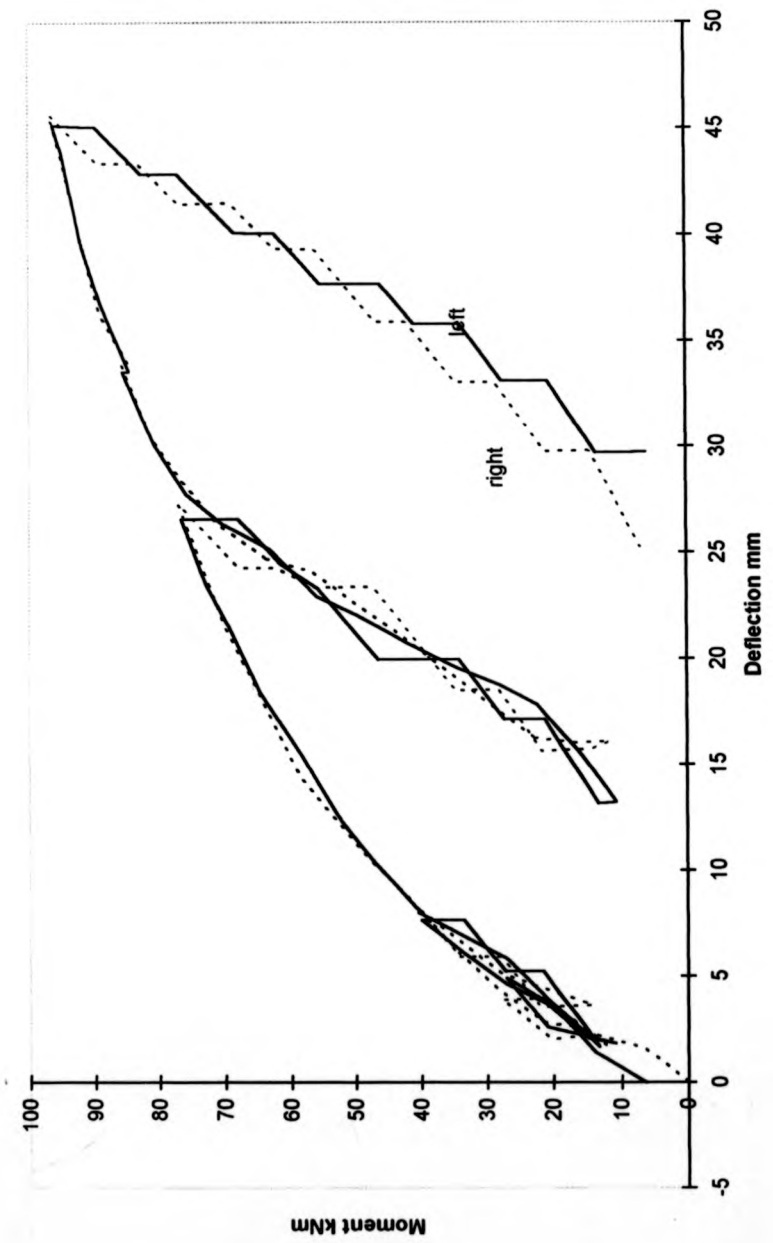
Fig. 4-13 : Moment vs Deflection for TEST5

SFB1
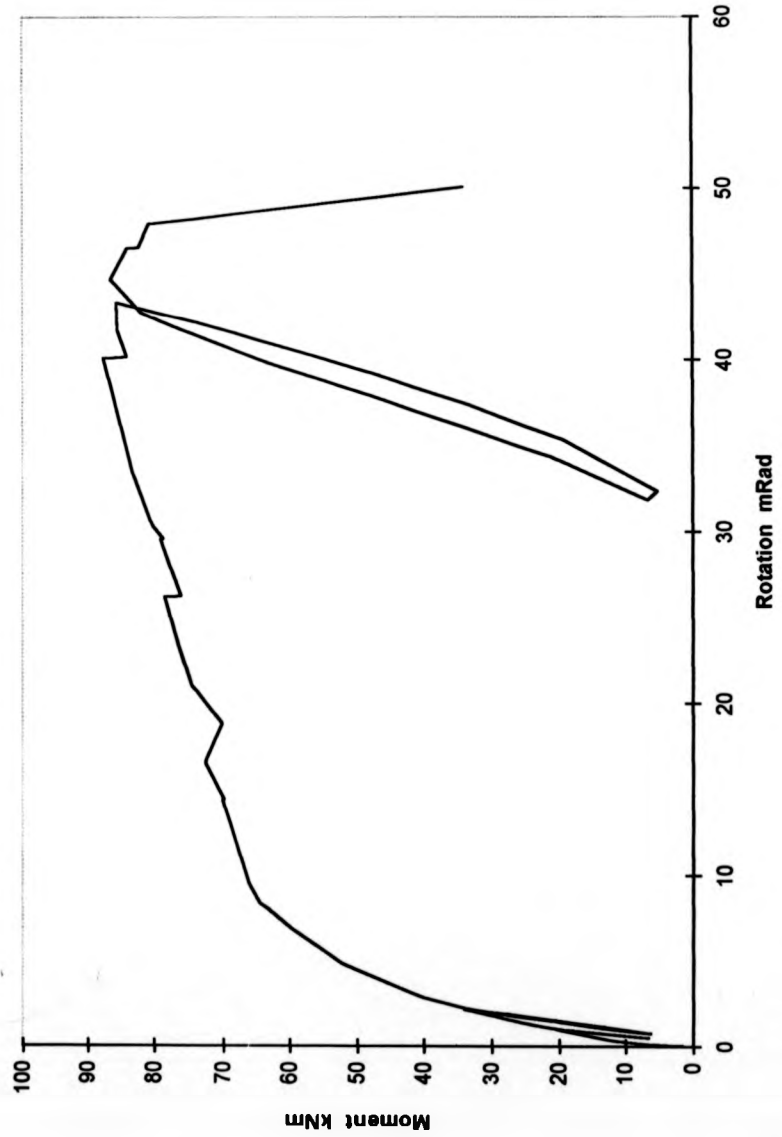
Fig. 4-14a : Average value of Moment vs Rotation for SFB1

Moment vs Rotation for SFB2(average)
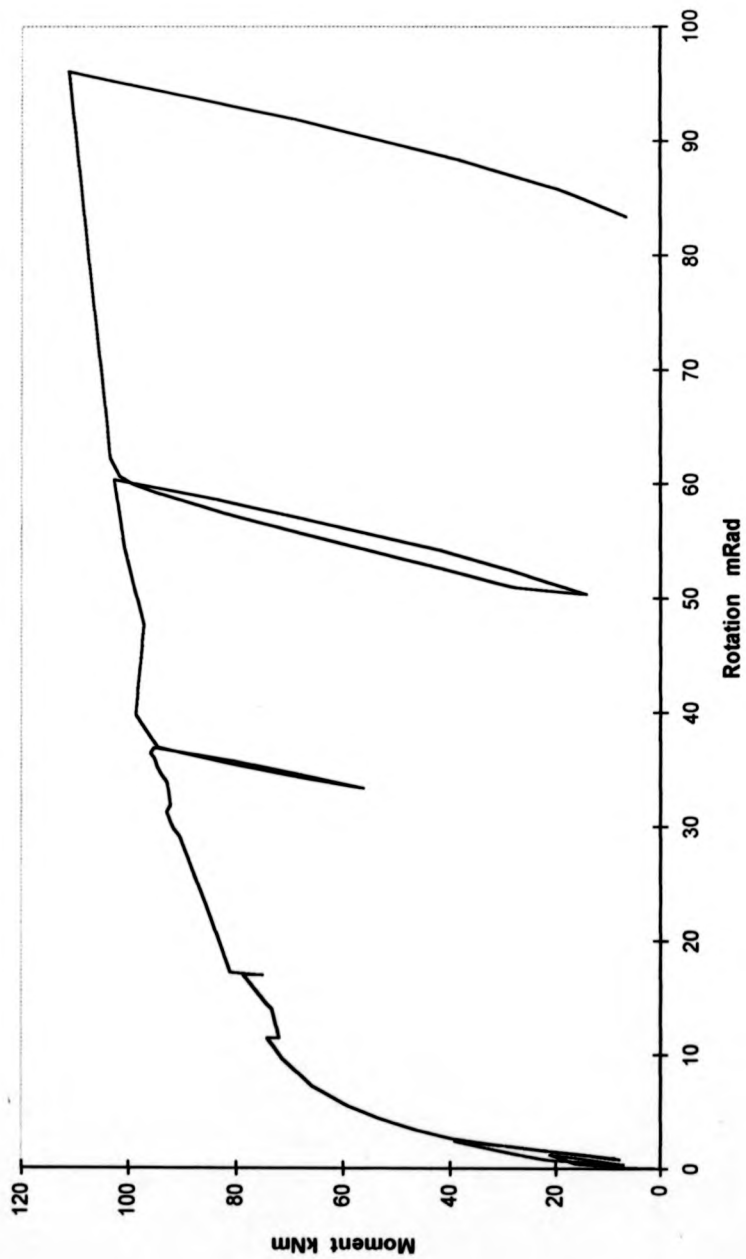
Fig. 4-14b : Average value of Moment vs Rotation for SFB2

SFB3
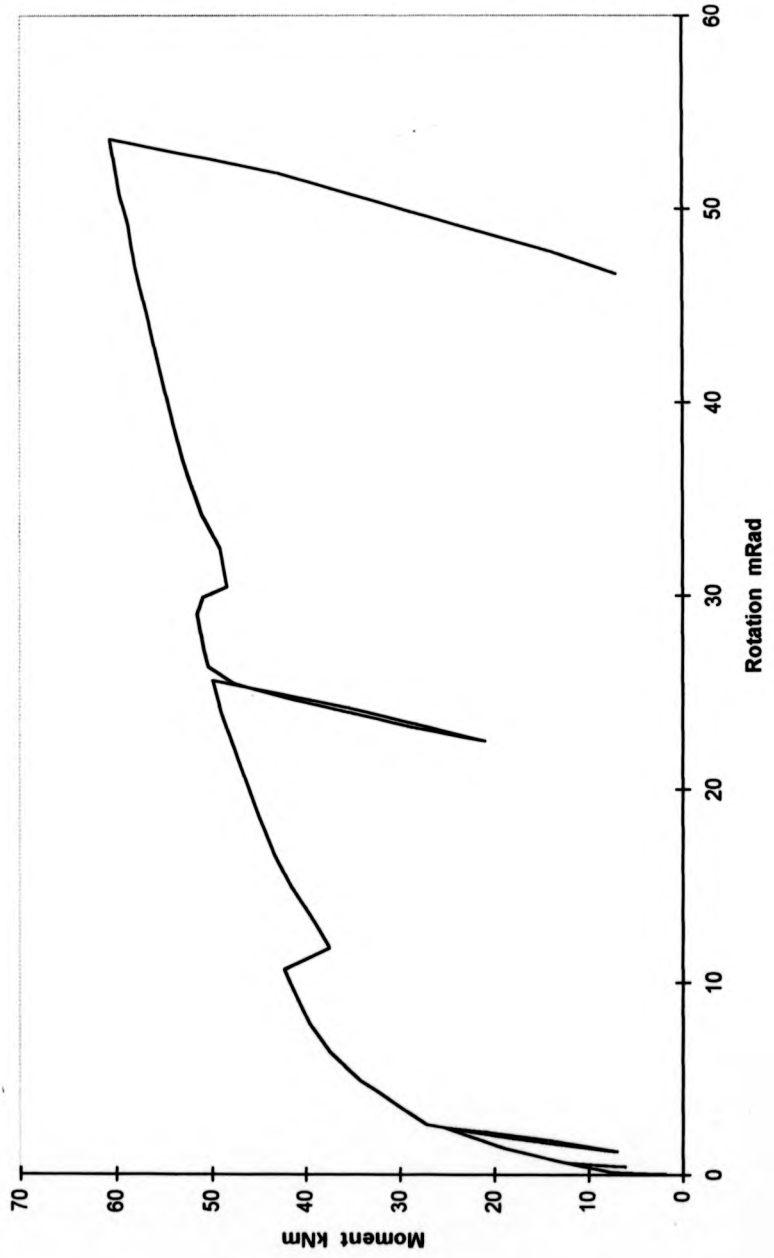
Fig. 4-14c : Average value of Moment vs Rotation for SFB3

TEST4
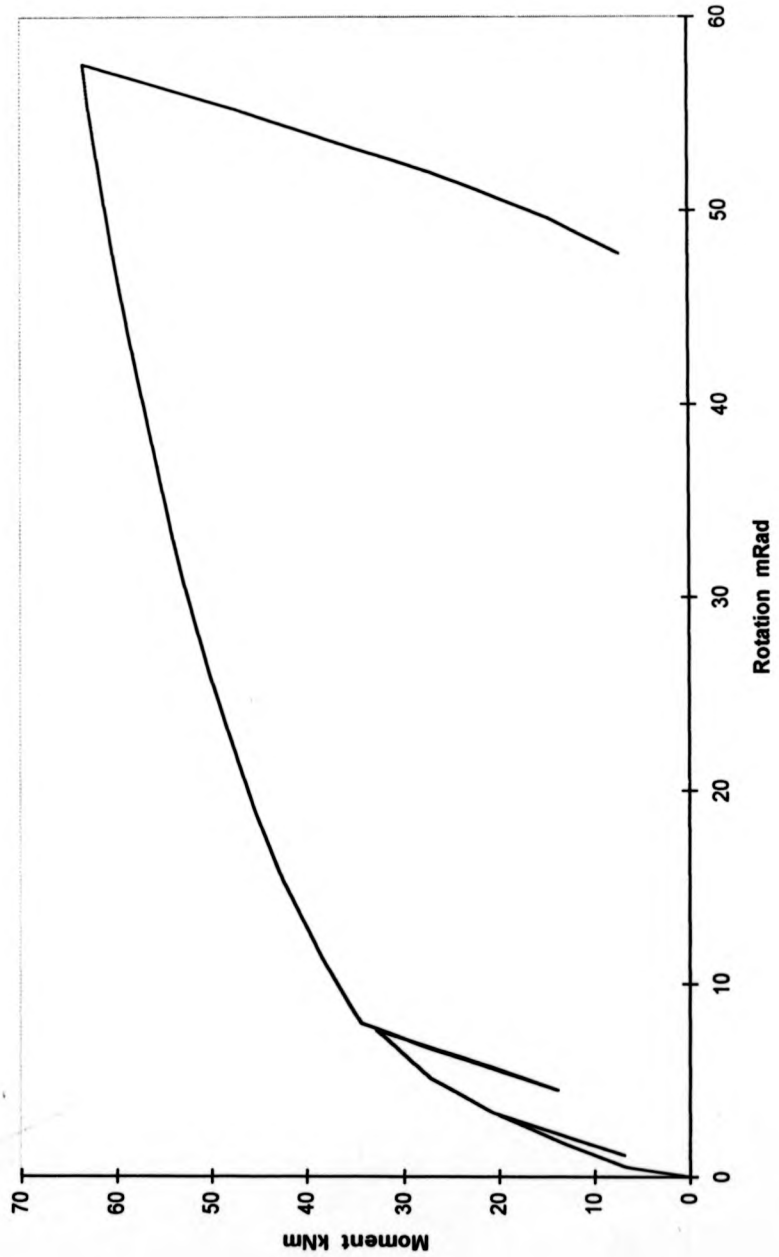
Fig. 4-14d : Average value of Moment vs Rotation TEST4

TEST5

average

Rotation mrad

Moment kNm
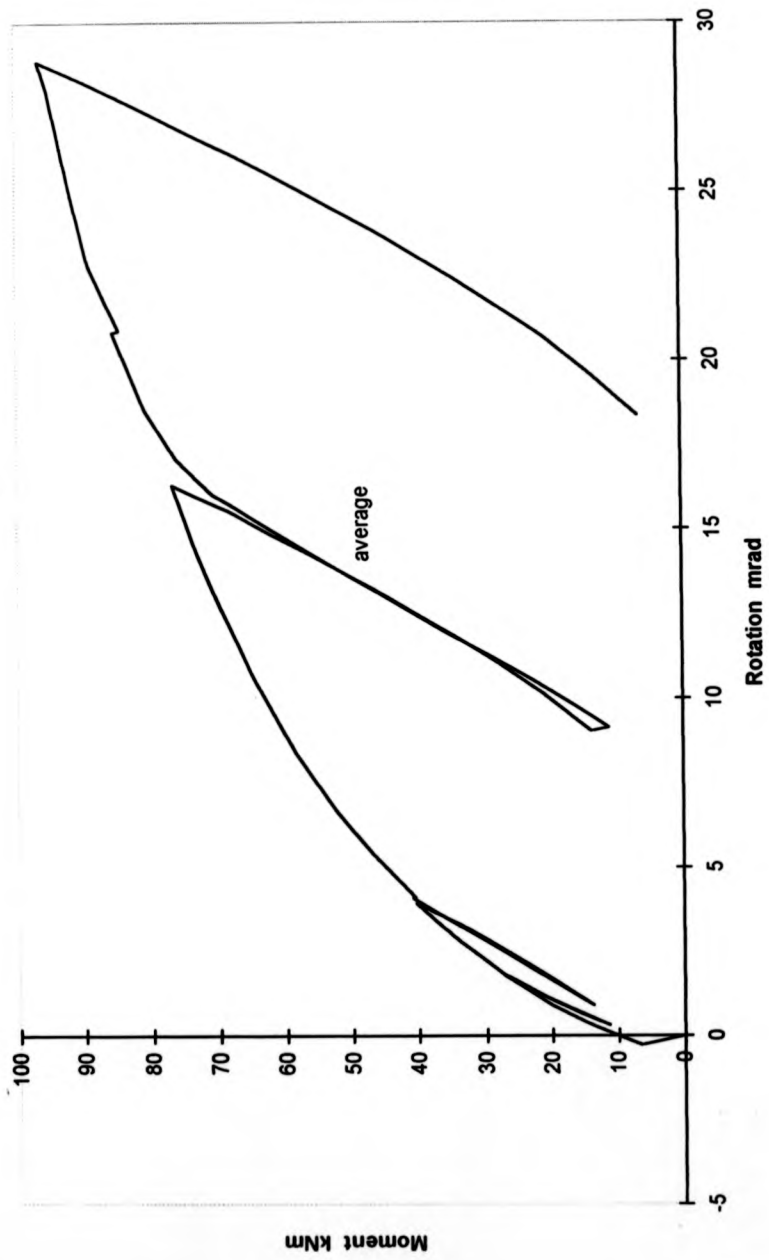
Fig. 4-14e : Average value of Moment vs Rotation for TEST5

Comparison between SFB3 and TEST4
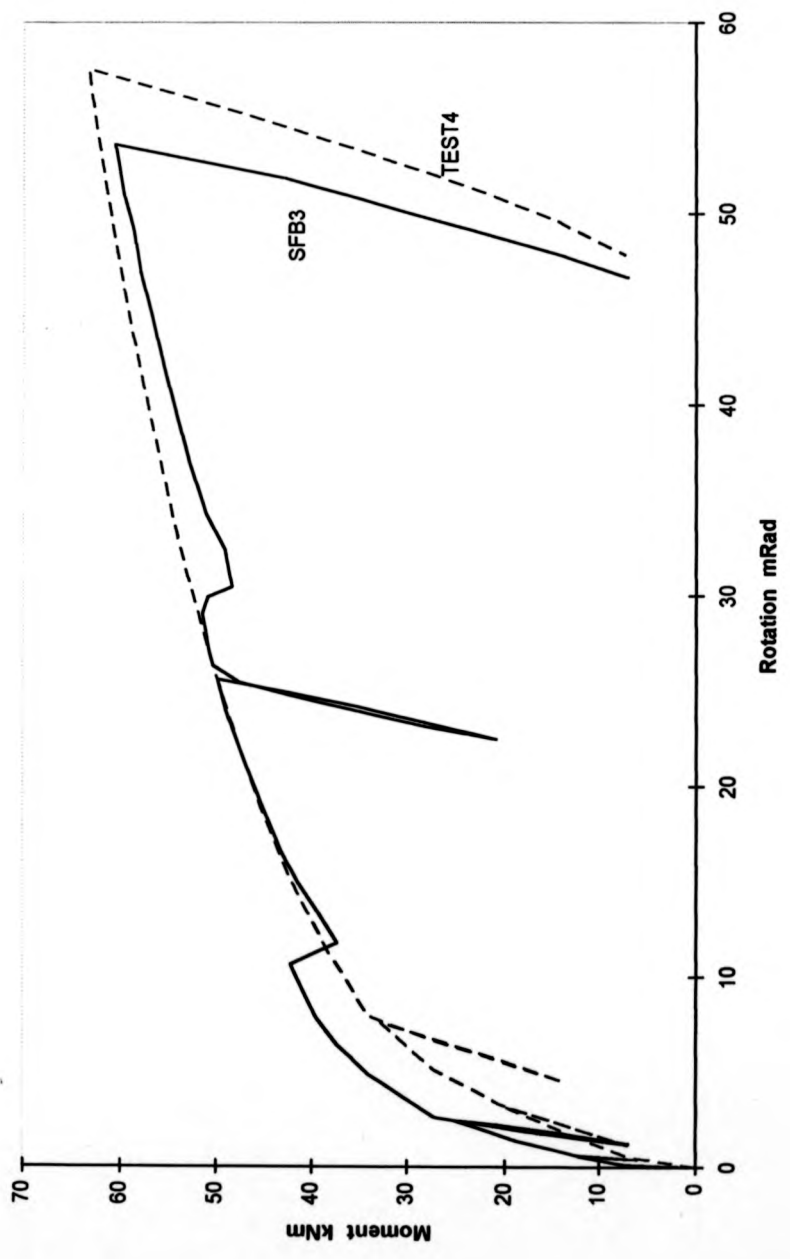
Fig. 4-15 : Effect of encasement

Comparison between SFB2 and TEST5
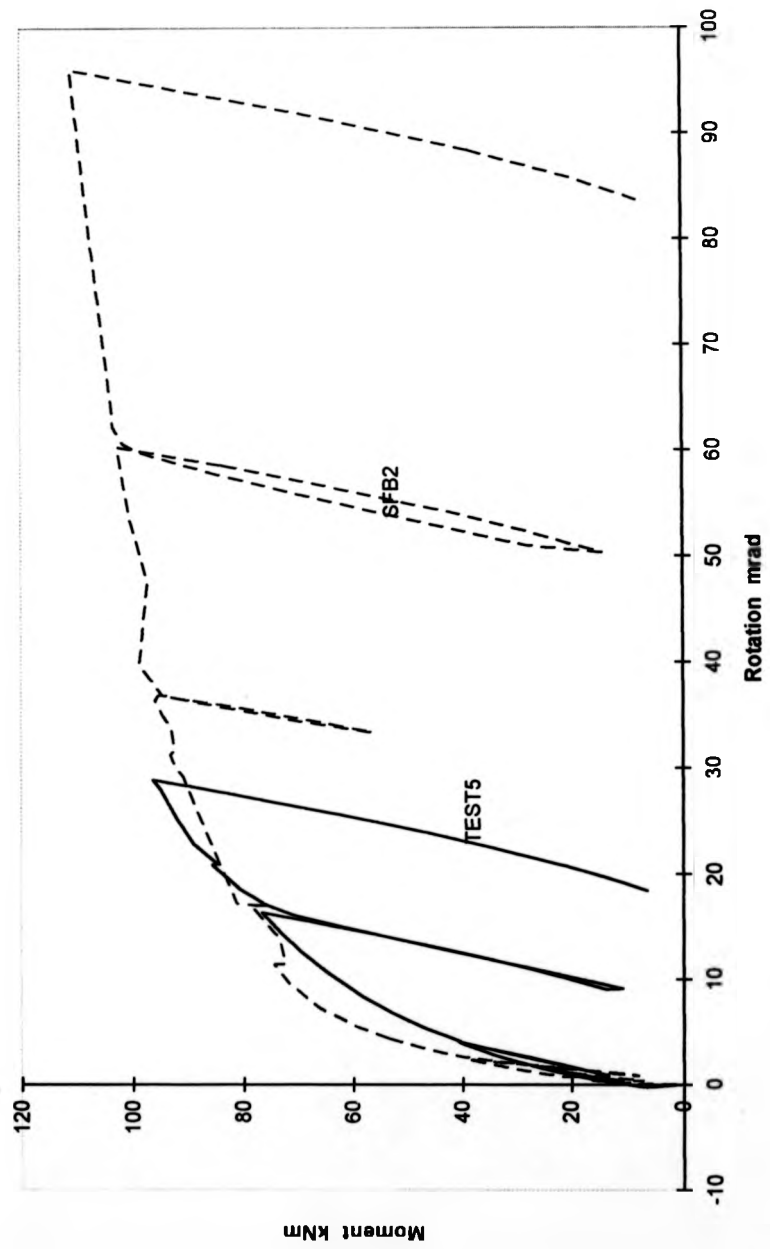
Fig. 4-16 : Effect of encasement

Comparison between SFB1 and SFB3
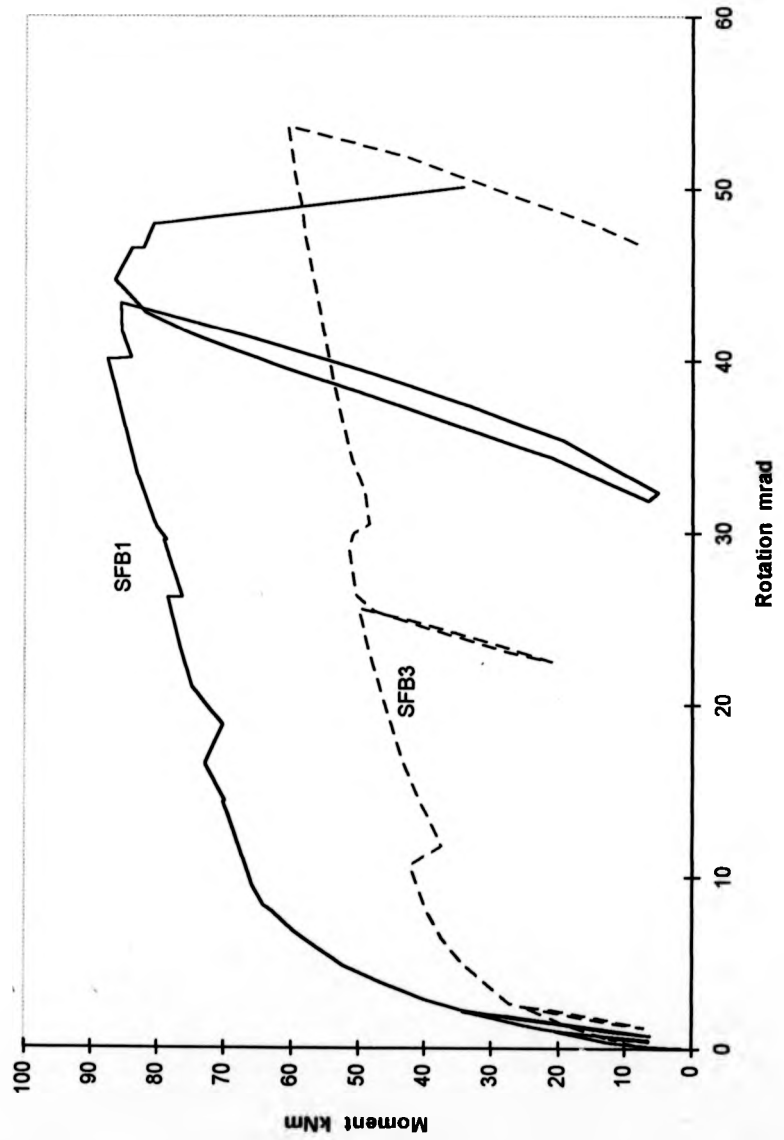
Fig. 4-17 : Effects of end plate thickness

Comparison between SFB1 and SFB2

Moment kNm

Rotation mrad
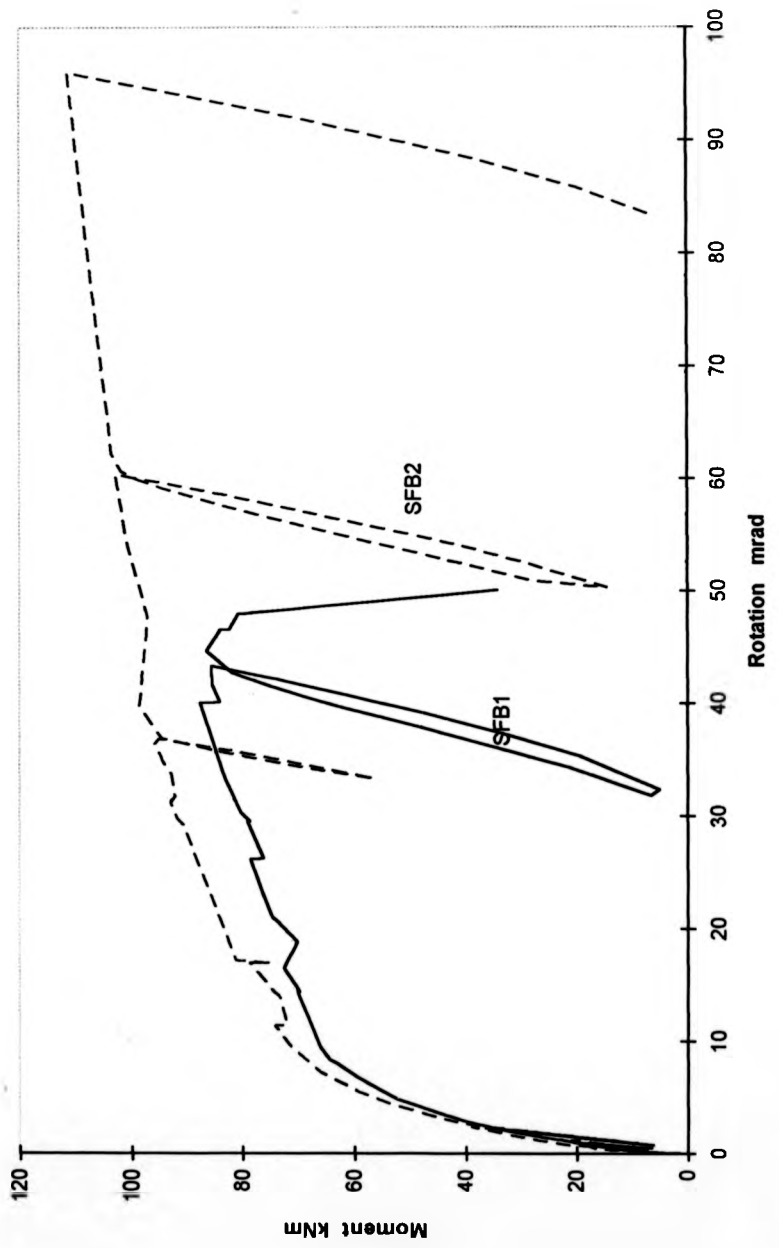
SFB2

SFB1

Fig. 4-18 : Effect of different bolt sizes

(SFB1)

$y = 0.914x + 0.3212$

$R^2 = 0.9998$
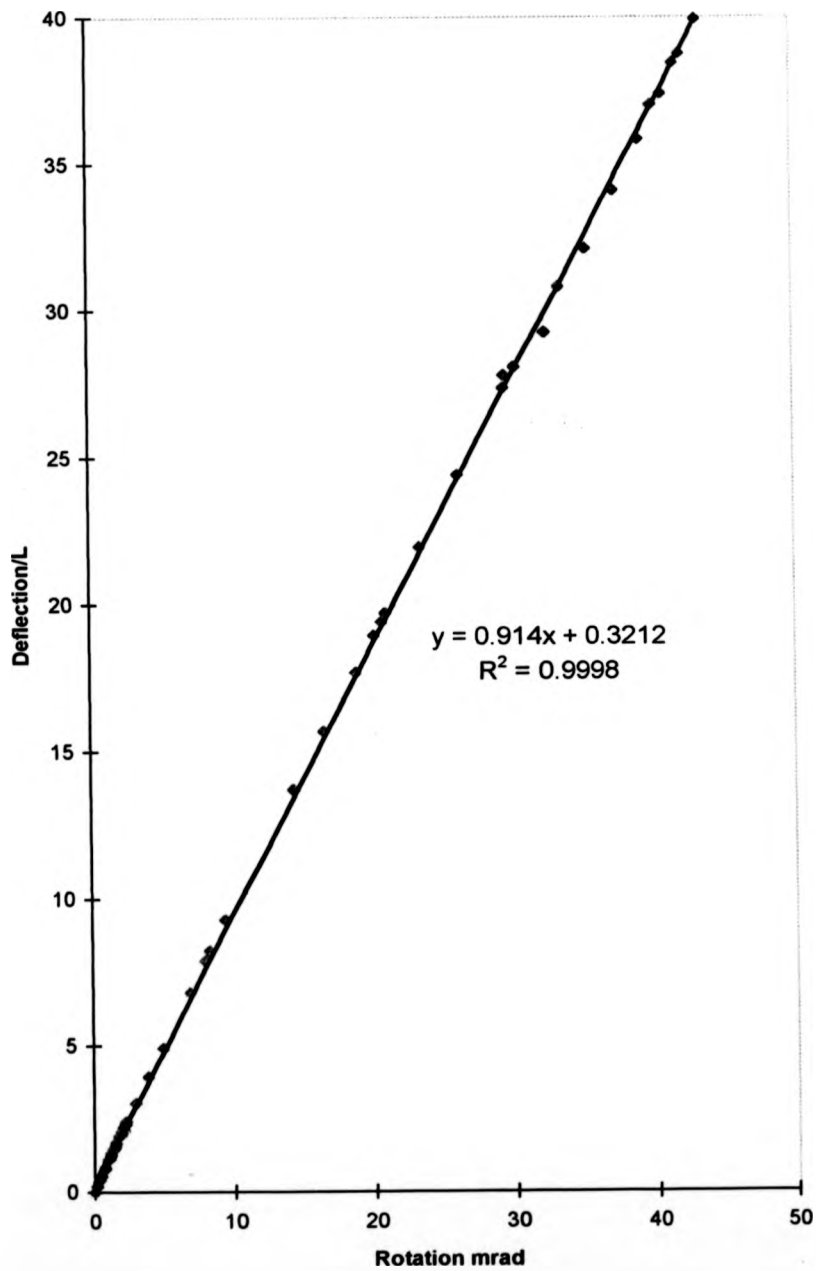
Fig. 14-19a : Comparison between transducer and inclinometer readings for SFB1

(SFB2)

$$y = 0.9231x + 0.3914$$
$$R^2 = 0.9999$$
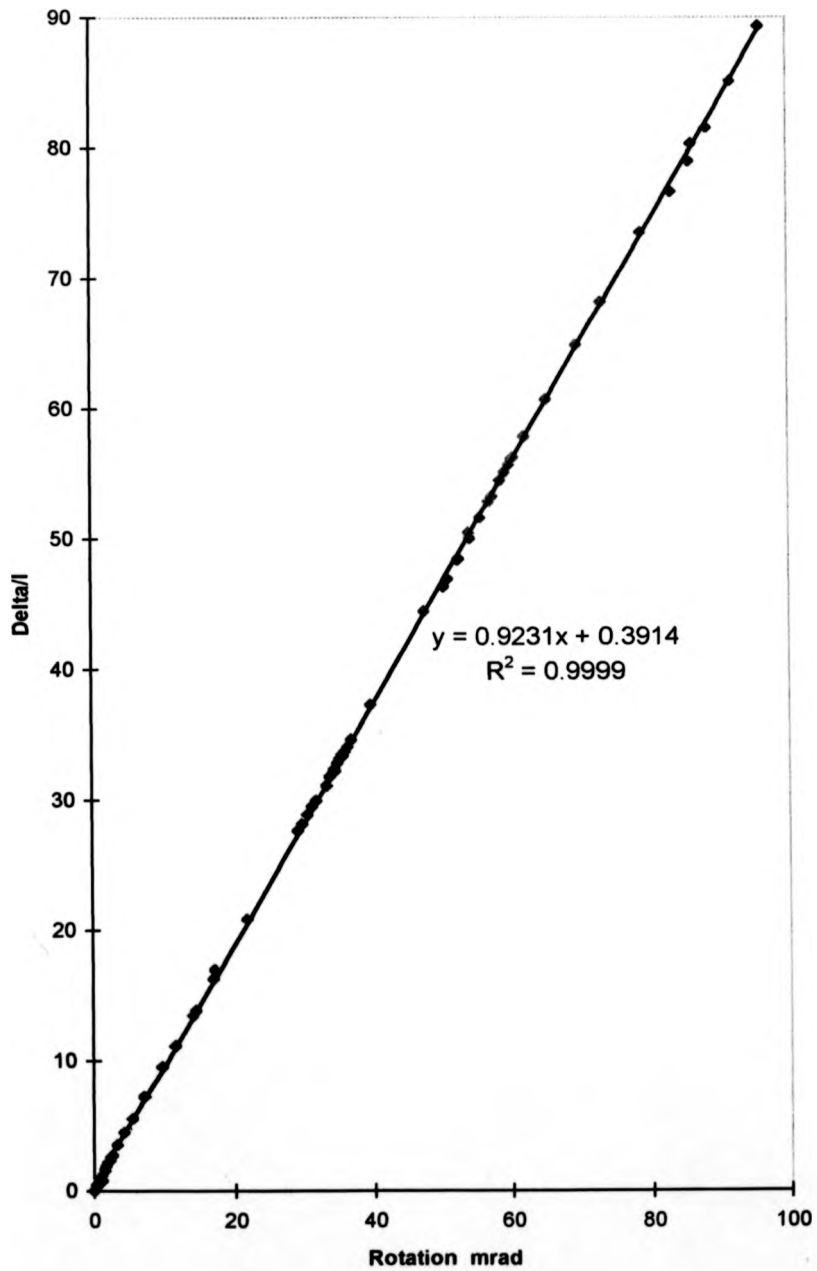
Fig. 14-19b : Comparison between transducer and inclinometer readings for SFB2

(SFB3)

$y = 0.9214x + 0.3468$

$R^2 = 0.9998$
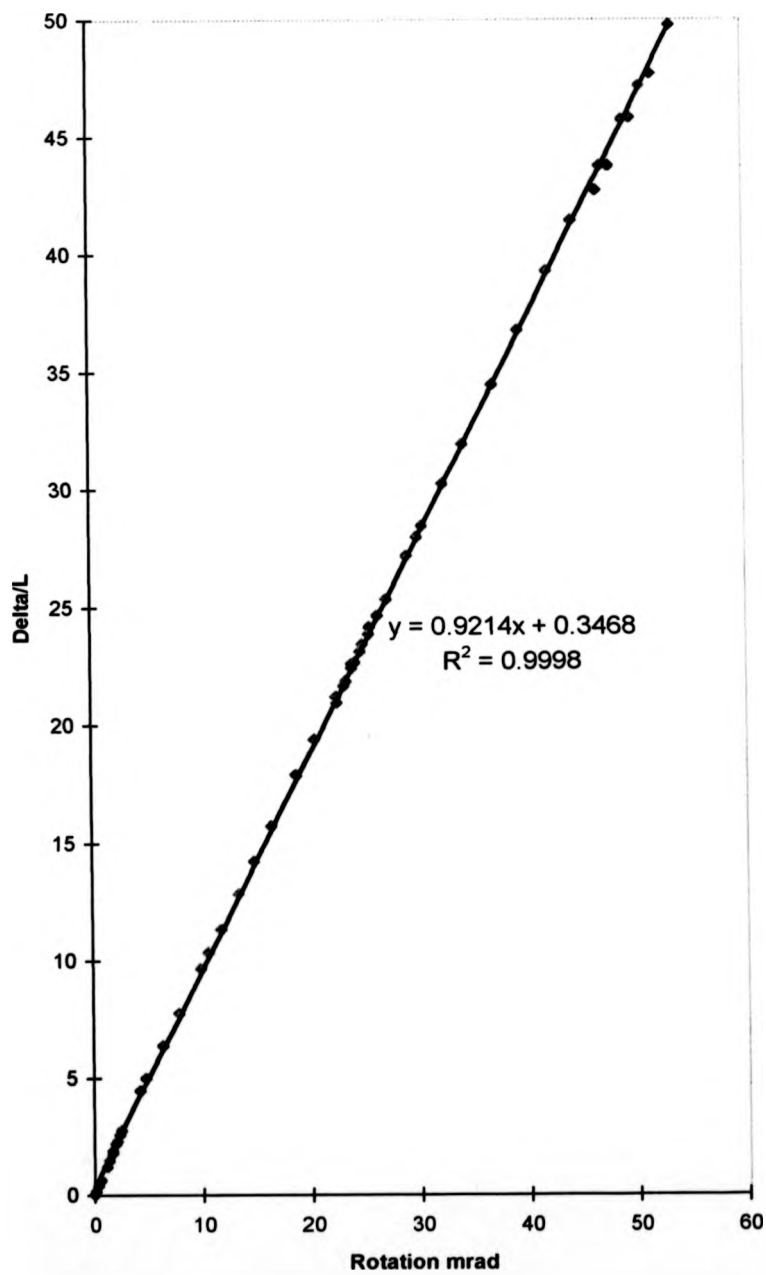
Fig. 14-19c : Comparison between transducer and inclinometer readings for SFB3.

(TEST4)

$$y = 0.9342x + 0.8022$$
$$R^2 = 0.9982$$
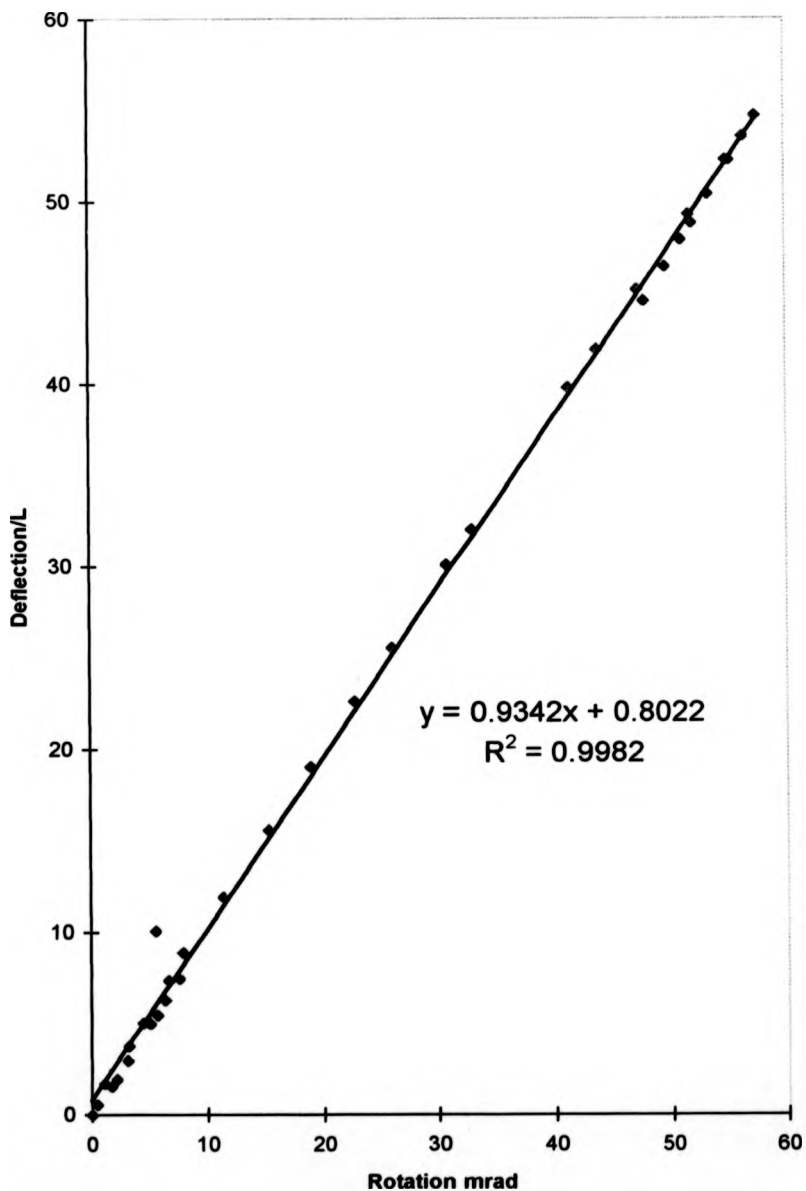
Fig. 14-19d : Comparison between transducer and inclinometer readings for TEST4

(TEST5)

$$y = 0.993x + 1.061$$
$$R^2 = 0.998$$
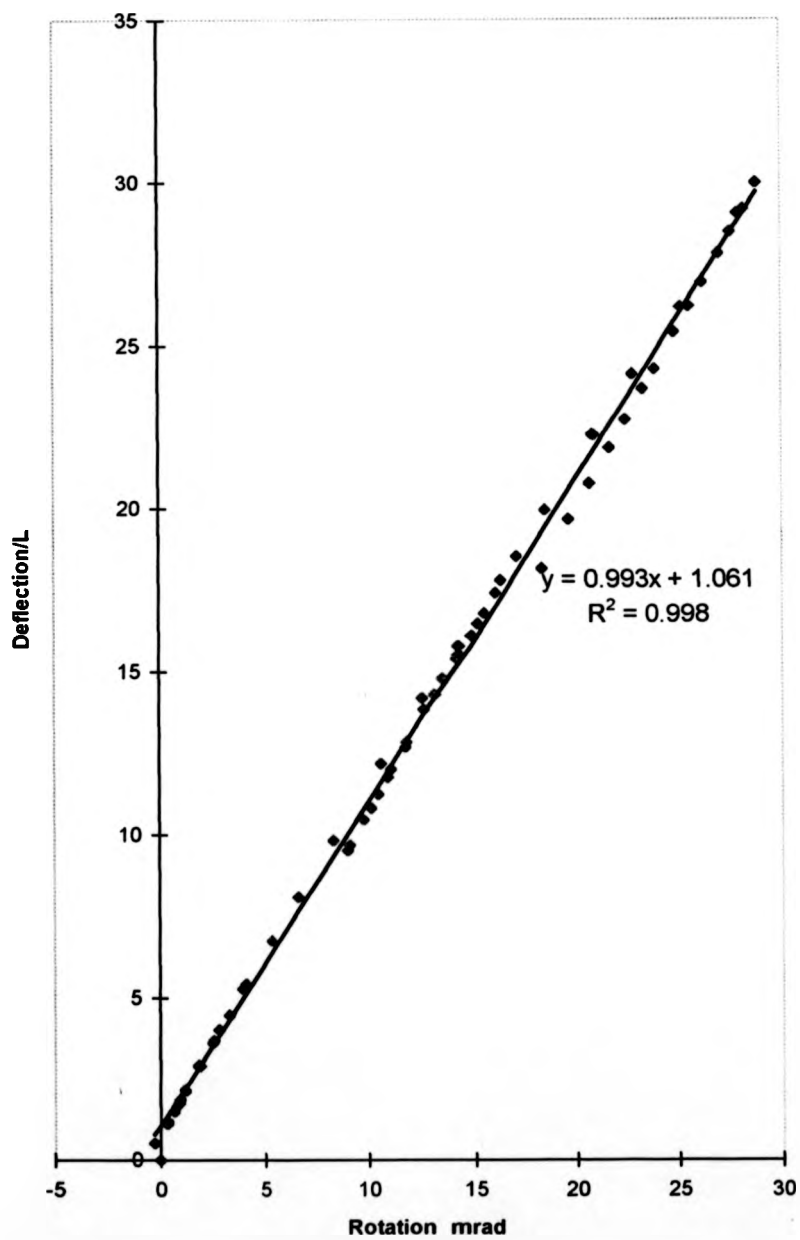
Fig. 14-19e : Comparison between transducer and inclinometer readings
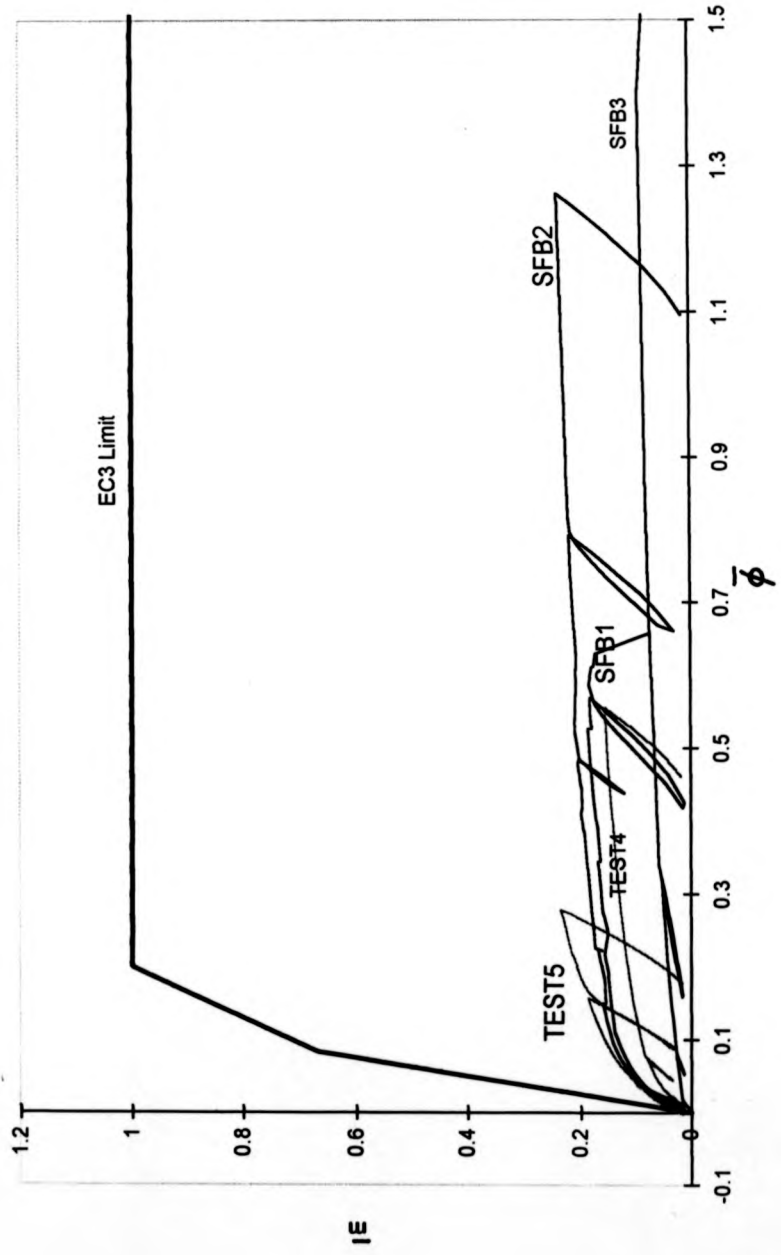
Fig. 14-20 : Connection classification
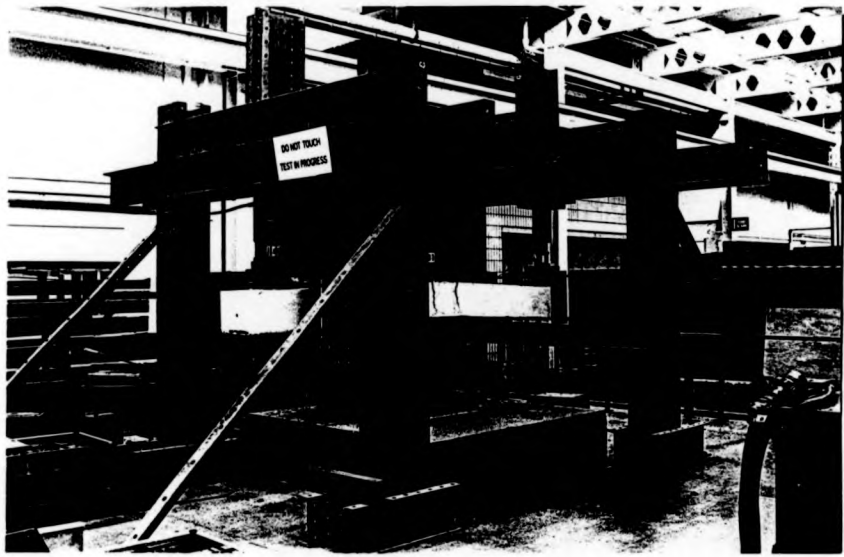
Plate 4-1 : Test Rig

Plate 4-2 : Steel base plate support
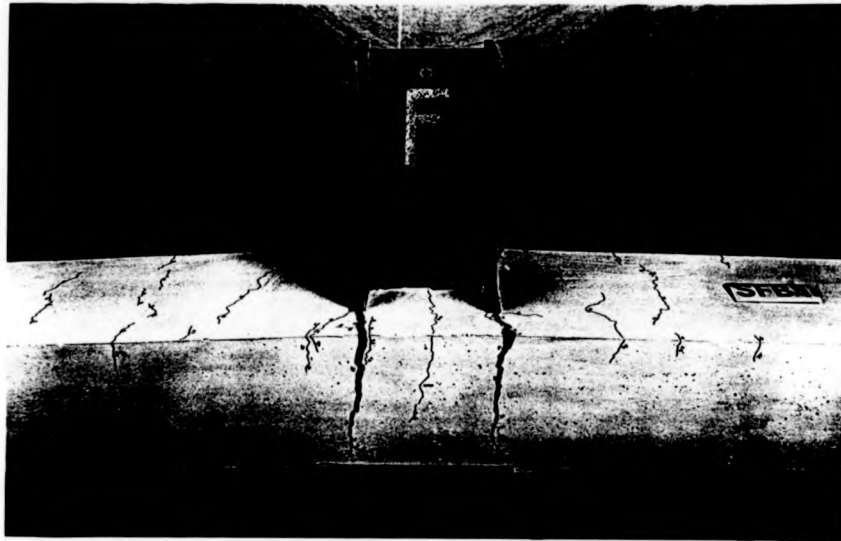
Plate 4-3 : Cracks pattern of SFB1
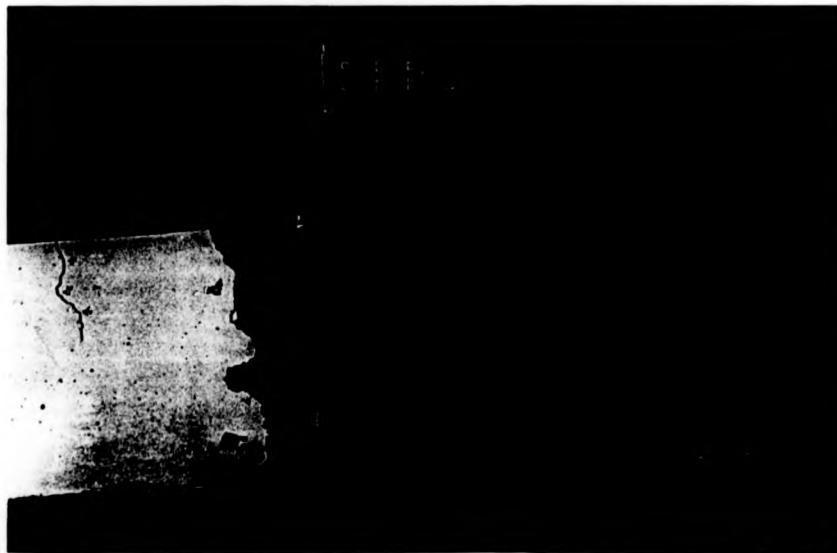
Plate 4-4 : Excessive deformation of column flanges and end plates
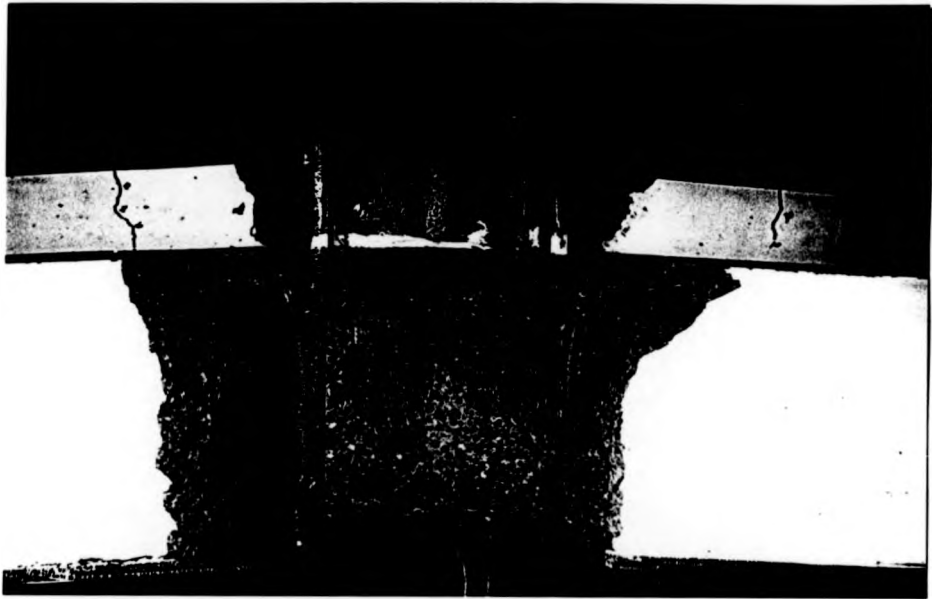
Plate 4-5 : Excessive deformation of end plates (SFB3)

Plate 4-6 : Deformation of end plate (TEST4)
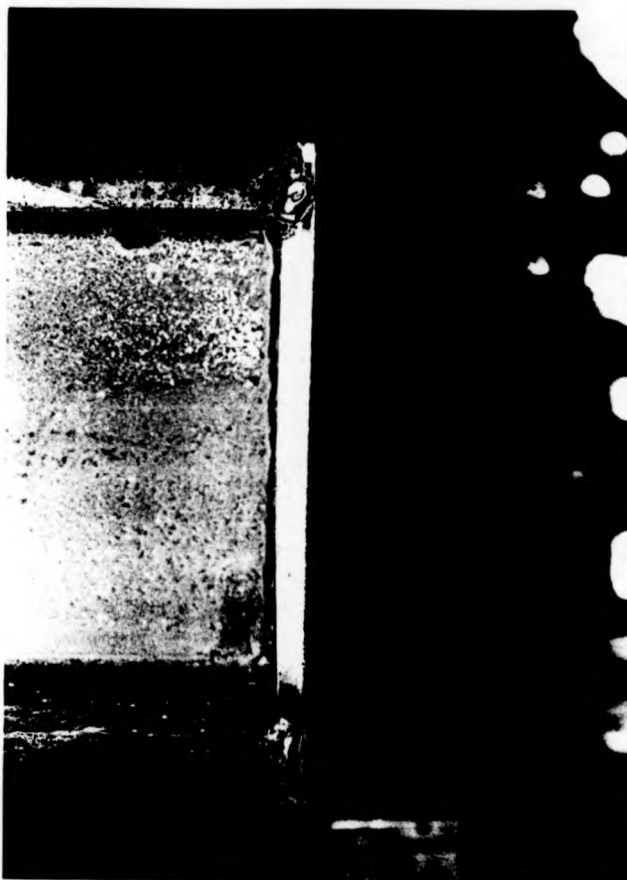
Plate 4-7 : Initial curvature of the end plate (TEST5)

Chapter 5

PUSH-OUT TESTS ON ENCASED STEEL SECTION WITH VARIOUS TYPES OF SHEAR ENHANCERS

5.1 Introduction

At any stage of loading, the horizontal shear that develops between the concrete slab and the steel beam needs to be resisted if the composite section is to act monolithically. Although the bond and the frictional force that develop between the concrete slab and steel beam can be significant, it is uncertain whether it may be relied upon to provide the required interaction. The state of knowledge developed in traditional systems (concrete slab connected to the top flange of I-shaped steel beam) may not be adapted to slim floor systems directly. The fact that the beam is encased in concrete may influence both the interactions and the flexural behaviour[5-1], and raises the possibility of composite action without stud connectors to the beam's flanges. In EC4[5-2] no application rules are given for the contribution of concrete encasement of a steel section to resistance in bending or vertical shear. However depending on the type of encasement, EC4[5-2] noted the average bond strength due to bond and friction in composite columns should be taken as between 0-0.6 N/mm^2. Several previous works

related to shear bond strength of encased steel sections have already been mentioned in Chapter 1.

There is currently considerable interest in improving the bond capacity of encased beams by introducing one of several types of 'shear enhancer'. The suitability of such innovations in the slim floor needs to be carefully appraised before they are introduced in practice. This chapter describes an investigation into the bond stress developed between concrete and steel sections with different 'shear enhancers'. A total of six push-out tests were performed.

5.2   Experimental Programme

5.2.1   General specimen description

Fig. 5-1 shows a typical push-out test for an encased steel section. A total of six push-out test specimens were performed, each having different type of shear enhancer. Fig. 5-2 to Fig. 5-7 indicate general details of the specimens. PT1 consisted of only a steel section without any 'shear enhancer' and acted as a control in order that comparison of performance can be made between the six specimens. In PT2 and PT3 two T20 rebars were provided through the web of the specimen, in PT2 these were straight while the rebars for PT3 were cranked upward. Two shorter and straight T20 rebars were positioned through the flanges of PT4 while four 19 mm diameter of 95 mm long shear studs were used to act as the shear enhancer in PT5. All the enhancers for PT1-PT5 were placed loose and needed temporary support during casting. Slightly bigger dimensions are provided for the concrete of PT6 to cater for placement of the enhancers on the outer flanges.

A 254UC89 grade S355 section with an embedded length of 900 mm was used for each specimen, to represent an encased steel beam. Although the results from the tests were to be applied to the type of slim floor construction studied in Chapter 4, it was decided to omit the bottom welded plate to the beam. In this way a balanced and symmetrical test could be carried out. The width of 1000 mm of the completed specimen was an approximation for an effective slab width based 0.125 of the assumed span.

5.2.2 Preparation of the specimen

The preparation and delivery of the steelwork was organised by The Steel Construction Institute. The fixing of the shear enhancers was done in the laboratory. Special plywood formwork was constructed according to the required dimensions. The steel section was lowered into the formwork followed by the fixing of shear enhancers and placement of A142 steel mesh. This was placed on the longer sides of the concrete to control the shrinkage cracks.

Concreting was carried out using the in-house laboratory concrete mixing facility. Light-weight concrete of grade 25 was employed. Concrete mix design was based on Boral Lytag technical notes[5-3]. Casting of 100x100x100 mm cubes for compression tests was carried out at the same time as the specimen was cast . The cubes were tested at 7 days, 28 days and on the day of the push-out tests. The tests on concrete strength conformed to BS1881[5-4] The average compressive strengths of concrete are summarised in Table 5-1.

5.2.3 Instrumentation

To measure the slip between the steel and the concrete two calibrated displacement transducers were used. The measurement of load was through one 200-ton load cell. The

instrumentation was wired to a data acquisition which was connected to a computer to monitor each test. All the tests were intended to be tested at University of Warwick using the test rig as shown in Plate 5-1. However after 1500 kN load had been applied to PT1, no significant slip had occurred and the test was stopped for safety reasons. It was decided to transport and carry out the tests at City University, where there is a rig capable of providing load up to 3000 kN. The test rig at City University is shown in Plate 5-2.

The load was applied by a hydraulic testing machine with analog pointer to indicate the load level. The load was transferred to the steel section of the specimen by a rocker bearing (Plate 5-3). Two transducers, one digital and one electronic, were used to record the slip. Load increments of 100 kN were applied until the load reached 1000 kN, after which the specimen was unloaded in increment of 100 kN to 2.5 kN. Load was increased again at the same load increment of 100 kN until 1000 kN, after which subsequent readings under higher load were taken after two minutes had elapsed.

5.3   Expected 'Shear Enhancer' Contribution

It was expected that the specimens with various 'shear enhancers' would show increased bonding capacity. The expected additional contribution to the bonding of the specimens is calculated using the recommended clauses of EC4[5-2].

Specimen PT2 (2 straight bar T20, 950mm long.)

(i)   As block connector. (Using clause *6.3.4 of EC4*)

Design resistance of a block connector,

$$P_{Rd} = \eta.Af_1\,f_{ck}/\gamma$$

$$= \eta.d.l.\,f_{ck}/\gamma$$

$$= \quad \eta.d.l. f_{ck} / \gamma$$

$$= \quad 1.0 \times 20 \times 60 \times 2 \times 45.6/1.0$$

$$= \quad 109 \text{ kN}$$

$\therefore$ Total Resistance $\quad = \quad$ 218 kN

Therefore expected contribution to PT3 $\quad = \quad$ **218 kN**

Specimen PT4 (2 Nos T20 bar, 270 mm length)

(i)   Referring to clause 6.3.4 of EC4

$$P_{Rd} \quad = \quad \eta.Af_1 f_{ck} / \gamma$$

$$= \quad 1.0 \times 20 \times (270-17) \times 46.95/1.0$$

$$= \quad 238 \text{ kN}$$

$\therefore$ Total Resistance $\quad = \quad$ 576 kN

(ii)   Referring to clause 6.3.4 but taking into account clause 6.4.4(1) and 6.3.4(1)

$$P_{Rd} \quad = \quad \eta.Af_1 f_{ck} / \gamma$$

$$= \quad 1.0 \times 20 \times (80 + 27) \times 46\ 95/1/0$$

$$= \quad 100 \text{ kN}$$

$\therefore$ Total Resistance $\quad = \quad$ 200 kN

(iii)   Referring to clause 6.3.2.1 of EC4

$$P_{Rd} \quad = \quad 0.8f_u (\pi d^2 /4)/\gamma_v$$

or   } whichever the lesser

$$P_{Rd} \quad = \quad 0.29\alpha\, d^2 (\sqrt{fck.Ecm})/\gamma_v$$

$P_{Rd} \quad = \quad 0.8 \times 500 \times 314.1 /1.0 \quad = \quad$ 125.6 kN

$P_{Rd} \quad = \quad 0.29 \times 1.0 \times 20^2 (\sqrt{46.95 \times 29 \times 10^3})/1.0 \quad = \quad$ 134.9 kN

$\therefore$ Total Resistance   =   251.2 kN

Therefore expected contribution to PT4   =   **200 kN**

Specimen PT5 (4 Nos shear connector 19dia x 95 long)

(i)   Referring to 6.3.4 of EC4

     P_{Rd} = $\eta . A f_i \, f_{ck} / \gamma$

            =   1.0 x 19 x (95-17) x 45.4/1.0

            =   67 kN

     $\therefore$ Total Resistance   =   268 kN

(ii)   Referring to 6.3.2.1 of EC4

     P_{Rd} = $0.8 f_u \, (\pi d^2 /4)/\gamma_v$ $\Big\}$

or   whichever the lesser

     P_{Rd} = $0.29\alpha \, d^2 \, (\sqrt{fck.Ecm})/\gamma_v$ $\Big\}$

P_{Rd} = $0.8 \times 500 \times (\pi \times 19^2 /4)/1.0$ =   113.4 kN

P_{Rd} = $0.29 \times 1.0 \times 19^2 (\sqrt{45.4 x 29 x 10^3})/1.0$ =   120.1 kN

     $\therefore$ Total Resistance   =   453.6 kN

Therefore expected contribution to PT5   =   **268 kN**

Specimen PT6 (2 Nos T20 welded to the outer flanges)

(i)   Referring to 6.3.4 of EC4

     P_{Rd} = $\eta . A f_i \, f_{ck} / \gamma$

            =   1.0 x 20 x 1010 x 41.8/1.0

            =   844 kN

     $\therefore$ Total Resistance   =   1688 kN

(ii)   Referring to 6.3.4 but considering 6.4.4(1) and 6.3.4(1) of EC4

$$P_{Rd} \quad = \quad \eta.Af_1 \, f_{ck} \, / \, \gamma$$

$$= \quad 1.0 \times 20 \times (160 + 256) \times 41.8/1.0$$

$$= \quad 348 \text{ kN}$$

∴ Total Resistance   =   696 kN

Therefore expected contribution to PT6   =   **696 kN**

A summary of the expected contribution of each type of 'shear enhancer' is presented in Table 5-2.

5.4   Tests Observation and Results

The experimental results and the modes of failure are summarised in Table 5-2. All the tested specimen are shown in Plate 5-4 to Plate 5-9.

Specimen PT1 failed by full slip of steel section. Longitudinal cracking of concrete was observed along the edges of the flanges. The failure load recorded for PT1 was 1320 kN. Plate 5-4b shows the slip at the bottom of the specimen PT1.

For specimens PT2-PT6 there were two consecutive audible 'sounds' just before the bond failure occurred. The concrete cracking pattern for specimens PT2-PT4 was almost identical to PT1. However for PT5-PT6 there were significant horizontal cracks which occurred at the level of shear enhancer (Plate 5-8a and Plate 5-9a).

For specimen PT6 the concrete burst on both sides of the specimen, followed by some spalling. This could be due to the cover provided for specimen PT6 being not adequate

to resist the bursting force. The mode of failure for PT6 was similar to PT1 i.e. failed by full slip of steel section (Plate 5-9b).

PT2-PT5 all showed a slip mode of failure. However, part of the encasement to the steel web split from the surrounding concrete, thereby showing a partial shear core failure occurred at the bottom of these specimens. The typical mode of failure is shown in Plate 5-8b.

The apparent average maximum bond stress were between 0.81 and 0.96 N/mm^2 in the experiments (see Table 5-2). However, if the contribution from the shear enhancer was discounted, the maximum bond stress were then between 0.46 and 0.96 N/mm^2 . Except for PT6 these values were greater than the value of 0.6 N/mm^2 suggested by EC4[5-2] for completely concrete encased sections. After testing on PT1 and PT4, it was decided for the remaining tests, to continue loading after bond failure to study the behaviour after slip had commenced. Load against slip curves were plotted (see Fig. 5.8 to Fig. 5-13). From the curves it was observed that after the bond failure had occurred some of the specimens showed that the bond capacity becomes almost independent of the slip.

One important observation was that the load at the initial slip for the enhanced specimens was never greater than the load of PT1.

It should be noted that the test at Warwick University (specimen PT1) was performed by the 'usual' push-out test method as employed by Roeder[5-1] and Hawkins[5-5]. The load was applied through the steel section with the concrete ends acting as supports. However in the experiments at City University the concrete ends were pushed upwards while the upper part of steel section was supported by the rig.

5.5 Discussion

Since bond stress failure involved cracks propagating through the concrete, concrete strength may effect the maximum bond stress. Comparison between Table 5-1 and Table 5-2 indicated that except PT1 bond stress tended to decrease with concrete strength.

It was observed that there were two general types of cracking pattern. In specimens PT1-PT4 concrete cracking mostly occurred along the edges of flanges. However in PT5-PT6 noticeable horizontal cracking was observed at the level of shear enhancers. This could be caused by the position of the enhancer. In PT2-PT4 the enhancers were placed at the web while in PT5-PT6 the enhancers were positioned at the flanges of the section.

There is no clear evidence from the tests that the types of enhancer increases the maximum bond stress attainable in the specimen. It is likely that the resistance of the enhancers only became effective after slip due to bond failure had occurred. From Fig. 5-9, after the bond failure had taken place, specimen PT2 was able to sustain higher load than before bond failure..

Specimens PT2-PT5 showed a slip mode of failure, but with partial shear core failure taking place at the bottom of these specimens. Theoretically the 'shear enhancer' would cause an increase in the resistance to slip. However in the experiments no significant contribution was demonstrated. All the specimens indicated a peak load. The peak load is highly dependent on the surface quality of the steel section. However a resistance due to frictional bonding remains and may provide the design shear strength[5-6]. There were indications that the enhancers become effective only after some slip had occurred.

For PT2 and PT3, the peak strength is roughly maintained (PT3) or reached again (PT2) by the action of the rebar enhancers. Comparing PT2 to PT3 it seems that the cranked upward shape of shear enhancers (Fig. 5-4) prevented a sudden loss of resistance. It is thought the cranked shaped enhancer enabled the mobilisation of resistance almost immediately there was bond failure and as the steel section-concrete bond deteriorated, the bent rebar became increasingly effective in maintaining the peak load.

In PT4 the load at debonding was 1120 kN, however the action of the shear enhancers could not be justified as the test was terminated after the recorded slip was only 1.3 mm. PT5 showed the characteristics of stud connectors with a gradual reduction in resistance with increasing slip. However for PT6 full resistance of enhancer was not utilised because of bursting of concrete due to the small cover above the enhancers.

For PT2, assuming the residual bond resistance is 50% of the peak strength, i.e. 660 kN, the remainder of the residual resistance must be due to enhancers, and is equal to

$$1400 \text{ kN (from Fig. 5-9) - 660 kN} \quad = \quad 740 \text{ kN}$$

$$\text{shear resistance of rebar} = 0.6 f_y \times \frac{\pi d^2}{4}$$

$$= 0.6 \times 500 \times \pi \times \frac{20^2}{4}$$

$$= 94 \text{ kN per leg}$$

$$= 376 \text{ kN per shear plane}$$

The rising strength could then be the onset of strain hardening.

From the tests the average maximum bond stress recorded was between 0.46 N/mm^2 and 0.96 N/mm^2 (see Table 5-2). If the result from PT6 is excluded the range is 0.62 N/mm^2 to 0.96 N/mm^2. These are comparable to the results obtained by Roeder[5-1] (0.6 N/mm^2 to 1.6 N/mm^2), Hawkin[5-5] (0.7 N/mm^2 to 1.1 N/mm^2) and Lawson[5-7] (0.85 N/mm^2 to 1.28 N/mm^2)

5.6 Conclusions

(1) Apparent values of bond strength (except PT6) measured in push-out test are considerably in excess of those recommended by EC4; the latter though are "design" values.

(2) Two modes of failure were identified ; the specimen without a 'shear enhancer' failed by full slip ; the specimens reinforced by a 'shear enhancer' also failed by slip but this was combined with a partial shear core failur.

(3) The load at debond failure is not greatly dependent on the type of 'shear enhancer'.

(4) Depending on the type of shear enhancer used, the mobilisation of the enhancers is still possible after the slip following bond failure.

(5) Rebars through the web are the most effective means of maintaining resistance after initial slip, and the configuration in PT3 is better than that in PT2.

(6) There is a correlation between bond capacity and compressive strength of concrete.

References

5-1. Roeder, C.W. "Bond stress of embedded steel shapes in concrete", Proc. of the US/Japan Joint Seminar on Composite and Mixed Construction, Washington July 1984. ASCE pp227-240.

5-2. Commission of the European Communities, Eurocode No. 4 Common unified Rules for Composite Steel and Concrete Structures.

5-3. Guidelines on properties, "Designs and Specification of Lytag structural lightweight concrete", Technical Notes, Boral Lytag.

5-4 BS 1881, "Testing of concrete", British Standard Institution, London, 1983.

5-5. Hawkins, N.M. "Strength of Concrete-Encased Steel Beams", Civil Engineering Transaction. Inst of Eng. Australia 1973 CE15 pp39-45.

5-6 Johnson, R.P., and Anderson, D., "Designers' handbook to Eurocode 4: Part 1.1, Design of steel and composite structures". Thomas Telford, London 1993.

5-7. Lawson, M., Mullet, and D., Rackham, J., "Slimdek: Development and Testing", New Steel Construction. June/July 1997. pp19-22.

Table 5-1 : Average concrete compressive strength

TEST	7 days N/mm²	14 days N/mm²	28 days N/mm²	Day of Testing
PT1	32.5	33.8	45.1	44.0 (*119 days*)
PT2	32.5	33.8	45.1	47.9 (*134 days*)
PT3	29.8	34.6	42.0	45.6 (*109 days*)
PT4	29.8	34.6	42.0	47.0 (*95 days*)
PT5	27.3	34.6	42.1	45.4 (*95 days*)
PT6	27.3	34.6	42.1	41.8 (*103 days*)

Table 5-2 : Summary of the result

TEST	Load at Initial Slip (debond load) kN	Slip at debond load mm	Shear bond stress based on the whole section perimeter* N/mm²	Shear bond stress based on flange perimeter" N/mm²	Expected contribution from 'shear enhancer'** kN	Failure mode
PT1	1320	1.35	0.96	1.37	-	Full slip
PT2	1320	1.79	0.74	1.05	306	Full slip with core failure
PT3	1220	2.17	0.74	1.04	218	-do-
PT4	1120	1.27	0.67	0.95	200	-do-
PT5	1120	2.23	0.62	0.95	268	-do-
PT6	1320	1.92	0.46	0.65	696	Full slip

Notes:

* $\dfrac{\text{Load at initial slip - Contribution from shear enhancer}}{\text{Nominal perimeter}}$

" $\dfrac{\text{Load at initial slip - Contribution from shear enhancer}}{\text{flanges perimeter}}$

** Based on calculation given in Section 5.3 using EC4
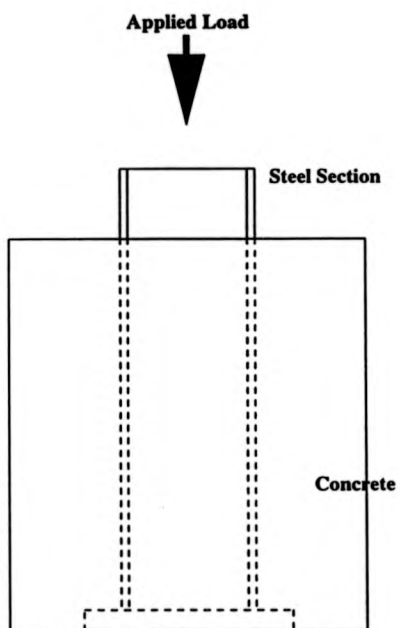
Fig. 5.1 : Typical Push Out Test
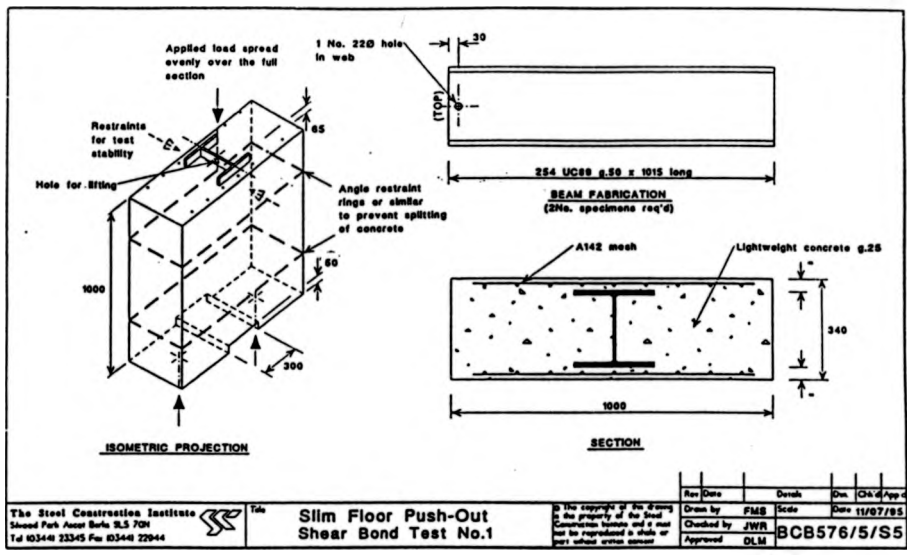
Fig. 5-2 : General details of PT1
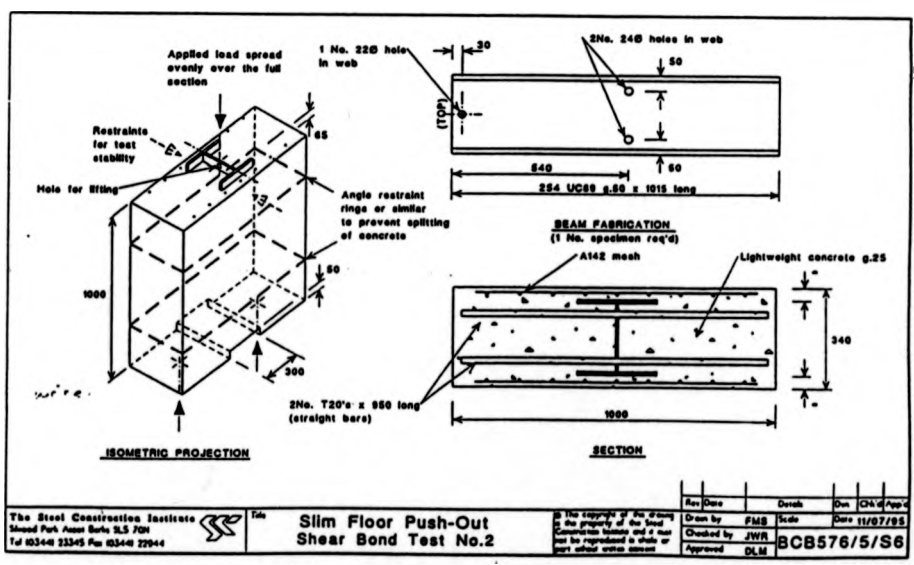
Fig. 5-3 : General details of PT2
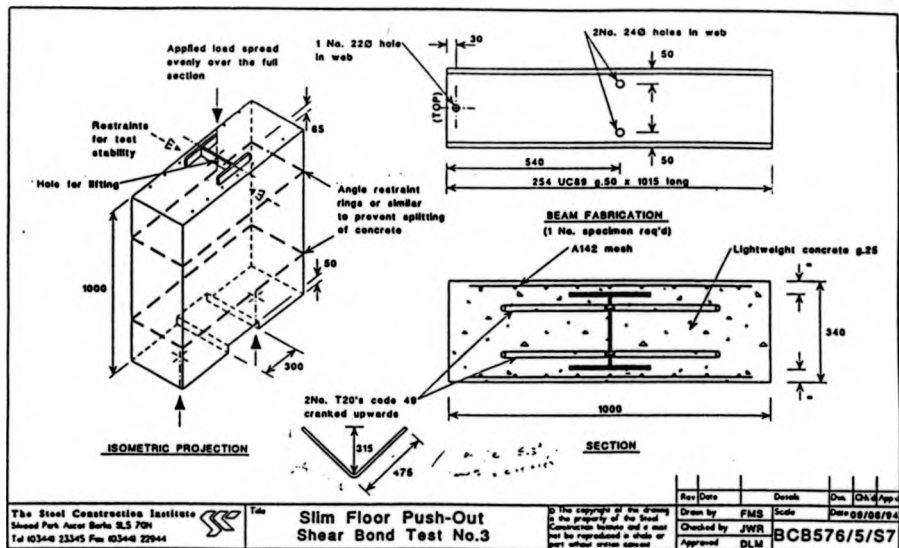
Fig. 5-4 : General details of PT3
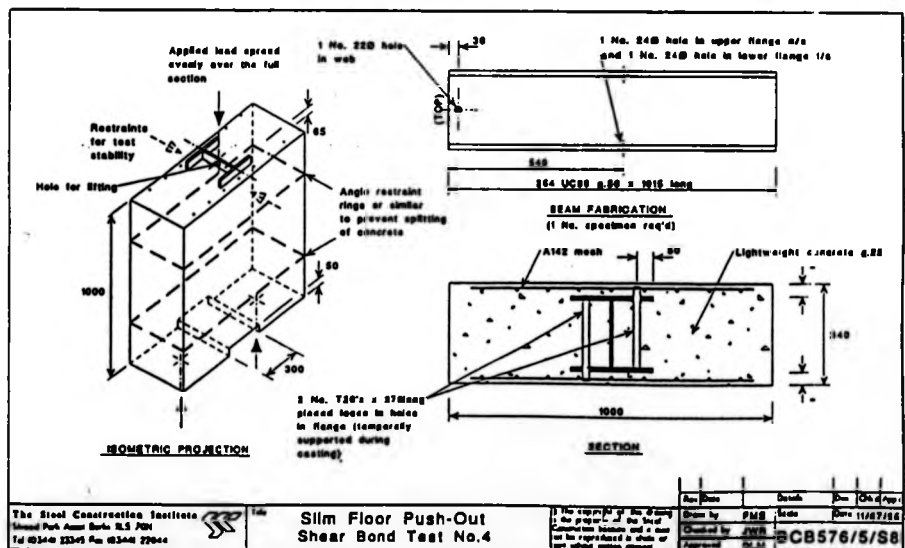
Fig. 5-5 : General details of PT4
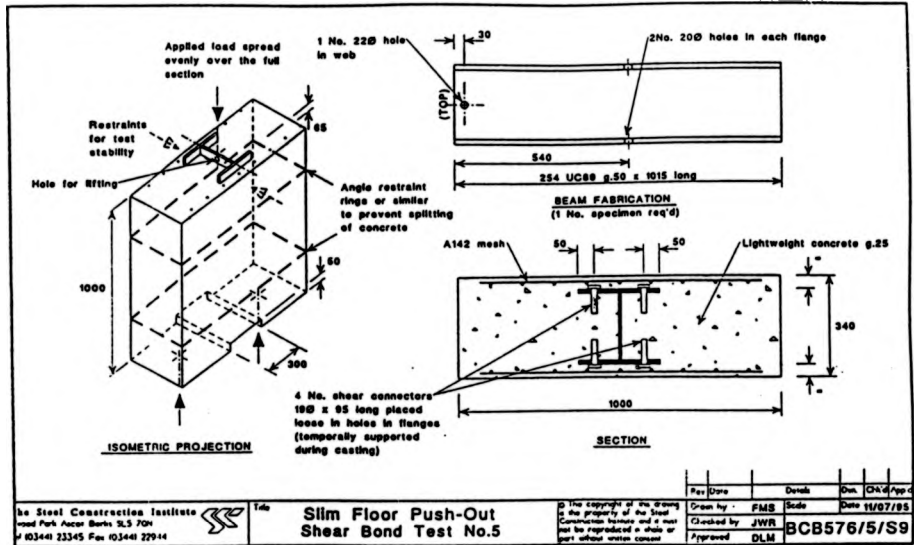
Fig. 5-6 : General details of PT5
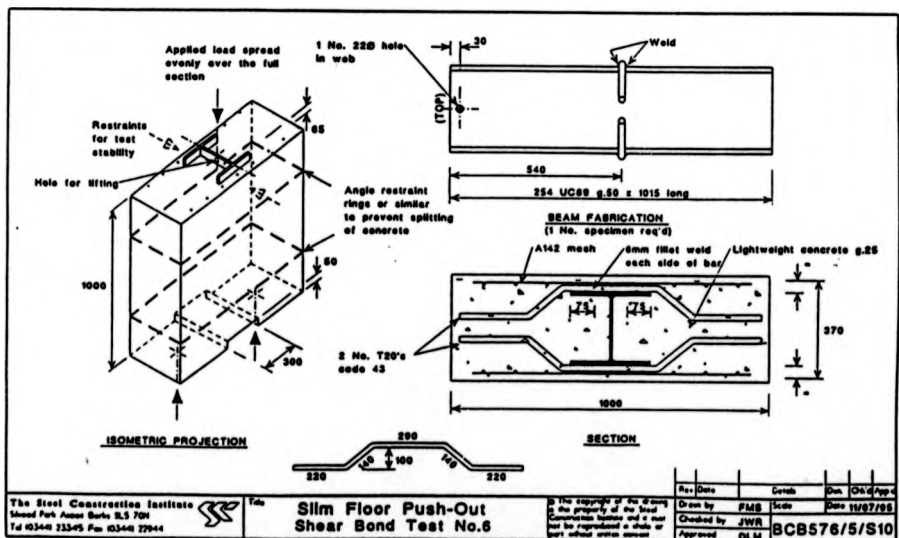
Fig. 5-7 : General details of PT6
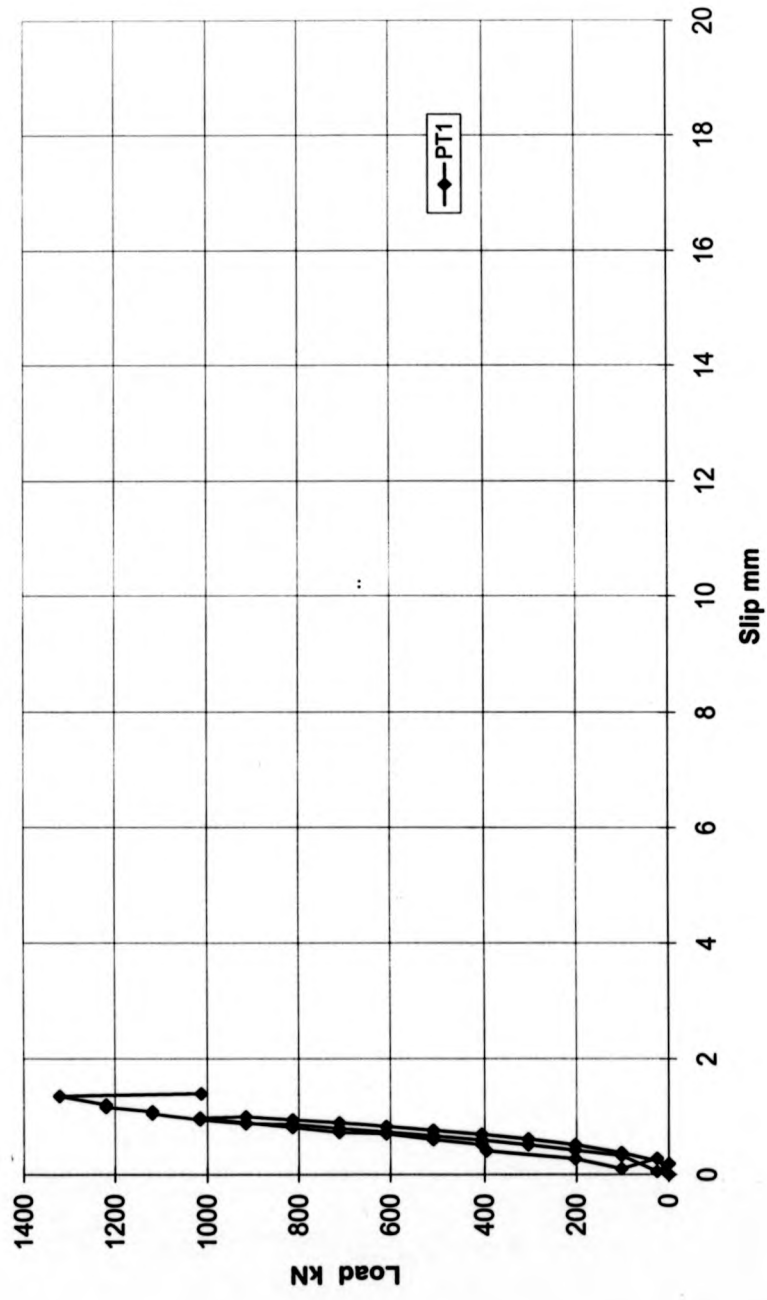
Fig. 5-8 : Load against slip curve for PT1
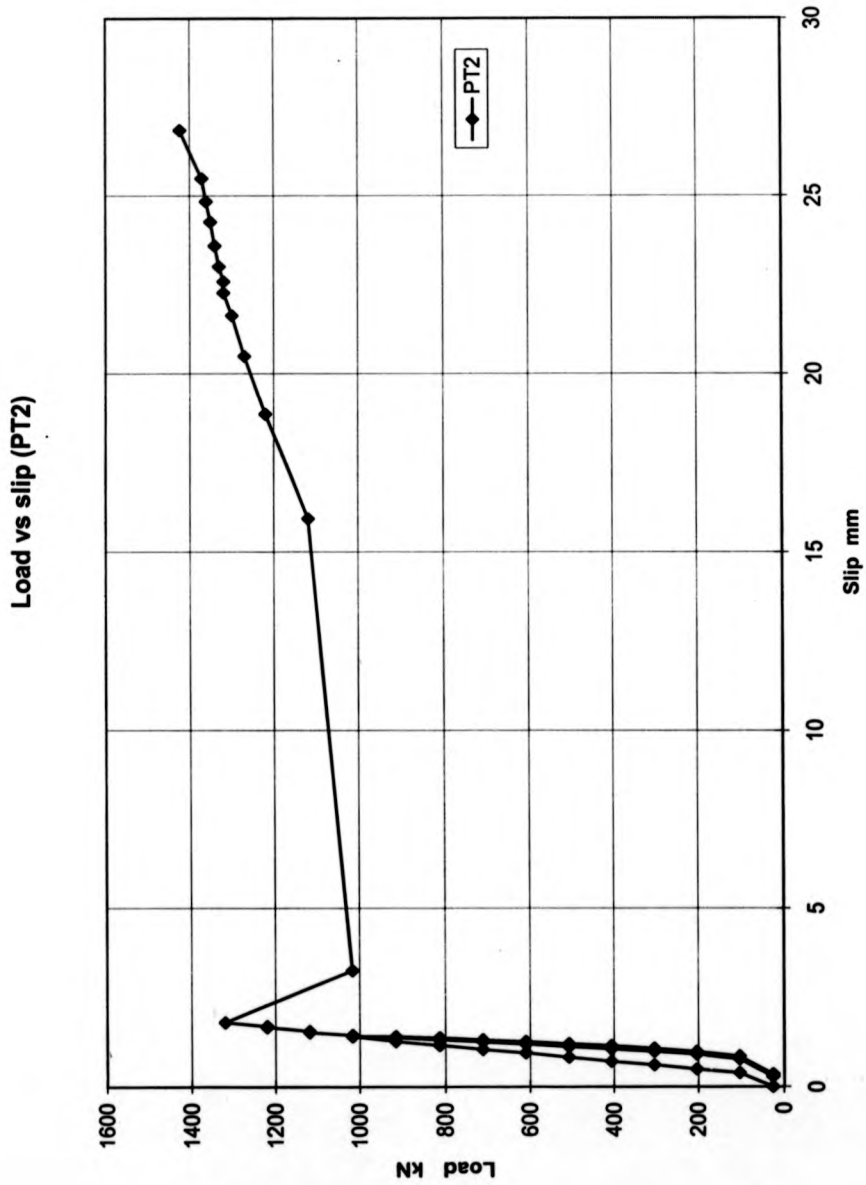
Fig. 5-9 : Load against slip for specimen PT2
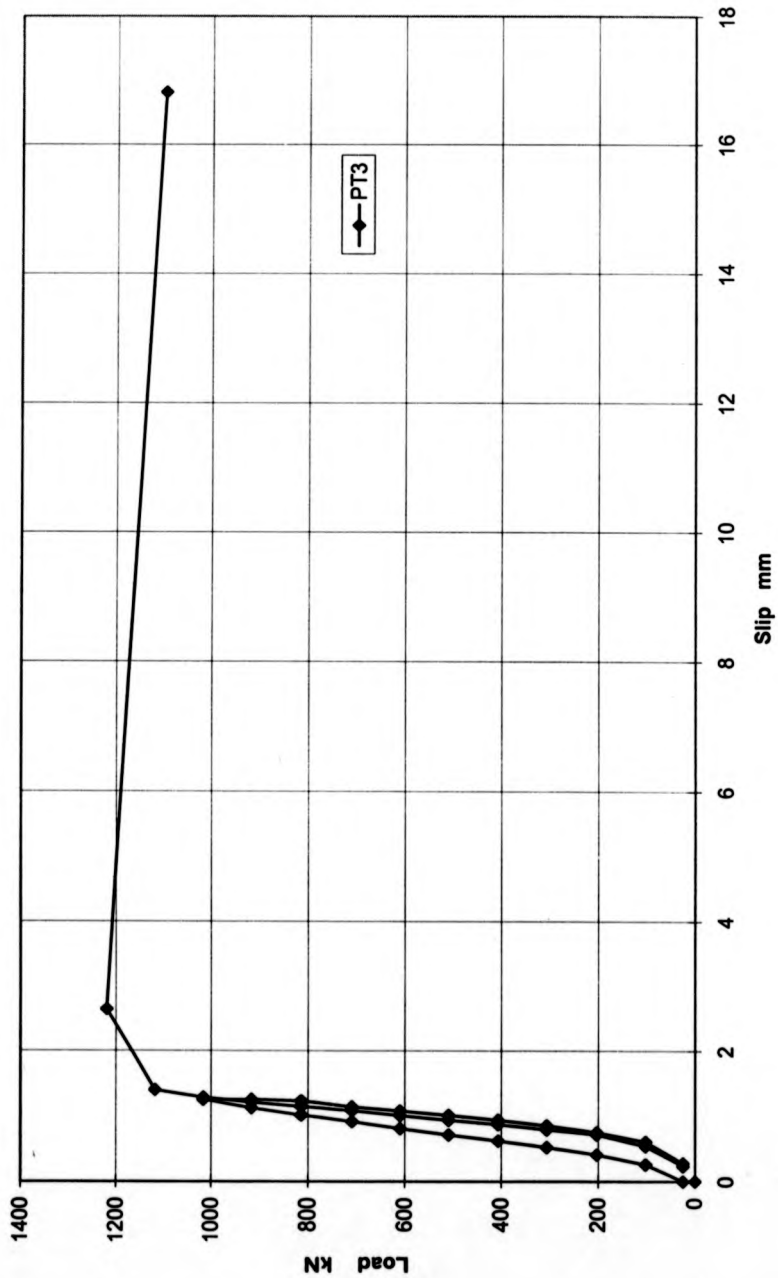
Fig. 5-10 : Load against slip of specimen PT3

Load vs slip (PT4)
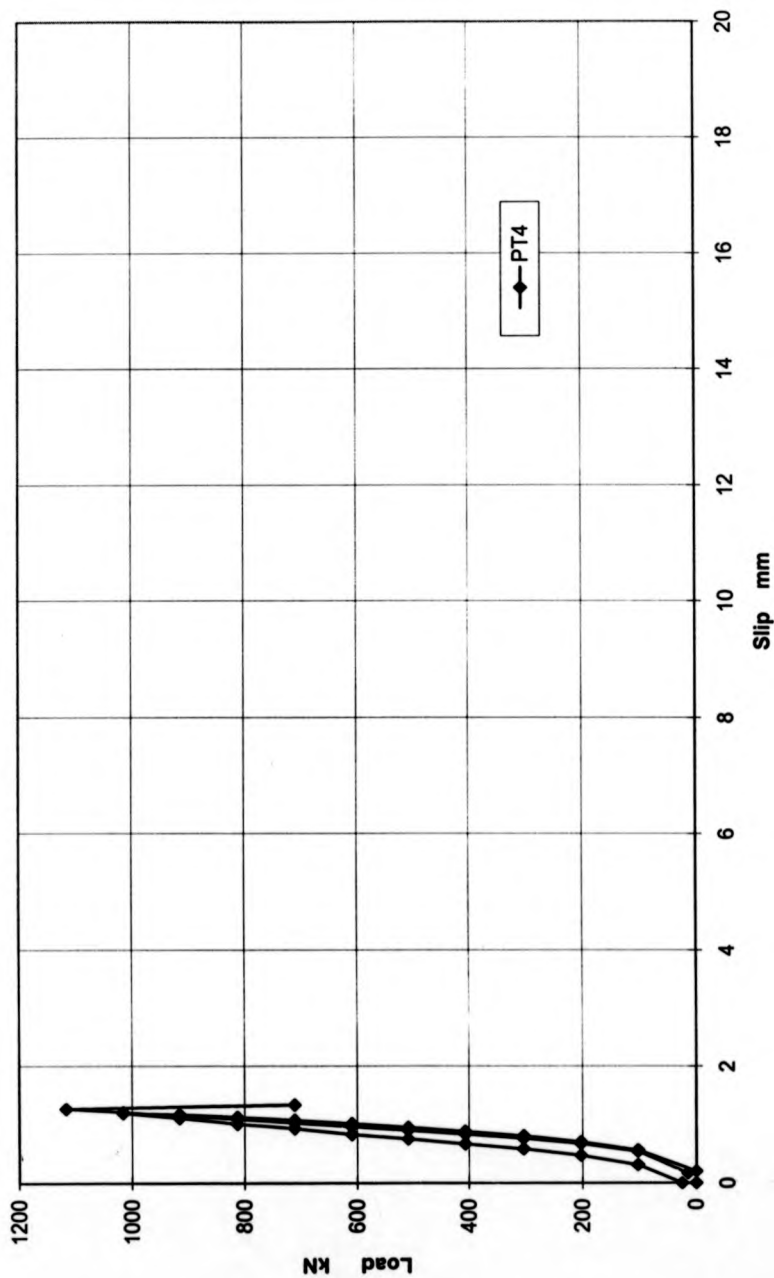
Fig. 5-11 : Load against slip for specimen PT4
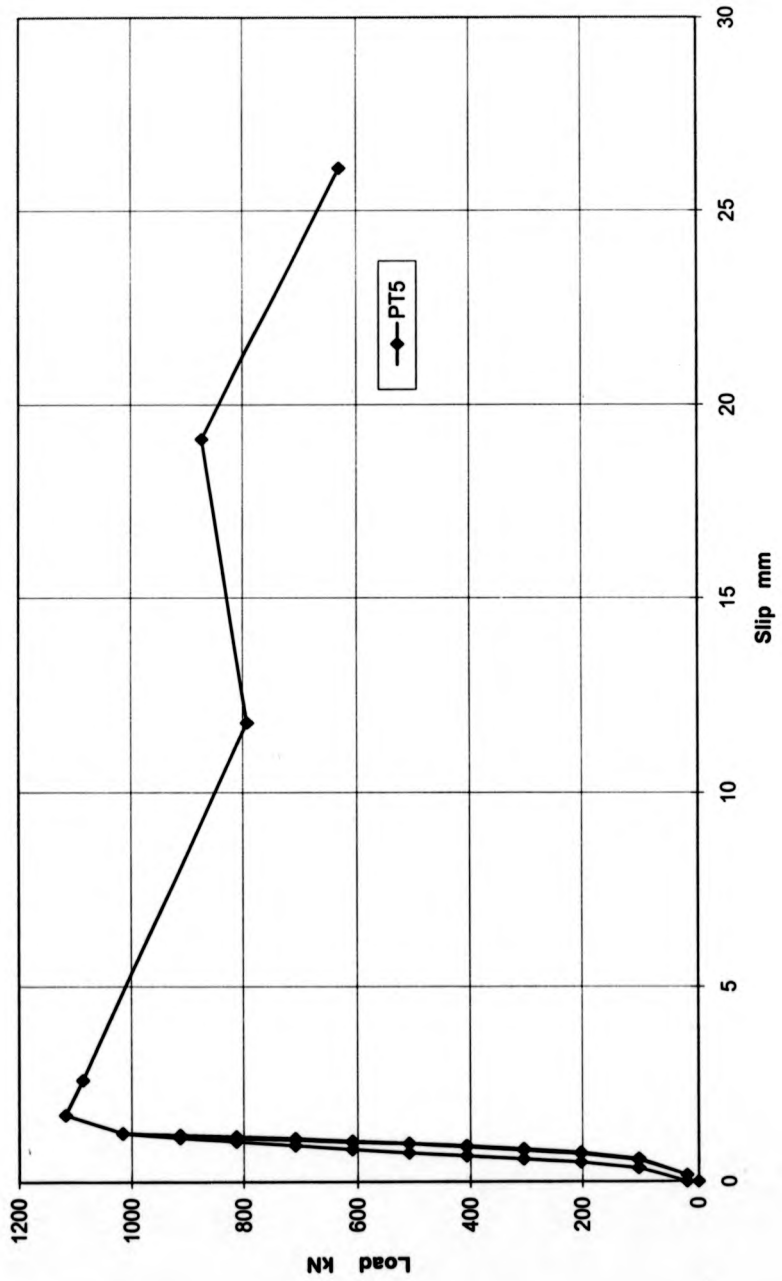
Fig. 5-12 : Load against slip for specimen PT5

Load vs slip (PT6)
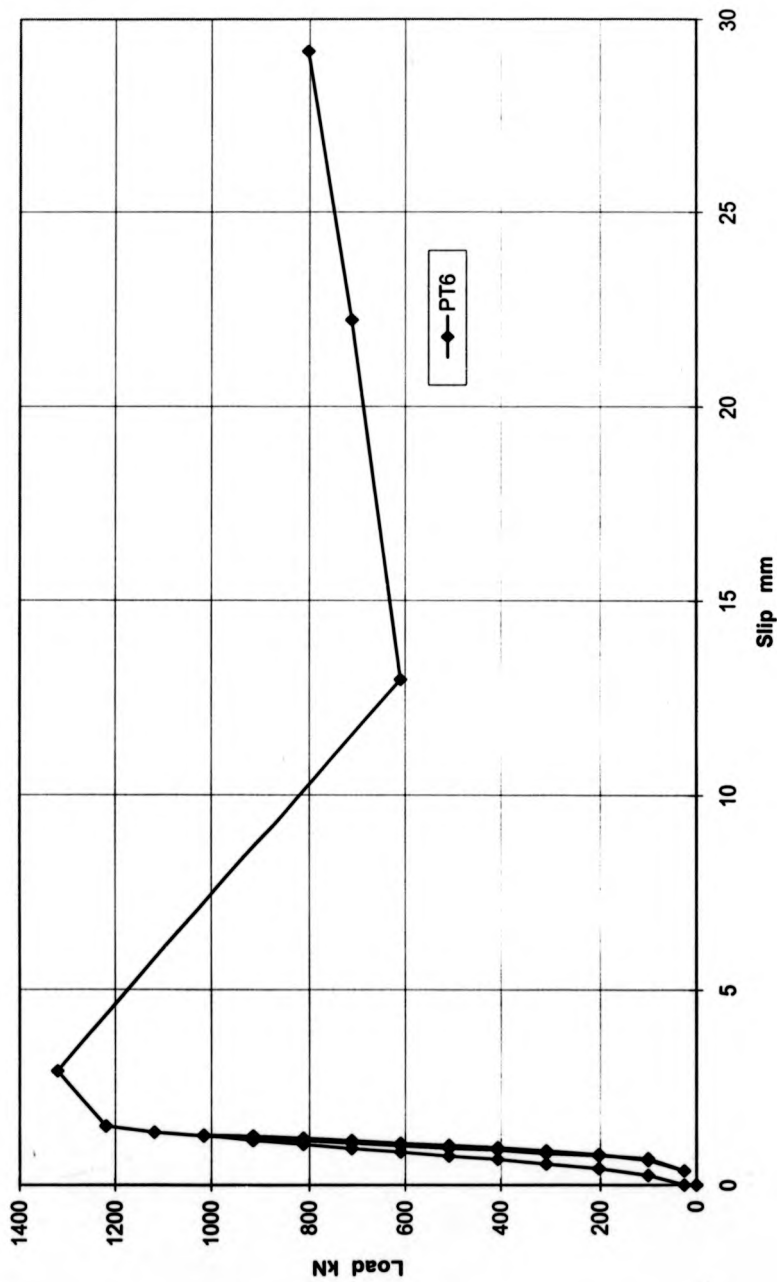
Fig. 5-13 : Load against slip for specimen PT6
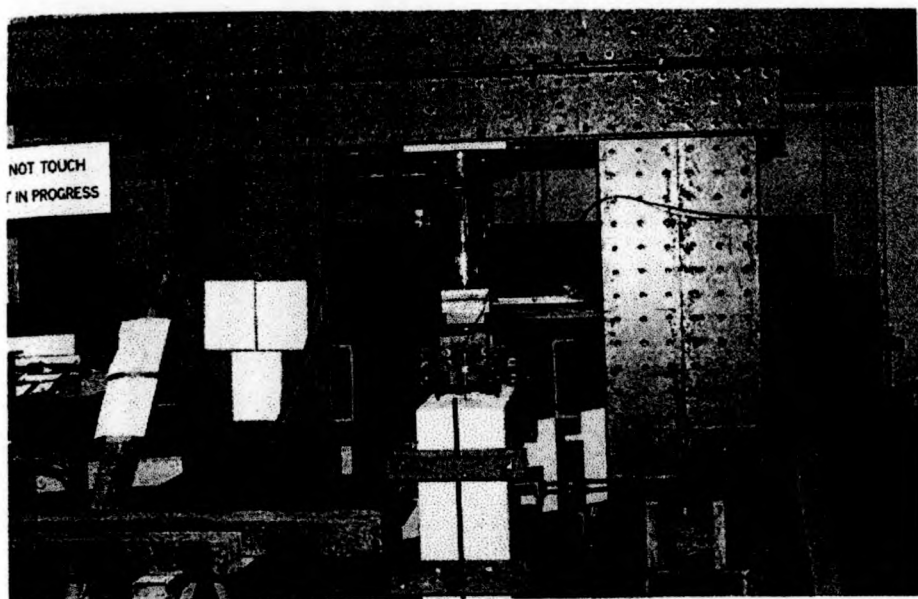
Plate 5-1 : Test rig at Warwick University
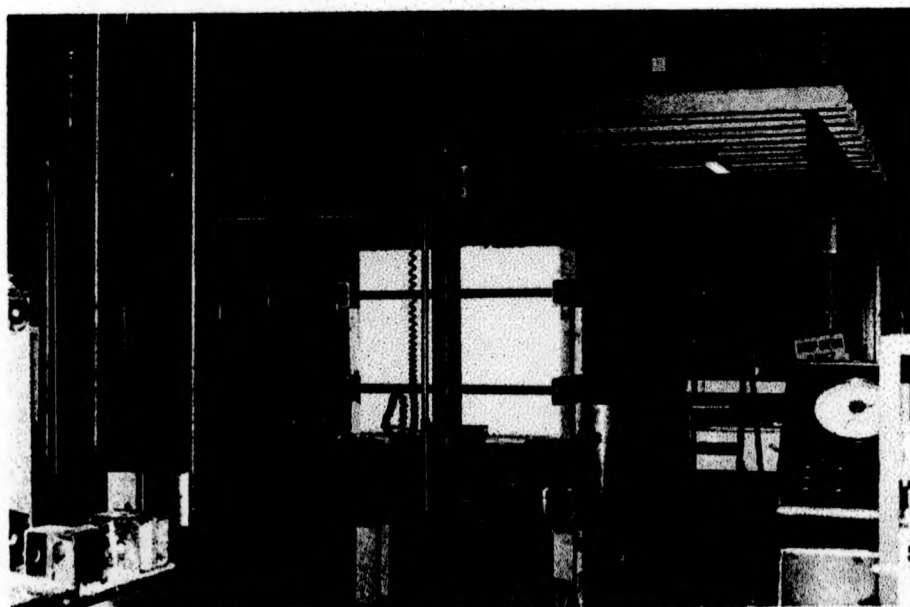
Plate 5-2 : Test rig at City University
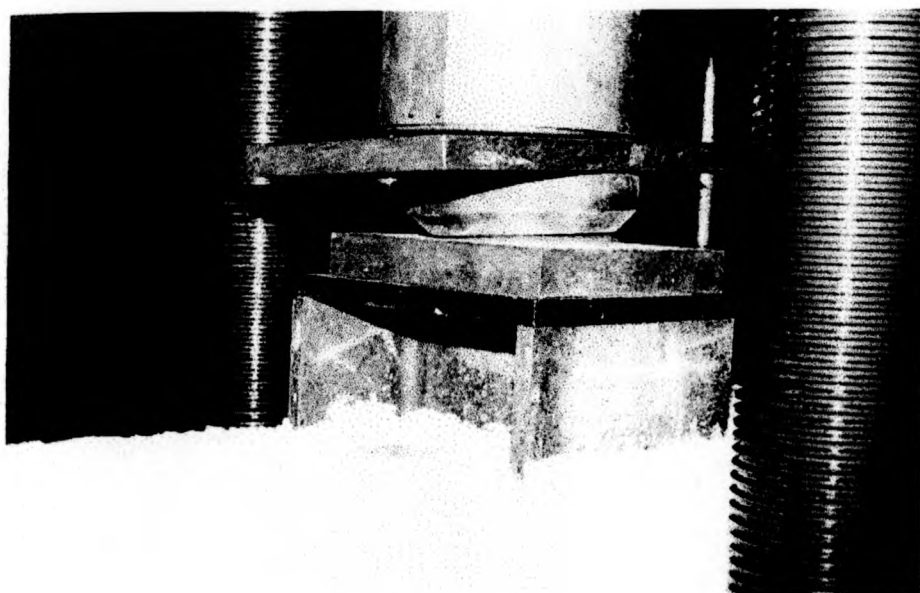
Plate 5-3 : Rocker bearing
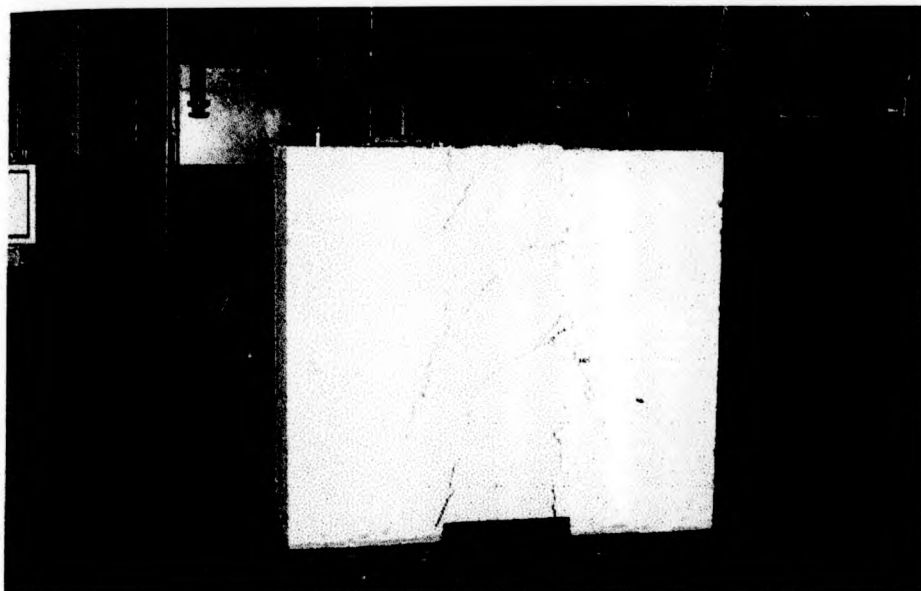
Plate 5-4a : Concrete cracks pattern (PT1)
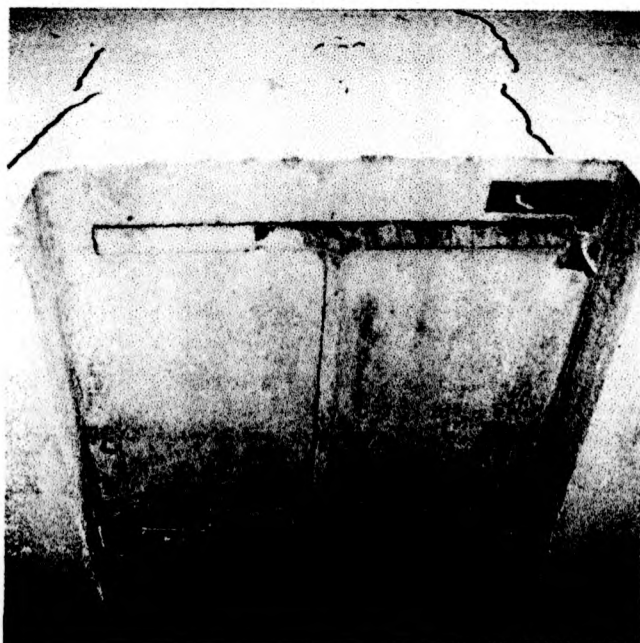
Plate 5-4b. : Slip between concrete and steel section
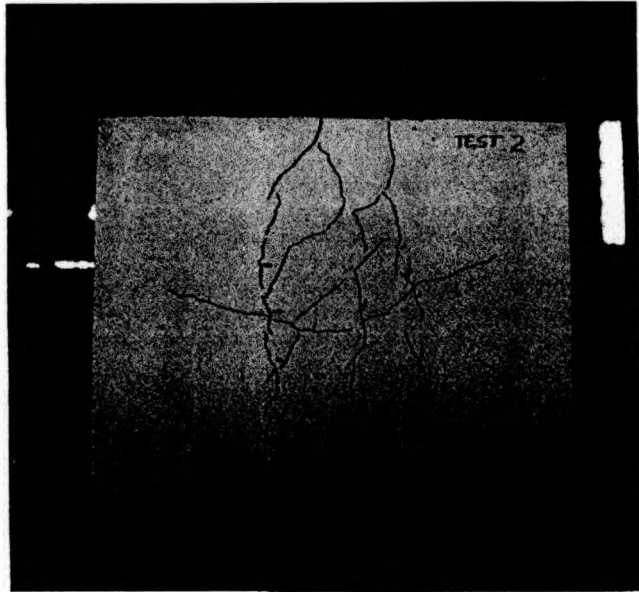
Plate 5-5a : Concrete cracks pattern (PT2)
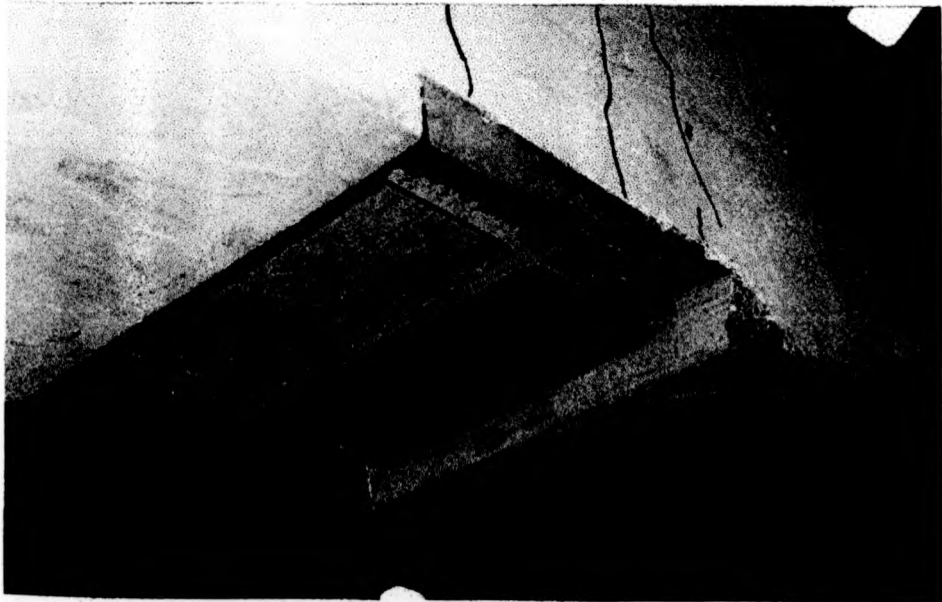
Plate 5-5b : Failure mode of PT2
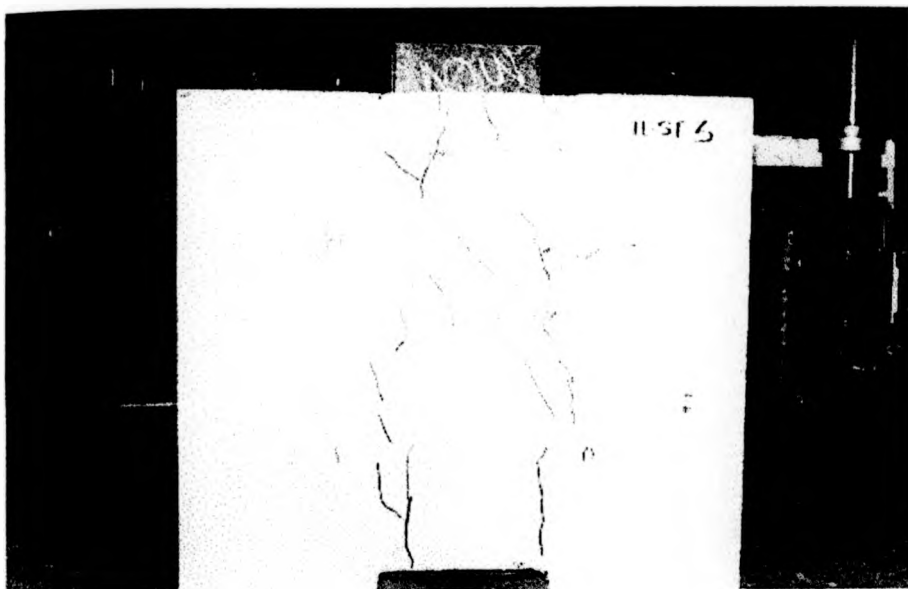
Plate 5-6a : Concrete cracks pattern of PT3
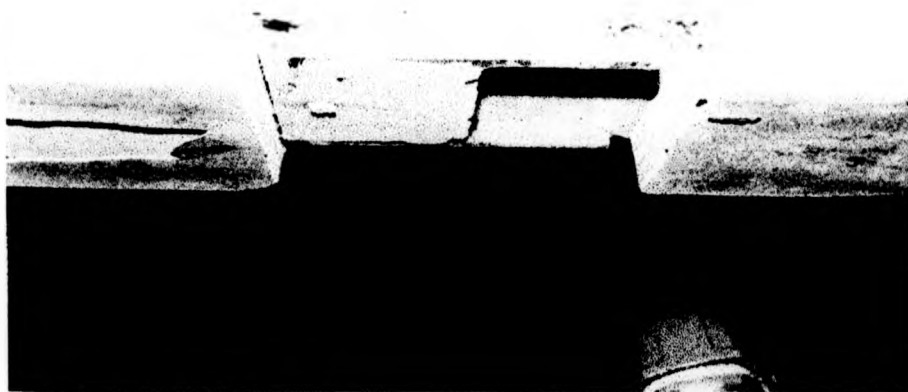
Fig 5-6b : Full slip with concrete core (PT3)
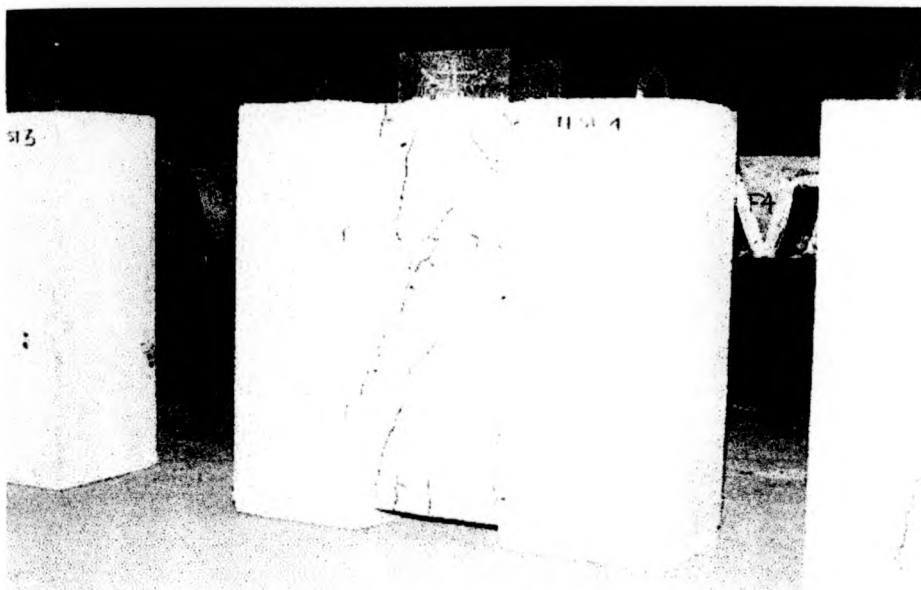
Plate. 5-7a : Concrete cracks pattern of PT4
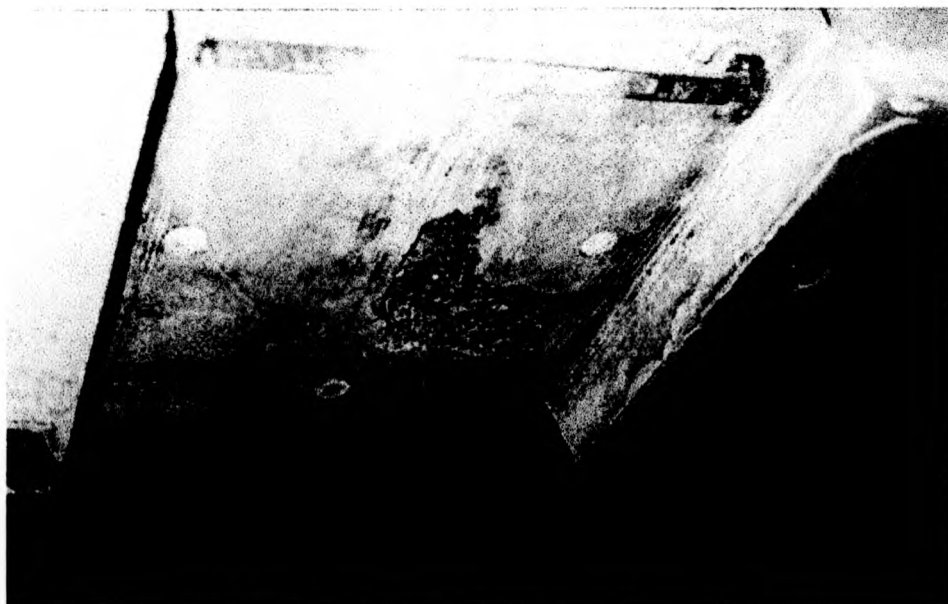
Plate 5.7b : Slip between concrete and steel section (PT4)
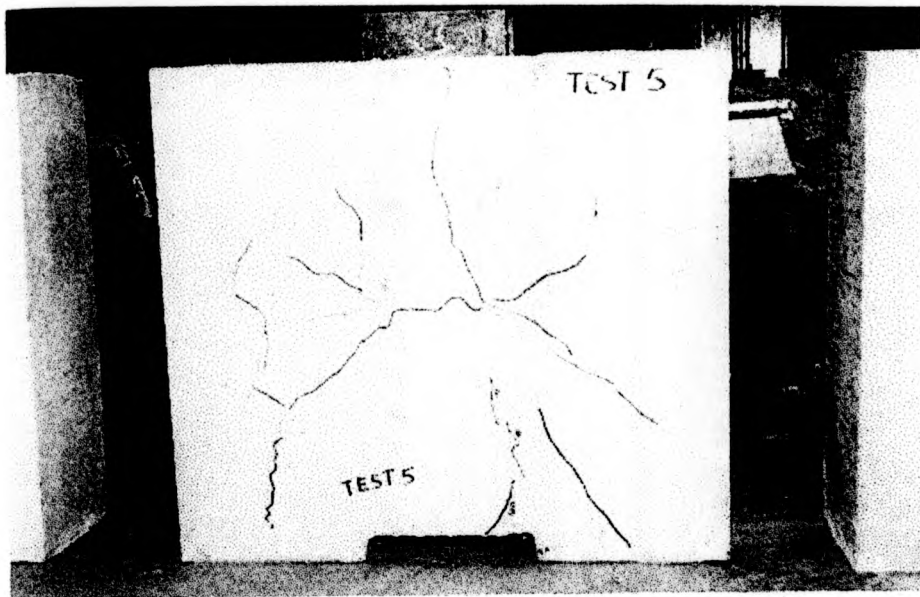
Plate 5-8a : Concrete cracks pattern of PT5

Plate 5-8b : Full slip with concrete core (PT5)
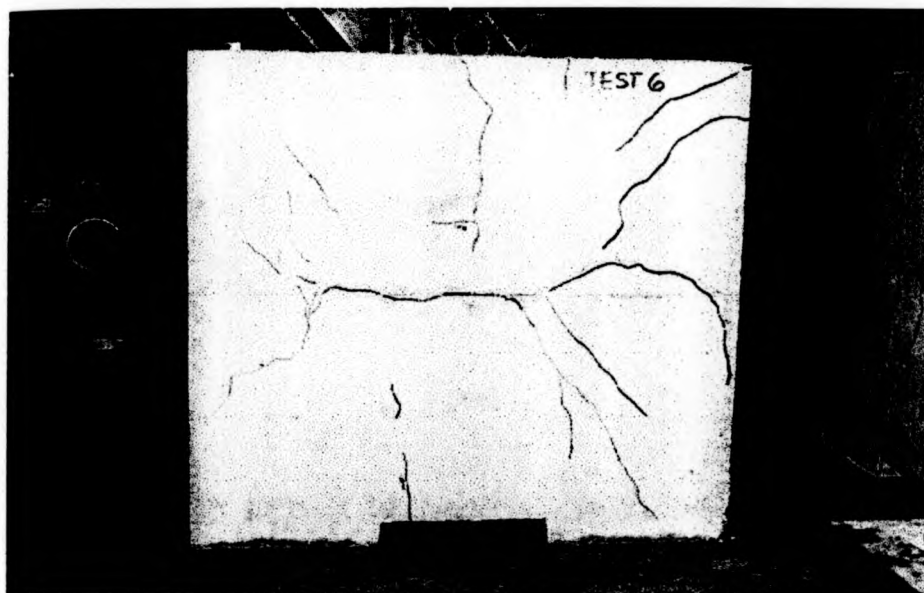
Plate 5-9a : Concrete cracks pattern of PT6
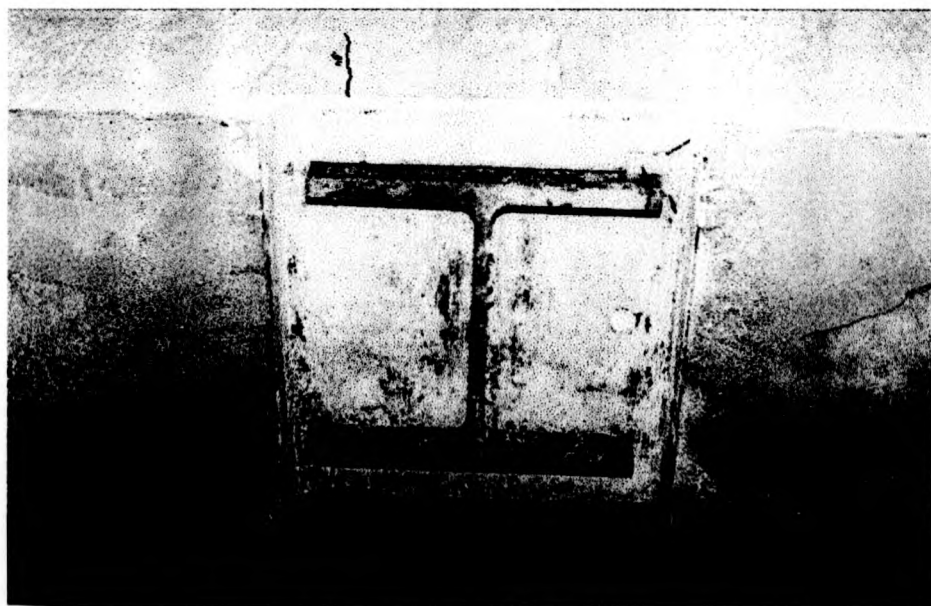
Plate 5-9b : Full slip (PT6)

Chapter 6

LOCAL BUCKLING AND SECTION CLASSIFICATION

6.1 Introduction

The cause and the adverse effect that local buckling has on steel and composite sections has been mentioned in Chapter 1. Design codes [6-1, 2, 3] provide a set of classifications based on limiting proportions of cross-sections. These classifications are performed separately for flange and web. Each flange or web in compression is placed in one of the four classes described in Chapter 1. The class of the cross-section is the less favourable of the classes of the flange and the web so found. This class determines appropriate design procedures for the resistance of the cross-section and for global analysis.

Ideally, the proportions of composite sections should be chosen so that they can be designed as Class 1 or Class 2, for the following reasons[6-4]:

- Rigid-plastic global analysis (also known as plastic hinge analysis) is available only for structures where the cross-sections at the plastic hinge locations are in Class 1 and other cross-sections of beams are in Class 2.

- Plastic theory for the bending resistances of beams is available only for cross-sections in Class 1 and Class 2.

- Where elastic global analysis is used, the limits to the redistribution of moments are more favourable for the higher classes.

- Where floor slabs are composite and in the sagging region, it is possible to use partial shear connection. This is allowed only for beams where the critical cross-sections are in Class 1 or Class 2.

In composite construction, the region of positive moment poses no problems because the concrete slab restrains the compression flange against local and lateral buckling, and the position of the plastic neutral axis is such that only a small depth of the web (if any) will be subject to compression.

However in the negative moment region, the lower flange is not restrained and its proportions influence classification of the section. The presence of reinforcement contributes to the resistance in hogging bending. It may also change the position of the plastic neutral axis and put more of the web into compression, which in turn tends to reduce the cross-section to a lower class.

The class of the web of a steel section effectively depends on the proportion of its clear depth, d , under compression as shown in Fig. 6-1. The limiting d/t ratios for the Class 1/2 and 2/3 boundaries (based on plastic stress blocks) are given in EC3 and EC4 as a function of α. Elastic stress distributions, defined by the ratio ψ , are used for the Class 3/4 boundary (see Tables 6-1 and 6-2). The classification is sensitive to the effect of reinforcement, which increases the depth of steel web in compression, αd. Johnson [6-5] has shown by way of the information in Fig. 6-2 that when $d/t > 60$, an increase in α of only 0.05 can move a web from Class 1 to Class 3. Elastic analysis would then cause a reduction of design moment resistance of up to 30%, compared to plastic stress-block analysis.

To avoid this, an approach known as the "hole-in-the web" method, first introduced in BS 5950 Pt. 3.1[6-3]. It discounts a portions of web which does not contribute to bending resistance. This method, which can be regarded as an extension of the effective width approach (long-used for elastic analysis of Class 4 sections[6-2]0, effectively eliminates the step reduction in moment resistance that would otherwise be caused by the sudden change from plastic to elastic section analysis at the Class 2/3 boundary[6-4]. The "hole-in-the web" method (see Fig. 6-1) has also been adopted in Eurocode 4[6-1] after a slight modification. By using this method, Class 3 sections are effectively upgraded to Class 2.

The published data on local buckling are used to review the classification of sections to Eurocode 4[6-1]. Specific attention given to the possibility of using the "hole-in-the web" approach to upgrade sections from Class 3 to Class 1, thereby permitting rigid-plastic global analysis in the design process.

6.2   Calculation of design resistance of composite beam $M_{pl \cdot Rd}$

A FORTRAN programme has been formulated to calculate the value of plastic design moment resistance, $M_{pl \cdot Rd}$, accounting for the hole-in-the web. The programme is able to classify the composite section, based on EC4 for both the flanges and the web. The listing of the programme is shown in Appendix A2.

The formulae used in the program were based on those published in *Appendix B* and *Appendix C* of BS 5950 Pt 3.1.[6-3]. The derivation of the formulae are given in Lawson et al.[6-6] in which the plastic moment resistance is expressed in terms of the resistance of various elements of the beam (refer to Fig. 6-3) as follows:

Resistance of concrete flange	R_c	=	$0.45f_{cu}B_e(D_s\text{-}D_p)$
Resistance of steel flange	R_f	=	BTp_y
Resistance of slender web	R_o	=	$38\varepsilon\, t^2\, p_y$
Resistance of shear connection	R_q	=	NQ
Resistance of reinforcement	R_r	=	$0.87f_y\, A_r$
Resistance of steel beam	R_s	=	$A\, p_y$
Resistance of clear web depth	R_v	=	$d\, t\, p_y$
Resistance of slender steel beam	R_n	=	$R_s - R_v + R_o$
Resistance of overall web depth	R_w	=	$R_s - 2R_f$

where :

A is area of steel beam

A_r is area of reinforcement

B is breadth of steel flange

B_e is effective breadth of concrete flange

D_p is the depth of profiled steel sheet

D_s is overall depth of concrete flange

d is the clear depth of web

f_{cu} is characteristic strength of the concrete

f_y is characteristic strength of reinforcement

N is number of shear connectors

p_y is design strength of steel

Q is resistance of shear connectors

T is the thickness of steel flanges

t is thickness of web

ε is constant $(275/p_y)^{0.5}$

However some modifications and adaptations were necessary in order to carry out to calculations to EC 4[6-1]:

1. Value of epsilon ε

The value of ε influences the ratios of *c/t* and *d/t* which limit the boundaries for each class of section. In the program, the value of $\varepsilon = \sqrt{(235/f_y)}$ is used in accordance with EC4 instead of $\varepsilon = \sqrt{(275/p_y)}$ used by BS 5950.

2. The classification of flanges and web.

The classification of flanges are based on the limits tabulated in Table 6-1 while the classification of the web are given to Table 6-2. Both of these tables are extracted from EC4[6-1].

2. Ratio of mean longitudinal stress in the web to the design strength

For Class 1 and Class 2, α is taken as $\alpha = 0.5(1 + R_r/R_v)$ where R_r is the resistance of the reinforcement and R_v is the resistance of the clear web depth. The possibility of the position of the plastic neutral axis in the top flange is not excluded by either EC4[6-1] nor BS 5950: Section 3.1[6-3]. However, Johnson and Anderson [6-4] in their commentary on EC4 recommend the limit on α as

$$\alpha \quad \leq \quad 0.5 + 20t\varepsilon / d$$

Any slab reinforcement that increases α above the recommended value is ignored. The program included this recommendation.

For Class 3 and Class 4 the position of zero stress is calculated down the web in order to determine the stress ratio ψ.

3.   Partial safety factors γ

γ-factors for all materials were included in the program, to provide flexibility of use for design or comparison with test results. $\gamma = 1.0$ is taken in calculating plastic moment of resistance to permit comparison against test results.

4.   Hole-in-the web

The hole-in-the web method is available only for webs of Class 3, provided the flange is in Class 1 or Class 2. This method was adopted by EC 4. However the formula in BS 5950 Pt 3.1 Appendix B only applies when the plastic neutral axis of the steel section alone is above the 'hole'. The programme however applies an alternative formula should the position of the plastic neutral axis be in the 'hole'. As can be seen from Appendix A3, if $Rr > (3R_o - R_v)/2$, the plastic neutral axis of the steel section lies in the hole. Different formula (derived in Appendix A3) are then needed to determine the plastic moment of resistance of the composite section allowing for the hole.

5.   Resistance of concrete flange

For EC4, this is given by:

$$R_c = 0.85(f_{ck}/\gamma_c) B_e(D_s - D_p)$$

where f_{ck} is the characteristic cylinder strength and γ_c is the partial safety factor for concrete.

For Class 3 and Class 4 the position of zero stress is calculated down the web in order to determine the stress ratio ψ.

3. Partial safety factors γ

γ-factors for all materials were included in the program, to provide flexibility of use for design or comparison with test results. $\gamma = 1.0$ is taken in calculating plastic moment of resistance to permit comparison against test results.

4. Hole-in-the web

The hole-in-the web method is available only for webs of Class 3, provided the flange is in Class 1 or Class 2. This method was adopted by EC 4. However the formula in BS 5950 Pt 3.1 Appendix B only applies when the plastic neutral axis of the steel section alone is above the 'hole'. The programme however applies an alternative formula should the position of the plastic neutral axis be in the 'hole'. As can be seen from Appendix A3, if $Rr > (3R_o - R_v)/2$, the plastic neutral axis of the steel section lies in the hole. Different formula (derived in Appendix A3) are then needed to determine the plastic moment of resistance of the composite section allowing for the hole.

5. Resistance of concrete flange

For EC4, this is given by:

$$R_c = 0.85(f_{ck}/\gamma_c) B_e(D_s - D_p)$$

where f_{ck} is the characteristic cylinder strength and γ_c is the partial safety factor for concrete.

6.   Resistance of slender web

In the programme the effective depth of the web in compression is taken as $40t\varepsilon$ as suggested in EC 4 instead of $38t\varepsilon$.

6.3   Experimental data

Data from several researchers were examined and comparisons were carried out using results from the computer programme. In line with its aim, the study concentrated on results which mainly reported local buckling as the failure mode and the classification of web as Class 3. The study considered results presented in the form of a moment-rotation (M-ϕ) relationship for the composite beams tested. Fig. 6-4 shows a typical moment-rotation behaviour of a section. Work carried out by previous researchers involving connection tests were also considered if they were full strength (i.e. moment resistance of connection > plastic resistance of the beam). Fig. 6-4 defines parameters whose values are quoted when assessing test results, with M_u, the experimental maximum moment, and M_p, the calculated resistance moment of beam cross-section given based on measured strength given by the reseachers. ϕ_p represents the rotation capacity at M_p of the specimen tested and ϕ_u describes the rotation at the experimental maximum moment M_u. $M_{pl.Rd}$ represents the the resistance moment of beam cross-section calculated by the programme using the given measured material properties. It uses the "hole-in-the-web" approach for sections with Class 3 webs.

The experimental programmes undertaken by several researchers are summarised in this section. Several types of test configuration have been tested, namely

i) Section continuous over internal support

In this type of configuration only one beam is used in each test. It is supported at the middle and loads are applied at each end or vice-versa.

ii) Continuous beam tests

This configuration involves at least a two-span beam in which the beam section at the internal support is continuous.

iii) Cruciform type

This consists of a column and two cantilever beams, with loads applied at the end of the cantilever. This arrangement is usually used to investigate the performance of a composite connection, and can be arranged to suite tests about the major or minor-column axis.

The three different test arrangements are summarised in Fig. 6-5.

6.3.1 Climenhaga & Johnson [6-7]

The aim was to provide more information on local buckling and its effect on rotation capacity in negative moment regions of continuous composite beams. Composite beams and simulated composite beams (by plating the steel section) were used in the tests. Results were reported as moment-rotation curves. The principal results of these tests are tabulated in Table 6-3. From Table 6-3 the beams can be group into three classes based on flange and web slenderness.

For Class 1 sections very large rotations were observed and the value of experimental maximum moment M_u exceeded M_p based on measured material properties. The values of over 100 mrad were recorded for all the three beams in Class 1. It worth noting that for stiffened beam SB13s (simulated composite beam) gives the highest M_u when compared to SB1 and SB7 (bare steel beams). It indicated the advantages of choosing a

composite section. A lower rotation of 40 mrad was recorded for SB13s at M_u, compared to 100 mrad for both SB1 and SB7.

The calculated values of plastic moment given by the author's programme, M_{plRd}, with γ-factors taken as 1.0 is also given. As the sections are Class 1 and do not therefore use the "hole-in-the-web" method, the values are (not suprisingly) very close to those calculated by Climenhaga and Johnson[6-7]. Small differences may be expected if treatment of the curved fillets to the steel section is not identical.

For the Class 2 group some of the beams, i.e. beams SB3, SB9 and HB40 behaved like Class 1 in that their rotation capacity, ϕ_p, observed to be greater than 100 mrad. Except for HB40, M_u for all the beams in the group is at least M_p. Local buckling failure then led to a fall-off in the applied bending moment, although never to a value less than M_p. The beams in the group had a range of rotation capacity, ϕ_p, from 20 to 100 mrad. From Table 6-3 comparable results are observed between M_p and $M_{pl.Rd}$.

Except for beams with stiffeners, i.e. SB15s and HB42s, the moment resistance obtained from the tests, M_u, did not reach the values of M_p in the Class 3 group. This is typical behaviour for Class 3 beams. Compared to beams of Class 1 and Class 2 in Table 6-3, the Class 3 beams (except SB15s and HB42s) registered lower rotation capacity. SB15s (simulated composite beam) and HB42s (composite beam) gave highest rotation capacities, ϕ_p, (27 mrad and 67 mrad respectively) in the group. By having stiffeners on the beam, the resistance moment of the beam may improve and premature local buckling is prevented thus leading higher rotations. These two beams had shown behaviour typical of Class 1 and Class 2 beams although they were classified as Class 3. It is an indication that the upgrading of Class 3 composite sections to a higher class is feasible.

From Table 6-3, it can be seen that, by discounting a portion of web which does not contribute to bending resistance, the author's computed values for $M_{pl.Rd}$ are reasonably accurate and provide conservative estimates of the maximum experimental moment M_u. This implies that the 'hole-in the web' method for Class 3 sections worked well.

The use of $\gamma_{structural\ steel} = 1.1$ and $\gamma_{rebars} = 1.15$ instead of $\gamma = 1.0$ increases the range of the design rotation capacity of Class 2 beams between 36 and 70 mrad while the rotation capacity of the Class 3 group improved greatly, giving a range of 17 to 34 mrad. However no significant changes in rotation capacity occur for the Class 1 group when the γ greater than 1.0 is applied.

6.3.2   Hamada and Longworth[6-8]

The behaviour of sections continuous over an internal support was investigated by Hamada and Longworth[6-8]. They carried out a study on the buckling of three steel-only beams and 19 composite beam specimens in negative bending. Four different groups of section were used. The 2438 mm span beams were tested under concentrated load at midspan 'upside down' to create the condition of negative bending (Fig. 6-5i).

In their paper the level of the longitudinal rebars is not given. In the author's programme to calculate $M_{pl.Rd}$ the distance from the top of slab to the centroid of rebars was assumed to be 25 mm. From Table 6-4 it can be seen that for all the beams that fail by a local buckling mode, the value of ultimate moment M_u exceeded the calculated plastic moment M_p, although the class of web varies from Class 1 to Class 3.

In group 1 tests the compression flanges of beams 4A,2,5,6,1 were reinforced by a cover plate which prevented local buckling from occurring and the beams failed by lateral buckling.

The effect of varying the amount of reinforcement on section classifications can be seen from Table 6-4 for group 2, 3, and 4. When no reinforcement was provided the sections are in Class 1. However when the reinforcement is gradually increased, the class of section decreased to lower class. It was also observed from the table that, the curvature, and hence the rotation capacity gradually decreased as the area of reinforcement increase. In general group 2 and group 3 specimens registered a higher ratio of M_u / M_p than group 4 because the flanges in group 4 had a lower class i.e. Class 2. This indicates the importance of flange classification in determining the moment resistance of the beam. It is also observed that group 4 specimens had a comparatively higher d/t ratio, thus indicating that the possibility of upgrading the classification of sections with relatively lower d/t ratios may be feasible.

Deformation is given by curvature, but this is 'at local flange buckling'. The level of moment corresponding to this is not given. The values of computed $M_{pl.Rd}$ showed some difference to the published M_p[6-8]. Those values cannot therefore be confirmed by the present author. One needs to be cautious concerning the stiffness properties of steel, particularly the ratio of the modulus of elasticity to the strain hardening modulus h=E/E$_{st}$ This is not given by Hamada and Longworth[6-8] but a value of the slope at the onset strain-hardening E$_{st}$ is taken as 6003 N/mm^2 and this does not correspond to typical values for European steels (E$_{st}$ =4200 N/mm^2)

Hamada and Longworth[6-8] concluded that the ultimate moment capacity of composite beams in negative bending is affected by local buckling unless compression flange is

stiffened by a cover plate. They found also that by increasing the flange width-thickness ratio there was a significant decrease in the moment resistance of the beams.

6.3.3 Najafi and Anderson[6-9]

A total of eleven tests on end plated beam-to-column connections were carried out by Najafi and Anderson[6-9]. Seven tests were performed about the major-axis and the remaining four about the minor-axis.

Except for one test where an extended end plate was used, the tests used flush end plates as the connecting medium. The amount of slab reinforcement was selected to provide percentages ranging from 0% to 1.5% of the area of concrete. All the tests were carried out on cruciform specimens to model internal joints in a braced frame. The variables investigated were the type of end plate connection, the amount of reinforcement and the depth of steel beam. All the composite specimens showed formation of cracks at low applied moment (at about 28 kNm) . As loading increased transverse cracks formed at increasing distance from the faces of column. Crack widths were measured, generally at two third of the predicted resistance of the connection.

Significant deformation of the column flange at higher load was observed in specimens S8F and S4F before fracture of mesh and rebars occurred. In specimen S8F slight local buckling of lower flange was also visible at failure.

Local buckling of the bottom flange was the failure mode for specimen S8E and S12F (extended end plate with 1% reinforcement and flush end plate with 1.5% reinforcement, respectively). For a deeper beam(specimen S8FD), failure occured at the very low rotation of 14 mrad.

From Table 6-5 specimens S8F, S8E, S12F and S8FD were noted to have flange of Class 1 and a web of Class 3. However, only specimens S8F, S8E and S12F were valid for the purpose of this study as only the connections were full strength compared to the resistance of composite beam. The ultimate experimental moments, M_u were greater than M_p with a substantial rotation for these specimens. It thus supports the view that the EC4 limits on classification of the web could be further relaxed. It is noted however from Table 6-5 that the web in specimens S8F, S8E and S8FD was close to Class 2 and this explains the response detailed above..

In the minor-axis tests unbalanced loading was applied to the specimens. In all specimens (except T11) cracks were observed at low moment. In specimens T5 and T8 there was signs of local buckling on further moment increase before there was fracture of the rebar.

From the tests, Najafi and Anderson[6-9] showed that an increase in the amount of reinforcement and the use of extended end plate will both increase the moment resistance and the rotation capacity of a composite connection. However, the use of a deeper beam did result in an increase in stiffness but a decrease in rotation capacity.

6.3.4   Uth[6-10]

Uth[6-10] carried out tests on the negative moment region of continuous beams in which local buckling was the failure mode. Table 6-6 shows the results from the tests. From the table it is observed that for the beams with flange of Class 1 and web of Class 3, (VT1, DV11) the value of M_u exceeded both M_p and $M_{pl.Rd}$. They gave substantial amount of rotation but the ratios of d/t were very close to Class 2 web. However for

beams in specimens A1 and A2, values of M_u were exceeded the M_p , but not $M_{pl.Rd}$. For these beams the ratios of d/t were near to the Class 3 limit.

For beams in specimens VT4, VT6 with flange of Class 4 and web of Class 1 (according to EC4 a Class 4 section) the M_u values obtained in the tests were above the published M_p values. The present author's programme does not address this case.

The rotation capacity of Class 3 beams in tests VT1, DV11, DV31, A1, A2, and A3 was considerable, in the range between 39 mrad to 82 mrad. In a number of cases these rotations are higher than for the Class 1 or Class 2 in the tests. The ability of Class 3 sections to show a high rotation capacity and moment resistance showed the possibility of upgrading the class of the section.

6.3.5 *Kemp et al.[6-11]*

Tests were carried out by Kemp et al[6-11] to study the ductility effects of end details in composite beams. Specimens LR and SR were continuous over the internal support and are suitable for assessment of rotation capacity. Except, for test SR, the other three tests were with beams of flange Class 1 and web Class 3. M_u exceeded M_p in tests LSR, SR, and SSR. Specimen LR had a very high lateral slenderness and lateral-torsional buckling occurred first, followed by local web buckling. No rotation capacity at the plastic moment was available, because this moment was not reached. Tests LSR and SSR are not relevant as they are not full-strength connections. Kemp et al suggested that the ductility classification of composite beams should reflect both lateral and local buckling and not just local buckling as in many existing codes.

6.3.6 *Aribert and Raoul[6-12]*
Two continuous beams B1 and B2 were tested. Beam B1 was a rolled I-section while beam B2 was an I-section made of welded plates. Specimen B1 had flanges in Class 1

and the web just in Class 3. Extensive local buckling of web and flange occurred, yet ultimate failure was due to crushing of concrete in sagging bending. This test met the EC4 requirements for rigid-plastic analysis because the loading was concentrated and the neutral axis depth in the slab, at 60.7mm below top surface, did not exceed 15% of the overall depth. B1 showed the behaviour of Class 1 in which the value of moment resistance obtained in the test M_u was higher than the predicted value M_p.

6.3.6 Gill and Johnson[6-13]

Three three-span continuous composite beams were tested. Beams CB10 and CB11 were intended to explore premature failure due to crushing of concrete (i.e. insufficient rotation capacity in the mid-span region). The critical cross-sections in CB12 were at internal supports, where rotation capacity would be limited by local buckling. All the beams flanges and webs in Class 1, and in each case M_u exceeded M_p with a large amount of rotation. This is the expected behaviour of Class 1 beams.

6.4 Discussion

The classification of composite beams in hogging bending has been checked by a computer programme using the published specimen data. All the beams which were classified as Class 3 (by the EC4 definition) are presented in Table 6-7. For the continuous beams tested it can be seen from the results in Table 6-7 that most had a value of M_u exceeding the moment predicted $M_{pl.Rd}$ using "hole-in-theweb" method. For $M_{pl.Rd}$ measured material properties were used. For the connection tests only a 'full strength connection' which exhibits this kind of behaviour was considered. From Table 6-5, fracture of the rebars was the failure mode for some composite beam details (S8F, S4F, S8FD, T5 and T8). This means that up to the reported final rotation, there was a

possibilty that local buckling had also occurred in the compression flange without an overall detrimental effect to moment resistance. Thus there is evidence that local buckling was not damaging the behaviour for Class 3 beams. It also meant that the rotation capacity is at least at the point where rebars snapped and that limits on classification permit at least that amount of rotation capacity to be obtained. This would indicate that upgrading from Class 3 to Class 2 and probably to Class 1 is appropriate for composite beams.

In EC4[6-1], the web slenderness relevant to a Class 2 section is defined as $\alpha d/t\epsilon$, where αd is the depth of web under compression, $\epsilon = (235/f_y)^{0.5}$ and t is its thickness. Slenderness limit for flanges of rolled section is given in EC4 to be $10 < b/T\epsilon \leq 11$ and for webs as α increases the slenderness limit reduces as follows:

for $\alpha = 1.0$, $33 < \alpha d/t\epsilon \leq 38$

for $\alpha = 0.5$, $36 < \alpha d/t\epsilon. \leq 41.5$

The relationships between these slenderness limits are plotted in Fig 6-6. The figure also show the class boundaries. From Fig 6-6 it can be seen that although all the beams plotted were Class 3 some of them were also within the boundaries of Class 2. It can therefore be concluded that some of the Class 3 beams can be upgraded to Class 2.

Fig. 6-7 shows the values of $M_u/M_{pl,Rd}$ plotted against web slenderness limit. From Fig. 6-7 it can be deduced that many Class 3 beams are able to reach the section's plastic moment resistance.

Ratio d/t could be used as an indicator to upgrade Class 3 to Class 2, or even to Class 1. However thus far, no conclusive boundary to d/t has been established to separate beams

in an upgrading process. Further tests and verification would be necessary in order to upgrade Class 3 to a higher class confidently.

6.5 *Conclusion*

The conclusion that can be drawn from this study are

i) From the available physical test data it was found that in many cases, where the connection was full strength, beams of Class 3 web according to EC4 showed the characteristics of beams with a higher class of web.

ii) It can be said that the type of connection contributed to the M_u of composite beams.

iii) The 'hole-in-the web' approach provides a satisfactory method to determine the moment resistance of beams with Class 1 or 2 flanges and Class 3 webs.

iv) Many of the Class 3 beams can be upgraded to Class 2. However there is no evidence to substantiate the possibility of upgrading such beams to Class 1.

References

6-1   *DD ENV 1994-1-1 : 1993 Eurocode 4: Design of Composite and concrete Structures: Part 1.1, General rules and rules for buildings*, British Standard Institution, London 1993.

6-2   *DD ENV 1993-1-1 : 1992 Eurocode 3: Design of Steel Structures: Part 1.1, General rules and rules for buildings*, British Standard Institution, London 1992.

6-3   BS 5950 *Structural use of steel work in buildings: part3.1: code of practice for composite construction.* British Standards Institution.

6-4   Johnson, R.P., Anderson, D., "Designers' handbook to Eurocode 4", Thomas Telford, London. 1993.

6-5   Johnson, R.P., "Composite structures of steel and concrete, Vol 1 Beams, Slabs, Columns, and Frames for Building", 2nd Edition. Blackwell Scientific Publication. 1994.

6-6   Lawson, R.M., Taylor, J.C., Smith, D.G.E., "Commentary on BS 5950 Part 3: Section 3.1 'Composite Beams'. The Steel Construction Institute. 1990.

6-7   Climenghaga J.J., Johnson, R.P. "Local buckling in continuous composite beams", *The Structural Engineer.* No 9 Vol 50, Sept. 1972, pp. 367-374.

6-8   Hamada, S., Longworth, J., "Buckling of composite beams in negative bending", Journal of the Structural Division. ASCE, Vol. 100 No. ST11, Nov. 1974. pp.10917-2221.

6-9   Najafi A.A., "End plate connections and their influence on steel and composite structures", PhD Thesis, University of Warwick, 1992.

6-10   Uth H-J., " Durchlaufende Verbundtrager im hochbau - Lokale Instabilitat im Negativen Momentenbereich.", Dr-Ing. Dissertation. Kaiserslautem. 1987.

6-11   Kemp A.R., Trinchero P, Dekker N. " Ductility effect of end details in composite beams", Composite Construction in Steel and Concrete II, *Proceedings of an Engineering Foundation Conference, ASCE*, Potosi, June 1992, pp. 413-428

6-12   Aribert J.M. and Roul J "Two full-scale tests of class 3 composite beams". Composite Construction in Steel and Concrete II, *Proceedings of an Engineering Foundation Conference, ASCE*, Potosi, June 1992, pp. 65-80.

6-13   Hope-Gill, M.C., Johnson, R.P., "Tests on three-span continuous composite beams", Proc. Instn Civ. Engrs, Part 2, June 1976, Vol 61, pp. 367-381.

Table 6-1[6-1] : Maximum width-to-thickness ratios for steel outstand flanges in compression
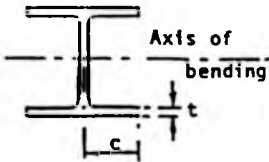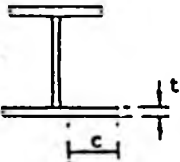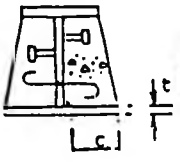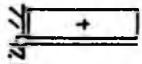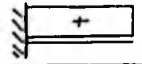
Class	Type	Web not encased		Web encased	
		Rolled		**Welded**	
		Welded		**Encased web**	
Stress distribution (compression positive)			+		+
1	Rolled	c/t ⩽ 10c		c/t ⩽ 10c	
	Welded	c/t ⩽ 9c		c/t ⩽ 9c	
2	Rolled	c/t ⩽ 11c		c/t ⩽ 15c	
	Welded	c/t ⩽ 10c		c/t ⩽ 14c	
3	Rolled	c/t ⩽ 15c		c/t ⩽ 21c	
	Welded	c/t ⩽ 14c		c/t ⩽ 20c	

$\varepsilon = \sqrt{235/f_y}$	f_y (N/mm^2)	235	275	355
	ε	1.0	0.92	0.81

Table 6-2[6-1] : Maximum width-to-thickness ratios for steel webs

Table	Maximum width-to-thickness ratios for steel webs		
Webs: (internal elements perpendicular to axis of bending)			

$$d = h - 3t$$

Class	Web subject to bending	Web subject to compression	Web subject to bending and compression
Stress distribution (compression positive)			
1	$d/t \leq 72\varepsilon$	$d/t \leq 33\varepsilon$	when $\alpha > 0.5$: $d/t \leq 396\varepsilon/(13\alpha - 1)$ when $\alpha < 0.5$: $d/t \leq 36\varepsilon/\alpha$
2	$d/t \leq 83\varepsilon$	$d/t \leq 38\varepsilon$	when $\alpha > 0.5$: $d/t \leq 456\varepsilon/(13\alpha - 1)$ when $\alpha < 0.5$: $d/t \leq 41.5\varepsilon/\alpha$
Stress distribution (compression positive)			
3	$d/t \leq 124\varepsilon$	$d/t \leq 42\varepsilon$	when $\psi > -1$: $d/t \leq 42\varepsilon/(0.67 + 0.33\psi)$ when $\psi \leq -1$: $d/t \leq 62\varepsilon(1-\psi)\sqrt{(-\psi)}$

$\varepsilon = \sqrt{235/f_y}$	f_y	235	275	355
	ε	1	0.92	0.81

Table 6-3 : Results from Climenhaga

1 Test No	2 Section sizes	3 MpRd (Comp)	4 Mp (Published)	5 Mu (Test)	6 φu mrad	7 φp mrad	8 Class F	9 Class W	10 d/t web	11 C1	12 C2	13 C3	14 Combined Slenderness	15 MpRd/Mp	16 φp at MpRd	17 MpRd when γs=1.1 γr=1.15	18 17/4	19 φp when 17/4	20 Comment
										Limit of web Classification									
SB1	127x76UB13	31	32.3	40	100	100	1	1	23	27.85	32.07	64.36	10.53	0.96	100	28.2	0.87	100	
SB7	127x76UB13	31	32.6	41	100	100	1	1	23	27.85	32.07	64.36	10.53	0.95	100	28.1	0.87	100	
SB13s	203x133UB25	98.9	97.6	133	40	100	1	1	29.71	30.07	34.63	67.67	16.64	1.01	100	89.6	0.92	100	
SB2	203x133UB25	108.5	108.1	119	26	52	1	2	29.71	27.28	31.41	61.38	17.87	1.00	40	98.3	0.91	70	
SB8	203x133UB25	108.5	108.1	114	18	28	1	2	29.71	27.28	31.41	61.38	17.87	1.00	28	104.4	0.91	46	
SB9	203X133UB30	114.3	114.5	140	48	100	1	2	29.71	28.64	32.98	65.89	14.6	1.00	100	104.4	0.91	100	
HB40	203x133UB30	146.6	138.9	134	32	100	1	2	29.71	28.64	32.98	65.33	14.6	1.06	100	127.2	0.92	100	
HB41	254x100UB15	127.4	125.5	128	14	20	1	2	38.79	36.27	41.77	71.31	17.85	1.02	19	114.5	0.91	36	
SB3	203x133UB30	114.3	114.5	144	46	100	1	2	29.7	28.64	32.98	65.89	14.6	1.00	100	104.4	0.91	100	
SB4	305x102UB25	152.1	188.3	170	6		1	3	47.55	29.52	33.99	56.62	22.38	0.81	13	137.9	0.73	26	
SB5	356x127UB33	210.5	254.8	219	6		1	3	52.73	26.84	30.91	60.5	23.8	0.83	9	190.9	0.75	17	
SB6	406x140UB39	261.9	317.2	294	6		1	3	57.08	30.36	34.96	61.15	24.5	0.83	10.5	237.6	0.75	20	
SB10	305x102UB25	151.3	179.6	176	7		1	3	47.55	32.48	37.4	61.16	21.43	0.84	20	138.2	0.77	34	
SB11	356x127UB33	204	230.7	212	7		1	3	52.73	35.96	41.4	68.58	20.83	0.88	9	186	0.81	25	
SB12	406x140UB39	260.6	284.7	271	NA	NA	1	3	57.08	38.56	44.4	69.42	22	0.92	-	237.1	0.83	-	
SB14	305x102UB33	206.6	202.4	194	10		1	3	41.79	34.25	39.44	64.43	15.37	1.02	-	188	0.93	23	
SB15s	406x140UB39	236.8	290.9	317	16	27	1	3	57.08	33.97	39.12	68.02	22.61	0.81	45	215	0.74	67	
HB42s	305x102UB25	163.1	177	194	31	67	1	3	47.55	32.78	37.75	64.73	20.99	0.92	85	147.5	0.83	90	

Table 6-4 : Results from Hamada and Longworth

Test No	Section sizes	M_{theu} (Comp)	M_p (Published)	M_u (Test)	Curvature rad/mm	Area of reinforcement mm sq.	Class F	Class W	d/t web	Limit of web Classification			Comment
										C1	C2	C3	
4A	W12 x 16.5	142.0	185.0	217.0	NA	774	1	3	49.61	38.23	44.02	44.02	lateral
2		155.0	224.0	238.7	NA	1599.6	1	3	49.61	27.86	32.08	32.08	lateral
5		155.0	224.0	239.1	NA	1599.6	1	3	49.61	27.86	32.08	32.08	lateral
6		155.0	224.0	244.1	NA	1599.6	1	3	49.61	27.86	32.08	32.08	lateral
1		164.3	255.4	255.4	NA	1999.5	1	3	49.61	27.65	31.84	31.84	lateral
18	W12 x 36	235.9	230.5	327.7	0.000343	—	1	1	35.89	61.95	71.42	106.7	local
11		297.2	280.2	375.2	0.000312	761.1	1	1	35.89	41.02	41.02	47.24	local
12		328.5	305.1	388.7	0.0002574	1264.2	1	2	35.89	33.53	33.53	38.61	local
13		346.2	313.0	393.2	0.0001911	1599.6	1	3	35.89	29.89	29.89	34.42	local
16		346.2	313.0	391.0	0.0001092	1599.6	1	3	35.89	29.89	29.89	34.42	local
17		346.2	313.0	388.7	0.0001911	1599.6	1	3	35.89	29.89	29.89	34.42	local
14		374.5	332.2	399.2	0.0000975	2399.4	1	3	35.89	28.4	28.4	32.7	local
15		374.5	332.2	403.4	0.0000858	2399.4	1	3	35.89	28.4	28.4	32.7	local
21	W12 x 31	205.5	207.6	2881.2	0.00017706	—	1	1	41.33	61.49	70.88	105.9	local
22		429.1	253.9	323.2	0.00014508	516	1	1	41.33	45.27	52.13	84.36	local
23		281.8	321.5	337.9	0.0001014	1199.7	1	3	41.33	33.55	38.63	72.27	local
24		291.5	285.0	340.1	0.0000881	1599.6	1	3	41.33	29.13	33.55	68.25	local
25		316.6	294.9	327.7	0.0000761	2399.4	1	3	41.33	28.18	32.45	63.12	local
31	W12 x 27	207.4	208.8	256.5	0.0001638	—	2	1	47.03	57.55	66.34	99.12	local
32		246.3	240.9	271.2	0.0001474	516	2	2	47.03	42.4	48.63	77.23	local
33		262.3	266.1	291.5	0.0001119	1032	2	3	47.03	33.57	38.65	67.87	local
34		292.9	296.9	305.1	0.0000893	1999.5	2	3	47.03	26.38	30.37	59.63	local

Notes: i) Compression flange of beam 4A, 2, 5, 6 and 1 was reinforced
with 76.2mm x 9.525 mm cover plate.

Table 6-5 : Results from Najafi and Anderson

1	2	3	4	5	6	7	8	9	10	11	12	13	14	15
Test No	Section sizes	Mp,Rd (Comp) kNm	Mp (Published) kNm	Mu (Test) kNm	φu mrad	φp mrad	Area of reinforcement mm sq.	Class F	Class W	WEB d/t	Limit of web classification C1	C2	C3	Comment
S8F	305x165UB40	241.5	248.5	262	28	35.8	905	1	3	41.83	31.43	36.19	78.34	fracture of rebar
S8E	305x165UB40	242.9	248.9	291	20	40	905	1	3	41.96	31.38	36.13	77.37	local flange buckling
S4F	305x165UB40	218.7	221	179	17.7	26.6	452	1	1	41.63	42.3	48.7	88.55	fracture of rebar
S12F	305x165UB40	263.8	271.3	302	22.7	55.7	1357	1	3	41.5	29.11	33.52	71.12	local flange buckling
S8FD	457x152UB52	439.1	443	416	14	14	905	1	3	51.41	40.85	47.04	79.91	fracture of rebar
T5	305x165UB40	247.1	NA	293	22.5	22.5	905	1	3	41.37	31.6	36.4	75.9	fracture of rebar
T6	305x165UB40	174.4	NA	138	2.8	11	nominal	1	1	41.6	62.9	72.5	106.3	fracture of mesh
T8	305x165UB40	219.9	NA	207	4.8	14.2	452	1	2	42.8	41.7	48.1	87.3	fracture of rebar
T11	305x165UB40	173.2	NA	105	22	22	-	1	1	41.8	63.5	73.2	109.4	plate deformed + bolt stripping

Notes: i) T5, T6, T8 and T11 are minor axis test.

Table 6-6: Results from other researchers

1	2	3	4	5	6	7	8	9	10	11	12	13	14	15
Researchers	Test No	M̄ (Comp) kN·m	M̄p (Published) kN·m	M̄tu (Test) kN·m	w mm²	Reinforcement w mm	Area of Reinforcement mm²	Class F	Class d̄r W	web	C1	C2 / C3		Comment
Arbst and Raoul	B1	310.5	299.1	315			1256.6	1	3	41.69	31.68	36.48	74	
Kemp	LR	171.2	174	154			360	1	3	47.55	34.14	46.22	72.4	local web buckling
Tninchero	LSR	182.1	124	167	31.7	53.7	628	1	3	46.2	34.15	39.32	64	local flange buckling
and	SR	163.4	161	165	7.9	11	393	1	2					flange + web buckling
Dekker	SSR	172.5	124	165	39.4	60.9	628	1	3	49.34	33.35	38.4	63.6	flange+web buckling
Gil	CB10	128.2	127	149.9			678.8	1	1					local flange buckling
and	CB11	133	128	154.9	34	60	678.6	1	1					crushing+buckling
Johnson	CB12	139.8	131	179.5	64	70	905	1	1					local flange buckling
Lim	VT1	227.33	228	240	27	63	1581	1	3	30.71	25.29	29.13	54.24	
	VT2	189.98	191	211	55	83	608	1	2					
	VT3	165.43	186.5	190		38	242	1	1					
	VT4		647.8	692	44	44	1162	4	1					elastic
	VT5		667	607	44	51	913	4	1					.
	VT6		570.6	592		8	376	4	1					.
	VT7		647.8	483	50		1162	4	1					.
	DV11	242.3	241.8	253	18	82	1555	1	3	29.29	24.42	28.12	52.63	elastic
	DV21		680.3	658		74	1100	3	2					elastic
	DV22		680.3	682		60	1100	3	2					elastic
	DV31	521.3	552.5	533	20	46	1100	1	3	40.35	25.39	29.24	60.38	
	DV3.1	148.6	149.2	127		30	614.1	1	2					
	DV4.1	140.8	144.5	146			504	1	2					
	DV5.1	132.7	136.9	133		27	276	1	1					
	A1	501.5	456.3	469	21	44	1590	1	3	44.57	26.02	29.96	63.64	
	A2	501.5	456.3	472	37	68	1590	1	3	44.57	26.02	29.96	63.64	
	A3	501.5	459.1	450	28	39	1590	1	3	44.57	26.02	29.96	63.64	

Table 6-7 : Results of beams with Class 1 flange and Class 3 web

	Beam	α	ε web	d/t	αd/tε	ψ	ε flange	c/t	c/tε	Mu	MplRd	Mu/MplRd	φu	φp
Climenhaga	SB4	0.856	0.755	47.55	53.911	-0.333	0.811	7.47	9.211	170	152.1	1.12	6	13
	SB5	0.989	0.803	52.73	64.944	-0.340	0.852	7.38	8.666	219	210.5	1.04	6	9
	SB6	0.866	0.786	57.08	62.843	-0.394	0.879	8.24	9.372	317.2	261.9	1.21	6	7
	SB10	0.785	0.755	47.55	49.445	-0.459	0.811	7.47	9.207	176	151.3	1.16	7	8
	SB11	0.758	0.804	52.73	49.711	-0.540	0.852	7.38	8.666	212	204	1.04	7	9
	SB14	0.773	0.782	41.79	41.272	-0.485	0.858	4.74	5.523	194	206.6	0.93	10	17
Uth	VT1	1.0	0.767	30.71	40.065	-0.232	0.803	6.12	7.621	240	227.3	1.06	27	63
	DV11	1.0	0.740	29.29	39.576	-0.24	0.778	6.32	8.123	253	242.3	1.04	NA	>82
	DV31	0.929	0.710	40.35	52.777	-0.587	0.774	10.95	14.147	533	521.3	1.02	20	>46
	A1	1.0	0.789	44.57	56.525	-0.453	0.823	6.54	7.948	469	501.5	0.94	21	44
	A2	1.0	0.789	44.57	56.525	-0.453	0.823	6.54	7.948	472	501.5	0.941	37	68
	A3	1.0	0.789	44.57	56.525	-0.453	0.823	6.54	7.948	450	501.5	0.9	26	39
Anderson & Najafi	S8F	0.945	0.896	41.83	44.1442	-0.575	0.931	8.11	8.709	262	241.5	1.08	28	35
	S8E	0.94	0.89	41.96	44.361	-0.574	0.928	8.14	8.774	291	241.9	1.2	20	40
	S12F	1.0	0.882	41.5	47.047	-0.452	0.930	8.26	8.886	302	263.8	1.14	22.7	55.7
	S8FD	0.706	0.844	51.41	43.017	-0.686	0.871	7.45	8.556	416	439.1	0.95	14	14
	T5	0.916	0.871	41.37	43.522	-0.571	0.930	8.11	8.725	293	247.1	1.86	22.5	22.5

Table 6-7(continued) : Results of beams with Class 1 flange and Class 3 web

	Beam	α	ε web	d/t	αd/h𝒸	ψ	ε flange	c/t	c/t𝒸	Mu	MplRd	Mu/MplRd	φu	φp
	B4A	0.744	0.838	49.61	44.05	-0.521	0.879	7.54	8.581	217	142	1.53	NA	NA
	B2	0.993	0.838	49.61	58.793	-0.31	0.879	7.54	8.581	238.6	155	1.54		
	B5	0.993	0.838	49.61	58.793	-0.31	0.879	7.54	8.581	239.1	155	1.54		
	B6	0.993	0.838	49.61	58.793	-0.31	0.879	7.54	8.581	244.1	155	1.57		
Hamada	B1	1.0	0.838	49.61	59.208	-0.237	0.879	7.54	8.581	255.4	164.3	1.55		
&	B13	0.954	0.860	35.89	39.786	-0.484	0.925	6.33	6.843	393.2	346.2	1.14		
Longworth	B16	0.954	0.860	35.89	39.786	-0.484	0.925	6.33	6.843	391	346.2	1.13		
	B17	0.954	0.860	35.89	39.786	-0.484	0.925	6.33	6.843	388.7	346.2	1.12		
	B14	1.0	0.860	35.89	41.713	0.356	0.925	6.33	6.843	399.2	374.5	1.07		
	B15	1.0	0.860	35.89	41.713	-0.356	0.925	6.33	6.843	403.4	374.5	1.08		
	B23	0.853	0.854	41.33	41.291	-0.526	0.91	7.41	8.143	337.9	281.7	1.2		
	B24	0.970	0.854	41.33	46.934	-0.438	0.91	7.41	8.143	350.4	291.5	1.2		
	B25	1.0	0.854	41.33	48.4	-0.308	0.91	7.41	8.143	327.7	316.6	1.04		
	B33	0.802	0.799	47.03	47.218	-0.531	0.839	8.51	10.145	291.5	262.3	1.11		
	B34	1.0	0.799	47.03	58.861	-0.324	0.839	8.51	10.145	305.1	262.3	1.04		
													NA	NA
Kemp	LR	0.643	0.746	47.55	40.987	-0.719	0.78	6.87	8.808	154	171.2	0.9		
	LSR	0.732	0.734	46.2	46.055	-0.572	0.811	7.49	9.236	167	182.1	0.92	31.7	53.7
	SSR	0.748	0.734	49.34	50.247	-0.563	0.811	7.01	8.644	165	172.5	0.96	39.4	60.9
Aribet	B1	0.928	0.885	41.69	43.716	-0.518	0.885	8	9.04	315	310.5	1.01	NA	NA
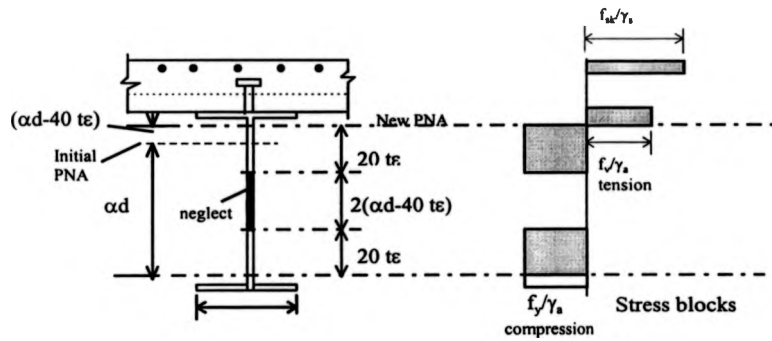
Fig. 6-1 :   Use of effective web in Class 2 for a section in hogging
bending with a web in Class 3
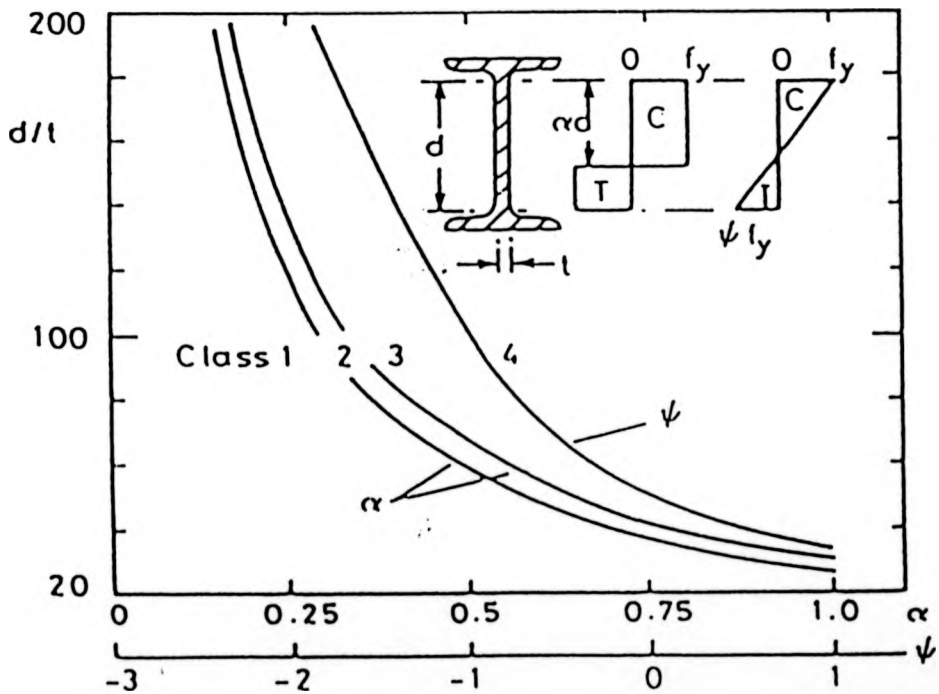
Fig. 6-2 :   Classification of webs, for fy = 355 N/mm²
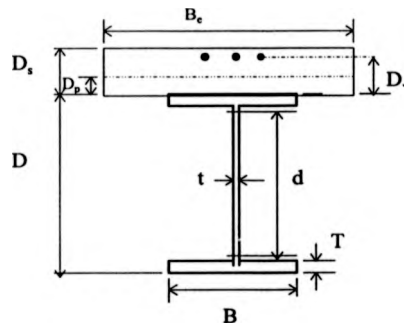
Fig. 6-3 : Dimension for plastic moment resistance resistance

Fig. 6-4 : Typical moment-rotation curve

(i) Section continuous over support

(ii) Continuous beam tests

(iii) Cruciform type : Major axis

(iv) Cruciform type : Minor axis
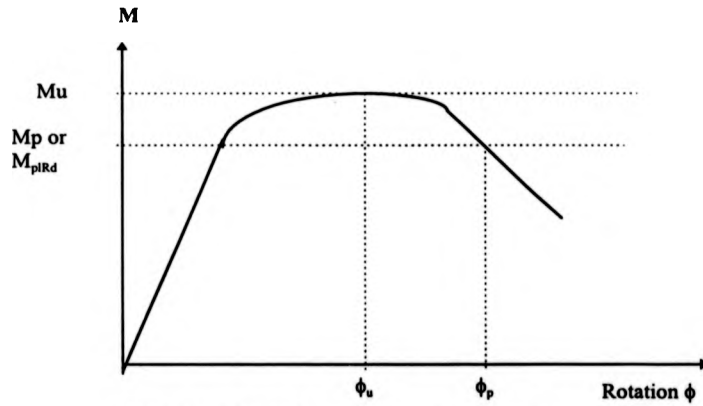
Fig. 6-5 :   Various tests configuration

Classification to EC4 of section tested
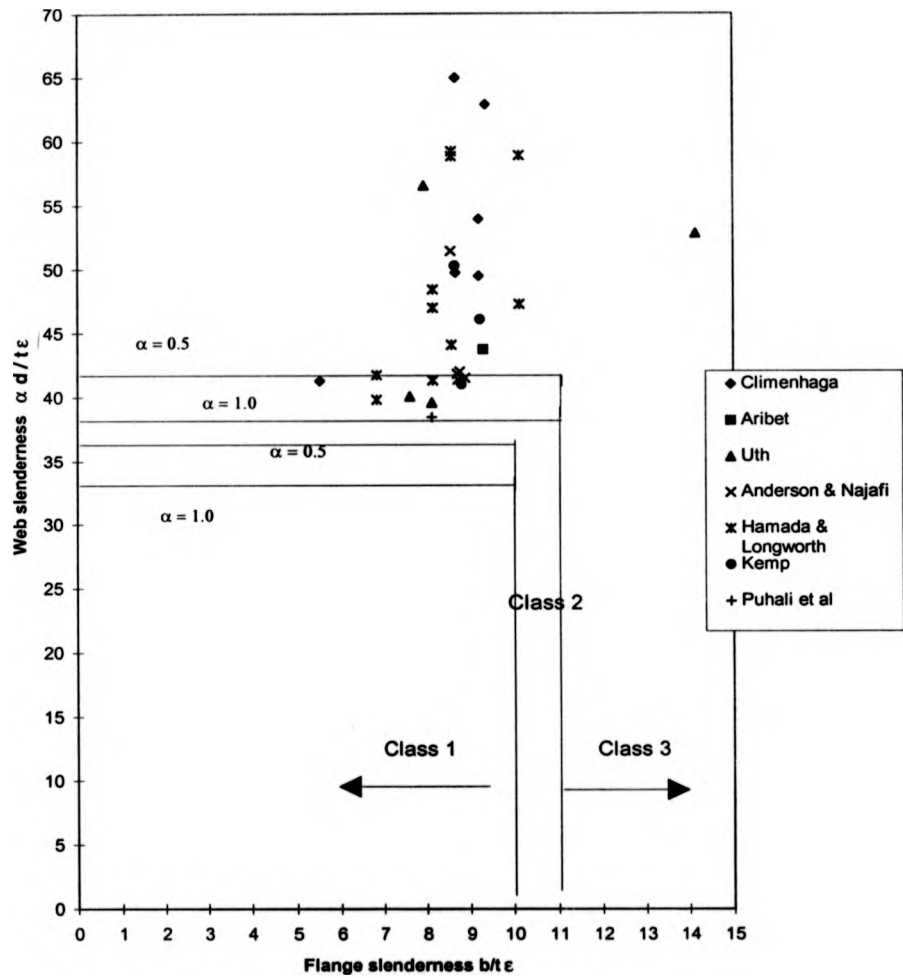
Fig 6-6 : Classification of sections
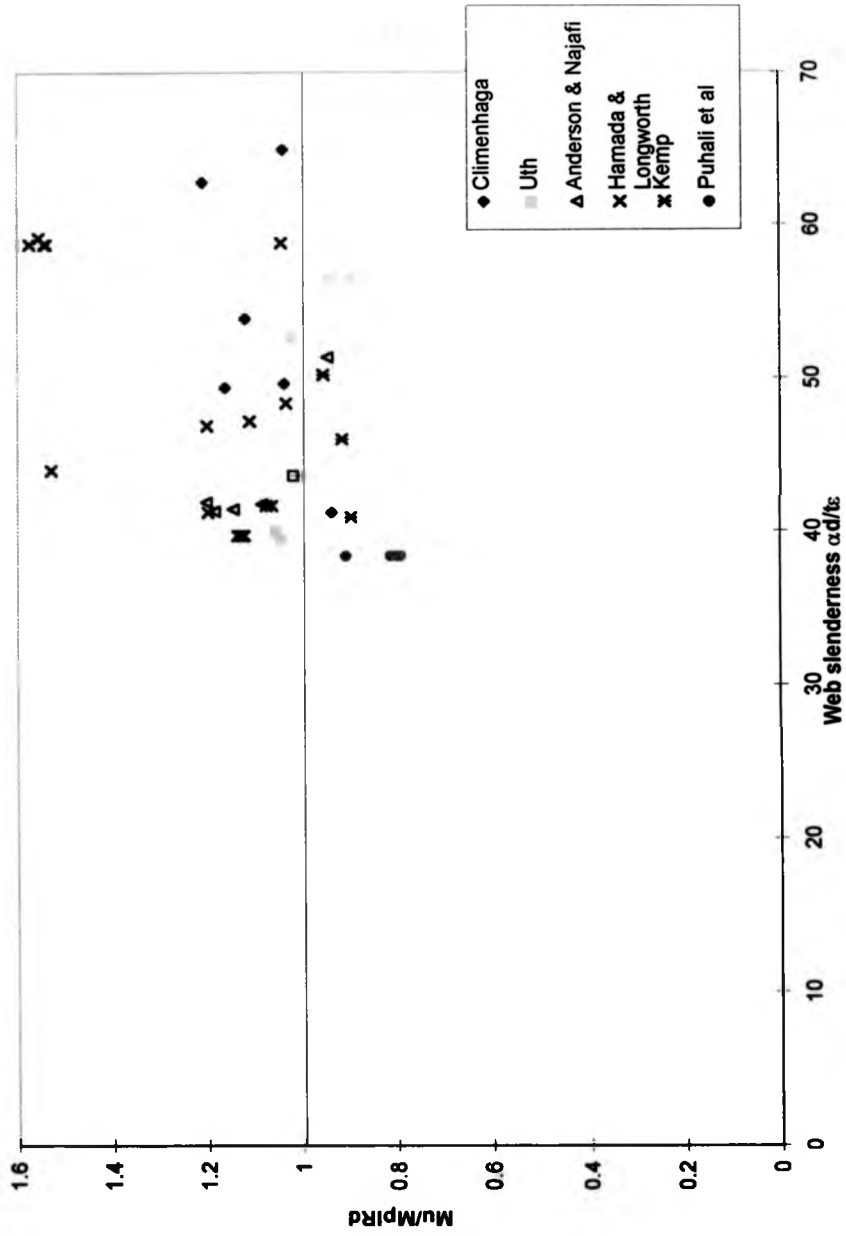
Fig. 6-7: Web slenderness vs M$_u$/M$_{plRd}$

Chapter 7

FURTHER DEVELOPMENT TO DIRECT DESIGN TO HORIZONTAL SWAY LIMITATION

7.1 Introduction

For unbraced frames, the control of sway deflection can be a more important criterion than strength; design to ultimate resistance will often result in excessive sway under service loading. This form of deflection arises mainly from the wind, and its contro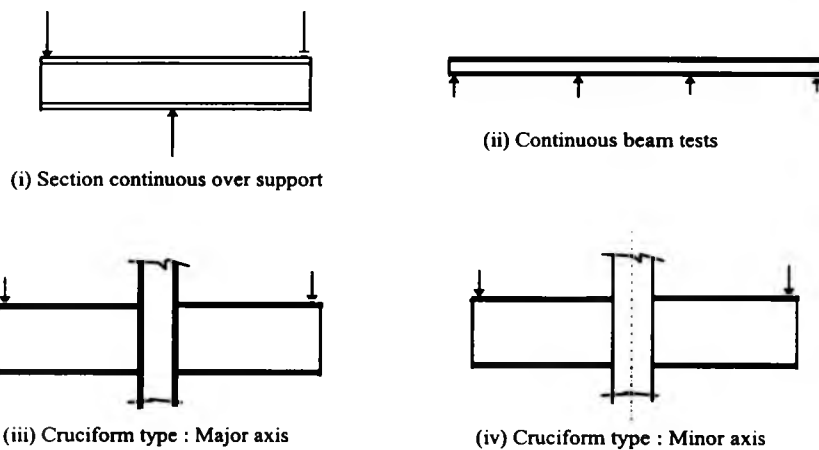l may govern the member sections. There were many limits for the sway (Δ):height (h) ratio, ϕ, to be used in design. A survey by the Council on Tall Buildings[7-1] showed that the limiting value varied from 1/1000 to 1/200. However a limit of 1/300 has been commonly used and recommended by present British and European guides.

A method applicable to the design of unbraced multi-storey steel frames to specified limits on horizontal sway deflection is presented here. This method of design is the extension and combination of the work by Wood and Roberts [7-2] and Anderson and Islam[7-3]. Both of these approaches have been introduced in Chapter 1. Only simple calculations are required by the method and its application is illustrated by worked examples. Regular and non-regular frames are considered. Semi-rigid joints may be included into the frame to be designed.

7.2   Derivation of design equations

As mentioned in Chapter 1, by way of analysing the frame using the stiffness distribution method suggested by Wood[7-4], Wood and Roberts[7-2] distribution coefficients, k_t and k_b (see Fig. 7-1) can be defined as

$$k_t = \frac{K_c + K_u}{K_c + K_u + K_{bt}} \tag{7.1}$$

$$k_b = \frac{K_c + K_u}{K_c + K_l + K_{bb}} \tag{7.2}$$

where,

K_{bt} is the top beam stiffness of substitute frame

K_{bb} is the bottom beam stiffness of substitute frame

K_c is the column stiffness of substitute frame

K_u is the upper adjacent column stiffness of substitute frame

K_l is the lower adjacent column stiffness of substitute frame

They[7-2] also obtained a non-dimensionless expression for sway index, $\overline{\Phi}$ where,

$$\overline{\Phi} = \left[1 + \frac{3(k_b + k_t - k_b k_t)}{4 - 3k_b - 3k_t + 2k_b k_t + s(1 - k_b k_t/4)/3} \right] \tag{7.3}$$

The actual sway index is then obtained from :

$$\overline{\Phi} = \frac{\Delta / H}{FH / (12EK_c)} \tag{7.4}$$

where,

Δ is the storey sway

H is the storey height

F is the wind shear

K_c is the Grinter substitute frame column stiffness

E is the elastic modulus of member

$\overline{s}$ is taken as zero if effect of cladding is ignored

To develop this into an expression for direct design the same devices used by Anderson and Islam[7-3] (i.e. assuming point of contraflexure at mid-height of column and also minimising the Σ second moment of area x length) are now applied to the substitute frame concept which Wood and Roberts[7-2] used as the basis for their analysis.

Imposing a central point of contraflexure on the column of a single 'cell' in Fig 7-2(a) implies that the distribution coefficients, k_t and k_b at the top and the bottom of the column are equal. This arises because, from Fig. 7-3 it can be seen that

$$M_t = M_b \qquad \text{and} \qquad \theta_t = \theta_b$$

Therefore

$$k_b = k_t = k \tag{7.5}$$

Substititing Eqn. (7.5) into Eqn. (7.3), the sway index now becomes:

$$\overline{\Phi} = 1 + \frac{3(2k - k^2)}{4 - 6k + 2k^2}$$

$$= \frac{4 - 6k + 2k^2 + 6k - 3k^2}{4 - 6k + 2k^2}$$

$$= \frac{4 - k^2}{(4 - 2k)(1 - k)} = \frac{(2 - k)(2 + k)}{2(2 - k)(1 - k)}$$

$$\therefore \qquad \overline{\Phi} = \frac{2 + k}{2 - k} \tag{7.6}$$

and from Eqn. 7.4 and Eqn. 7.6,

$$\frac{\Delta / H}{FH / (12EK_c)} = \frac{2 + k}{2 - k} \tag{7.7}$$

As:

$$(\Delta/H) = \left[(FH)/(12EK_c)\right] \cdot \overline{\Phi} \qquad (7.8)$$

Eqn. (7.8) refers to point which lies on the diagonal of Fig. 7-1.

By taking the limit of sway:height ratio recommended by the UK guides,

Δ/H = 1/300 gives:

$$K_c \quad = \quad (25\, FH/E)\,\overline{\Phi} \qquad (7.9)$$

or more generally :

$$K_c \quad = \quad f\,\overline{\Phi} \qquad (7.10)$$

where the constant, f in Eqn. (7.10) may be adjusted to suite other deflection requirements.

7.3   Design equation for intermediate storey of a frame

Fig. 7-4 shows a typical intermediate storey in a building frame indicating the column and beam stiffnesses. For an intermediate storey, the distribution coefficients k_t and k_b are given by Eqn. (7.1) and Eqn. (7.2). The requirement that these be equal can be satisfied by making the column stiffnesses K_{cu}, K_c and K_{cl} (Fig. 7-4) the same while insisting that the upper and lower beam stiffnesses K_{bt} and K_{bb} are also equal.

Allowing for continuity between the storeys, the distribution coefficient from Eqn.(7.1) and Eqn. (7.2) can be rewritten as:

$$k = \frac{2K_c}{2K_c + K_b} \qquad (7.11)$$

where K_b denotes the beam stiffness.

Substituting Eqn. (7.11) into Eqn. (7.6) gives :

$$\overline{\Phi} = \frac{(3K_c + K_b)}{K_b} \tag{7.12}$$

When this expression for sway index is substituted into Eqn.(7.10) the following relationship is obtained :

$$K_c = \frac{f \cdot K_b}{(K_b - 3f)} \tag{7.13}$$

For multi-bay frames Anderson and Islam[7-3] made the 'weight', W, per storey of each equal bay width as approximately :

$$W = \Sigma(H I_c) + \Sigma(B I_b) = \Sigma(H^2 K_c) + \Sigma(B^2 K_b) \tag{7.14}$$

where B is the bay width.

Now if K_c and K_b refer instead to the equivalent Grinter-frame concept which Wood and Roberts[7-2] used to formulate the graphical method, we have:

$$K_c = \Sigma(I_c / H)$$
$$K_b = \Sigma(3I_b / B)$$

The 'weight' is now :

$$\therefore \quad W = H^2 \cdot K_c + \frac{B^2}{3} \cdot K_b \tag{7.15}$$

For unequal bay widths, B may approximately be taken as the average span.

Substituting K_c of Eqn.(7.13) into Eqn.(7.15) and differentiating the expression with respect to K_b and setting zero for a minimum leads to

$$\frac{dW}{dK_b} = \frac{B^2}{3} + H^2 f \left(\frac{1}{K_b - 3f} + \frac{-K_b}{(K_b - 3f)^2} \right) = 0$$

$$\frac{B^2}{3} + H^2 f \left(\frac{K_b - 3f - K_b}{(K_b - 3f)^2} \right) = 0$$

$$\therefore \qquad H^2 f \left(\frac{K_b - 3f - K_b}{(K_b - 3f)^2} \right) = \frac{B^2}{3}$$

$$\therefore \qquad 9 H^2 f^2 = B^2 (K_b - 3f)^2$$

$$\therefore \qquad K_b - 3f = \frac{3Hf}{B}$$

$$\therefore \qquad K_b = 3f \left(1 + \frac{H}{B} \right) \qquad\qquad (7.16)$$

Substituting K_b into Eqn.(7.14), K_c follows from:

$$K_c = \frac{f K_b}{K_b - 3f} = \frac{3f^2 \left(1 + \dfrac{H}{B} \right)}{3f \left(1 + \dfrac{H}{B} \right) - 3f}$$

$$\therefore \qquad K_c = \frac{f \left(1 + \dfrac{H}{B} \right)}{\dfrac{H}{B.}} = f \left(1 + \frac{B}{H} \right) \qquad\qquad (7.17)$$

7.4 Column and beam tapering

The simple expression of Eqn (7.16) and Eqn.(7.17) can be applied to each storey in turn. However the increasing wind shear down the frame results in more than one design for each member. This can be avoided by 'tapering' the design to resist the increasing wind shear.

7.4.1 Beam tapering

The assumptions used by Anderson and Islam[7-3] resulted in relationships between the stiffness of the upper and lower beam (Fig. 7-5). With second moments of area I_{bu} and I_{bl}, then from Fig. 7-5(b) the 'weight' is :

$$W = H^2 K_c + B^2 I_b$$

$$= H^2 K_c + \tfrac{1}{2} B^2 I_b + \tfrac{1}{2} B^2 I_b$$

$$= H^2 K_c + B^2 \frac{(I_{bu} + I_{bl})}{2}$$

$$\therefore \qquad I_b = \frac{(I_{bu} + I_{bl})}{2} \qquad\qquad (7.18)$$

The relationship between the I_{bu}, I_{bl} and the wind shear are:

$$I_{bl} = \frac{(F_2 h_2 + F_3 h_3)}{(F_1 h_1 + F_2 h_2)} \cdot I_{bu} \qquad\qquad (7.19)$$

7.4.2 Column Tapering

Consider a column subjected to pure sway as shown in Fig. 7-6

By slope-deflection equation:

$$M = 6EI \frac{\Delta}{h^2}$$

$$\therefore \qquad I = \frac{Mh}{6E\left(\dfrac{\Delta}{h}\right)}$$

but $$\qquad M = F \cdot \frac{h}{2}$$

$$\therefore \qquad I = \frac{F h^2}{12E\left(\dfrac{\Delta}{h}\right)}$$

$$\frac{I_c}{h} = K_c = \frac{Fh}{12E\left(\dfrac{\Delta}{h}\right)} \qquad\qquad (7\text{-}20)$$

Therefore for the limiting Δ/h to arise at consecutive storeys, the rules for column

tapering should be (see Fig. 7.7):

$$I_{cu} = I_c \cdot \frac{F_1 h_1^2}{F_2 h_2^2} \qquad\qquad (7.21)$$

$$I_{cl} = I_c \cdot \frac{F_3 h_3^2}{F_2 h_2^2} \qquad\qquad (7.22)$$

It is also necessary to consider the effect of the proposed taper, on the values of the

distribution coefficients k_t and k_b. By substituting Eqn. (7.21) and Eqn. (7.22) into

Eqn.(7.1) and Eqn.(7.2) it can be shown that $k_t = k_b$ (see the derivation in Appendix A4).

7.5   Design example

The method discussed above is demonstrated by designing a six storey frame was under

unfactored wind loading. The frame is shown in Fig. 7-8. It is designed by both the

tapered and untapered approaches to a limiting sway index of 1/300; E is taken as 205

kN/mm². Attempts were made to derive special equations to limit sway of the top storey

without much success. However as strength under vertical loading would normally

control the design of the top storey, the equations for sway are therefore not important.

Design for sway limitation is commenced at the sixth (top) storey for the untapered

method. For the tapered approach, the columns are considered as continuous over two

storeys and the design is commenced at the fifth storey. Eqns. (7.17), (7.21) and (7.22)

are used to calculate the second moment area for an internal columns. The required

second moment of area for the external column is half of the internal column. The beam

second moment of areas are then calculated from Eqns. (7.18) and (7.19). A similar procedure is followed for the third storey. The results are compared to those from the Anderson and Islam[7-3] method of design. Table 7-1 summarises the comparison. From Table 7-1 it can be seen that the results of the design of the columns are almost consistent for the upper storeys. The same cannot be said for the lower storey. This is because Anderson and Islam[7-3] used a separate analysis for the bottom two storeys and considering fixed bases for the frames.

Designing of beams using untapered direct design resulted in similar section second moment of area for both the beams and the columns. As the difference between the section second moment of areas are not large the resulting beam or column sections will be the same as those given by the design method of Anderson and Islam method[7-3].

Concluding Remarks

The method proposed in this chapter is suitable for the design of unbraced multi-storey frames if the choice of sections is controlled by sway deflection. However it has a limitation in that a unique design cannot be obtained for frames of irregular storey height. A strategy and engineering judgement are needed for such cases in applying the proposed method.

References

7-1. Council on Tall Buildings, Committee 17 Stiffness, Monograph on Planning and Design of Tall Buildings, ASCE, New York. Vol. SB, Chapter SB-5, pp.345-400.

7-2. Wood. R.H., and Roberts, E.H.: "A graphical method of predicting side-sway in the design of multi-storey buildings", Proc. ICE, Pt. 2, **59**, 1975, p.353.

7-3. Anderson, D. and Islam, M. A. : "Design of multi-storey frames to sway deflection limitations", The Structural Engineer, **57B**(1), pp.11-17.

7-4. Wood. R. H.,:"Effective lengths of columns in multi-storey buildings", The Structural Engineer, **52**(7), pp 235-244; (8), pp. 295-302; (9), 341-346.

7-5. Anderson, D. : 'Design of multi-storey steel frames to sway deflection limitation'. Stability in Frame. (ed. R.Narayanan) Elsevier Applied Science Publishers, London, 1986. pp. 55-80.

Table 7-1 : Comparison of Results

Storey	Internal Column (cm⁴)			External Column (cm⁴)			Lower Beam (cm⁴)			Upper Beam (cm⁴)		
	I_c (ref [7-5])	I_c (Direct Design)	I_c (After Tapering)	I_c (ref [7-5])	I_c (Direct Design)	I_c (After Tapering)	I_{bl} (ref [7-5])	I_{bl} (Direct Design)	I_{bl} (After Tapering)	I_{bu} (ref [7-5])	I_{bu} (Direct Tapering)	I_{bu} (After Tapering)
5	5673	5663	5663	2836	2836	2831	7252	5666	7554	3626	5666	3778
3	13234	13215	13216	6617	6608	6608	14447 15993	13218	15105	10835 11995	13218	11332
2	16314	16991	16990	8157	8496	8495	16243	16995	18883	14862	16995	15107
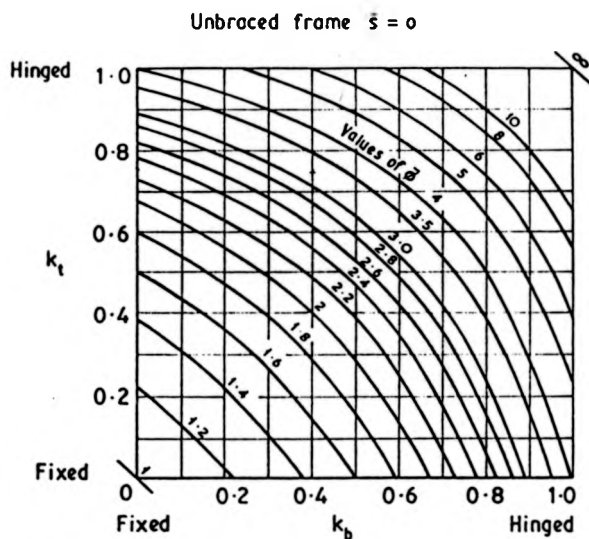
Fig. 7-1 : *Sidesway deflection for unbraced frame values of $\overline{\Phi}$*

(a) "Cell" with beam split up   (b) Forward intergration
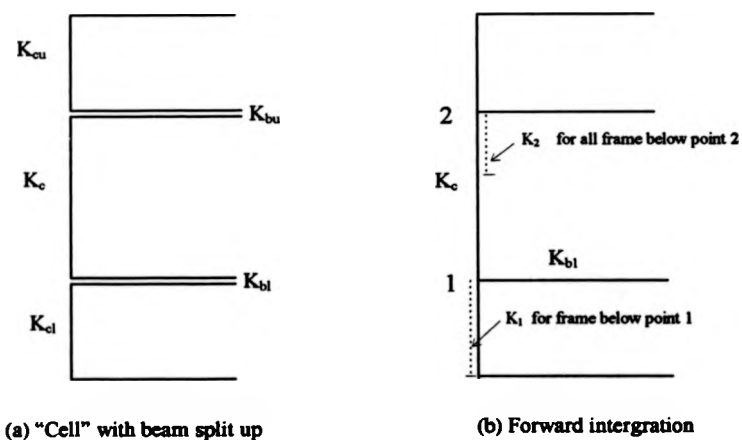
Fig. 7-2 : *Illustrating stiffness concept*
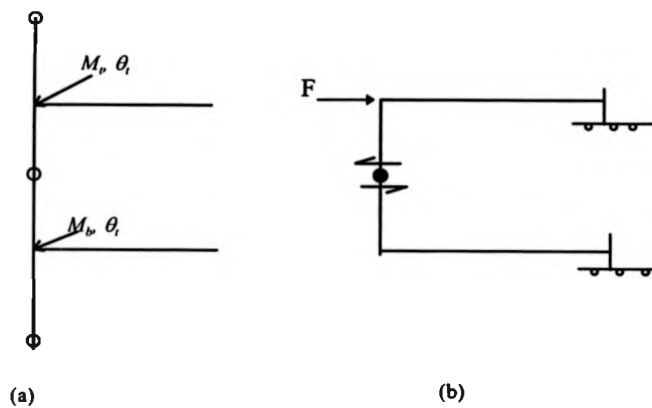
Fig. 7-3 : Distribution under sway

Fig. 7-4 : Typical intermediate storey of a frame

(a) Wind shear (b) Optimization
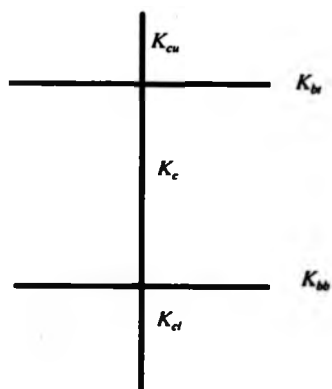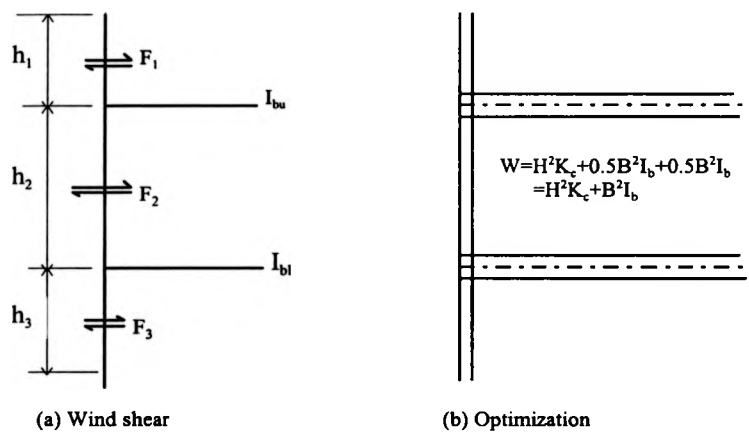
Fig. 7.5 : Relationship between upper and lower beam

Fig. 7-6 : Column subject to pure sway

$$I_c \cdot \frac{F_1}{F_2} \cdot \frac{h_1^2}{h_2^2}$$

For beam, moment = $F_1 h_1 / 2 + F_2 h_2 / 2$

I_c

For beam, moment = $F_2 h_2/2 + F_3 h_3/2$

$$I_c \cdot \frac{F_3 h_3^2}{F_2 h_2^2}$$

Fig. 7-7: Column tapering
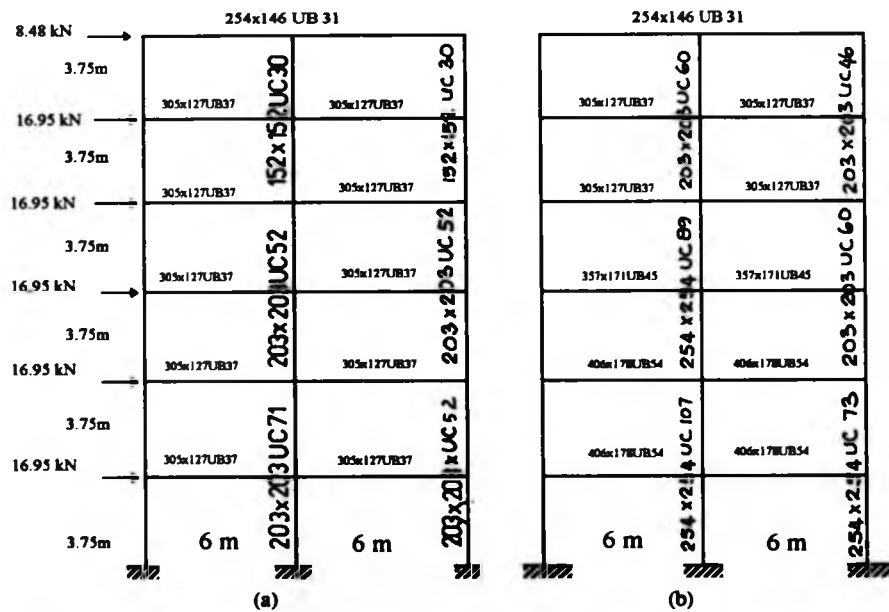
Fig. 7-8 : Designs for six-storey two-bay frame [ref. 7-5]: (a) initial design;
(b) design

Chapter 8

CONCLUSIONS AND SUGGESTIONS FOR FURTHER WORKS

8.1   Conclusions

The research work presented in this thesis was carried out by the author from October 1993 to January 1998. The conclusions are drawn from results and observations presented in this thesis which are acquired from the investigation carried out in this research programme. Detailed conclusions have been given at the end of each selected chapter. However, as a summary, final discussions and conclusions are given below.
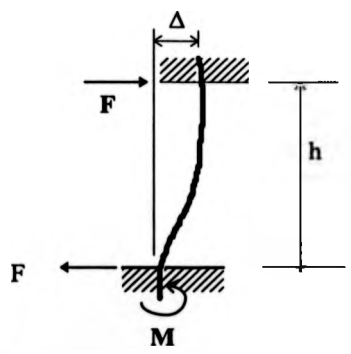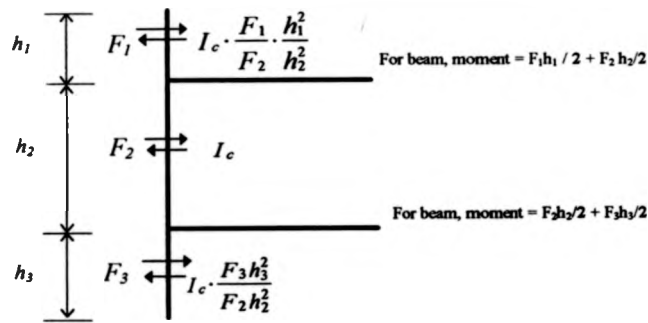
In general, this study is concerned with aspects of continuity in steel and composite frame, particularly at joint regions. The work described Chapter 1 has contributed to a better understanding of theoretical and practical aspects of steel and composite frames design for buildings. The review of previous research shows that further work is justified in order to realise in practice the benefits of continuity and composite action in frames.

An experimental work on beam-to-beam end plate composite connections (see Chapter 2) was carried out to realise the benefit of continuity consistently throughout the building frame. The results indicate a similar overall response of M-ϕ curves to beam-

to-column tests. The failure modes such as local buckling mesh and rebar fracture, are also generally similar to those of beam-to-column connection tests.

The assessment and analysis of the above tests was carried out in Chapter 3. It confirmed the effects of reinforcements to composite connections. A moderate amount of reinforcement provided an increase in the strength and the rotation capacity of the connections. However a higher amount could reduce the degree of shear connection from full to partial. The results justified the restriction imposed by current design codes having partial shear connection in hogging moment region. Methods specified by the SCI[8-1] and EC3[8-2] may be used to predict the moment resistance of end plate composite beam-to-beam connection conservatively. The rotation capacity of composite joint can be estimated satisfactorily by a method proposed by Kronenberger[8-3].

In Chapter 3 a prediction method to estimate the initial stiffness is presented. Comparable results were obtained when compared to the test findings of the author and other researchers[8-4, 5].

Tests were conducted to investigate the effect of concrete encasement to the joints of continuous slimflor beams (see Chapter 4). The tests showed that the encasement increases the initial stiffness of end plate connections. However, the initial stiffness decreased to that of bare steel connections after fracture of the mesh. As all the mesh fractured at a moment level greater than two-thirds of the value of the design moment , the mesh could be assumed effective in deflection calculations.

The author's tests have provided evidence of the suitability of composite beam-to-beam joints, sufficient to justify their inclusion in forthcoming British and European design recommendations[8-6, 8-7].

Various types of "shear enhancer" incorporated in order to improve the bond capacity of encased beams(see Chapter 5) were tested. The tests showed that the load at initial slip does not greatly depend on the type of enhancer and the mobilisation of the enhancers is still possible after the slip due to bond failure. Rebars through the web are found to be the most effective enhancer. There is a correlation between the bond capacity and the compressive strength of concrete.

The study on published data on local buckling (Chapter 6) showed that the "hole-in-web" approach provides a satisfactory method to determine the moment resistance of beams with Class 1/Class 2 flanges and a Class 3 web. No evidence emerged from the study to substantiate the possibility of upgrading such beams to Class 1. This conclusion will influence the drafting of the EN-version of Eurocode 4.

A method applicable to the design of unbraced multi-storey frames to specified limits on horizontal sway deflection is proposed in Chapter 7. The method is found to be suitable for the design of multi-storey frames with uniform storey height. Such work is important in view of the increasing popularity of unbraced construction which arises from the freedom provided to the architect.

8.2   Suggestions for further work

The following represents several suggestions whereby the work undertaken by the author could be extended to further improve the research described in this thesis.

For the beam-to-beam composite connection tests, a better method of fixing the strain gauges to the rebars without reducing the diameter needs to be considered so that the level at which the rebars fracture can be determine more accurately.

The predicted rotation capacity model by Kronenberger[8-3] does not include any account of plastic deformations of the beams. Refinements to this model by including these deformations may further improve the model.

The "boltless" connection such as BTB3 could be utilised to provide a viable economic solution in connections. Additional studies and experimental tests are necessary to investigate its validity.

To improve the moment capacity of connections of slimflor beams, further studies are needed on connections considered as composite connections. Other geometrical configurations of slimflor beam could be used. The latest information from the SCI has revealed a very recent configuration in the form of an asymmetrical beam ASB[8-8]. The push-out test results showed that rebars through the web are the most effective means of maintaining resistance after initial slip for an encased steel section. More experimental tests are needed with other shape of rebars to established its performance. The expressions for the direct design to horizontal sway limitations may further be improved to include all types of steel frame such as non-uniform storey height.

References

8-1   Lawson, R. M., and Gibbons C., "Moment connections in composite construction: Interim guidance for end plate connections". SCI Publication 143, The Steel Construction Institute, 1995.

8-2   Eurocode 3: Part 1.1, "Revised annex J : Joints in building frames". ENV 1993-1-1.

8-3   Composite steel-concrete joints in braced frames for buildings. (ed. D. Anderson), European Commission European Cooperations in the Field of Scientific and Technical Research, COST-C1, Brussels, 1997.

8-4   Brown N. D., "Aspects of sway frame design and ductility of composite end plate connections", PhD Thesis, University of Warwick, UK, 1995.

8-5   Najafi, A. A., "End plate connections and their influence on steel and composite structures", PhD Thesis, University of Warwick, UK, 1992.

8-6   Joints in Steel Construction : Composite Connection, to be publish by The Steel Construction Institute, Ascot, 1998.

8-7   Design of Composite Connections, European Connection for Constructional Steelwork, Brussels, expected publication late 1998 / early 1997.

8-8   Lawson, M., Mullet, D., and Rackham, J., "Slimdek: Development and Testing", *New Steel Construction*. June/July 1997. pp.19-22.

APPENDIX A1

Worked example of initial stiffness prediction

The worked example below is based on test BTB2 of beam-to-beam test conducted by the author.

Reinforcement provided
$$A_{s1} = 4 \times \pi \times (16/4)^2 = 804 \text{ mm}^2$$
$$A_{s2}(\text{mesh}) = 162 \text{ mm}^2$$
$$\Sigma A_s = 966 \text{ mm}^2$$

Take $h_s = 120 - 28 - 8 + 352 - 4.5 = 431.5$ mm

Distance from centre-line of primary beam to first stud $= 199$

$\therefore k = (966 / 199) = 4.85$

$f_{ctm} = 4.26$ N/mm^2 $f_{cu} = 50$ N/mm^2

$E_s = 195$ kN/mm2 $E_c = 35$ kN/mm^2

$E_a = 191$ kN/mm2 $I_a = 12091$ cm^4

reinforcement ratio $\rho = \dfrac{966}{(1100)(120 - 46)} = 1.19\%$

$\therefore \rho_{s,eff} = 2.38\%$

$\therefore \sigma_{sr1} = \dfrac{4.26 \times 100}{2.38}\left(1 + \dfrac{195000}{35 \times 10^3} \cdot \dfrac{2.38}{100}\right)$

$= 202.7$ N/mm^2

$\therefore \Delta\varepsilon = \dfrac{202.7}{195000} - \dfrac{4.26}{35 \times 10^3} = 0.00092$

$\therefore \varepsilon_{sm} = \dfrac{505}{195000} - 0.4(0.00092) = 0.0022217$

$\therefore$ Effective $E = \dfrac{505}{0.0022217} = 227.3$ kN/mm^2

Allowance for slip:

$$\alpha = \dfrac{(191000)(120910000)}{260^2(227300)(966)}$$

$$= \quad 1.56$$

$$\beta \quad = \quad \sqrt{\left(\frac{2.56x6x100x10^3x1410x260^2}{191000x120910000}\right)}$$

$$= \quad 2.52$$

$$K_{sc} \quad = \quad \frac{6x100x10^3}{2.52 - \dfrac{1.52}{2.56} \cdot \dfrac{431.5}{260}}$$

$$= \quad 390981$$

$$\therefore \quad \frac{1}{1 + \dfrac{227300}{390981}x4.85} \quad = \quad 0.262$$

$$\therefore \quad k_{reduced} \quad = \quad 0.262 \times 4.85 \quad = \quad 1.271$$

For the steelwork : from test result

$$S_j \quad = \quad 10.9 \text{ kNm/mrad}$$

$$k_i \quad = \quad \frac{10900x10^6}{191000(352 - 90 - 4.5)^2} \quad = \quad 0.86$$

$$z \quad = \quad \frac{0.86x257.5^2 + 1.271x431.5^2 x(227.3/195)}{0.86x257.5 + 1.271x431.5(227.3/195)} = \quad 386.7 \text{ mm}$$

$$k_{eq} \quad = \quad \frac{0.86x257.5 + 1.271x431.5x(227.3/195)}{386.7} = \quad 2.23$$

$$\therefore \quad \text{predicted initial stiffness of composite joint}$$

$$S_L \quad = \quad 195000 \times 2.23 \times 386.7^2$$

$$= \quad 65 \text{ kNm/mrad}$$

Page 1

Sep 5 1997 16:10:39   comp2.f   Page 1

```fortran
1   C*************************************************
2   C* A SIMPLE PROGRAM TO CLASSIFY A GIVEN SECTION  *
3   C* AND CALCULATE THE MOMENT RESISTANCE OF COMPOSITE SECTION *
4   C* USING EC4                                     *
5   C* THE EFFECTS OF REINFORCEMENT IS ALSO INVESTIGATED *
6   C*************************************************
7   C
8   C    D   - Depth of steel section
9   C    DW  - Depth of web
10  C    B   - Width of steel section
11  C    TF  - Flange thickness
12  C    TW  - Web thickness
13  C    A   - Area of steel section
14  C    S   - Plastic Modulus
15  C    SL  - Span Length
16  C    DS  - Depth of Slab
17  C    DP  - Depth of Profiled Steel Sheeting
18  C    AS  - Area of Reinforcement
19  C    FY  - Yield stress of steel section
20  C    FS  - Yield stress of steel reinforcement
21  C
22        CHARACTER*12 NAME,BEAM,YEAR
23        REAL D,B,TF,TW,DW,A,S,SL,FYF,FYW,GA,GS,FCK,GC,FCD
24        REAL B2,EPSF,EPSW,RR,FLAN,FLAN1,FLAN2,Y1,Y2,YBAR
25        REAL FLAN3,WEB,BE,RRS,TAU,DS,DP,FYDF,FYDW,COMSLEN
26        REAL ASB,AST,DRB,DRT,FSDT,FSDB,FSKT,FSKB,FRATIO
27        INTEGER CASE,FCLASS,MCLASS
28
29        PRINT*,'ENTER RESEARCHERS NAME, BEAM NO,YEAR'
30        READ*,NAME,BEAM,YEAR
31        PRINT*,'TYPE IN THE VALUE OF D,DW,B,TF,TW,A,S,SL'
32        READ*,D,DW,B,TF,TW,A,S,SL
33        PRINT*,'TYPE THE VALUES OF FYF,FYW,GA,FSKT,FSKB,GS,FCK,GC,DS,DP,
34       +DRT,AST,DRB,ASB'
35        READ*,FYF,FYW,GA,FSKT,FSKB,GS,FCK,GC,DS,DP,DRT,AST,DRB,ASB
36        PRINT*,'WHAT ARE OTHERS REQUIRED DATA'
37        PRINT 1,NAME,BEAM,YEAR
38   1    FORMAT('NAME:',A12,6X,'BEAM NO:',A12,3X,'YEAR:',A12)
39        PRINT*,'
40        PRINT*,'
41
42        PRINT 2,D,DW,B,TF,TW,A,S,DS,DP,DRT,AST,DRB,ASB,SL
43   2    FORMAT('D =',F6.2,3X,'DW =',F6.2,3X,
44       +'B =',F6.2,3X,'TF =',F6.2,3X,'TW =',F6.2/
45       +'AREA OF SECTION A =',F9.2/
46       +'PLASTIC MODULUS S =',F7.2//
47       +'DS =',F6.2,3X,'DP =',F6.2,3X,
48       +'DRT =',F6.2,3X,'AST =',F8.2/
49       +'DRB =',F6.2,3X,'ASB =',F8.2/
50       +'SL =',F8.2)
51
52        FYDF = FYF/GA
53        FYDW = FYW/GA
54        FSDT = FSKT/GS
55        FSDB = FSKB/GS
56        FCD = FCK/GC
57        PRINT 3,FYDF,FYDW,FCD,FSDT,FSDB,GA,GS,GC
58   3    FORMAT('FYDF =',F6.2,6X,'FYDW =',F6.2,6X,'FCD = ',F6.2/
59       +'FSDT=',F6.2,6X,'FSDB =',F6.2/
60       +'GA =',F6.2,3X,'GS =',F6.2,3X,'GC = ',F6.2)
61        PRINT*,'
62
63  * Classification of Section from table 4.1&4.2 and from Fig 4.4 EC4
64        BE=SL/8.
65        PRINT*,'EFFECTIVE BREADTH OF SECTION BE = ',BE
66
```

Page 2

Sep 5 1997 16:10:39   comp2.f   Page 2

```fortran
67        EPSF = (235./FYF)**0.5
68        EPSW = (235./FYW)**0.5
69        PRINT*,'VALUE OF EPSILON OF FLANGE = ',EPSF
70        PRINT*,'VALUE OF EPSILON OF WEB = ',EPSW
71        B2 = B/2.
72        FLAN = B2/TF
73
74  *Calculate the Force Ratio
75        FRATIO = (AST*FSDT+ASB*FSDB)/(TW*DW*FYDW+(A-DW*TW)*FYDF)
76        PRINT*,'THE FORCE RATIO = ',FRATIO
77        PRINT*,'
78
79  * To calculate ALPHA ie depth of web in compression
80  * Need to check the elastic stress for web limit class 4
81  * Need to calculate position of elastic neutral axis
82        RRT=FSDT*AST/1000.
83        RRB=FSDB*ASB/1000.
84        RR =RRT+RRB
85        RV = TW*DW*FYDW/1000.
86        RS = RV*(A-DW*TW)*FYDF/1000.
87
88        YBAR = A*(D/2.+DRT)/(A+AST+ASB) + ASB*(DRT-DRB)/(A+AST+ASB)
89        Y1 = DRT + D - (D-DW)/2.- YBAR
90        Y2 = DW -Y1
91        PRINT*,'Y1 =',Y1,     'Y2 =',Y2,     'YBAR = ',YBAR
92
93        TAU = -Y2/Y1
94        PRINT*,'RATIO TAU = ',TAU
95        IF(TAU .GT.1.)PRINT*,'WARNING TAU IS GREATER THAN 1'
96        IF (TAU .GT.-1.)WEB3=42.*EPSW/(0.67 + 0.33*TAU)
97        IF (TAU .LE.-1.)WEB3=62.*EPSW/(1.-TAU)*SQRT(-TAU)
98  * Note that in hogging bending TAU must be .GT. -1
99
100       ALPHA=0.5*(1.+RR/RV)
101 *--Recommendation by Johnson & Anderson : ALPHA LT 0.5=20tEPS/d
102       ALPHA1 = 0.5+20.*TW*EPSW/DW
103       IF (RR .GT. RV) ALPHA = 1.0
104       IF (ALPHA .GT.ALPHA1)PRINT*,'WARNING ALPHA IS EXCEEDING ALPHA1'
105       ALPHAD=ALPHA*DW
106       PRINT*,'ALPHA1 = ',ALPHA1
107       PRINT*,'ALPHA = ',ALPHA
108       PRINT*,'INITIAL PNA POSITION WITH NO HOLE IN WEB= ',ALPHAD,'mm'
109       WEB =DW/TW
110 *--Combined Slenderness
111       COMSLEN=((ALPHA*WEB*3.*TW*DW/(A*EPSW))*
112      +(FLAN*3.*B*TF/(A*EPSF)))**0.5
113       PRINT*,'COMBINED SLENDERNESS = ',COMSLEN
114
115       IF (ALPHA .EQ.0.5)THEN
116       WEB1=72.*EPSW
117       WEB2=83.*EPSW
118       ENDIF
119       IF (ALPHA .GT.0.5)THEN
120       WEB1=396.*EPSW/(13.*ALPHA-1.)
121       WEB2=456.*EPSW/(13.*ALPHA-1.)
122       ENDIF
123       IF (ALPHA .LT.0.5)THEN
124       WEB1= 36.*EPSW/ALPHA
125       WEB2= 41.5*EPSW/ALPHA
126       PRINT*,'SINCE ALPHA LE 0.5, NEED NOT TO CONSIDER'
127       ENDIF
128       PRINT 4,WEB,WEB1,WEB2,WEB3
129  4    FORMAT('WEB= ',F6.2,2X,'WEB1= ',F6.2,2X,'WEB2= ',F6.2,2X,
130      + 'WEB3= ',F6.2)
131       FLAN1=10.*EPSF
132       FLAN2=11.*EPSF
```

Page 4

```fortran
199       IF(WEB.LE.38.*EPSW .OR.WEB .LE.WEB2)THEN
200          IF(RR.LT.RW)THEN
201             CASE = 1
202             PRINT*,'WEB COMPACT & PNA IS IN THE WEB'
203             MR = MRS+RRT*(D/2.+DRT)/1000.+
204       +RRB*(D/2.+DRB)/1000.-((RR*RR/RV)*0.25*DW/1000.)
205          ENDIF
206       ENDIF
207   !-
208       IF(WEB .GT.38.*EPSW .AND.WEB.GT.WEB2)THEN
209          IF(RR.LT.RD )THEN
210             CASE = 2
211             PRINT*,'WEB NOT COMPACT & PNA IS IN THE WEB'
212             V1=(RV+RR)*(D/2.+RR-2.*RD)
213   140   MR=MRS+RRT*(D/2.+DRT)/1000.+RRB*(D/2.+DRB)/1000.
214       +-(RR**2+V1)/RV)*(DW/4000.)
215             ENDIF
216   !-
217          IF(RR.LT.RD .AND.RR.GT.DA)THEN
218             PRINT*,'CENTROID OF STEEL SECTION WITHIN HOLE'
219             PRINT*,'USE FORMULA BY D ANDERSON'
220             V2=MRS+RRT*(D/2.+DRT)/1000.+RRB*(D/2.+DRB)/1000.
221             V3=RD*RV-2.5*RD**2+2.*RD*RR
222             V4=(0.5*RV-1.5*RD+RR)**2
223             V5=(0.5*RV-0.5*RD)**2
224             V6=DW/(2.*RV)
225             MR = V2-(V6/1000.)*(V3-V4+V5)
226          ENDIF
227       ENDIF
228
229   !!
230       IF(WEB.LE.38.*EPSW)THEN
231          IF( RR.GE.RW .AND. RR.LT.RS)THEN
232             CASE = 3
233             PRINT*,'WEB COMPACT & PNA IN STEEL FLANGE'
234             MR= (RS*0.5*D+(RRT*DRT+RRB*DRB)-((RS-RR)**2*0.25*TF/RF))/1000.
235          ENDIF
236          IF( RR.GE.RW .AND. RR.GE.RS)THEN
237             CASE = 4
238             PRINT*,'WEB COMPACT & PNA OUTSIDE STEEL BEAM'
239             MR= RS*((0.5*D+DRT)/1000.)
240             PRINT*,'THIS MOMENT RESISTANCE NEGLECTS ANY LOWER LAYER OF
241       +REBARS IN SLAB'
242          ENDIF
243       ENDIF
244       IF(WEB .GT.38.*EPSW .AND. RR.GE.RD)THEN
245          IF(RR.LT.RN)THEN
246             CASE = 5
247             PRINT*,'WEB NOT COMPACT & PNA IN STEEL FLANGE'
248             MR = (RN*0.5*D+(RRT*DRT+RRB*DRB)-((RN-RR)**2*0.25*TW/RF))/1000.
249          ENDIF
250          IF( RR .GE. RN)THEN
251             CASE = 6
252             PRINT*,'WEB NOT COMPACT & PNA OUTSIDE STEEL BEAM'
253             MR = RN*(0.5*D+DRT)/1000.
254             PRINT*,'THIS MOMENT RESISTANCE NEGLECTS ANY LOWER LAYER OF
255       +REBARS IN SLAB'
256          ENDIF
257       ENDIF
258
259       PRINT*,'CASE TO CONSIDER IS CASE = ',CASE
260       PRINT*,'MOMENT RESISTANCE OF SECTION Mg1.Rd = ',MR, 'kNm'
261       STOP
262       END
```

Page 3

```fortran
133          FLAN3=15.*EPSF
134       IF (FLAN.LE.FLAN1)THEN
135          FCLASS=1
136       ELSEIF (FLAN.LE.FLAN2)THEN
137          FCLASS=2
138       ELSEIF (FLAN.LE.FLAN3)THEN
139          FCLASS=3
140       ELSE  FCLASS=4
141       ENDIF
142       PRINT*,
143       PRINT 5,FLAN,FLAN1,FLAN2,FLAN3
144     5 FORMAT('FLAN= ',F6.2,2X,'FLAN1= ',F6.2,2X,'FLAN2= 'F6.2,2X,
145       + 'FLAN3= ',F6.2)
146       PRINT*,'FLANGE IS IN CLASS = ',FCLASS
147   !-
148       IF( WEB.LE.WEB1)THEN
149          WCLASS=1
150       ELSEIF( WEB.LE.WEB2)THEN
151          WCLASS=2
152       ELSEIF(WEB.LE.WEB3)THEN
153          WCLASS=3
154       ELSE   WCLASS=4
155       ENDIF
156       PRINT*,'WEB IS IN CLASS = ',WCLASS
157       IF ( FLAN .GT.FLAN2 .OR.WEB .GT.WEB3)THEN
158       PRINT*,'FLANGE IN CLASS 3 OR 4 OR WEB IS IN CLASS4'
159       PRINT*,'DESIGN USING ELASTIC METHOD'
160       STOP
161
162       ENDIF
163
164   !
165       PRINT*,'IF FLANGE IS IN CLASS 1 OR 2 AND WEB IS IN CLASS 3'
166       PRINT*,'CONSIDER HOLE IN WEB METHOD'
167       PRINT*,
168
169   !
170       PRINT*,'-------------------------------------------------------'
171       MRS = FYDF*S/1000.+(FCYK-FYDF)*0.25*TW*DW/1000000.
172       PRINT*,'MOMENT RESISTANCE OF STEEL SECTION MRS = ',MRS,  'kNm'
173       RS = RV*(A-DW*TW)*FYDF/1000.
174       PRINT*,'RESISTANCE OF STEEL BEAM           RS = ',RS,   'kN'
175       RC = 0.85*FCD*BE*(DS-DP)/1000.
176       PRINT*,'RESISTANCE OF CONCRETE FLANGE      RC = ',RC,   'kN'
177       RF = B*TF*FYDF/1000.
178       PRINT*,'RESISTANCE OF STEEL FLANGE         RF = ',RF,   'kN'
179       RD = 40.*EPSW*TW*TW*FYDW/1000.
180       PRINT*,'RESISTANCE OF SLENDER WEB          RD = ',RD,   'kN'
181       RV = TW*DW*FYDW/1000.
182       PRINT*,'RESISTANCE OF CLEAR WEB DEPTH      RV = ',RV,   'kN'
183       RW = RS-(2.0*RF)
184       PRINT*,'RESISTANCE OF OVERALL WEB DEPTH    RW = ',RW,   'kN'
185       RR = RV-RRB
186       PRINT*,'RESISTANCE OF REINFORCEMENT        RR = ',RR,   'kN'
187       RN = RS-RV-RD
188       PRINT*,'RESISTANCE OF SLENDER STEEL BEAM   RN = ',RN,   'kN'
189       PRINT*,
190       PRINT*,
191       PRINT*,
192       PRINT*,'-------------------------------------------------------'
193       DA = (3.*RD-RV)/2.
194       PRINT*,'VALUE FROM D ANDERSON  DA = ',DA
195       PRINT*,'IF RR.LT.RD .AND.RR.GT.DA THEN CENTROID OF STEEL SECTION
196       +WITHIN HOLE-IN-WEB'
197       PRINT*,
198
```
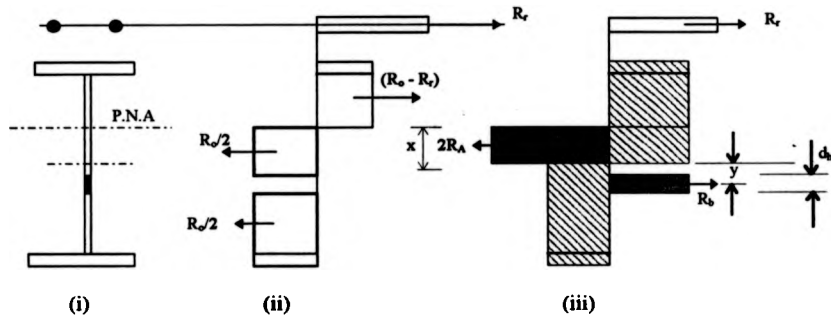
APPENDIX A3

Formula for hole-in web method for a symmetrical steel section

(i)　　　　　　　　(ii)　　　　　　　　(iii)

From Fig. (ii) and (iii),

$$\frac{R_v}{2} + 2R_A = R_B + R_r + R_A + (R_o - R_r)$$

$$\therefore \quad R_B \quad = \quad R_A + \frac{R_v}{2} - R_o$$

$$R_A \quad = \quad R_B - \frac{R_v}{2} + R_o$$

$$2R_A \quad = \quad 2R_B - R_v + 2R_o = \quad R_B + R_r$$

$$\therefore \quad R_B \quad = \quad R_r + R_v - 2R_o$$

$$R_A \quad = \quad x\, t\, p_y$$

$$R_v \quad = \quad d\, t\, p_y \qquad\qquad \therefore \quad p_y \quad = \quad \frac{R_v}{dt}$$

$$\therefore \quad R_A \quad = x\, t\, \frac{R_v}{dt}$$

$$R_o \quad = 38\, \varepsilon\, t^2\, p_y$$

$$\therefore 38\, t\, \varepsilon \quad = \quad \frac{R_o}{t \cdot p_y} \qquad \text{But} \quad t\, p_y \quad = \quad \frac{R_v}{d}$$

$$\therefore 38 \, t \, \varepsilon \quad = \quad R_o \cdot \frac{d}{R_v}$$

$$R_B \quad = \quad d_h \cdot t p_y$$

where,

d_h is depth of "hole"

$$\therefore \quad d_h \quad = \quad \frac{R_B}{t \cdot p_y} = R_B \cdot \frac{d}{R_v}$$

$$\therefore \quad y + d_h/2 + 19 \, t\varepsilon \quad = \quad d/2$$

$$\therefore \quad y + \frac{R_B}{2}\left(\frac{d}{R_v}\right) + \frac{R_o}{2}\left(\frac{d}{R_v}\right) = \frac{d}{2}$$

$$\therefore \quad y = \quad \frac{d}{2} - \frac{d}{R_v}\left[\frac{R_B}{2} + \frac{R_o}{2}\right]$$

$$\therefore \quad y = \quad \frac{d}{R_v}\left[\frac{R_v}{2} - \frac{R_B}{2} - \frac{R_o}{2}\right]$$

Substitute for R_B :

$$y \quad = \quad \frac{d}{R_v}\left(\frac{R_v}{2} - \frac{R_o}{2} - \frac{R_r}{2} - \frac{R_v}{2} + R_o\right)$$

$$= \quad \frac{d}{R_v}\left(\frac{R_o}{2} - \frac{R_r}{2}\right)$$

For centroid of steel section to be above "hole" :

$$y - \frac{d_h}{2} \geq 0$$

$$\therefore \quad y \geq \frac{d_h}{2}$$

$$\therefore \quad \frac{d}{R_v}\left(\frac{R_v}{2} - \frac{R_o}{2} - \frac{R_B}{2}\right) \geq R_B \frac{d}{2R_v}$$

$$\therefore \quad R_v - R_o - R_B \quad \geq \quad R_B$$

$$\therefore \quad R_v - R_o \geq \quad 2R_B$$
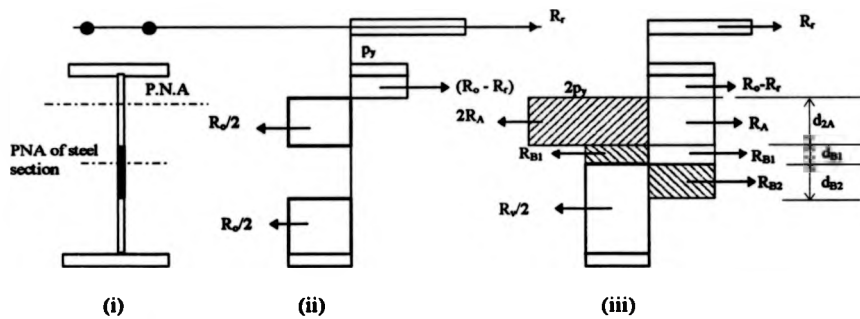
But $\quad R_B \quad = R_r + R_v - 2R_o$

$R_v - R_o \geq \quad 2R_r + 2R_v - 4R_o$

$\therefore \quad 3R_o - R_v \geq 2R_r$

$2R_r \leq 3R_o - R_v$

$R_r \leq \dfrac{3R_o - R_v}{2}$

Now consider PNA of steel section within the web hole:

| (i) | (ii) | (iii) |

$2R_A + R_{B1} = R_{B2} + R_r \qquad\qquad (1)$

$R_A = R_o/2$

$\therefore 2R_A = R_o$

$R_v/2 + R_{B1} + 2R_A = R_{B2} + R_{B1} + R_A + (R_o - R_r) + R_r$

$\therefore R_{B2} = R_v/2 + R_A - R_o \qquad\qquad (2)$

Substitute for R_A :

$R_o + R_{B1} \quad = \quad R_{B2} + R_r \qquad\qquad (3)$

$R_{B2} = R_v/2 + R_o/2 - R_o \qquad\qquad (4)$

$\therefore \quad R_{B2} = R_v/2 - R_o/2$

From Eqn.(3) : $\qquad R_o + R_{B1} = R_v/2 - R_o/2 + R_r$

$$\therefore \quad R_{B1} = R_v/2 - 3R_o/2 + R_r$$

Moment about centriod of steel beam

$$M = M_s + R_r\left(\frac{D}{2} + D_r\right) - 2R_A\left(\frac{d_{2A}}{2} + d_{B1}\right) - R_{B1} \cdot \frac{d_{B1}}{2} - R_{B2} \cdot \frac{d_{B2}}{2}$$

where

M_s is the resistance moment of steel beam only
D and D_r are defined in Fig. 6.3

Now $\quad 2R_A \quad = \quad d_{2A} \cdot t \cdot \left(p_y \times 2\right)$

$R_v = d\, t\, p_y \qquad\qquad \therefore t\, p_y \quad = R_v/d$

$$\therefore d_{2A} = \frac{(2\,R_A)}{2t \cdot p_y} = \frac{R_o}{2\,R_v} \cdot d$$

Also $\qquad R_{B1} = d_{B1} \cdot t\, p_y$

$$\therefore \qquad d_{B1} = \frac{R_{B1}}{t\,p_y} = \frac{d}{R_v}\left[\frac{R_v}{2} - \frac{3R_o}{2} + R_r\right]$$

Also $\qquad R_{B2} = d_{B2}\, t\, py$

$$d_{B2} = \frac{d}{R_v}\left[\frac{R_v}{2} - \frac{R_o}{2}\right]$$

Therefore plastic moment resistance when PNA in the "hole" :

$$M = M_s + R_r\left(\frac{D}{2} + D_r\right) - R_o\left[\frac{d}{R_v}\right]\left\{\frac{R_o}{4} + \frac{R_v}{2} - \frac{3R_o}{2} + R_r\right\}$$

$$-\frac{d}{2R_v}\left\{\frac{R_v}{2} - \frac{3R_o}{2} + R_r\right\}\left\{\frac{R_v}{2} - \frac{3R_o}{2} + R_r\right\} - \frac{d}{2R_v}\left\{\frac{R_v}{2} - \frac{R_o}{2}\right\}\left\{\frac{R_v}{2} - \frac{R_o}{2}\right\}$$

$$M = M_s + R_r\left(\frac{D}{2} + D_r\right) - \frac{d}{2R_v}\left\{2R_o\right\}\left\{\frac{R_v}{2} - \frac{5R_o}{4} + R_r\right\}$$

$$-\frac{d}{2R_v}\left(\frac{R_v}{2} - \frac{3R_o}{2} + R_r\right)^2 - \frac{d}{2R_v}\left(\frac{R_v}{2} - \frac{R_o}{2}\right)^2$$

$$M = M_s + R_r\left(\frac{D}{2} + D_r\right) - \frac{d}{2R_v}\left(\left(R_o R_v - \frac{5}{2}R_o^2 + 2R_o R_r\right) + \left(\frac{R_v}{2} - \frac{3}{2}R_o + R_r\right)^2 + \left(\frac{R_v}{2} - \frac{R_o}{2}\right)^2\right)$$

APPENDIX A4

Derivation to show that column taper rules gives $k_t = k_b$

From Eqn.(7.1) and Eqn.(7.21),

Distribution coefficient $\quad k_t \quad = \quad \dfrac{\dfrac{I_c}{h_2} + \dfrac{I_{cu}}{h_1}}{\dfrac{I_c}{h_2} + \dfrac{I_{cu}}{h_1} + \dfrac{I_b}{L}}$

$$= \frac{\dfrac{I_c}{h_2} + I_c \cdot \dfrac{F_1}{F_2}\dfrac{h_1}{h_2^2}}{\dfrac{I_c}{h_2} + I_c \cdot \dfrac{F_1}{F_2}\dfrac{h_1}{h_2^2} + \dfrac{I_b}{L}}$$

$$= \frac{\dfrac{I_c}{h_2} \cdot \left(1 + \dfrac{F_1}{F_2}\dfrac{h_1}{h_2}\right)}{\dfrac{I_c}{h_2} \cdot \left(1 + \dfrac{F_1}{F_2}\dfrac{h_1}{h_2}\right) + \dfrac{I_b}{L}}$$

Distribution coefficient $\quad k_b \quad = \quad \dfrac{\dfrac{I_c}{h_2} + \dfrac{I_{cl}}{h_3}}{\dfrac{I_c}{h_2} + \dfrac{I_{cl}}{h_3} + \dfrac{I_b}{L}\dfrac{(F_2 h_2 + F_3 h_3)}{(F_1 h_1 + F_2 h_3)}}$

$$= \frac{\dfrac{I_c}{h_2} + I_c \cdot \dfrac{F_3 h_3}{F_2 h_2^2}}{\dfrac{I_c}{h_2}\left(1 + \dfrac{F_3 h_3}{F_2 h_2}\right) + \dfrac{I_b}{L}\left(\dfrac{F_2 h_2 + F_3 h_3}{F_1 h_1 + F_2 h_2}\right)}$$

$$= \frac{\dfrac{I_c}{h_2}\left(\dfrac{F_2 h_2 + F_3 h_3}{F_2 h_2}\right)}{\dfrac{I_c}{h_2}\left(\dfrac{F_2 h_2 + F_3 h_3}{F_2 h_2}\right) + \dfrac{I_b}{L}\left(\dfrac{F_2 h_2 + F_3 h_3}{F_1 h_1 + F_2 h_2}\right)}$$

$$= \frac{\dfrac{I_c}{h_2}}{\dfrac{I_c}{h_2} + \dfrac{I_b}{L}\left(\dfrac{F_2 h_2}{F_1 h_1 + F_2 h_2}\right)}$$

$$= \frac{\dfrac{I_c}{h_2}\left(\dfrac{F_1 h_1 + F_2 h_2}{F_2 h_2}\right)}{\dfrac{I_c}{h_2}\left(\dfrac{F_1 h_1 + F_2 h_2}{F_2 h_2}\right) + \dfrac{I_b}{L}}$$

$$= \frac{\dfrac{I_c}{h_2}\left(1 + \dfrac{F_1 h_1}{F_2 h_2}\right)}{\dfrac{I_c}{h_2}\left(1 + \dfrac{F_1 h_1}{F_2 h_2}\right) + \dfrac{I_b}{L}}$$

$$= k_t$$

Published work

Two reports have been published by The Steel Construction Institute based upon the work in Chapter 4 and Chapter 5 of this thesis.

(1)   Bending Resistance and Rotational stiffness of Connection in Encased Steel Sections. Document RT594. September 1996.

(2)   Bond Strength of Encased Steel Sections. Document RT593. September 1996.

One of the beam-to-beam connection test (BTB2) was cited in Chapter 5 of "Composite steel-concrete joints in braced frames for buildings", a European COST-C1 publication. (Ed. D. Anderson). November 1996.

THE BRITISH LIBRARY
BRITISH THESIS SERVICE

COPYRIGHT

REPRODUCTION QUALITY NOTICE